Acoustics Australia

SPECIAL ISSUE

Underwater Acoustics

SignalCalc ACE
QUATTRO

ACE-QUATTRO has:

- Standard FFT, Synthetic 1/3 Octave standard,
- Quality Control, Point & Direction,
- Sound Power, Sound Intensity,
- Acoustic Intensity, Human Vibration,
- Sound Quality, Demodulation,
- Disk Record & Playback Analysis,
- Frequency Domain Compensation,
- Real Time Octave Analysis, Event Capture,
- 4-32 Inputs (Abacus), 2-8 Outputs + Tachy,
- ActiveX command & control macro programs,
- Single to Multi-Plane Balancing ...and more

2, 3 or 4 Inputs
0, 1 or 2 Outputs
1 Tachy + Trigger
Fast USB 2 for
Data & Power.

BSWA TECH

MEASUREMENT MICROPHONES.
microphones & accessories for Australian & NZ.

**High quality, calibrated electret prepolarized
microphones to class 1 & 2 & preamplifiers.**
Some of the Accessories available:
- IEPE power sources, - portable sound level calibrators,
- USB powered 2 channel measurement soundcard
- a 12 speaker dodecahedral sound source,
- compact light weight 2 channel power amplifiers,
- a self contained Tapping Machine sound source for
     foot fall measurements.
- impedance tubes providing 125 Hz to 3200 Hz range,
- Outdoor noise monitoring, terminal and software
- Small Reverberation chamber,
- Artificial Ear, Mouth & Head

VibraScout USB DC Triaxial Vibration Measurement System
from KINGDOM PTY LTD.
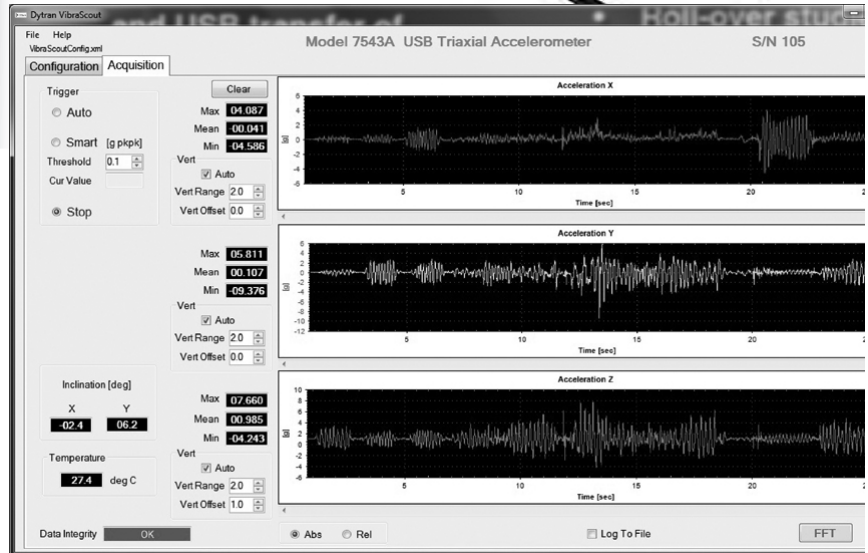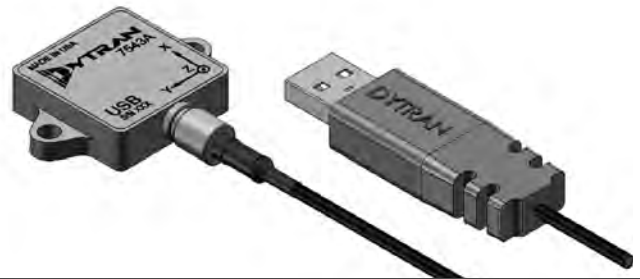
VibraScout system is an intelligent sensor including a USB digital Triaxial MEMS accelerometer, a microprocessor, a USB 4.6 m 4 pin cable, Data Acquisition software and Post Processor software. Just add your PC to get power and data exchange from the PC bus. VibraScout provides real-time 3 axis acceleration, static inclination, auto & smart triggering, RT Temperature recording, data logging with export to ascii, jpg, TDMS binary and conversion to PSD & FFT. Frequency span Zero to 1100 Hz.
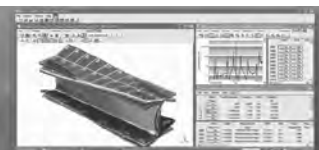Highly suitable for NVH, Vibration, calibration, rotating and more.

For more information phone: **02 9975 3272**
or visit: ***www.kingdom.com.au***

KINGDOM PTY LTD
Phone 02 9975 3272

AAS 07/10

Acoustics Australia

EDITORIAL COMMITTEE:

Nicole Kessissoglou ,

Marion Burgess, Tracy Gowen

BUSINESS MANAGER: Leigh Wallbank

LETTERS

PAPERS

TECHNICAL NOTES

REGULAR ITEMS

Cover design: Helena Brusic

MESSAGE FROM THE EDITOR

Welcome to the April 2013 special issue on Underwater Acoustics. I'd like to thank Dr Christine Erbe, who got the ball rolling on this special issue, and Dr Alec Duncan, who rounded up contributors and reviewers. I'd also like to extend my gratitude to two wonderful reviewers for their thorough and timely reviews when time was running out (unfortunately I am not able to name you but you know who you are!). Considering the concept of a special issue on underwater acoustics only originated six months ago, it has been a fantastic effort by all involved to bring this issue together so quickly.

I'd like to share the moment in the photo shown here. Dr Paul Dylejko was awarded the President's prize for best paper at the Acoustics 2012 conference. Paul was my first PhD student when I joined UNSW 10 years ago and I am a proud "academic parent" of his achievements.

Two upcoming conferences in Australia are the Acoustics 2013 Victor Harbor conference in South Australia in November this year, and Inter-Noise 2014 in Melbourne in November next year. Both of these conferences are shaping up to be exciting events!

Nicole Kessissoglou

ACOUSTICS 2013 VICTOR HARBOR
Science, Technology and Amenity
VICTOR HARBOR, SOUTH AUSTRALIA
NOVEMBER 17-20 2013

Inter-Noise 2014
MELBOURNE AUSTRALIA 16-19 NOVEMBER 2014

The Australian Acoustical Society will be hosting Inter-Noise 2014 in Melbourne, from 16-19 November 2014. The congress venue is the Melbourne Convention and Exhibition Centre which is superbly located on the banks of the Yarra River, just a short stroll from the central business district.

The congress theme is *Improving the world through noise control*. Major topics will include community and environmental noise, building acoustics, transport noise and vibration, human response to noise, effects of low frequencies and underwater noise.

Further details are available on the congress website **www.internoise2014.org**

SAVTek Sales+Rentals

DO YOU FEEL THE GROUND SHAKING?

SYSCOM MR3000C

SYSCOM MR3000C

- The **NEW** MR300C from SYSCOM from Switzerland – state of the art ground vibration measurement equipment.

- Internal or external Triaxial Velocity meter or Accelerometer.

- 3G and Wireless connectivity built in – can send emails/SMS alerts and push data to the Cloud or an FTP

- Settings can be changed by wi-fi, via iPhone, Android phones, tablets or Laptop or by LAN

- Stores triggered events and background levels on an SD card on the unit and also uploads via 3G.

- Ideal for monitoring construction vibration, roads, tunnelling, dams, bridges, piling and railways.

SAVTek Pty Ltd
Sound and Vibration Technology

Phone: (07) 3300 0363 | **www.savtek.com.au**

MESSAGE FROM THE PRESIDENT

A lot is happening in our Society right now. Preparations are moving along very nicely for the AAS Annual Conference in Victor Harbor 17th to 20th November 2013. There will be some very interesting Plenary talks by leaders in their respective fields and the Sponsorship and Exhibition opportunities are being snapped up. Look out for the notice on submission of abstracts and put the dates down for you to attend.

Planning for Internoise 2014 in November 2014 in Melbourne is also well underway. We anticipate there will be four keynote lectures and two plenary talks during the Congress. Details of the speakers and their subjects will be posted on the web-site, www.internoise2014.org once they are finalised. Already, over 80 people from many parts of Europe, UK, USA and Asia have agreed to chair or co-chair sessions during the Congress with many Australian based researchers and consultants agreeing to assist. Charles Don and John Davy will attend Internoise 2013 in Innsbruck on our behalf and present to the INCE Board re our planning.

A special committee of Federal Council headed by Matthew Stead has been progressing our goal to promote and advance acoustics in all its branches and to facilitate the exchange of information and ideas in relation thereto. Another objective is to encourage research and the publication of new developments relating to acoustics. This AAS project aims to activate these two objectives. One outcome from the committee is a survey to seek YOUR input on the proposal for research grants and to identify priority research areas. The survey can be accessed at: http://www.surveymonkey.com/s/9DNB6M6 and will be open to the end of April. Please assist us by filling your ideas regarding research priorities.

We are also progressing towards a revamp of our website to bring us up to date and to make our website more functional. Stay tuned.

We were very saddened to hear of the sudden untimely passing in January of Michael John Smith, Managing Director and CEO of Vipac Engineers and Scientists Ltd. Michael was a major contributor to acoustics in Australia. Michael was one of four young engineers who established Vipac Engineers and Scientists in Sydney in 1973. Over the next 40 years, he steered it to become an engineering powerhouse, employing 280 staff. Many acoustic consultants around Australia owe their thanks to Michael for giving them the opportunity to get into the field of acoustics, including myself. We honour his contribution to acoustics in general and give our condolences to his family for their loss.

Norm Broner
President Internoise 2014

MESSAGE FROM THE GUEST EDITOR

It is with great pleasure that I welcome you to this special edition of Acoustics Australia on underwater acoustics. This special edition seems particularly timely as there has been a dramatic transition over recent years, as increasing community concerns about the impacts of man-made underwater sound on marine animals have moved this discipline, once considered of interest to only a small number of specialists, into the mainstream. At the same time, advances in technology have given us wonderful active acoustic tools such as multibeam sonars that can be used for surveying and characterising the seabed, and allowed the development of relatively low cost, autonomous, underwater recording systems that have vastly increased our knowledge of the ocean soundscape and the animals that contribute to it.

In this special edition you will find thirteen papers that provide a sample of the broad discipline of underwater acoustics. These papers are revised and expanded versions of a small selection of the fifty-five papers on underwater acoustics that were presented at last year's Australian Acoustical Society national conference in Fremantle. Among them you will find papers on the impacts of man-made sound on marine animals, on the use of both passive and active acoustics for monitoring marine animals, on factors that influence the propagation of sound through the ocean, and on techniques for communicating information through the ocean using acoustics.

If you are a specialist in this discipline then I am sure you will find these papers both interesting and useful. If this area is new to you then I trust that you will find a browse through this issue a rewarding and intriguing journey.

A final thought – the average depth of the oceans is just under 4000m, but sunlight only penetrates to a depth of 200m. Other forms of electromagnetic radiation, such as radio waves, attenuate much faster than light. The only form of radiation that travels any significant distance in the oceans is sound, so the importance of underwater acoustics in helping us increase our knowledge of the marine environment cannot be overstated.

Alec Duncan

LETTER TO THE EDITOR

Ray Tumney, RCA Australia, Newcastle, NSW 2294
rayt@rca.com.au

Response to article by S. Cooper, "Wind farm noise - an ethical dilemma for the Australian Acoustical Society?", *Acoustics Australia* **40**(2), 139-142 (2012)

I wish to respond the strident criticism of Steven Cooper's article published in Acoustics Australia Vol. 40, No. 2, pp 139-143 (2012). It is disappointing that the respondents, all senior members of the AAS, seem to have misunderstood Mr Cooper's article and appear to have responded in an ill considered fashion and not in the context of ensuring that the profession ensures that the issue of noise from wind farms is properly and adequately considered in the same manner as noise from other sources has been in the past.

The main points of Mr Cooper's article are:-

- that there has been insufficient study conducted on the effects of wind farm noise to enable the profession to confidently and adequately walk the fine line between balancing the competing needs of the community to have productive industries without paying too high a price in environmental impact.

  and

- that published assessment criteria are being used to make evaluations of community impact which based on the existing available information seem likely to be flawed.

Mr Cooper is also concerned, quite rightly in my view, that the un-certainty in the prediction of human response that results from a shortage of detailed and reliable scientific knowledge is not acknowledged in the assessment documents. If an uncertainty arises due to a lack of scientific evidence it must be considered by the assessors of the application in accordance with the requirements of the Environmental Planning and Assessment Act [1] and the relevance and application of the "Precautionary Principal" must be evaluated. If a technical assessment document does not disclose uncertainty then the planning assessor would correctly accept that there is no significant uncertainty in the outcomes expressed in the technical assessment. In the case of Industrial Wind Turbine farms the acceptance that there is no significant uncertainty would be erroneous at best and there may be some potential for any consent based on such a noise impact assessment to be found to be invalid. Given the nature of the planning review system it is likely that an invalid consent may not be identified or determined by court until after the IWTs are constructed. The consequences of an invalid consent for the client of an acoustician who made the assessment upon which planning consent is invalidated are truly terrifying.

It seems beyond dispute that the community has a high level of concern with wind farm noise. A recent health study by Nissenbaum et al. [2] clearly indicates that there is much work yet to be done in understanding the human response to Industrial Wind Turbines (IWTs).

Participants living near IWTs had worse sleep, as evidenced by significantly greater mean PSQI and ESS scores [Table 3]. More participants in the near group had

PSQI > 5 (P = 0.0745) and ESS scores > 10 (P = 0.1313), but the differences did not reach statistical significance. Participants living near IWTs were significantly more likely to report an improvement in sleep quality when sleeping away from home.

This study supports the conclusions of previous studies, which demonstrate a relationship between proximity to IWTs and the general adverse effect of 'annoyance', but differs in demonstrating clear dose-response relationships in important clinical indicators of health including sleep quality, daytime sleepiness, and mental health. The levels of sleep disruption and the daytime consequences of increased sleepiness, together with the impairment of mental health and the dose-response relationships observed in this study (distance from IWT vs. effect) strongly suggest that the noise from IWTs results in similar health impacts as other causes of excessive environmental noise. The degree of effect on sleep and health from IWT noise seems to be greater than that of other sources of environmental noise, such as, road, rail, and aircraft noise. Bray and James have argued that the commonly used noise metric of LAeq (averaged noise level adjusted to human hearing) is not appropriate for IWT noise, which contains relatively high levels of low frequency sound and infrasound with impulsive characteristics. This has led to an underestimation of the potential for adverse health effects of IWTs.

It is also clear from the recent Australian experience (there is an active Senate inquiry) that there is a reasonable level of good quality well informed community engagement in the debate.

In the Acoustics Australia journal special issue on wind turbine noise, Cooper et al. [3] recommends that AS 4959:2010 [4] be revised as soon as practical because of error inherent in the modelling process specified in the standard.

Articles by Tonin [5] and Evans and Cooper [6] provide information determined from predictive noise models that are only defined over the range to 63Hz to 8 kHz, but Doolan et al. [7], Tickell [8] and Thorne [9] clearly show substantial sound generation below 20 Hz with the BTI frequency in the range 0-5 Hz with multiple harmonics above that.

Despite claims to the contrary, good quality, well informed community engagement is often not truly welcome either by a proponent industry or their consultants as it makes the path to development approval far more testing that it might otherwise be.

I have long been concerned with the effects of low frequency noise (LFN) on the general public and the fact that

there are many areas where there is potential for the impacts to not be adequately recognised or assessed because guideline documents are either too narrow or out of date because science and engineering have moved ahead of the guideline.

In my opinion the ultimate responsibility rests with the professional in the technical field and I am disappointed to note that Dr Tonin's response [10] suggests that an acoustician should simply follow a guideline to adequately assess a noise impact. While guidelines are very useful tools, it will never be the case that guidelines are either completely comprehensive or completely up to date. Also while it may the case that a planning authority may reject an application because it has not adequately covered the information sought in a planning assessment guideline, it will never be the case that a planning application is rejected because the acoustic assessment examined additional information above and beyond that which is included in the guideline.

It may, however, be the case that the additional information provides a basis on which it may be decided that a development application should not be approved, but that is no reason for a professional to simply ignore that information and only address what a guideline may request.

It would not be the first time that the acoustics profession has become lazy or complacent and followed a flawed guideline only to pay the price in increased claims and insurance premiums. The recent history of changes to the Building Code of Australia comes to mind.

I think it extraordinary that Dr Tonin has so misread Mr Cooper's article that he considers Mr Cooper is accusing consultants of being pro or anti a particular form of development. It is quite clear that Mr Cooper is translating a view he considers is present in the Wind Turbine industry not one that he considers is present in the acoustics industry.

On the other hand Marks et al. [11] have quite clearly grasped the issues that Mr Cooper is seeking to bring to the attention of society members but for reasons that mystify me seek published interpretive guidance from the AAS on how to apply the code of ethics to the practice of environmental noise impact assessment.

In my view the key element of Mr Cooper's concern relates to the diligent compliance by members with Item 1 of the Code of Ethics "Responsibility". The code of ethics already contains a set of explanatory notes as to what this means for members of the society and it is very clear that the "health and welfare and safety" of the community is to be paramount in the conduct of members. If there is any lack of clarity in a members mind as to what this means in their day to day work then I would suggest that they are either already in breach of their ethical duty or are not fit to be full members of the society.

In considering Dr Burgemeister's response [12] I am led to consider that Mr Cooper's concerns may indeed be valid. Dr Burgemeister makes the point that he has never consulted to any part of the industry or community but has conducted a desk top review of the available information. He goes on to make the point that guidelines and criteria are not perfect and that he considers that consultants are doing their best to make a fair and reasonable assessment given the limitations under which they work. He quotes numerous works that provide

information on the assessment of wind farms and makes some technical criticism of Mr Cooper's measurement techniques.

Eventually Dr Burgemeister gets to, what I think is the heart of the problem, and that which Mr Cooper has sought to bring to our attention. That the demographic and psycho-acoustic studies necessary to enable society members to confidently and accurately "protect the "health and welfare and safety" of the community do not presently exist and neither do reliable measurement methods or guidelines.

The situation appears to be as follows:-

- Mr Cooper has identified that some of the submitted environmental impact assessments do not contain an adequate description of the potential impacts on the community (as distinct from a compliance with a guideline that is recognised by all to be imperfect) and neither did they contain a statement as to the level of uncertainty about the impacts brought about by the shortage of the necessary psycho-acoustic studies.
- Dr Burgemeister agrees that the necessary information is not available but believes that consultants and engineers are "trying their best" to get there.
- The Code of Ethics requires that community "health and welfare and safety" is paramount and it requires society members to avoid work that would cause conflict with that that pre-eminent requirement,
- The Planning and Assessment Act in NSW requires the application of the "precautionary principal" which stipulates that "a lack of scientific certainty may not be a premise for granting planning approval for a project"
- Marks et al. do not know what to think and want the society to bail them out, and
- Dr Tonin seems to have completely missed the point.

In reviewing my own work I often ask myself the question:-

If, instead of being an acoustician, I was a structural engineer designing a difficult new bridge in uncertain conditions or an aeronautical engineer designing a new passenger aircraft - am I satisfied that my assessment of the design is good enough to avoid failure?

I find this question, if answered honestly in the context of a development assessment, can be very enlightening.

In my view the Society is firmly on the horns of a 2000 kg (about the size of a fully grown bull for you city folk) ethical dilemma.

Given that renewable energy in the form of Industrial Wind Turbines is not necessarily something we must have now, it is extremely disappointing that senior members of the society have failed to take up the opportunity to press for greater funding for research into the effects of wind turbines.

The current state of uncertainty surrounding methods of assessment, acceptable sound levels, and human response requires that members involved in the development assessment of Industrial Wind Turbines should ensure that any work they conduct fully examines and documents all of the potential issues, and clearly states any uncertainty or unknowns that result from the work. Acoustic assessment reports should not recommend approval for a development while the situation remains unresolved but should properly describe the known outcomes and discuss the issues associated with the unknowns

or the poorly quantified. The proponents of the developments need to be required to ensure that adequate research work is conducted in this area until the questions surrounding human response and appropriate measurement methods are resolved to a satisfactory level.

REFERENCES

[1] NSW Planning and Infrastructure, *Environmental Planning and Assessment Act 1979* http://www.austlii.edu.au/au/legis/nsw/consol_act/epaaa1979389/

[2] M.A. Nissenbaum, J.J. Aramini and C.D. Hanning, "Effects of industrial wind turbine noise on sleep and health", *Noise Health* **14**, 237-243 (2012)

[3] J. Cooper, T. Evans and L. Najera, "Comparison of compliance results obtained from the various wind farm standards used in Australia", *Acoustics Australia* **40**(1), 37-44 (2012)

[4] Australian Standard AS 4959:2010 *Acoustics – Measurement, prediction and assessment of noise from wind turbine generators*

[5] R. Tonin, "Sources of wind turbine noise and sound propagation", *Acoustics Australia* **40**(1), 20-27 (2012)

[6] T. Evans and J. Cooper, "Comparison of predicted and measured wind farm noise levels and implications for assessments of new wind farms", *Acoustics Australia* **40**(1), 28-36 (2012)

[7] C.J. Doolan, D.J. Moreau and L.A. Brooks, "Wind turbine noise mechanisms and some concepts for its control", *Acoustics Australia* **40**(1), 7-13 (2012)

[8] C. Tickell, "Low frequency, infrasound and amplitude modulation noise from wind farms - some recent findings", *Acoustics Australia* **40**(1), 64-66 (2012)

[9] B. Thorne, "Finding the character of wind turbine sound", *Acoustics Australia* **40**(1), 62-63 (2012)

[10] R. Tonin, Letter to the Editor, *Acoustics Australia* **40**(3), 167-168 (2012)

[11] T. Marks, C. Delaire, J. Adcock and D. Griffin, Letter to the Editor, *Acoustics Australia* **40**(3), 168 (2012)

[12] K. Burgemeister, Letter to the Editor, *Acoustics Australia* **40**(3), 169-171 (2012)

LETTER TO THE EDITOR

Graeme E. Harding, Donvale, VIC 3111, Australia
gandg@tpg.com.au

Wind Farm Noise - The Debate

The debate in Acoustics Australia has quite rightly continued; rightly because the debate has not reached a conclusion matching all the available information. In drafting this I found it easier to set it out as numbered points for which I hope readers will forgive me.

1. As an Applied Physics student I was taught that theory and practice always agree - if theory and practice do not agree then it is the theory that must be modified. In conformity with this concept we should not declare a design or calculating procedure as correct until community subjective responses agree with predicted response.

2. That we have people who benefited financially from their agreement to allow wind turbines on their land abandoning their homes because they could not stand the noise strongly indicates that the theory used to predict a noise climate acceptable to residents needs modification.

3. I note there are AAS Members who, at hearings, are happy to advise that compliance with legislated or established design criteria will be safely achieved (and undoubtedly will); but do not comment on the likely actual acoustical amenity potentially affected residents are likely to have to live with.

4. I note that the noise climate that matters most is that at the resident's ears when he/she goes to sleep. This noise level is dependent on the sound insulation of the home; and highly dependent on room geometry and location of the bed. I have measured very high low frequency sound levels at trihedral corners of rooms, and in the middle of small rooms like toilets relative to centre of room noise.

5. I believe that when an AAS Member is giving expert evidence, he or she should advise the court or panel not just of the external noise level to residences when calculated in accordance with recognised procedures relative to established limits, but also on the likely noise inside the residence(s), and the likely response disinterested people would have if they lived in the potentially affected residences.

6. A "Sound Jury" has been successfully and rightly used to establish relationships between subjective response and character and magnitude of noise, such as car drive-past, or office air conditioning, etc. The results of such experiments are relatively easily replicated by others and a consensus reached as to what constitute acceptable design noise limits for those circumstances.

7. The sound jury approach cannot be used to establish acceptable noise limits as regards the limits of acceptable character and magnitude of noise wind turbines as received inside and outside homes cannot be easily done because:-

   a. The assessment as regards acceptability of the potentially disturbing noise is a judgement of what can be lived with and needs time for assessment relative to the various normal home activities and conditions such as windows open or closed, occupants studying, sleeping or other activities.

   b. The sound level and character vary significantly from room to room and with position in the room, generally having much higher low frequency sound levels at the bed head position in the corner of the bedroom; thus assessment should not be based on a single position in a room.

c. Existing residents are not disinterested and hence likely to be biased if used as part of the sound jury, if alternatively non-residents were to act as members of the sound jury, they would need to live in a potentially affected "test" houses for a time (2 weeks?, 6 weeks?) for acclimatisation before the turbines run and a similar time? for acclimatisation with the wind turbines running.

d. The sound source (the wind turbine noise) cannot altered in sound output magnitude, and character in a controlled manner; excepting by pitch angle changes and braking to some or all of the turbines.

8. Having established acceptable internal noise character and magnitude limits it would be necessary to establish by test on various home designs and constructions how the free field external noise relates to the internal sound levels.

9. AAS Members may have noticed The "Weekend Australian" for February 9-10 2013 had a prominent article in the centre of page 9 titled "Wind-weathered residents await turbine test"; and a bigger article on page 17 titled "World's eyes will be on Waterloo as turbines go on trial". The text informs of the forthcoming investigations by the South Australian EPA of noise associated with wind turbines, perhaps for the first time measuring sound levels at low frequencies and with it organised that wind turbines can be turned off and on so as to distinguish turbine generated sound from other environmental noise under various wind conditions.

10. Measurements necessary to assess compliance or otherwise in accordance with standardised or legislated procedures may take a month or more of multi-band recording and analysis perhaps during more than one season but would allow potentially excessive noise to be measured where it is heard. One difficulty may be the need for absolute silence by the residents

11. The work proposed above might hopefully give us all a better idea of what aspects, characteristics and magnitudes of noise from wind turbines, as heard inside dwellings, is disturbing.

a. Just imagine that we had a large enough sample and enough measurements and analysis to reasonably say what was unreasonably disturbing to 1%, 2%, 4% and 8% of people living in their home and exposed to 'Wind Farm' noise within their dwelling.

b. Further imagine that from the large sample we, as acousticians, did establish what measurable magnitudes and attributes of wind turbine noise contributed to a resulting 1%, 2%, 4% and 8% of the potentially affected population.

c. Finally imagine the responsible body established noise measuring and analysis procedures and limits for assessment of compliance of wind turbine noise that was directly and only related to the assessment of wind turbine noise within dwellings.

In summary I believe that it behoves us as acousticians and AAS Members when acting as experts to be

a. Clear and candid in our evidence and admit the facts that many residents have complained bitterly about the adverse effect of the noise from the wind turbines when located at distances and circumstances so as to be in accordance with currently established procedures.

b. It also behoves the member to state that the current state of acousticians' knowledge does not guarantee freedom from disturbance to all potentially affected residents at some or the most of the time.

Finally an AAS Member should be wary of relying on their own judgement as their hearing may be much dulled by city living, they should remember the story of an investigation into intrusive noise by a Melbourne consulting firm; the two acousticians being totally unable to hear any disturbing noise conducted a test with one acoustician in the factory and the other in the house; the dear old lady could tell the acoustician the machine is on or off as the case was before radio contact was made; such can be the difference in the acuity and "tuning" of ears.

Graeme E. Harding
F.AAS, M.ASA, M.AIRAH, M.IIAV

INTERNATIONAL REGULATION OF UNDERWATER NOISE

Christine Erbe

Centre for Marine Science and Technology, Curtin University, Perth 6845, Western Australia
Christine.erbe@curtin.edu.au

Underwater noise is a by-product of marine industrial operations, that plays an increasing role in environmental impact assessments. It can have a variety of temporary to chronic bioacoustic impacts on marine fauna, such as behaviour modification, changes in habitat usage or migration, communication masking, and auditory and non-auditory physiological impacts. There are still lots of unknowns. Audiograms (curves of hearing sensitivity) have only been measured of few individuals of about 20 marine mammal species, and even fewer individuals and species of other marine genera. No audiograms exist for sperm whales or baleen whales. Behavioural responses likely depend on prior experience (habituation versus sensitisation), age, gender, health, context, current behavioural state etc., but we don't understand the details or mechanisms. Data on hearing loss and acoustic trauma is even scarcer. Finally, what is the biological significance of individual acoustic impacts? Environmental agencies and regulators struggle for data to support environmental management. Research on the impacts of underwater noise is being undertaken around the globe, but there is a substantial delay in publication and science transfer. In the face of uncertainty, what is being done? This article aims to provide a brief overview of underwater noise regulation in Australia and overseas. Regulations vary from country to country. Some jurisdictions use specific do-not-exceed thresholds, which are very broadly applied across differing species and environments, and sound sources. Others use more conceptual requirements such as 'minimising impact to acceptable levels', yet what this means has to be defined and demonstrated by each proponent for their specific situation (i.e., operation, environment and organisms). Furthermore, in many situations, multiple differing Acts and policies apply.

INTRODUCTION

The ocean is not a quiet place. It is naturally noisy with sounds from physical (wind, waves, rain, ice) and biological sources (whales, dolphins, fish, crustaceans etc.). Anthropogenic contribution to underwater noise has increased rapidly in the past century. In some parts of the world, low-frequency ambient noise has increased by 3.3 dB between 1950 and 2007, which was attributed to commercial shipping [1].

As ocean water conducts light very poorly but sound very well, many marine animals have evolved to rely primarily on their auditory system for orientation, communication, foraging and sensing their environment. For example, humpback whales (*Megaptera novaeangliae*) sing songs for hours to days. Killer whale (*Orcinus orca*) pods sharing the same geographic habitat have different dialects, and can be told apart from their calls. Odontocetes (toothed whales) use echolocation (active sonar) to navigate and forage. Fish and shrimp sing evening choruses. Coral larvae tune in to reef sounds for homing purposes.

Underwater noise can interfere with all of these functions on an individual yet ultimately population level. The effects of noise and the ranges over which they happen depend on the acoustic characteristics of the noise (level, spectral distribution, duration, duty cycle etc.), the sound propagation environment, and the characteristics of the acoustic receptor (the animal). Figure 1 shows a sketch of the potential zones of impact. These types of impact have been demonstrated in species of marine mammal and fish. As sound spreads through the ocean away from its source, the sound level decreases. At the longest ranges, a sound might barely be detectable. For

behavioural responses to occur, a sound would mostly have to be significantly above ambient levels and the animal's audiogram. However, avoidance at tens of km has been reported that was estimated to be at the limit of audibility in beluga whales (*Delphinapterus leucas*) [2].

Figure 1. Potential zones of bioacoustic impact around a noise source (red star).With increasing distance from the source, the impacts might include permanent or temporary hearing loss, communication masking and alterations of behaviour. All of these effects, including mere audibility, could induce stress.

Noise can mask communication, echolocation and the sounds of predators, prey and the environment. Masking

depends on the spectral and temporal characteristics of signal and noise [3]. The potential for masking can be reduced due to an animal's frequency and temporal discrimination ability, directional hearing, co-modulation masking release (if noise is amplitude modulated over a number of frequency bands) and multiple looks (if the noise has gaps or the signal is repetitive) [4], as well as anti-masking strategies (increasing call level, shifting frequency, repetition).

Auditory threshold shifts (hearing loss) can be either temporary (TTS) or permanent (PTS). Marine mammal TTS data have formed the basis for regulation of impulsive sounds in Germany [5] and the USA [6]. Noise—under certain circumstances—can affect non-auditory systems including the vestibular and nervous systems, can cause physical damage to tissues and organs, and can lead to concussion, cavitation, and stress. Pro-longed stress can cause health problems. Many of the discussed effects might be related, e.g. TTS affects audibility of a signal and thus alters the normal behavioural response of an animal. Or, noise received by a diving animal might induce stress leading to a flight response involving rapid surfacing that can cause decompression sickness or injury. How do temporary and individual impacts relate to population impacts? The Population Consequences of Acoustic Disturbance (PCAD) and Population Consequences of Disturbance (PCOD) models try to link noise characteristics to population effects [7]. While cumulative exposures from multiple sources over large geographic scales and long durations can be modelled fairly easily and reliably [8-10], we do not yet understand how acoustic exposures integrate in terms of impact. And finally, acoustic stressors can "add" synergistically to non-acoustic stressors such as light, chemical pollution, food depletion etc.

Given that data on bioacoustic impact is mostly limited to short-term individual responses, management of underwater noise is focussed on specific events limited in space and time. An animal, however, would experience multiple separate events along its migration, for example. A more holistic approach is needed, but complicated by a lack of information on cumulative impacts, the impracticability of managing multiple events separated in space and time, and the involvement of multiple jurisdictions.

Low-frequency (< 100 Hz) sound, in particular, can cross entire ocean basins. Noise that originates in one country or jurisdiction travels into neighbouring jurisdictions, making its regulation an international affair. Ocean noise can legally be treated as a "transboundary pollutant" [11] - "transboundary" because it crosses boundaries between jurisdictions, and "pollutant", because it fits the United Nations Convention on the Law of the Sea (UNCLOS) definition of marine pollution, which can be a substance or energy released into the marine environment, and which may result in deleterious effects on marine life [12]. UNCLOS has been signed by 138 countries. A framework for a holistic approach to the management of underwater noise is established by some international agreements—specifically within Europe.

INTERNATIONAL AGREEMENTS

The most widely signed agreements relating to underwater noise are discussed below.

Marine Strategy Framework Directive (MSFD)

The MSDF [13] is a European initiative that considers a multitude of anthropogenic "stressors" and their potentially cumulative effects. Member States are requested to develop an ecosystem-based approach to the management of human activities, enabling a sustainable use of marine goods and services. The objective is to achieve and maintain "good environmental status" by 2020, measured by 11 descriptors, the 11th of which refers to underwater noise: "The introduction of energy, including underwater noise, must be at levels that do not adversely affect the marine environment." [14].

Three indicators for descriptor 11 were suggested in 2010, requiring 1) the registration of low- and mid-frequency (10 Hz – 10 kHz) impulsive sounds exceeding either a sound exposure level (SEL) of 183 dB re 1 μPa^2s @ 1m or a peak pressure level (SPLpk) of 224 dB re 1 μPa @ 1m, as well as the spatial and temporal distribution of such events; 2) the tracking and possibly limitation of the number of vessels equipped with sonar systems (50 - 200 kHz) in order to reduce potential impact on high-frequency cetaceans inhabiting coastal waters in the EU; and 3) the monitoring of continuous low-frequency sound with the aim of keeping the annual average ambient noise level in the 1/3 octave bands centred at 63 Hz and 125 Hz, as measured by a statistical representative set of observation stations, below the baseline values of the year 2012 or 100 dB re 1 μPa root-mean-square (rms). Noise mapping (through measurement and modelling) was further suggested to analyse noise budgets. A low-frequency level of <100 dB re 1 μPa rms is very ambitious and not achievable in areas of busy commercial shipping as demonstrated by Erbe et al.'s cumulative ship noise model [9]. The original indicators were refined in 2012 [15] requiring member states to register any impulsive events that "are likely to entail significant impact on marine animals", in terms of both SEL and SPLpk, and to monitor trends in ambient noise in two 1/3 octave bands centred at 63 and 125 Hz. All target levels were removed, as was the suggestion to register sonar systems.

HELCOM

The Helsinki Commission (HELCOM) aims to protect the marine environment of the Baltic Sea from all sources of pollution through intergovernmental co-operation involving Denmark, Estonia, Finland, Germany, Latvia, Lithuania, Poland, Russia, Sweden and the European Community. Project CORESET (2010-2013) is developing a set of core indicators to assess the effectiveness of the implementation of the Baltic Sea Action Plan and the above-mentioned MSDF. One indicator will relate to underwater noise and impacts on marine mammals and likely involve mapping of anthropogenic sound sources and modelling of cumulative noise levels. Under the LIFE+ Environment Policy & Governance programme, the European Commission is currently funding the Baltic Sea Information on the Acoustic Soundscape (BIAS) project to establish and implement standards and tools for the management of underwater noise, in accordance with the MSFD. Soundscape maps will be produced as part of a GIS-based planning tool, initially showing the underwater noise generated by commercial vessels and allowing the modelling of noise footprints of intermittent operations (e.g. pile driving

and underwater explosions). Standards will be developed for hardware sensors and data, as well as data recording and processing.

OSPAR Convention

OSPAR guides international cooperation on the protection of the marine environment of the northeast Atlantic. The OSPAR Commission includes 15 European countries and the European Commission, representing the European Union. The Commission recently reviewed the potential effects of man-made underwater sound on marine life and concluded that there was not enough scientific information to evaluate the effectiveness and adequacy of current measures for the protection of marine life, and called for more research on animal audition, behaviour and distribution, as well as man-made noise characteristics, distribution and budgets, and mitigation. A lack of standardisation of environmental impact assessments was noted [16]. Following suite to conclusions of the Quality Status Report 2010 and the Environmental Impact of Human Activities Committee, a drafting group under the lead of Germany and the UK is currently developing a proposal for OSPAR guidance on the environmental impacts of underwater noise and mitigation measures.

ASCOBANS

The Agreement on the Conservation of Small Cetaceans of the Baltic and North Seas (ASCOBANS) was signed by eight countries bordering the Baltic and North Seas and focused on bycatch rates, habitat deterioration and anthropogenic disturbances to small cetaceans [17]. ASCOBANS specifically requires that all parties address underwater noise. Regarding seismic surveys, operators are asked to time surveys outside of marine mammal presence, to reduce noise levels as much as possible, to monitor marine mammal presence, and to ensure no marine mammals are within short-range exclusion zones when operations commence. With regards to pile driving, operators are additionally asked to employ technical measures for sound absorption, and to employ measures for alerting marine mammals to the onset of pile driving (e.g., acoustic deterrence devices) [18].

ACCOBAMS

The Agreement on the Conservation of Cetaceans of the Black Sea, Mediterranean Sea and Contiguous Atlantic Area (ACCOBAMS) was signed by eight countries bordering these waters. While ACCOBAMS calls for research and monitoring, few explicit recommendations on noise mitigation have been released, apart from reductions in vessel speed, maintenance of propellers, timing of operations when marine mammals are less present, and noise reduction mechanisms [19].

International Convention on Migratory Species

116 countries, including Australia, signed this Convention. The draft resolution on adverse anthropogenic marine/ocean noise impacts on cetaceans and other biota (UNEP/CMS/Res.9.19/Rev.3/5 December 2008) urges Parties to undertake environmental assessments of underwater noise, adopt mitigation measures and develop guidelines by monitoring of ambient noise, studying the sources of noise, compiling a reference noise signature database, characterising sound propagation, studying bioacoustic impacts, and investigating the benefits of noise protection areas.

There is no shortage of international agreements, in particular within Europe, intending to protect marine ecosystems and recognising noise as an environmental stressor. However, there is no international agreement on the methods for protection. Guidelines and regulations are up to individual countries. Explicit guidelines have only been issued for certain operations, mostly pile driving and seismic surveying (both impulsive sound sources), primarily with regards to impacts on marine mammals—mostly cetaceans [20,21].

COUNTRY-SPECIFIC GUIDELINES

The following paragraphs provide examples of underwater noise regulation in countries with a more stringent approach. While specific requirements differ from country to country, the general approaches are similar and may involve:

The Source
- Source selection: Some countries stipulate that a (seismic) source with minimal practical power be used, or that alternative foundation techniques be used instead of pile driving of offshore wind-turbines.

Location & Timing
- Time/area closures: These are mostly applied to seismic surveys during seasons of whale breeding and calving in habitats with significant animal presence.

Operational Parameters
- Soft-start/ramp-up: Seismic surveys or pile driving are required to start at a low acoustic power, ramping up to full power over 20-40 minutes. The idea is to send a warning to animals allowing them to desert the area. There are currently no scientific results validating this concept. The Behavioral Responses of Australian Humpback Whales to Seismic Surveys (BRAHSS) study funded by the Oil and Gas Producers' (OGP) Joint Industry Program (JIP) is currently investigating the effectiveness of soft-starts.
- Use of vibratory pile driving instead of or at the beginning of impact pile driving.

Mitigation Equipment
- Bubble screens: Almost all European countries require bubble curtains to absorb and scatter some of the energy from impact pile driving.

Mitigation Procedures
- Safety zones: Real-time mitigation methods are implemented within a zone (radius) around the pile driving or seismic source. These could be shut-down zones close to the source, low-power zones at longer radii and mere observation zones at the longest radii.
- Marine mammal observers (MMO): Dedicated visual observers are required to monitor safety zones for animal presence.
- Pre-shoot survey: For commonly 30 minutes prior to operations, the observation zone is surveyed for marine animal presence. If none are detected during this time, operations can commence.

- Low-power and shut-down: If animals enter the corresponding zones, operations have to switch to low power or shut down. Operations can recommence once animals have left, and (depending on country) after an additional pre-shoot survey and/or soft-start.
- Passive acoustic monitoring (PAM): In addition to MMOs, PAM is recommended specifically for operations in poor visibility.

United Kingdom

The Joint Nature Conservation Committee (JNCC) released a pile driving protocol for minimising the risk of injury to marine mammals [22], and similar guidelines for seismic surveys [23]. The developer must determine what species are present when, and consider seasonal timing. The Best Available Technique (BAT) has to be employed within the constraints of commercial affordability and practicality. Hammer modifications, sleeving or muffling, as well as vibratory and gravity-based piling instead of percussive piling, might be necessary. Simultaneous visual and passive acoustic monitoring (PAM) is suggested during operations. There are requirements for marine mammal observer (MMO) and PAM operators' training and work schedules, location (viewing platform) and equipment. The size of the monitoring and mitigation zones is established during the environmental impact assessment and agreed with the regulator and is no less than 500 m, see Figure 2a. Piling should not be commenced during darkness or poor visibility (*e.g.*, fog or Sea State > 4). MMOs and/or PAM operators should monitor the mitigation zone for at least 30 minutes prior to piling. Piling should not begin if marine mammals are detected within the mitigation zone or until 20 minutes after the last visual or acoustic detection. A soft-start (i.e., gradual ramping up of piling power) period of at least 20 minutes is recommended. If an animal enters the mitigation zone during soft-start, the power should not be increased until the animal exists and remains outside of the zone for 20 minutes. Acoustic deterrent devices (ADDs) may be utilised if the effectiveness of candidate devices on the key marine mammal species can be demonstrated during the environmental impact assessment process.

After the end of the piling activity, a written report should be sent to the regulator including completed marine mammal reporting forms; date and location of the piling operations; a record of all occasions when piling occurred, including details of the duration of the pre-piling search and soft-start procedures, and any occasions when piling activity was delayed or stopped due to presence of marine mammals; details of watches made for marine mammals, including details of any sightings, details of the PAM equipment and detections, and details of the piling activity during the watches; details of any acoustic deterrent devices used, and any relevant observations on their efficacy; details of any problems encountered during the piling process including instances of non-compliance with the agreed piling protocol; and any recommendations for amendment of the protocol.
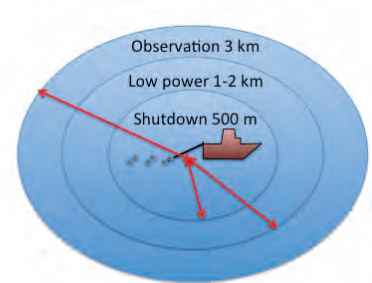
Figure 2. a) The mitigation radius, measured from the pile location, must not be less than 500 m [22]; b) Precaution zones surrounding the seismic airgun source (Australian EPBC Act Policy Statement 2.1).

Germany

The German Federal Government requires an exclusion zone of 750 m from pile driving for marine mammals. Measures must be employed by the operator to keep the received level at 750 m below a sound exposure value of 160 dB re 1 $\mu Pa^2 s$ and below a peak-to-peak sound pressure value of 190 dB re 1 μPa [24]. These levels were based on TTS measurements in a harbour porpoise after exposure to single impulsive signals [5], and were rounded down to allow for cumulative effects and intra-species variability. While this exclusion zone is intended to avoid TTS, behavioural effects are acknowledged to be likely. Temporal and spatial restrictions are additionally considered in critical habitats during seasons of high animal abundance.

United States of America

The Endangered Species Act (ESA) protects endangered species across the classes (including marine mammals). The National Marine Sanctuaries Act protects marine environments with special national significance based on conservation, recreational, ecological, historical, scientific, cultural, archaeological, educational or aesthetic qualities. The Marine Mammal Protection Act (MMPA) specifically protects marine mammals from anthropogenic noise. It is administered by the National Marine Fisheries Service (NMFS) and the Fish and Wildlife Service. The latter has jurisdiction over species such as manatees, polar bears, walrus and sea otters. NMFS has taken the more active role in issues related to underwater noise.

The MMPA defines 'take' as harassment, hunting, capture, killing or collection - or the attempt thereof. Under the 1994 Amendments to the MMPA, harassment is defined as any act of pursuit, torment or annoyance, that has the potential to injure (Level A Harassment) or to disturb (Level B Harassment) a marine mammal or stock in the wild. Level B Harassment includes the disruption of behavioural patterns, e.g. migration, breathing, nursing, breeding, feeding, or sheltering. Authorisation for incidental 'takings' may be granted by NMFS if the taking will have a 'negligible' impact on the animal populations, i.e. not affect annual rates of recruitment or survival. Notices of a proposed Incidental Harassment Authorization (IHA) are published by NMFS and public comments are considered in developing, if appropriate, IHAs.

NMFS' policy for pulsed sound is currently under review and requires that cetaceans and pinnipeds not be exposed to SPLrms > 180 and 190 dB re 1 µPa respectively [25], to prevent Level A Harassment. The threshold for Level B Harassment from pulsed sound is generally set at 160 dB re 1 µPa rms.

As an example, in 2008, the Port of Anchorage applied for and was granted an IHA to take, by Level B Harassment, up to 34 beluga whales (*Delphinapterus leucas*), 20 harbour seals (*Phoca vitulina*), 20 harbour porpoises (*Phocoena phocoena*), and 20 killer whales (*Orcinus orca*) during port expansion [26]. Level B Harassment was expected to consist of short-term, mild to moderate behavioural (altered headings, fast swimming changes in dive, surfacing, respiration and feeding patterns, and changes in vocalisations) and physiological responses (stress). Under the IHA, three years of sighting data around the Port had to be collected prior to construction yielding information on animal abundance, group size, group composition, and behaviour, from which expected monthly takes were calculated. Bubble curtains were considered for mitigation, however, due to strong currents were determined impractical. NMFS required that construction activities be scheduled during low presence of beluga whales. Pile driving was not to occur within two hours before and after low tide, as animal presence peaked during low tide. Through modelling and *in situ* transmission loss measurements, ranges to 160 dB re 1 µPa rms (Level B Harassment from percussive pile driving) and to 120 dB re 1 µPa rms (Level B Harassment from vibratory piling) were determined. NMFS imposed a 200 m shut-down zone for any single animal, and a 350 m shut-down zone for more than five beluga whales in a group or calves.

Piles had to be driven with a vibratory hammer to the maximum depth possible before switching to impact pile driving. A soft-start was employed: For vibratory piling, this meant 15 s at reduced energy followed by a 1-minute break, three times in a row. For impact pile driving, this meant three strikes at 40% energy followed by a 1-minute rest, then two subsequent three-strike sets. If an animal moved into the 200 m safety zone during the soft-start procedure, pile driving had to be delayed until the animal had left the zone or until it was not resighted within 15 minutes. The safety zone was monitored by trained observers 30 minutes prior to and during pile driving. Additional land-based MMOs recorded beluga behavioural responses to construction activities. Pile driving was not to occur if weather conditions prohibited adequate monitoring of the 200 m safety zone. Passive acoustic detection was required for validation of visual data and for monitoring noise exposures to be correlated with behavioural responses. For in-water heavy machinery operations other than pile driving (hydraulic excavators, clamshell equipment used to place or remove material, dump-scows, barges and tugs), if a marine mammal came within 50 m, operations would cease and vessels would slow down while still maintaining control of the vessel and safe working conditions. If the maximum authorised take was reached, any beluga entering into the Level B Harassment isopleth would trigger mandatory shut-down. Weekly monitoring reports had to be submitted to NMFS.

New Zealand

New Zealand does not have any policies for underwater noise exposure of marine fauna yet. A Code of Conduct for Minimising Acoustic Disturbance to Marine Mammals from Seismic Survey Operations was published in 2012 [27], and will be subject to an implementation performance review in 2015, prior to further consideration of mandatory regulations. The current code is neither legally binding nor enforceable. In general, marine seismic surveys should not happen in sensitive, ecologically important areas during key biological periods where species of concern are breeding, calving, resting, feeding or migrating. The lowest practicable power level for the seismic source should be used. The code considers three levels of seismic surveys. The Director-General must be notified of Level 1 & 2 surveys at least three months in advance. The proponent must prepare a Marine Mammal Impact Assessment (MMIA), describing the proposed activities, identifying all potential effects on marine species and habitats, and detailing an impact mitigation plan to reduce impacts to acceptable levels. Expert technical advice should be sought. While there is no formal approval process resulting in a consent, the Director-General will advise if the MMIA suffices or needs further mitigation measures. Where activities are planned in Areas of Ecological Importance or Marine Mammal Sanctuaries, sound propagation modelling must be included in the MMIA and ground-truthed during the course of the survey. If sound levels are predicted to exceed either 171 dB re 1 μPa^2s within the following mitigation zones for Species of Concern or 186 dB re 1 μPa^2s at 200 m, the mitigation zone might be extended. In addition:

1. Level 1 (source > 427 in^3): minimum of 2 MMOs and 2 PAM operators present at all times; pre-operation MMO and PAM survey of 30 minutes over mitigation zone; 20-40 minute soft-start; 1.5 km shut-down zone for Species of Concern with calves; 1 km shut-down zone for Species of Concern without calves; delayed start if Other Marine Mammal within 200 m

2. Level 2 (source 151-426 in^3): minimum of 2 MMOs present at all times; PAM optional; pre-operation MMO survey of 30 minutes over mitigation zone; 20-40 min soft-start; 1 km shut-down zone for Species of Concern with calves; 600 m shut-down zone for Species of Concern without calves; delayed start if Other Marine Mammal within 200 m

3. Level 3 (source < 150 in^3, sparkers, pingers, boomers): no specific mitigation zones

Requirements for minimum training and experience, and on-duty shift duration for both MMO and PAM observers exist. A written report on sightings must be submitted to the Director-General within two months after completion of the survey. While the code explicitly treats marine mammals, operators are strongly encouraged to consider and mitigate impacts on other key species (*e.g.* turtles, penguins, seabirds). Guidelines for borehole seismic surveys are similar depending on the acoustic source. The use of explosives is prohibited in New Zealand continental waters.

Australia

The National Offshore Petroleum Safety and Environmental Management Authority (NOPSEMA) came into effect on 1.1.2012 and is responsible for monitoring and enforcing compliance with the Offshore Petroleum and Greenhouse Gas Storage Act 2006 and (Environment) Regulations 2009 in Commonwealth waters. The Environment Regulations require that petroleum activities in Commonwealth waters be carried out in a manner consistent with the principles of ecologically sustainable development and in accordance with an accepted environment plan (EP). The operator must develop an EP for assessment and acceptance by NOPSEMA prior to operations [28]. The intent of the EP is to act not only as a regulatory compliance document, but also as a practical implementation and management tool to be used by operators in the field. The EP will describe the operations in enough detail to determine potential environmental risks and impacts. The EP will further describe the natural physical and biological environment, including any environmental receptors that may be affected by the proposed operations (both planned and unplanned), and spatiotemporal sensitivities (e.g. breeding and nesting seasons and habitats, animal migrations, spawning events). Consultations with stakeholders (people or organisations whose functions and interests may be affected by the operations) are required by the Regulations, might include workshops and should be ongoing. An operator may need to complete relevant studies to support the assessment and ongoing management of environmental impacts (literature reviews, biological surveys, modelling, specialist consultation etc.). The EP must establish management measures and demonstrate that any environmental risks and impacts are as low as reasonably practicable (ALARP) and at an acceptable level. Where uncertainty about impacts and likelihood exists, a precautionary approach should be adopted. The EP must have environmental performance objectives outlining the environmental goals of the operator, environmental performance standards stating the level of performance required of control measures, and measurement criteria that allow operators to measure if the objectives and standards were met during operations. The EP must include an implementation strategy and monitoring, recording and reporting arrangements that allow NOPSEMA to determine if the objectives and standards were met. Once NOPSEMA has accepted an EP, the operator must submit a summary for publication on the NOPSEMA website[1], where many examples of accepted EPs for various operations emitting underwater noise can be found.

Different from many other jurisdictions, these regulations do not prescribe a specific approach to environmental risk reduction (e.g. acoustic exposure thresholds); rather, operators are encouraged be flexible in their approach and employ innovative measures that are tailored to their specific circumstances. These regulations recognise that every situation (local environment, organisms, operations) is different and that no single approach (threshold or minimum standard) suits all situations and that what is "reasonably practicable" changes over time as technology, expertise and our understanding of environmental impacts evolve.

While NOPSEMA is responsible for Commonwealth waters, States and Territories are responsible for managing the marine environment within 3 nautical miles from the coast. An example of a mitigation and monitoring program to protect dolphins from pile driving impacts in State waters is given in [29].

Under the Environment Protection and Biodiversity Conservation (EPBC) Act 1999, the onus is on the operator to decide whether a proposal is likely to have an impact on a matter of national environmental significance and also needs to be referred to the Department of Sustainability, Environment, Water, Population and Communities (SEWPaC) for assessment and decision. The EPBC Act Policy Statement 2.1 (2008), published by SEWPaC (formerly DEWHA), provides standards and a framework designed to minimise the risk of acoustic impacts to whales (baleen whales and large toothed whales) from marine seismic operations. Seismic surveys should be planned outside of whale breeding, calving, resting or feeding habitats and times. Thirty-minute pre-operation visual observation, 30-minute soft-start, start-up delay if whales are sighted within the low-power zone, ongoing visual observation during operations, and power-down or shut-down if a whale is sighted within the low-power or shut-down zone are required irrespective of location and time of year of survey. Passive acoustic monitoring is recommended in addition to visual observation, specifically during low visibility. This policy statement requires the computation of the SEL from single emissions at 1 km range. If SEL > 160 dB re 1 $\mu Pa^2 s$ for 95% of the time, an observation zone of 3 km, a low-power zone of 2 km and a shut-down zone of 500 m are imposed (Figure 2b). Else, these zones are 3 km, 1 km and 500 m respectively. Time/area closures are imposed in the Great Australian Bight during winter (right whale breeding & calving). The requirements of the policy are often applied as Conditions of Approval by SEWPaC on seismic and other petroleum activities. There are no policy statements for smaller dolphins and porpoises; and none for sources other than seismic airguns.

DISCUSSION

Regulation and enforcement are handled differently from country to country. In fact, even within the same country, different states or jurisdictions regulate noise differently. Political boundaries are meaningless to animals; migratory species experience sequential exposures, and impacts might "accumulate". The United Nations Environmental Programme called for an international approach to research and regulation of anthropogenic noise effects on marine mammals as early as 1985 [30]. The International Maritime Organization (IMO) urged the "development of globally uniform regulations rather than a proliferation of diverse regional or local standards" [31]. There are regional directives involving multiple countries, in particular in the European Union, providing a framework for potentially more "holistic" management. Most of these

---

[1] http://www.nopsema.gov.au/environmental-management/environment-plans/environment-plan-summaries/

directives stipulate that marine ecosystems must be protected, but do not specify how, and often conclude in a call for further investigation. It is up to each country to interpret and act upon these directives, leaving us with disjoint and disparate management.

Tangible guidelines based on sound science, and effective measures by which noise impact can be mitigated would help, but are still lacking. This is partly because scientific research is still needed on biological impacts and the significance thereof, and partly because of a lack of standards in underwater noise measurement, analysis and reporting. Also, one number is not going to fit all situations (i.e., populations, environments and operations). Rather, guidelines would have to be multivariate and allow for different measures in different circumstances. A large amount of data is needed to tailor guidelines. Based on the author's experience with offshore petroleum projects, the number of, the size of and hence the cost of environmental impact assessments seems to be steadily increasing, yet without an apparent increase in quality or effectiveness. Humungous amounts of data are often collected in these environmental noise monitoring and impact mitigation programs, but do not flow into the public domain and hence do not advance our understanding—a loss to both science and the environment.

REFERENCES

[1] G. Frisk, "Noiseonomics: The relationship between ambient noise levels in the sea and global economic trends", *Scientific Reports* **2**, 437 (2012)

[2] C. Erbe and D.M. Farmer, "Zones of impact around icebreakers affecting beluga whales in the Beaufort Sea", *Journal of the Acoustical Society of America* **108**(3), 1332-1340 (2000)

[3] C. Erbe and D.M. Farmer, "Masked hearing thresholds of a beluga whale (*Delphinapterus leucas*) in icebreaker noise", *Deep-Sea Research Part II* **45**(7), 1373-1388 (1998)

[4] C. Erbe, "Critical ratios of beluga whales (Delphinapterus leucas) and masked signal duration", *Journal of the Acoustical Society of America* **124**(4), 2216-2223 (2008)

[5] K. Lucke, U. Siebert, P.A. Lepper and M.-A. Blanchet, "Temporary shift in masked hearing thresholds in a harbor porpoise (*Phocoena phocoena*) after exposure to seismic airgun stimuli", *Journal of the Acoustical Society of America* **125**(6), 4060-4070 (2009)

[6] B.L. Southall, A.E. Bowles, W.T. Ellison, J.J. Finneran, R.L. Gentry, C.R.J. Greene, D. Kastak, D.R. Ketten, J.H. Miller, P.E. Nachtigall, W.J. Richardson, J.A. Thomas and P.L. Tyack, "Marine mammal noise exposure criteria: Initial scientific recommendations", *Aquatic Mammals* **33**(4), 411-521 (2007)

[7] National Research Council, *Marine Mammal Populations and Ocean Noise: Determining when noise causes biologically significant effects*, National Academies Press, Washington, 2005

[8] C. Erbe and A.R. King, "Modeling cumulative sound exposure around marine seismic surveys", *Journal of the Acoustical Society of America* **125**(4), 2443-2451 (2009)

[9] C. Erbe, A.O. MacGillivray and R. Williams, "Mapping cumulative noise from shipping to inform marine spatial planning", *Journal of the Acoustical Society of America* **132**(5), EL 423-428 (2012)

[10] C. Erbe, "Modeling cumulative sound exposure over large areas, multiple sources, and long durations", in: A.N. Popper, A.D. Hawkins (Eds.), *The Effects of Noise on Aquatic Life. Advances in Experimental Medicine and Biology 730*, Springer Verlag, New York, 2012, pp. 477-479

[11] E. McCarthy, *International Regulation of Underwater Sound: Establishing Rules and Standards to Address Ocean Noise Pollution*, Kluwer Academic Publishers, Boston, 2004

[12] United Nations Division for Ocean Affairs and the Law of the Sea, *United Nations Convention on the Law of the Sea (UNCLOS)*, 1982

[13] European Parliament, "Directive 2008/56/EC of the European Parliament and of the Council of 17 June 2008 establishing a framework for communicity action in the field of marine environmental policy (Marine Strategy Framework Directive)", *Official Journal of the European Union* **L 164**, 19-40 (2008)

[14] M.L. Tasker, M. Amundin, M. Andre, A.D. Hawkins, W. Lang, T. Merck, A. Scholik-Schlomer, J. Teilman, F. Thomsen, S. Werner and M. Zakharia, *Marine Strategy Framework Directive*: Task Group 11 Report: Underwater noise and other forms of energy, JRC Scientific and Technical Report No. EUR 24341 EN - 2010, European Commission and International Council for the Exploration of the Sea, Luxembourg, 2010

[15] A.J. van der Graaf, M.A. Ainslie, M. Andre, K. Brensing, J. Dalen, R.P.A. Dekeling, S. M. Robinson, M.L. Tasker, F. Thomsen and S. Werner, *European Marine Strategy Framework Directive - Good Environmental Status (MSFD GES)*: Report of the Technical Subgroup on Underwater noise and other forms of energy, JRC Scientific and Technical Report, TSG Noise & Milieu Ltd., Brussels, 2012

[16] OSPAR Commission, *Overview of the impacts of anthropogenic underwater sound in the marine environment*, OSPAR Report No. 441, London, UK, 2009

[17] Marine Mammal Commission, *The marine mammal commission compendium of selected treaties, international agreements, and other relevant documents on marine resources, wildlife, and the environment: Agreement on the conservation of small cetaceans of the Baltic and North Seas (1992)*, Washington, DC, 1994

[18] ASCOBANS Secretariat, *Adverse effects of underwater noise on marine mammals during offshore construction activities for renewable energy production*, Resolution No. 2, Bonn, Germany, 2009

[19] G.N. di Sciara, *Cetaceans of the Mediterranean and Black Seas: State of knowledge and conservation strategies*, Report to the ACCOBAMS Secretariat, Monaco, 2002

[20] C.R. Weir and S.J. Dolman, "Comparative review of the Regional Marine Mammal Mitigation Guidelines implemented during industrial seismic surveys, and guidance towards a worldwide standard", *Journal of International Wildlife Law & Policy* **10**, 1-27 (2007)

[21] R. Compton, L. Goodwin, R. Handy and V. Abbott, "A critical examination of worldwide guidelines for minimising the disturbance to marine mammals during seismic surveys", *Marine Policy* **32**(3), 255-262 (2008)

[22] Joint Nature Conservation Committee (JNCC), *Statutory nature conservation agency protocol for minimising the risk of injury to marine mammals from piling noise*, Aberdeen, UK, 2010

[23] Joint Nature Conservation Committee (JNCC), *Guidelines for minimising the risk of injury and disturbance to marine mammals from seismic surveys*, Joint Nature Conservation Committee, Aberdeen, UK, 2010

[24] S. Werner, Towards a precautionary approach for regulation of noise introduction in the marine environment from pile driving, Federal Environment Agency, Stralsund, (2010)

[25] National Marine Fisheries Service (NMFS), *Environmental Assessment on the effects of controlled exposure of sound on the behaviour of various species of marine mammals*, Silver Spring, Maryland, USA, 2000

[26] National Marine Fisheries Service (NMFS), "Small Takes of Marine Mammals Incidental to Specified Activities; Port of Anchorage Marine Terminal Redevelopment Project, Anchorage, Alaska", *Federal Register* **73**(139), 41318-41330 (2008)

[27] New Zealand Department of Conservation, *Code of conduct for minimising acoustic distrubance to marine mammals from seismic survey operations*, Department of Conservation, Wellington, New Zealand, 2012

[28] National Offshore Petroleum Safety and Environmental Management Authority (NOPSEMA), *Environment Plan Preparation*, Guidance Note No. N-04700-GL0931 Rev. 0, NOPSEMA, 2012

[29] C. Erbe, "Underwater noise from pile driving in Moreton Bay, Qld", *Acoustics Australia* **37**(3), 87-92 (2009)

[30] United Nations Environmental Programme, Marine Mammals: Global Plan of Action , *UNEP Regional Seas Reports and Studies* **55** (1985)

[31] International Maritime Organization, *International Maritime Organization Resolution* A.927(22), 2001

THEME

ACOUSTICS 2013, the annual conference of the Australian Acoustical Society, will be held in Victor Harbor, South Australia, at the McCracken Country Club, from 17-20 November 2013.

With its theme of Science, Technology and Amenity, Acoustics 2013 Victor Harbor will include plenary sessions addressing the impact of science and technology on acoustics and amenity, whether it be environmental or internal spaces. Other major streams will address airport / road / railway noise, standards and guidelines including those from EPAs, underwater acoustics, marine bioacoustics and vibration.

Acoustics 2013 Victor Harbor will provide in-depth coverage of many topics of interest to professionals in related fields including educationalists, consultants, planners, developers, government authorities, and EPA/noise officers

VENUE

Acoustics 2013 Victor Harbor will be held at the McCracken Country Club. The 4.5 star McCracken Country Club offers guests luxurious accommodation in the beachside township of Victor Harbor. The country club highlights are its golf course, day spa and the gorgeous panoramic view of Hindmarsh Valley. Visit www.countryclubs.com.au/mccracken/

TOPICS

In addition to the main conference themes, Acoustics 2013 Victor Harbor will include sessions on:

• Environmental acoustics
• Industrial acoustics
• Wind turbine noise
• Low frequency noise
• Internal spaces and amenity
• Architectural acoustics
• Underwater acoustics
• Marine bioacoustics
• Legislation and standards
• Transportation noise

WORKSHOPS

A series of workshops are planned. The following workshop will be held:

• Flow induced noise

For up-to-date information regarding the Acoustics 2013 Victor Harbor conference, please visit the conference website: www.acoustics.asn.au/joomla/acoustics-2013.html
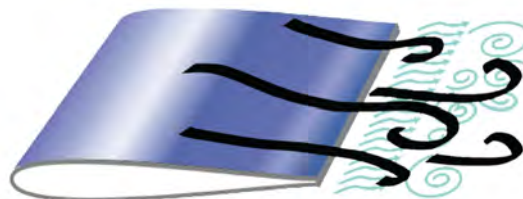
INVESTIGATION OF UNDERWATER ACOUSTIC MULTI-PATH DOPPLER AND DELAY SPREADING IN A SHALLOW MARINE ENVIRONMENT

Michael Caley and Alec Duncan

Curtin University, Department of Imaging and Applied Physics, Centre for Marine Science and Technology, Perth, Australia
michaelcaley@westnet.com.au

Doppler frequency spreading and arrival delay spreading of underwater acoustic communication signals under the influence of surface waves and transmitter-receiver motion were investigated in a channel probing experiment conducted primarily with binary pseudo-noise (PN) sequences ranging from 21ms to 1.4s duration. Testing was conducted in a 13.5m deep environment at transmission distances ranging from 44m to 1007m. The channel Doppler response was investigated both by time-domain Doppler search of the transmit-receive correlation for successive repeats of a 1.4s probe sequence, and by Fourier analysis of the channel impulse response history from a repeated 21ms probe sequence (i.e. Spreading Function). The bounds of Doppler shift imparted by relative transmitter/receiver motion and surface wave motion to idealised sound-ray transmission paths has been compared with experimental Doppler indicated by the Spreading Function. The coherence of the experimental channel response was also examined for different propagation ranges and at different delayed arrivals of the experimental signals.

INTRODUCTION

The choice for the wireless transmission of data underwater is between electromagnetic waves (e.g. light or radio) or sound waves. Light and radio waves are valuable for high-rate data transmission through water over short ranges of the order of a few metres. When transmission is required over longer distances through water, sound waves are the only viable wireless option.

Underwater acoustic data transmission is not without significant constraints intrinsic to the marine environment. The underwater acoustic environment is highly reverberant, resulting in multiple reflected copies of any transmitted signal arriving at the receiver at delayed intervals (delay spreading), and with the relative delays generally changing with time. The frequency of transmitted signals is also significantly distorted by transient Doppler effects generated by elongation and contraction of surface reflected transmission paths (Doppler frequency spreading), or Doppler frequency shifts from movement of either (or both) the transmitter and receiver. Transient delay spreading and Doppler spreading of the received signal present significant challenges to the decoding of incoming data symbols by a communications receiver, with the problem becoming more difficult as the rate of data transmission increases.

In 2011 the Department of Electrical and Computer Engineering and the Centre for Marine Science and Technology (CMST) at Curtin University commenced a project to develop high-rate underwater acoustic communications to support developing ocean-based industries in Australia [1]. The authors' role is to develop an underwater acoustic communication channel simulator to support this project. The purpose of the simulator is to simulate the way that the real ocean produces transient distortion of acoustic communication signals between a transmitter and a receiver, including interference effects from highly variable natural and anthropogenic noise. The simulator provides a configurable analogue of the real ocean that can be used to improve understanding of the influence of the marine acoustic environment on communications signals, and assists the development of underwater communication modulation and demodulation algorithms and hardware.

Transient phenomena that are key to the development of an acoustic channel simulator for high-rate data communications are the transient delay and Doppler frequency spreading of the received signal imparted by the moving sea-surface, shown schematically in Fig. 1, and the transient Doppler imparted by moving transmitter and/or receiver platforms [2,3].
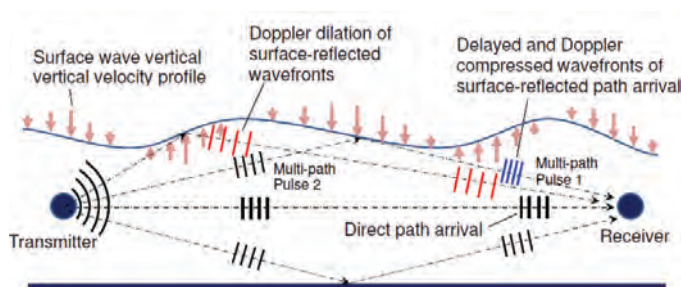
Figure 1. Conceptual signal Doppler shift and path delay

Experimental channel probing was conducted primarily with binary pseudo-noise (PN) sequences ranging from 21ms to 1.4s duration. The signal was created by phase-modulating a continuous 12kHz sinusoid with the binary sequence. This method is described in communication literature as Direct Sequence Spread Spectrum (DSSS) signalling.

In this investigation the channel Doppler response to probe

signals was investigated both by a time-domain resampling Doppler search method on successive transmit-receive (txrx) PN sequence blocks, and also by Fourier analysis of the channel response with respect to time, to generate the frequency-domain Doppler Spreading Function.

It is customary to present the channel Doppler axis of the Spreading Function $S(\tau,f)$ in the units of Hz. $S(\tau,f)$ was calculated in Eq. (1) by discrete Fourier analysis of the channel response $h(\tau,t)$.

$$S(\tau,f) = \sum_{n=N-1}^{n=0} h(m,n)\exp\left(-\frac{i2\pi np}{N}\right) \qquad (1)$$

$S(\tau,f)$ was calculated from $N = 1400$ impulse responses $h(\tau,t)$ spaced in the time (t) dimension at intervals $T = 21$ms, with time $t = nT$. The impulse response in the delay dimension (τ) was calculated from sampling at frequency $f_s = 96$kHz, with response delay $\tau = m/f_s$ and Doppler frequencies $f = p/NT$ where $p \in [-N/2+1,...,N/2]$.

When the complex channel response $h(\tau,t)$ is determined by cross-correlation of a modulated transmit and receive signal, the rate at which the phase of $h(\tau,t)$ changes with respect to time (t) is scaled by the probe signal carrier frequency (f_0). Accordingly the Doppler shift spectrum at each delay (τ) calculated by DFT of $h(\tau,t)$ is also scaled by the probe signal carrier frequency.

For a physical layer modeller it is helpful to note that the Doppler shift derived by (1) is responsive to $h(\tau,t)$ phase changes originating not only from Doppler phase compression/dilation, but also from what will be described as 'apparent' Doppler due to phase changes associated with transient phase interference of clustered multipath arrivals, and transient angular scattering of propagation paths by a moving sea surface [4].

The channel Doppler response may be expressed either as an equivalent velocity shift δv or as an equivalent signal-dependent frequency shift δf as linked by Eq. (2), where positive δv represents an equivalent velocity shift that contracts the propagation path length and c is the speed of sound in water.

$$\delta f(f_0) = \delta v/c \qquad (2)$$

In this paper the measured channel Doppler response has generally been reported as a frequency shift (Hz), but in the case of Spreading Function plots a secondary axis with Doppler velocity shift was added to enable comparison with Doppler velocity shift estimates from geometrical considerations.

CHANNEL PROBING TESTS

A shallow (13.5m) channel probing experiment was conducted in April 2012 over distances ranging from 44m to 1007m. The transmitter and receiver arrangements are illustrated in Figs. 2 and 3, respectively. The transmitter was inverted (relative to conventional vertical downwards primary axis alignment) to maximise the signal strength for surface reflected transmission paths.
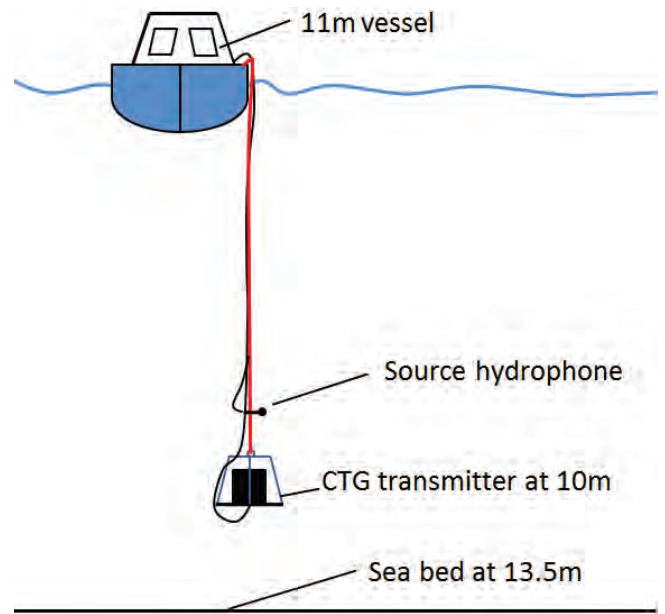
Figure 2. Transmitter configuration
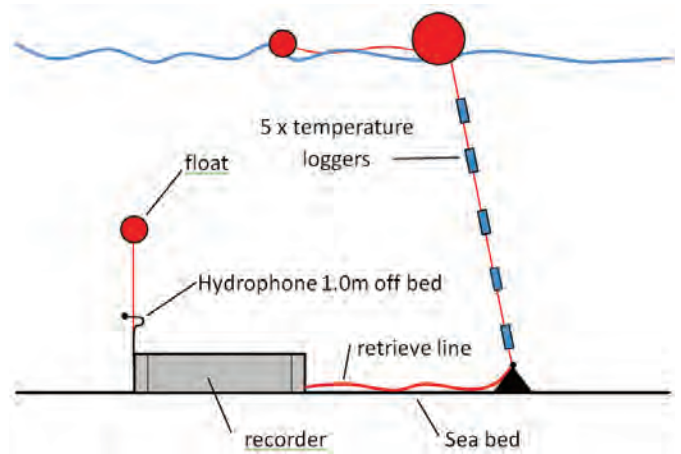
Figure 3. Receiver configuration

Experimental arrangement and instrumentation

Transmitted and received signals were sampled with 24 bit resolution at 96kHz. Directional surface wave data was obtained from a Directional Wave Rider Buoy (DWRB) located approximately 1.5km NE of the receiver. The sound-speed profile at each site was sampled with a Conductivity Temperature Depth (CTD) probe. The vessel was fitted with pitch, heave and roll data acquisition sampling at 100Hz. Five temperature loggers sampling at 60 second intervals were suspended from the surface float line. Grab samples were collected of the sandy bottom material.

Probe signals

Probe signals for simultaneous Doppler shift and delay detection consisted of a 12kHz continuous wave (CW) carrier modulated at a 3kHz chipping rate by binary phase pseudorandom (PN) sequences. The longer temporal effects

associated with wave and swell were explored by continuing the sequence repetitions over an interval greater than the swell period. A repeated pattern was transmitted consisting of 60s of 1.4s PN sequence (n-bits = 4095), 30s of 170ms PN sequence (n-bits = 511) and 30s of 21ms PN sequence (n-bits = 63). This was followed by 30 repeats of a 16ms 8kHz-16kHz linear frequency sweep at 1s intervals. The sweeps were utilised to provide an unambiguous check on the channel delay spread and structure.

The bandwidths of trial signals were guided by the ±3dB transmit sensitivity of the Chelsea Technologies CTG052 transmit transducer. Signals were written to a 24 bit wav file then replayed on a digital audio player with output amplification to the transmitter.

Doppler and delay resolution – single block processing

The delay resolution δ_t of multi-path arrivals for a PN probe signal is determined by the sequence chipping interval t_{chip} as per Eq. (3). For a linear frequency sweep, δ_t is the inverse of the maximum sweep frequency.

$$\delta_t = \frac{t_{chip}}{2} \qquad (3)$$

The Doppler velocity shift resolution δ_v for a PN sequence probe signal depends on the sequence repeat interval T and the signal carrier frequency f_0 as per Eq. (4) where c is the speed of sound. For a linear frequency sweep, f_0 is replaced by the maximum sweep frequency.

$$\delta_v = \frac{c}{f_0 T} \qquad (4)$$

The probe signal frequencies, repeat intervals, bandwidths and associated delay and Doppler resolutions are detailed in Table 1.

Table 1. Trial test signals

Signal type	f_0 (kHz)	Period T (s)	Chipping rate	δ_t (ms)	δ_v (m/s)
PN	12	1.4	3	0.16	0.094
PN	12	0.17	3	0.16	0.75
PN	12	0.021	3	0.16	6.1
Sweep	8-16	0.016	-	0.06	6.0

Doppler resolution – 21ms ensemble block processing

The Doppler velocity resolution of the Spreading Function from the 21ms probe impulse response history is also calculated by Eq. (4), but with T evaluated with the block ensemble duration of 30s. The resultant Doppler resolution is 0.0043m/s, or 0.033Hz, with Nyquist frequency of 23.8Hz.

Test sea conditions

The water column was well mixed during testing with the sound speed ranging almost linearly from 1537m/s at the surface to 1536m/s at the bottom. Wind conditions were light to still, with low swell and sea conditions reported at 15 minute intervals from the nearby (1.5km distant) Cottesloe Directional Wave Rider Buoy (DWRB) as summarised in Table 2. The appearance of the sea surface during testing is illustrated in Fig. 4. It is notably free of surface bubbles.

Table 2. Wave height data for presented results

Wave type	Significant height H_s	Wave period T_m	Wave frequency
Swell	0.4m	13-14s	0.07Hz
Sea	0.25m	3s	0.33Hz

Figure 4. Experimental sea surface

IDEALISED CHANNEL DELAY STRUCTURE

The arrival delay structure for an idealised ocean waveguide with specular surface and bottom reflections and constant sound speed shown schematically in Fig. 5 is graphed in Fig. 6 to assist with the interpretation of the measured delay structure. 'B' stands for a bottom-bounce, and 'S' a surface-bounce. It may be noted that at increasing ranges the time separation between delays becomes less than the delay resolution of test signals listed in Table 1.
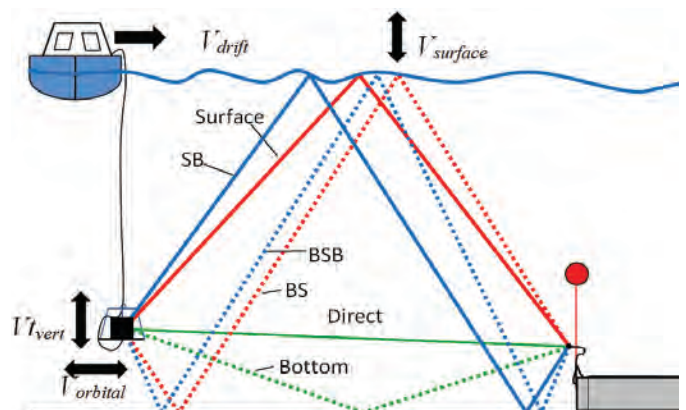
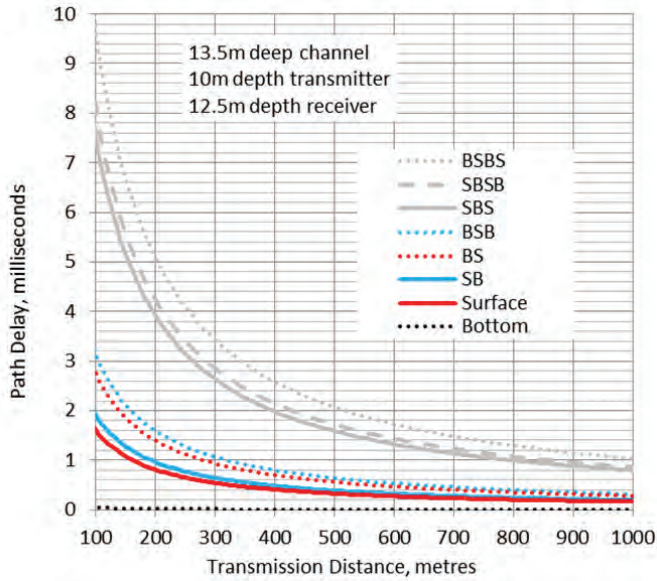

Figure 5. Low order reflected paths

Figure 6. Idealised delay structure of reflected paths relative to the direct path

DOPPLER CONTRIBUTIONS FROM RELATIVE MOTION

The primary geometrical sources of relative motion that contribute to the experimental Doppler shift are sea-surface motion, wave orbital motion coupling to the suspended transmitter, and transmitter movement generated by vessel rolling and drift as illustrated in Fig. 5. These components were resolved into the idealised acoustic transmission paths, then combined to provide a Doppler velocity shift interpretation of the Doppler effect indicated by the experimental Spreading Function.

The slow-changing contributions (drift and swell orbital motion) have been treated as constant values, whereas the rapidly changing stochastic Doppler velocity contributions from sea-surface reflections and vertical transmitter oscillation have been quantified as 3σ estimates where σ is the standard deviation. Successive surface reflections and vertical transmitter oscillations have been treated as independent processes. Only the vertical motion of surface reflections has been considered. The more complex horizontal surface-wave velocity components are not considered.

Vessel drift closing speed

The average closing speed V_{drift} was calculated from GPS data for the vessel drift. This speed ranged from 0.11m/s to 0.19m/s for the data presented. This relative motion contributes almost the same Doppler shift to all transmission paths as per Eq. (5), where θ is the path launch angle from horizontal.

$$V_d = V_{drift} \cos\theta \tag{5}$$

Transmit-receive motion coupled to orbital wave motion

The cable tether of both the transmitter (tx) at 10m depth and the receiver (rx) hydrophone 1m off the bottom make both susceptible to orbital wave motion, however the movement of the receiver hydrophone would be limited compared to that of the transmitter. At the depth of the transmitter the horizontal component of swell orbital motion is significant in the shallow test channel, with the contribution from wind-waves not extending below mid-depth. If it is conservatively assumed that the transmitter is completely compliant horizontally, the relative horizontal orbital motion $V_{orbital}$ is calculated at up to 0.17m/s for the Table 2 data. This relative motion contributes almost the same Doppler to all transmission paths as per Eq. (6).

$$V_o = V_{orbital} \cos\theta \tag{6}$$

Surface vertical velocity

The maximum vertical surface velocity $V_{surface}$ at the point of surface reflections was estimated based on the 3σ wave height for swell and sea by Eq. (7), providing estimates of 0.39m/s for the $H_s = 0.25$m sea-waves, and 0.13m/s for the $H_s = 0.4$m swell. The higher estimate obtained from the wind-waves was utilised as an upper bound estimate of $V_{surface}$. The vertical surface motion from a single surface reflection can be resolved in the direction of an idealised surface-reflected path as per Eq. (8).

$$V_{surface} = 3\pi H_s / 2T_m \tag{7}$$

$$V_s = 2V_{surface} \sin\theta \tag{8}$$

Vertical transmitter motion

The vertical velocity spectral density of the transmitter in Fig. 7 was calculated from the combined vessel pitch, heave and roll data by averaging 18 x 160s blocks of data with Hamming windowing. This data shows a peak at 0.07Hz that corresponds to the DWRB swell data, and peaks at frequencies similar to the DWRB data for wind-driven surface waves. These higher frequency peaks were likely influenced by the resonant pitch and roll frequencies of the vessel. The vertical root-mean-square (RMS) velocity from the data in the 0-2Hz range was 0.13m/s, providing a 3σ estimate of 0.39m/s for this component.
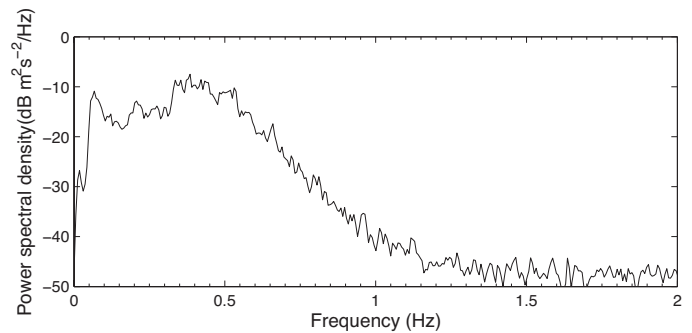

Figure 7. Transmitter vertical velocity power spectrum

The vertical transmitter velocity Vt_{vert} can be resolved in the direction of all surface and/or bottom reflected transmission paths as per Eq. (9).

$$V_t = Vt_{vert} \sin\theta \qquad (9)$$

Combination of geometrical Doppler velocity components resolved in path

An estimate of the 3σ total in-path Doppler shift for a path involving n_b surface bounces was calculated from components assuming independence of stochastic processes as per Eq. (10).

$$V_{total} = V_d + V_o + \sqrt{V_t^2 + n_b V_s^2} \qquad (10)$$

Figure 8. 3σ estimates of maximum geometrical Doppler velocity shifts resolved along idealised paths for path delays < 10ms

The geometrical Doppler components discussed in previous sections are compared in Fig. 8 for all idealised ray paths within 10ms delay relative to the direct path, for the example test distances of 110m, 500m, 1007m. The experimental txrx drift rate varied at each distance. Records of wave conditions from the nearby DWRB were comparable for all transmission ranges. This analysis indicates that the potential maximum in-path Doppler shift increases significantly with the number of surface bounces at short range, with the vertical surface Doppler delay per surface bounce diminishing with range.

It is noted that the test results relate to relatively low experimental surface wave heights as per Table 2. Sea and swell are commonly 4-5 times higher at the test site which would lead to all related Doppler velocity components increasing commensurately.

EXPERIMENTAL DELAY RESULTS

The transmit-receive correlation versus delay histories are presented for 110m, 500m and 1007m transmit ranges in Figs. 9-11. The correlation response for each time block was normalised by the product of the transmit and receive signal power. The plots are the absolute value of the correlation R, so do not reveal the phase changes occurring in R with time.

Successive block impulse responses were aligned on the first correlation maxima (with a 0.01ms numerical time step), without resampling to adjust for cyclical Doppler shift from txrx movement. Consequently the resultant channel response history will include distortion of the delay between the first maxima and subsequent arrivals due to this txrx relative movement. However the magnitude of this delay distortion is less than 0.01ms, less than a tenth of the delay resolution for the experimental probe signal. It is concluded that the 'approximate' delay history obtained in this manner is reliable.

The correlation results from 16ms frequency sweeps at 1s intervals (not shown) were used to check on the delay structure out to 60ms, confirming that the 10ms delay structure revealed by the 21ms probe sequence contains the significant arrivals for this channel.

Utilising the idealised delay structure in Fig. 6 for 110m range for reference, the first correlation maximum in Fig. 9 represents the combined direct and bottom-reflected paths, with the second group of arrivals extending between 1ms and 3ms corresponding to Surface, BS, SB and BSB reflected paths. The next group of arrivals for paths involving two surface reflections are apparent between 6ms and 10ms.

At 500m range (Fig. 10) the contracting of the delay spread is apparent with two additional bands of higher order surface reflections evident. The results at this range are notable as the first correlation maximum is suppressed relative to the second as a consequence of destructive phase interference between the Direct and Bottom paths. In this channel the Surface, SB, BS and BSB paths combine to provide a stronger arrival, but with interruption at intervals matching the swell period, presumably relating to destructive interference associated with differential path elongation/contraction.

At 1007m range the relative phases of the Direct, Surface and Bottom bounce again combine constructively to produce a strongest first correlation maximum.
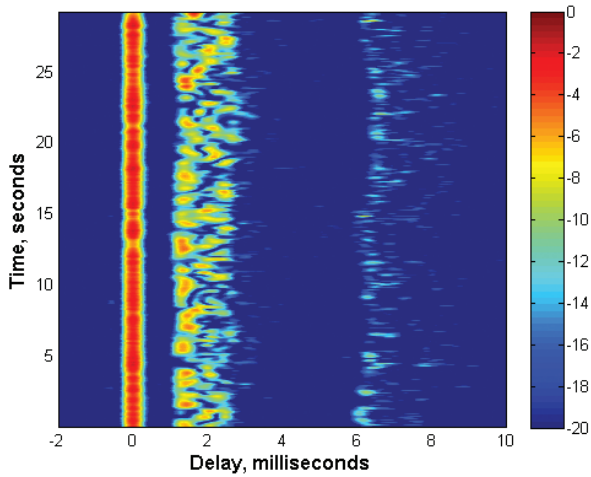
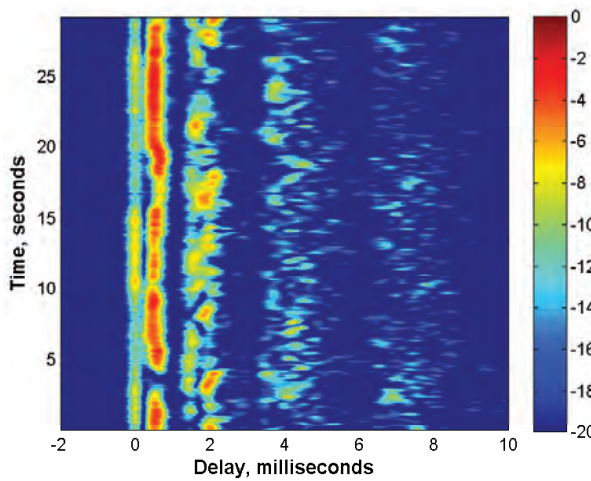Figure 9. Normalised txrx correlation history (dB)–21ms PN sequence @ 110m

Figure 10. Normalised txrx correlation history (dB)–21ms PN sequence @ 500m
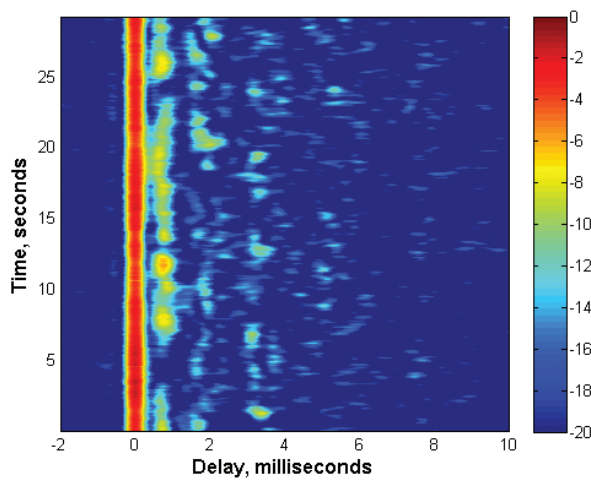

Figure 11. Normalised txrx correlation history (dB)–21ms PN sequence @ 1007m

EXPERIMENTAL DOPPLER SHIFT RESULTS

Spreading Function Doppler Shift Indication

The Spreading Functions corresponding to the 110m, 500m and 1007m ranges are presented in Figs. 12-14. The Spreading Functions are over-plotted with white markers representing the 3σ Doppler estimates from geometrical consideration as per Fig. 8, making use of the correspondence between Doppler frequency shift and velocity shift in Eq. (2). The corresponding delays of the white markers relate to an idealised waveguide with parallel boundaries. In reality the delays will vary with the path elongation and contraction associated with vertical surface movement, and with the moving reflection position linked to travelling surface waves. The variation in actual delay of surface-interacting paths is indicated by the substantial delay-spreading (x-axis) evident in the Spreading Function compared to the idealised discrete delay points.
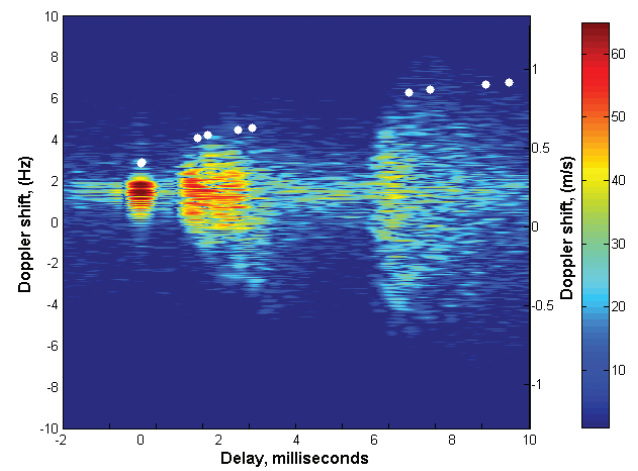

Figure 12. Spreading Function (dB) with 3σ geometrical Doppler estimates @ 110m
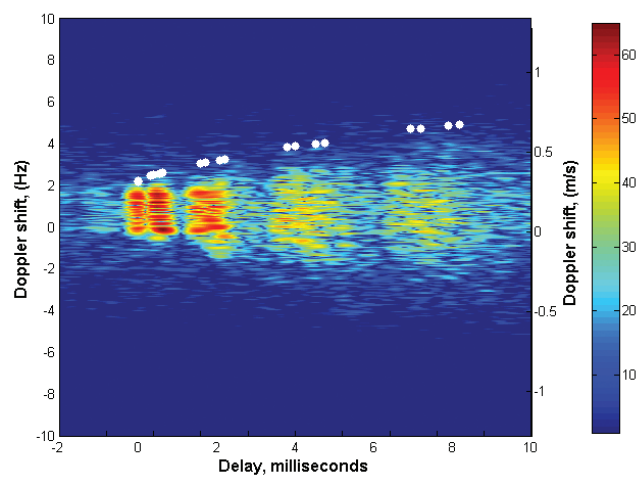

Figure 13. Spreading Function (dB) with 3σ geometrical Doppler estimates @ 500m

The 3σ estimates of total Doppler velocity shift from relative movement on idealised transmission paths and a simplistic treatment of surface wave movement readily account for Doppler shifted arrivals within 25dB-30dB of the strongest arrival at all delays. This Doppler estimate from velocity shift is therefore considered useful to interpretation of the Spreading Function Doppler.

Time domain Doppler search method

The results presented below relate to approximately the same channel as the 110m results in Fig. 9 and Fig. 12, but with transmitter drift extending the average range to 122m, and reducing the averaging closing speed from 0.19m/s to 0.13m/s.

Comparison of the short PN-sequence channel response history in Fig. 9 with the long PN-sequence channel response history in Fig. 15 illustrates how time varying channel Doppler degrades the txrx correlation for a relatively long 1.4s Doppler-sensitive sequence.

The correlation versus Doppler and time results presented in Figs. 16, 17 and 18 have been generated by block-by-block Doppler search for delay ranges relating to the first, second and third delayed path groups illustrated in Fig. 15. Whilst not shown, the equivalent Doppler frequency range of these figures is $\pm$ 10 Hz, as for the short-sequence spreading function plots.

The 'ripples' either side of the correlation maximum in Fig. 16 result from the ambiguity function Doppler side-lobes of the 1.4s PN sequence. The cyclical influence of swell orbital motion on relative motion is apparent in the Doppler time history for the first, second and third delay arrival groups. This time-dependent Doppler information is not obtainable from the Spreading Function or the time-domain channel response for the short 21ms sequence, for which the Doppler resolution of 6.1m/s is too coarse to enable detection of Doppler shift from orbital motion.

It appears from the time-domain Doppler analysis that there are no strong signal arrivals at large Doppler shift, however this
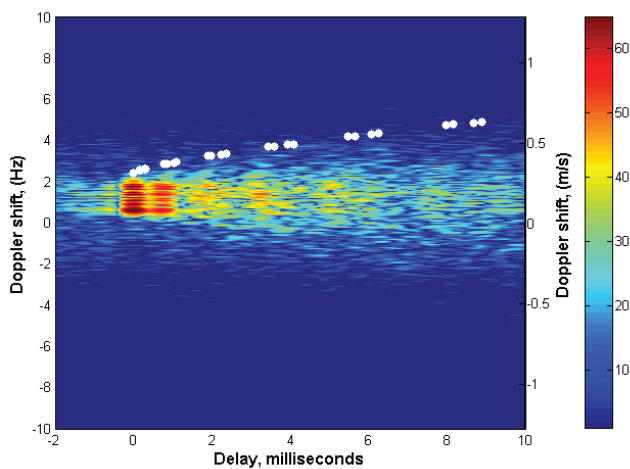

Figure 14. Spreading Function (dB) with 3σ geometrical Doppler estimates @ 1007m
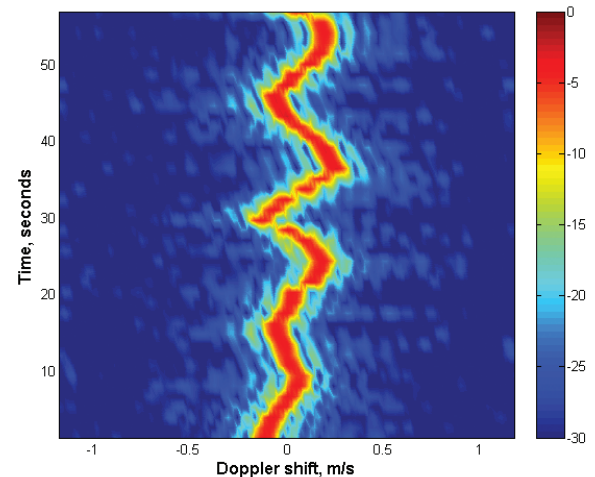

Figure 16. First arrivals normalised correlation (dB) versus time and Doppler, 1.4s PN sequence @ 122m
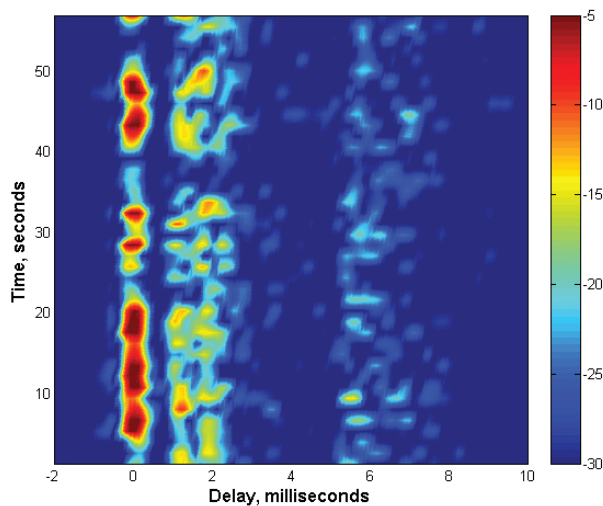

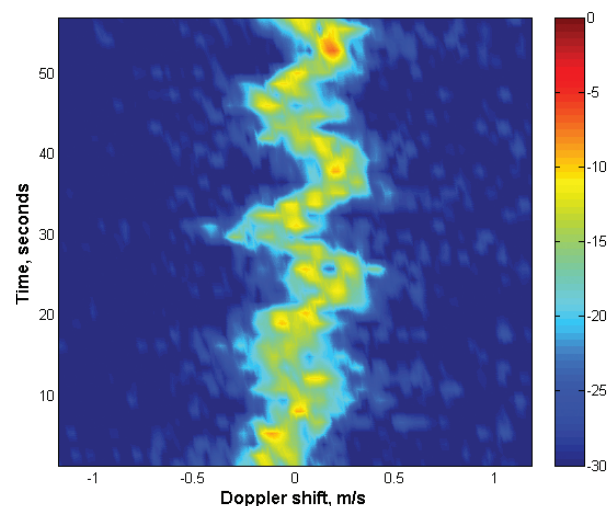Figure 15. Normalised txrx correlation (dB)–1.4s PN sequence @ 122m

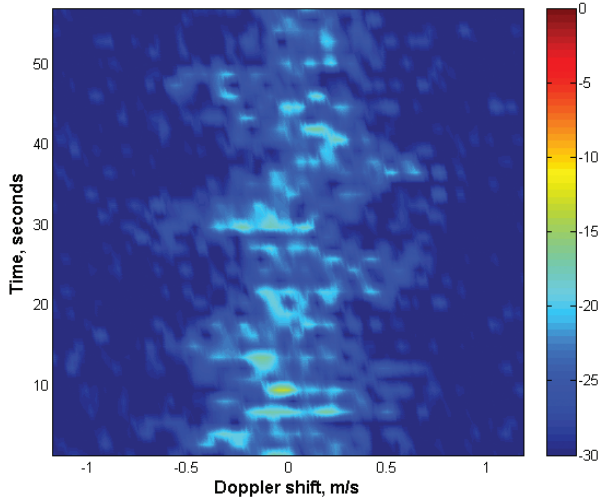Figure 17. Second arrivals normalised correlation (dB) versus time and Doppler, 1.4s PN sequence @ 122m

Figure 18. Third arrivals normalised correlation (dB) versus time and Doppler, 1.4s PN sequence @ 122m

Figure 19. Channel coherence versus time and delay group @ 110m

does not exclude the possibility of such transients occurring at a significantly shorter time-scale than the 1.4s probe sequence. However the same time-domain analysis was conducted for the shorter 170ms PN-sequence channel response (0.75m/s Doppler resolution) (not presented), which also indicated the absence of isolated strong transients at high Doppler shift.

It is concluded that whilst the Doppler resolution by direct Doppler search is low, the time history provides valuable insights into channel behaviour from a channel modelling perspective.

CHANNEL COHERENCE

The coherence of the channel response was explored for the repeated 21ms probe sequence to investigate the channel response update rate that would be necessary for a high-fidelity channel simulator. Results corresponding to the 110m, 500m and 1007m channels are presented in Figs. 19, 20 and 21, respectively. Markers on the figures indicate the calculated coherence at 21ms intervals. The results for each channel represent the average of ten three-second sub-blocks of the full 30s sample. The coherence $C(t)$ of each sub-block is calculated for the response within a given delay range (τ_1, τ_2) relative to reference time t_0 by Eq. (10).

$$C(t) = \frac{\sum_{\tau_2}^{\tau_1} h^*(\tau,t_0)h(\tau,t)}{\sqrt{\sum_{\tau_2}^{\tau_1} h^*(\tau,t_0)h(\tau,t_0) \sum_{\tau_2}^{\tau_1} h^*(\tau,t)h(\tau,t)}} \qquad (10)$$

The results in Figs. 19 to 21 demonstrate high coherence for the first arrival group at all ranges. Although the strength of subsequent correlation maxima generally degrades with range, the coherence of later arrivals generally improves with range, consistent with the geometrical trend of diminished in-path Doppler contributions from the moving sea surface as range increases.
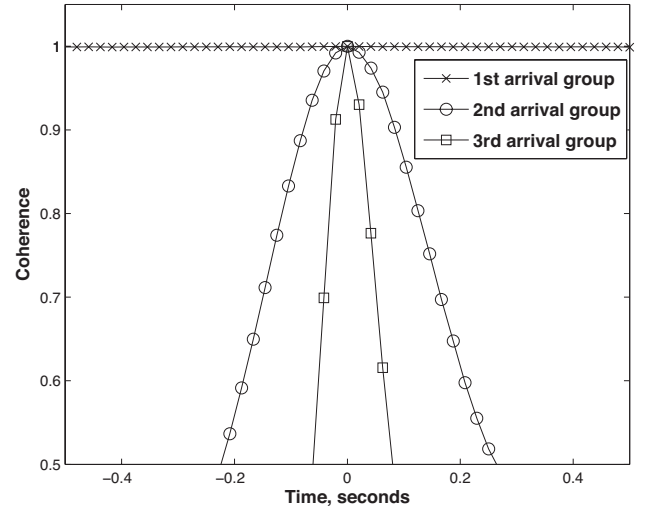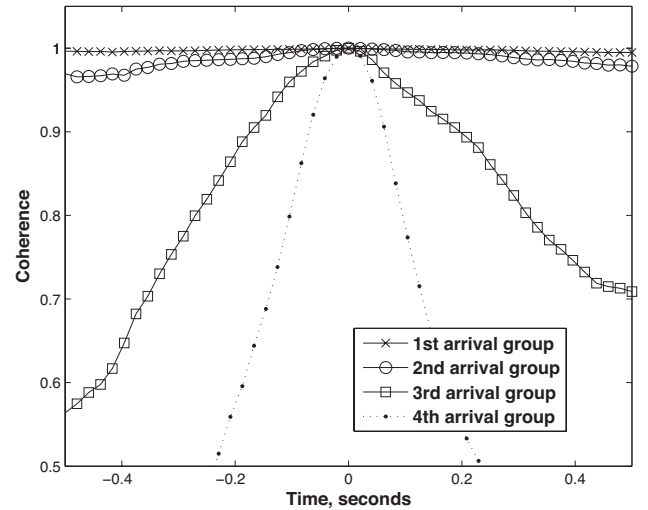

Figure 20. Channel coherence versus time and delay group @ 500m
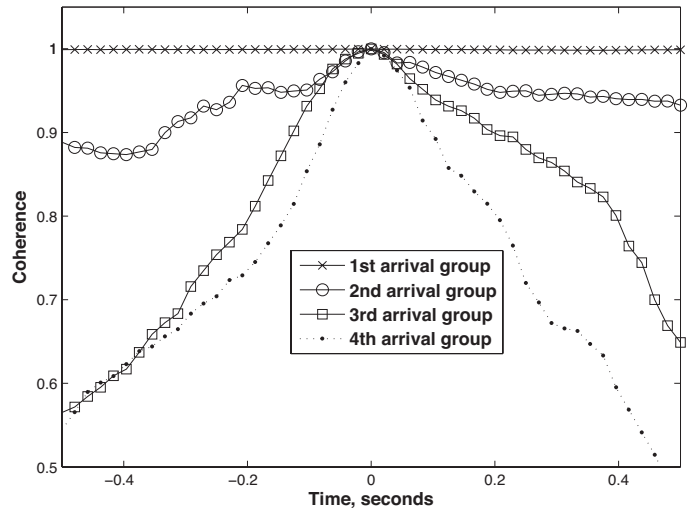

Figure 21. Channel coherence versus time and delay group @ 1007m

SUMMARY

Time and frequency domain analyses of experimental Doppler shift and delay spreading of underwater acoustic transmissions have been conducted for a shallow marine environment influenced by transmitter drift and heave, surface waves, and swell orbital motion. This analysis was conducted to ascertain channel coherence times and the significant sources and scale of channel Doppler spreading and delay spreading that need to be incorporated into a dynamic channel simulation for underwater communications.

The analysis has shown that the 3σ estimation of maximum channel Doppler shift in the units of equivalent velocity from simplified consideration of surface movement and relative motion is a useful approach to explaining the trends in experimental Doppler indicated by the Spreading Function.

Whilst the Doppler resolution achieved by direct Doppler search in the time domain is relatively low compared to that achievable by frequency domain analysis of a series of probe responses, it is concluded that the coarse Doppler time history provided by this approach is complementary to the Spreading Function in that it clarifies the origins of Doppler shifts associated with strong channel responses.

Coherence analysis of the channel response indicates that the coherence of later arrivals improves with increased transmission range, consistent with the geometrical trend of diminished in-path Doppler contributions from the moving sea surface as range increases.

REFERENCES

[1] S. Nordholm, Y. Rong, D. Huang, A. Duncan, "Increasing the range and rate of underwater acoustic communication systems using multi hop relay", Australian Research Council Discovery Project DP110100736, Curtin University, 2010.

[2] T.H. Eggen, A.B. Baggeroer and J.C. Preisig, "Communication over Doppler spread channels – Part 1: Channel and receiver presentation", *IEEE Journal of Oceanic Engineering* **25**, 62-71 (2000)

[3] P.A. van Walree, T. Jenserud and M. Smedsrud, "A discrete-time channel simulator driven by measured scattering functions", *IEEE Journal on Selected Areas in Communications* **26**, 1628-1637 (2008)

[4] P.H. Dahl, "High frequency forward scattering from the sea surface: The characteristic scales of time and angle spreading", *IEEE Journal of Oceanic Engineering* **26**, 141-151 (2001)

[5] P.A. van Walree, T. Jenserud and R. Otnes, "Stretched-exponential Doppler spectra in underwater acoustic communication channels", *Journal of the Acoustical Society of America Express Letters* **128**(5), EL329-EL334 (2010)

Distance Learning for Acoustics

The Professional Education in Acoustics program was established some years ago on the request from the industry due to a lack of regularly available appropriate courses in the formal University programs. It is aimed at providing appropriate modules to meet the needs of those embarking on a career in Acoustics and has the support of the Association of Australian Acoustical Consultants (AAAC). It is also be of value for those working in government agencies and allied organisations needing a fundamental understanding of acoustics. The program is based on a similar program that has been offered via universities and the UK Institute of Acoustics (IOA).

The program is fully flexible and all undertaken in distance learning mode. This means the modules can be commenced at any time and there is no requirement to complete at a specific date. This is an advantage to those who are unsure of future work demands – but of course a disadvantage as the lack of a deadline means that completion depends on the commitment of the registrant.

Each module of the program will be offered separately in distance learning mode so that it can be undertaken throughout Australia or elsewhere in the world and can be commenced at any time. Each module comprises course notes, assignments and two modules include practical exercises and a test. Registrants work through this material at their own pace and in their own location submitting the work electronically. The practical work and the test are undertaken at the registrant's location under supervision of their employer. It is expected that those registrants working for acoustical consultancies will receive support and supervision by their supervisors. For registrants who are working on the program without support from their employer will be given assistance by phone or email from the course coordinator. This assistance can be supplemented with assistance from a company that is a member of the AAAC.

For more information on the program see http://www.aaac.org.au/au/aaac/education.aspx

INFERENCE OF GEOACOUSTIC MODEL PARAMETERS FROM ACOUSTIC FIELD DATA

N. Ross Chapman

School of Earth and Ocean Sciences, University of Victoria, Victoria, BC V8P5C2, Canada
chapman@uvic.ca

The interaction of sound with the ocean bottom has a significant impact on the acoustic field in the ocean, especially in shallow water. Over the past several decades, there has been a high level of research activity in ocean acoustics to understand the physics of sound propagation in the ocean bottom. This work has led to the general practice of using geoacoustic models, - profiles of the sound speed, attenuation, and density of ocean bottom materials ñ to describe the bottom. Much of the research was focused on developing inversion methods to determine geoacoustic model parameter values from the information about the model contained in measurements of the acoustic field ñ or quantities that can be derived from the field ñ in the water. This paper reviews the stages in the development of geoacoustic inversion as a statistical inference process to estimate geoacoustic model parameter values and their associated uncertainties. Applications of linear inversions and non-linear inversions based on matched field processing are presented for analysis of their performance in estimating realistic geoacoustic models. The paper concludes by pointing out limitations in the present day inversion techniques that can severely limit performance, and discusses some new approaches that provide robust performance without compromising the accuracy of the estimated model parameters.

INTRODUCTION

Accurate representation of the acoustic field in the ocean is fundamentally important for many applications in ocean acoustics, from traditional naval interests in evaluating sonar performance to present day environmental concerns in assessment of the impact of anthropogenic sound sources on marine life. The measured field from a sound source in the ocean is uniquely determined by the physical conditions of temperature and salinity in the water, and the depth and geoacoustic properties of the ocean bottom. The mapping between the physical properties of the ocean waveguide and the acoustic field is non-linear, and the relationship is expressed by the acoustic wave equation [1, 2]. In all but a few simplified ocean waveguide models, analytic solution of the wave equation is not possible and sophisticated numerical techniques such as ray theory approximations, normal mode methods, wave number integral methods and parabolic equation approximations have been developed for calculating the field in realistic ocean waveguide environments [2]. These methods have been tested extensively in benchmarking sessions against simulated waveguide environments of varying complexity, and are in widespread use for applications with experimental data.

Solution of the wave equation involves satisfying boundary conditions of pressure release at the sea surface, and continuity of pressure and vertical particle velocity at the ocean bottom for the conventional assumption that the bottom is a fluid system; if the bottom is an elastic solid, there is an additional constraint of continuity of horizontal stress. The effect of the bottom on the acoustic field in the water is significant, particularly in shallow water environments, and there has been considerable research effort to understand the physics of sound propagation in ocean bottom materials. The interaction of sound with the ocean bottom is described in calculations of the acoustic field

using geoacoustic models of the physical bottom structure that generally consist of profiles in depth, range and cross-range of the sound speed, c, attenuation, α, and density, ρ, of the bottom materials. In most cases, the cross-range variation is negligible, but range dependence of the profiles in depth is common. Knowledge of these physical properties is necessary for constructing geoacoustic models that will enable accurate representation of the field. An example of a simple geoacoustic model is shown in Figure 1; the form of this model is typical of those used for applications with experimental data.

The geoacoustic model in the figure does not explicitly include shear wave parameters. Although shear wave effects in elastic solid material can be modelled in most numerical propagation codes, the impact of shear wave losses is not significant in most shallow water environments that consist of fine-grained, high porosity sediment material in which the shear wave speed near the sea floor is very low (< 300 m/s). Consequently, in most of the geoacoustic inversions reported in the literature, the bottom is modelled as a fluid. Exceptions to this approach include shallow or deep water environments where elastic solid material is found relatively close (within a few wavelengths) to the sea floor, e.g. calcarenite and limestone sea bottom regions off the west coast of Australia, and thin-sediment basalt regions of the Pacific Ocean. In those environments, the shear wave speed is comparable to or greater than the sound speed in water, and so the coupling with the compressional wave generated in the water is very strong. Inversions of data from such environments must take account of shear wave propagation in the bottom.
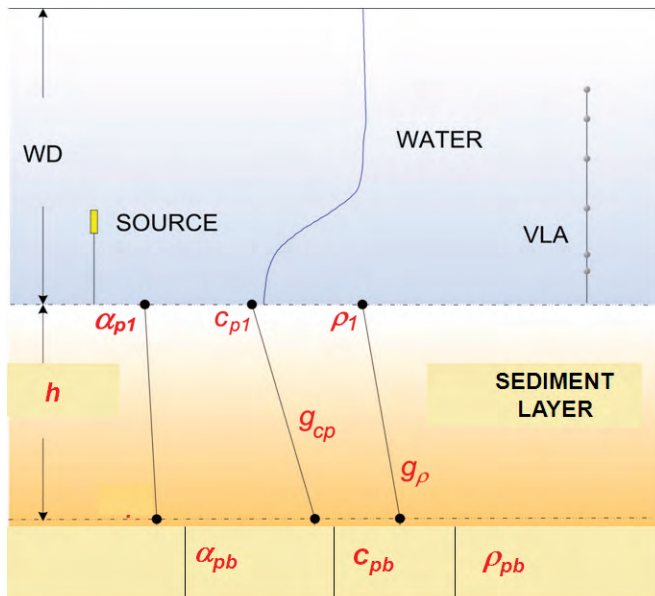
Figure 1. Geoacoustic model consisting of a simple layered structure of sound speed, c, attenuation, α, and density, ρ

The sensitivity of the acoustic field to geoacoustic model parameters was recognised many years ago by researchers who noted that improvements in modelling transmission loss data [3] and bottom loss data [4] could be obtained by adjusting specific model parameters. The simplicity of the approach is very appealing, and it continues to be applied in some studies [5]. However, an approach to inversion by changing model parameters in a trial and error fashion is highly subjective, and there is no measure of the uncertainty of the parameter value that provides the best fit to the data. More importantly, it ignores the sensitivities and the impact of errors in other model parameters that are held at fixed values. A more systematic approach of iteration over forward models was suggested by Frisk [6], but the computation time in executing such a grid search over many geoacoustic model parameters was and remains prohibitively long.

Over the past twenty years, there has been considerable interest in ocean acoustics in developing objective inversion techniques to estimate geoacoustic model parameters from measurements of the acoustic field – or quantities that can be derived from the acoustic field – in the water [7]. This approach using remote acoustic sensing is attractive because it is an efficient means for characterising the ocean bottom over large areas, and the estimates are made on material in its natural setting. By comparison, estimates based on point measurements that involve analysis of physical samples of the bottom material are expensive and time consuming, and may introduce additional problems in making measurements in other than *in situ* conditions. However, as will be seen later, the general practice is to compare the inferences from inversions to ground truth data from physical samples or other *in situ* measurements.

The inversion methods fall into two main categories, linear methods that assume small changes from an initial profile, and methods that are fully non-linear [8]. Linear inverse

problems are described by a well-established analytical theory that provides measures of the resolution and variance of the estimated parameters [9], and they have the additional appealing advantage of being computationally very fast. The non-linear methods are examples of model-based signal processing techniques that were made possible by the introduction of efficient numerical techniques for exploring multi-dimensional model parameter spaces. Inversion methods based on both approaches have been benchmarked in exercises with simulated data [10, 11], and have also been applied for use with data from experiments in many different ocean bottom environments - with varying degrees of success.

This paper reviews the stages in the development of geoacoustic inversion as a statistical inference process. The next section describes the background for the inverse problem, and describes some initial attempts in ocean acoustics to estimate geoacoustic parameters from experimental data. Linear inverse methods are then introduced, with examples of applications that use wave number measurements to infer the sound speed profile in marine sediment. Following this, non-linear model-based inversion is introduced with a discussion of matched field processing, followed by a description of inversion by Bayesian inference and demonstration of its performance with examples of applications to experimental data.

GEOACOUSTIC INVERSION METHODS

Inverse problems

Inversion can be described as the process of inferring information about a physical system from measurements of physical quantities that result from an interaction with the system. For geoacoustic inversion, this statement translates roughly as: given measurements of the acoustic field that has interacted with the bottom, what information can be inferred about the properties of the ocean bottom that generated the measured data? It might be expected that the inversion provides estimates of the material properties and structure of the real ocean bottom. However, this is not the case. Inversion provides the estimates of the parameters of a geoacoustic model that is designed to represent the bottom. Since the model is never exactly the true ocean bottom and since the data contain errors, the inverse problem is inherently non-unique. In the inversion process, we are comparing measured data with calculated replicas of the data based on the parameters of the designed geoacoustic model, and there are many different models that will provide very good fits to the data. One of the most significant challenges is designing an appropriate model, whether this is done by judicious choice based on prior information about the bottom structure, or within the inversion process itself.

Formally, the inverse problem in ocean acoustics is developed in terms of the relationship through the wave equation between the model parameters $\boldsymbol{m} = [m_1, m_2, \dots m_M]^T$ and the measured data $\boldsymbol{d} = [d_1, d_2, \dots d_N]^T$. The model parameters may be sound speeds, attenuations, densities and thicknesses of sediment layers. The primary physical quantity is the sound pressure, which can be measured directly with hydrophones in experiments. However, other quantities that are derived from

the pressure field such as horizontal wave numbers of normal modes; bottom reflection loss; modal amplitudes; modal dispersion and particle velocity are also used; travel time of received signals is also a useful quantity.

Measured data contain noise n that is assumed to be additive: $d = d_0 + n$. The vector d_0 is the data predicted by the wave equation that would be obtained in an ideal, perfectly accurate experiment in which the ocean waveguide is described by the set of model parameters m:

$$d_0 = F(m) \qquad (1)$$

As mentioned above, this problem has a unique and stable solution. The inverse problem of inferring the set of model parameters that generated the data is expressed by

$$m = F^{-1}(d) \qquad (2)$$

This problem is very difficult to solve, if a solution exists. Existence is usually addressed by constructing a geoacoustic model that provides an adequate fit to the data, within some specified uncertainty. However, the solution is non-unique, due to incomplete or inaccurate data, and is generally unstable–small errors in the data can lead to large changes in the estimated model parameter values. The complete solution to the inverse problem must provide both a set of estimated values and their associated uncertainties.

It is worthwhile to stress here what is meant by data errors. Errors can arise from two different sources: measurement errors that are due to inaccurate readings or ambient noise, and theory errors due to inaccurate or incomplete parameterisation of the geoacoustic model or approximations in the physics of the forward propagation problem. The data errors are not known explicitly, and it is usually assumed that d is a random variable with a Gaussian distribution. The theory errors are more difficult to estimate, and they can be the dominant source of uncertainty in the inversion.

Linearised inversion

Although the relationship between the pressure and the geoacoustic model parameters is non-linear, linear relationships can be developed for some observables that are derived from the acoustic field. In this approach, the problem is linearised in the vicinity of a reference model m_0, and it is assumed that the unknown model is related to the reference model by a small perturbation. Perturbation inversion has the advantage of the fast computational speed of linear methods, but there are many problems that offset this advantage. The most serious concern is that one is never sure that the final model is independent of the reference model. In many cases, the inversion does not converge if the starting model is not close to the solution, or more likely, it converges to a local minimum. Another serious issue is that because the relationship is nonlinear, it can be very misleading to use only the parameter space near the final estimated model to characterise the solution. Nevertheless, if used carefully, the approach can generate remarkably useful models.

An outstanding example of perturbation inversion was reported by Frisk et al. who developed an elegant method for estimating sound speed profiles in marine sediments by linearising the relationship between changes in the horizontal wave numbers of propagating modes and changes in the sound speed [12, 13]. The method assumes a background model for the sound speed profile $c_0(z)$ that generates a set of horizontal wave numbers k_{0m} and corresponding modal functions $Z_{0m}(z)$ for a sound frequency ω that are solutions of the depth-separated wave equation,

$$\left(\rho_0(z) \frac{d}{dz} \left(\frac{1}{\rho_0(z)} \frac{d}{dz} \right) + k_0^2(z) \right) Z_{0m}(z) = k_{0m}^2 Z_{0m}(z) \qquad (3)$$

where $\rho_0(z)$ is the density profile. The true model is thus

$$c(z) = c_0 + \delta c(z) \qquad (4)$$

and the wave numbers are changed from those for the background model,

$$k(z) = \omega/(c_0(z) + \delta c(z)) \qquad (5)$$

Applying first-order perturbation theory, an approximation can be obtained for the change in wave number with respect to that for the background model in terms of the change in sound speed [13]

$$\delta k_m = k_m - k_{0m} = \frac{1}{k_{0m}} \int_0^\infty |Z_{0m}(z)|^2 \frac{k_0^2(z)\, \delta c(z)}{\rho_0(z)\, c_0(z)}\, dz \qquad (6)$$

For a discretely sampled sound speed profile in depth, (6) can be cast in terms of a linear relationship between $\delta k(z)$ and the geoacoustic model parameters,

$$\delta k = Gm \qquad (7)$$

where G is a NxM matrix consisting of the background sound speed, density and mode functions; N is the number of discrete samples of the sound speed profile, and M is the number of model parameters [13].

Application of the method requires estimation of the horizontal wave numbers of propagating modes. The basis for this is the Hankel transform relationship between the depth-dependent Green's function and measurements of the variation of pressure with range for a specific sound frequency [12]. Good results have been obtained for experimental data from range independent waveguides, and an extension of the technique for range dependent waveguides using a short-time Fourier transform was developed by Becker [14]. Figure 2 shows an example of wave number estimation using this technique applied to data from the Shallow Water '06 (SW06) experiment that was carried out on the New Jersey continental shelf [15]. The estimated wave numbers of eight modes that are resolved in the data change slightly with the increasing water depth along the track. The estimated value of mode 6 is sensitive to a slow speed layer that pinches out and disappears towards the end of the track (Figure 3).
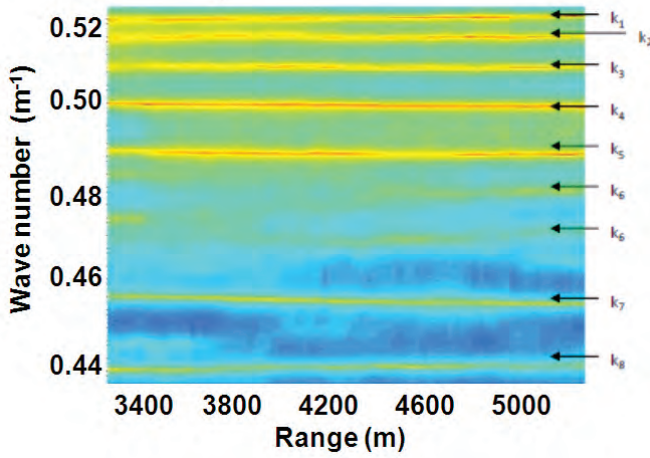
Figure 2. Modal wave numbers of 8 propagating modes that were estimated from SW06 experimental data of sound pressure versus range for a frequency of 125 Hz
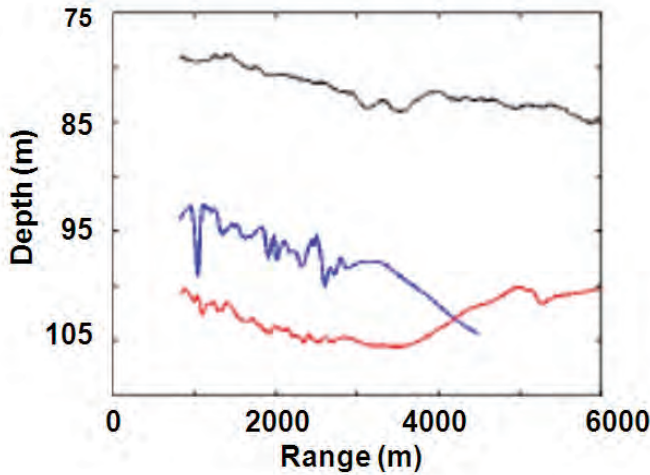

Figure 3. Chirp sonar depth profile from the SW06 experiment showing the depths of interfaces detected in the survey (upper curve: sea floor; middle curve: slow-speed erose layer boundary; bottom curve: R-reflector)

The inverse problem in Eq. (7) is ill-posed and requires some form of regularisation to obtain a solution. Ballard et al. [16] introduced a simple approach for piece-wise regularisation that enabled solution of a discontinuous sound speed profile, and used it to invert a range-dependent sound speed profile from the SW06 data. The method requires *a priori* knowledge of the locations of sound speed discontinuities in the sub-bottom material. This information was obtained from chirp sonar surveys of the SW06 experimental sites before the experiment, and the resulting section in depth (converted from two-way sonar signal travel time) is shown in Figure 3. The combined inversion of modal wave number data and two-way travel time information was able to estimate the sound speed in the three different sediment layers that were defined by the sonar data. However, without this type of additional information, the perturbation inversion can generate only a smoothed approximation to the profile [16].

MODEL-BASED INVERSION

Sophisticated numerical methods for solving non-linear geoacoustic inverse problems have been developed and implemented within the last two decades. The methods have been critically evaluated in workshops with simulated data [10, 11], and are in widespread use in applications with experimental data. The initial development of these methods was based on the use of matched field processing (MFP). The concept of MFP was known for a very long time, from the first simple experiments of Parvulescu and others at Hudson Laboratories that were reported in the mid 1960's [17] and the first formal paper by Homer Bucker in 1976 [18]. However, the method could not be applied effectively until modern numerical propagation models and fast computers with large storage capacity became available. The next section describes the background of MFP and the evolution of its use in ocean acoustics for source localisation and then geoacoustic inversion.

Matched field processing

A harmonic sound source in the ocean creates a unique distribution of the acoustic field in range and depth that can be expressed in terms of the propagating modes in the waveguide:

$$P(r,z) = \frac{e^{i\pi/4}}{\sqrt{8\pi}\,\rho_0\,(z_s)} \sum_{m=1}^{M} Z_m(z_s)Z_m(z) \frac{\exp(ik_m r)}{\sqrt{k_m r}} \qquad (8)$$

It can be seen from Eq. (8) that the spatial variation of the acoustic field contains information about the source/receiver geometry (r,z_s) and the waveguide model parameters that generate the modes.

Matched field processing was developed first as a method for extracting information about the source location from the spatial coherence of the acoustic field. In its most basic form, MFP compares measurements of the complex pressure $P(r,z)$ at specific sensor locations with calculated replica fields $Q(r,z)$ for the same locations. If the propagation model is correct (i.e., if the propagation model includes the correct physics of the problem), and if the physical model of the waveguide is a sufficiently accurate representation of the ocean environment, then the calculated field for the correct values of the true source depth and range (r_s,z_s) will be equal to the measured field $P(r_s,z_s)$ (to within a complex constant). This simple description defines MFP in terms of physically intuitive comparisons between measured and calculated acoustic fields. It is useful to retain this very physical picture of MFP in order to understand the more formal development.

In analogy with a conventional beamformer, the comparison process can be quantified by projecting the calculated replicas of the acoustic field on the measured data. The output of the MF processor can then be expressed in terms of the normalized Bartlett correlation for a frequency ω:

$$B(r,z,\omega) = |Q^\dagger(r,z,\omega)P(r,z,\omega)|^2 / |Q(r,z,\omega)|^2 |P(r,z,\omega)|^2$$

$$= Q^\dagger(r,z,\omega)P(r,z,\omega)P^\dagger(r,z,\omega)Q(r,z,\omega) / |Q(r,z,\omega)|^2 |P(r,z,\omega)|^2 \qquad (9)$$

where $P = [P_1, P_2, \ldots P_N]^T$ is the vector of measurements at

an array of N elements, $Q = [Q_1, Q_2, ...Q_N]^T$ is the vector of calculated replicas for the array and † denotes complex transpose. The quantity $PP†$ is the data covariance matrix that contains the relative phase information of the signal field across the array of sensors in the off-diagonal terms, as well as the signal power at each sensor in the diagonal terms. The difference between MFP and conventional beamforming is that the relative phase is determined from the full field solution to the wave equation instead of from plane waves.

The Bartlett processor described here is just one of many matched field processors that were developed and used for source localisation [19]. In all cases, the approach involved a systematic grid search to calculate an ambiguity surface of the matched field processor output over range and depth, as shown in Figure 4. This could be implemented very efficiently using normal mode propagation models because the environment model was constant for all points in the grid so that only one calculation of the field was needed. The true source location occurred at the ambiguity surface peak, assuming that the ocean waveguide environment model was correct.
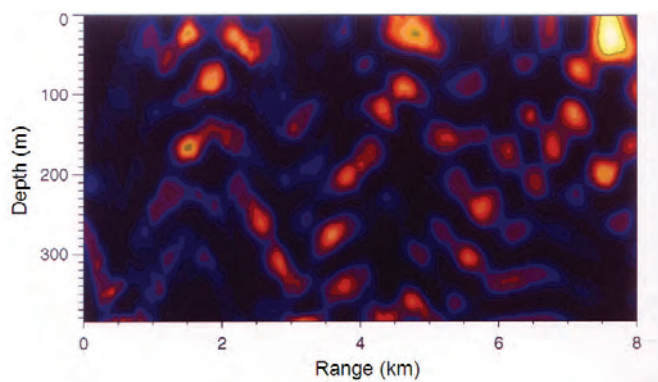

Figure 4. Matched field ambiguity surface for 45-Hz source from an experiment off the west coast of Vancouver Island, British Columbia. The peak at ~30 m depth and 7.7 km range indicates the source location

The example shown in Figure 4 displays the Bartlett matched field ambiguity surface based on data from an experiment carried out in shallow water (~400 m) on the continental shelf off the coast of Vancouver Island, British Columbia. The ambiguity surface peak at a depth of ~30 m and a range of 7.7 km indicates the location of the continuous wave 45-Hz source that was towed in the experiment. The sidelobes in the surface indicate locations of relatively high correlations. Since the propagation is bottom limited, there is a strong sidelobe at roughly half the distance to the source, approximately the range of the first bottom reflection for the shallow-angle propagating modes.

Optimisation inversions

Although the source/receiver geometry is generally more sensitive in MFP, there is also sensitivity to the ocean bottom properties that can be exploited to estimate geoacoustic model parameters. This hierarchy in sensitivity of geometric and geoacoustic parameters was formalised in the concept

of focalisation by Collins and Kuperman [20]. Their work showed that an accurate source location could be obtained for 'effective' models of the ocean bottom that were not necessarily realistic. This result is not unexpected, since the inverse problem is non-unique and there are many models that can provide a good fit to the data in model-based inversions. However, the application of MFP for geoacoustic inversion did not follow directly. The reason was simply that the inversion process required a computationally expensive calculation of the acoustic field to assess each new parameterisation of a multi-parameter geoacoustic model, and this prohibited a simple grid search for most cases of realistic models. The breakthrough that enabled matched field inversion (MFI) came with the introduction of numerical search algorithms such as simulated annealing [21] and genetic algorithms [22] for efficient navigation of multi-dimensional model parameter spaces. These methods reduced the computation time of the search process that was implemented to assess the models. The inversions were initially cast in terms of optimisation algorithms that consisted of four basic components:

- A prior geoacoustic model for the ocean bottom environment

- An accurate method for calculating the replica acoustic fields

- A cost function for comparing the measured and calculated fields

- An efficient search method for navigating the multi-dimensional model parameter space

The form of the prior geoacoustic model determined the structure and properties of the model that was inverted, and so the design of the model required careful development. The model was based on knowledge of the local environment that was available from 'ground truth' information such as sediment cores and physical grab samples, and high resolution seismic and chirp sonar surveys. Model structure was generally based on homogeneous or gradient layers of sound speed, attenuation and density to represent the sediment material in the ocean bottom, and the distribution of model parameter values was assumed to be uniform within the bounds that were set. The water sound speed profile was usually taken from measurements at the experimental site and was assumed known in the inversion. The cost function was generally based on the Bartlett processor, although other measures such as the high resolution minimum variance processor were sometimes used [19]. Models that were tested in the search process were selected or rejected based on the change in the cost function. Convergence was controlled either by pre-selecting the number of iterations, or by a criterion that set a minimum value for the change of the cost function (e.g. [24]).

A number of highly efficient numerical search methods were developed and implemented in various applications with data. Inversions based on simulated annealing were reported in the early 1990s [23, 24]. Simulated annealing is an example of an approach based on importance sampling for efficiently navigating multi-dimensional model parameter spaces. By analogy with thermodynamic cooling, SA uses a Boltzmann criterion to accept models that do not decrease the cost function. This feature allows the search to move away from areas of local

minima in the model parameter space, thus enabling a more extensive search. The genetic algorithm that is distributed in the widely used SAGA software package is another example of a global search technique based on importance sampling [22]. A number of hybrid search methods were also developed that combined global and local search processes such as the downhill simplex method, e.g. simulated annealing and downhill simplex [25]; genetic algorithm and Gauss-Newton [26]; genetic algorithm and downhill simplex [27].

Results of optimisation inversions using simulated annealing were conventionally presented in terms of the annealing history of each model parameter during the search process. However, the annealing history shows only the rate at which the optimal values were obtained in the search process. Although the annealing rate gives a rough impression of which parameters are more sensitive in the inversion, it does not give a good indication of how well each parameter was estimated. A better but still qualitative sense of the hierarchy of sensitivities of the model parameters and a rough measure of the uncertainties of the estimated values can be obtained from a scatter plot of the cost function values for each model that was tested in the search process. Figure 5 shows scatter plots for two different model parameters. Scatter plots that appear like 'tornadoes' as in the left panel indicate well-estimated parameters with values that cluster in a small region of the allowed range. Those that appear broader at the base, as in the right panel, indicate less sensitive parameters that are not well estimated; the flatness of the display essentially indicates that the experimental data do not contain any useful information about the parameter.
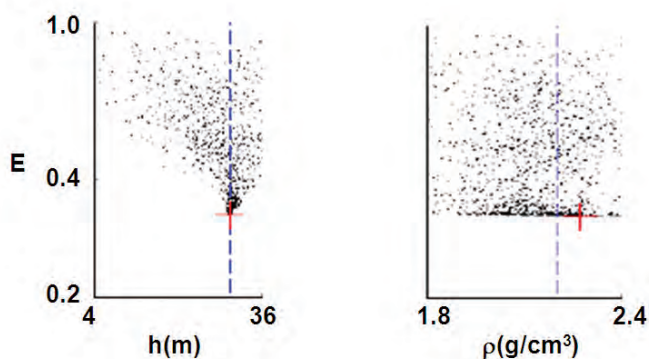

Figure 5. Typical scatter plots of cost function values ($E = 1 - B(r,z;\omega)$) for two different geoacoustic model parameters. The left panel shows clustering of accepted models in a favoured region of the allowed range of values; the right panel shows a flat scatter indicating that no particular value of this parameter provides a better estimate than any other

Examination of scatter plots from optimisation inversions reveals the inherent weakness of the approach. Optimisation inversions always provide an 'optimal' estimate for each model parameter. However, it is usually the case for inversions with experimental data that some model parameters are insensitive, so that the 'optimal' values of those parameters do not significantly affect the acoustic field. As a result, inversions can be over-parameterised, with meaningless estimates for some of the model parameters. In close scrutiny, optimisation inversions do not generate statistically valid measures of the errors in the estimated values, and consequently do not provide a complete solution to the inverse problem. However, it usually turns out that the spread of values obtained for a large number of optimisation runs (each one with different starting values) is contained within the error bounds of inversions carried out by Bayesian inference. Thus, the shape of the scatter plot generally gives a reasonable qualitative sense of the uncertainty of the estimate.

Model parameter correlations

An inherent problem in geoacoustic inversion arises from the correlations that exist between model parameters. At the very least, this leads to inefficient searches in the inversions. Optimisation inversions addressed this problem by re-parameterising the initial set of model parameters during the initial stages of the inversion [28]. Although this enables more efficient navigation of the model parameter space in the search process and is widely used, it does not eliminate the basic problem. The fundamental issue of mismatch remains: due to the model parameter correlations, errors in the estimate of one parameter will affect the estimates of all the others.

A simple but striking example of model parameter mismatch is the acoustic 'mirage' in source localisation by MFP. D'Spain et al. [29] showed that the range and water depth were strongly correlated in matched field source localisation. If the water depth used in calculating the replica fields was in error, the range was shifted in a predictable way. Since water depth and source range are not known exactly in experiments, the uncertainty in these parameters generates errors in the estimates of all the other model parameters in matched field inversions. The impact of this type of mismatch could be reduced by including geometric parameters of the experimental arrangement in the inversions, at the expense of increased computation time in searching a greater number of model parameters. This approach was adopted by many researchers. It supplied a useful consistency check on the quality of the inversions, provided that the inversion generated accurate estimates of the geometric parameters. Another well known example of mismatch is the correlation between source range and sound frequency through the waveguide invariant [1]. Errors caused by this effect were encountered initially when it was common practice to use only single frequency data in the inversions. The use of multi-frequency data (multiple tones or broad band signals) mitigates the impact of this mismatch to some degree.

These examples of mismatch errors in model-based inversions stress the fundamental issue of non-uniqueness of the solution to the inverse problem. Some researchers reported attempts to generate probabilities of the parameter values from the models that were tested in the search process as a means to address the uncertainties of the estimated values [30, 31]. However, the full resolution of the inverse problem as a statistical inference process was provided by Dosso [32] who introduced Bayesian inference [33] for geoacoustic inversion in ocean acoustics.

GEOACOUSTIC INVERSION BY STATISTICAL INFERENCE

Bayesian inference

The Bayesian formulation of the matched field geoacoustic inverse problem follows from Bayes' relationship between measured data and a set of environmental model parameters that is expressed in terms of conditional probabilities:

$$P(\boldsymbol{m}|\boldsymbol{d})P(\boldsymbol{d}) = P(\boldsymbol{d}|\boldsymbol{m})P(\boldsymbol{m}) \qquad (10)$$

Here, $P(\boldsymbol{m}|\boldsymbol{d})$ is the conditional probability of the model given the data, $P(\boldsymbol{d}|\boldsymbol{m})$ is the conditional probability of the data given a model $\boldsymbol{m}$, and $P(\boldsymbol{m})$ is the prior information about the model $\boldsymbol{m}$. The quantity $P(\boldsymbol{d})$ is the probability of the data, for the selected model parameterisation. If we assume that the model parameterisation is correct, then for observed data, $P(\boldsymbol{d})$=1. However, in general the correct parameterisation is not known, and P(d) can be considered as the likelihood of the parameterisation given the data.

In the Bayesian framework, the complete solution of the inverse problem is given by $P(\boldsymbol{m}|\boldsymbol{d})$, the *a posteriori* probability distribution (or PPD) of model parameter values. It is evident from Eq. (10) that Bayesian inversion involves an interaction between the information about the model that is contained in the data and the prior knowledge about the model. If there is no information in the data about a model parameter, the probability of that parameter is close to the original prior probability distribution. Otherwise, the final probability distribution is determined by the information contained in the data.

The relationship between the data and the set of environmental model parameters can be interpreted in terms of the mismatch between the measurement and a prediction of the measurement $\boldsymbol{q}$ based on the model:

$$\boldsymbol{d} - \boldsymbol{q}(\boldsymbol{m}) = \boldsymbol{n} \qquad (11)$$

The mismatch $\boldsymbol{n}$ can be interpreted as noise that arises from either the uncertainty in the experimental data itself or theory errors owing to differences between the environmental model and the real earth, or differences caused by an inaccurate model of the physics of the problem (in this case, the wave equation). The statistical distribution of $\boldsymbol{n}$ is generally not known.

Bayesian inversion is implemented by assuming that the conditional probability of the data for a given model, $P(\boldsymbol{d}|\boldsymbol{m})$, in Eq. (10) can be expressed in terms of a likelihood function of the data and model mismatch, $L(\boldsymbol{m},\boldsymbol{d})$ for data:

$$L(\boldsymbol{m},\boldsymbol{d}) = \frac{1}{\pi^N |C_d|} \exp\{-[E(\boldsymbol{m},\boldsymbol{d})]\} \qquad (12)$$

where C_d is the data error covariance matrix, N is the number of sensors and the data and model mismatch is defined as $E(\boldsymbol{m},\boldsymbol{d})$:

$$E(\boldsymbol{m},\boldsymbol{d}) = [(\boldsymbol{d} - \boldsymbol{q}(\boldsymbol{m}))^\dagger \, C_d^{-1} \, (\boldsymbol{d} - \boldsymbol{q}(\boldsymbol{m}))] \qquad (13)$$

In many applications, the assumption is made that the covariance matrix is diagonal. However, this condition is not usually correct, and some attempt must be made to evaluate C_d

in the inversion. This involves making assumptions about the statistics of the data mismatch distribution, and these must be verified by statistical tests [34, 35].

Although the complete solution of the inverse problem is given by the PPD, it is a multi-dimensional distribution that is difficult to visualise. Its interpretation in terms of model parameter estimates and their uncertainties involves computation of the properties of the PPD, such as the maximum *a posteriori* estimate (MAP), the mean values and covariances, and marginal probability distributions. Parameter uncertainties can be quantified in terms of credibility intervals, i.e. the γ% highest probability density interval (HPD) that represents the minimum width interval that contains γ% of the marginal probability distribution.

The Bayesian formulation is quite general, and the method can be applied to any of the types of data that are derived from the acoustic field. For the usual case in matched field inversion that the phase (θ) and amplitude (A) of the source sound pressure are unknown, the modeled data can be expressed as

$$\boldsymbol{q}(\boldsymbol{m}) = Ae^{i\theta} F_\omega(\boldsymbol{m}) \qquad (14)$$

where F_ω is the forward propagation model used to calculate the replica field at frequency ω for the geoacoustic model $\boldsymbol{m}$. The dependence on the source can be removed by maximizing over θ and A to obtain a misfit function that is given by the covariance-weighted Bartlett mismatch

$$E_\omega(\boldsymbol{m},\boldsymbol{d}) = \boldsymbol{d}_\omega^+ C_d^{-1} \boldsymbol{d}_\omega - \frac{|F_\omega(\boldsymbol{m}) C_d^{-1} \boldsymbol{d}_\omega|^2}{F_\omega^+(\boldsymbol{m}) C_d^{-1} F_\omega(\boldsymbol{m})} \qquad (15)$$

For multi-frequency data the different frequencies are usually combined incoherently, so that Eq. (12) becomes a product over the number of frequencies, and Eq. (15) becomes a summation.

Limitations of matched field Bayesian inference

Inversions based on the Bayesian formulation were applied to experimental data from many different experiments, with remarkable successes in estimating geoacoustic profiles that compared favourably with ground truth information for the local environment [36-39]. However, most of the experiments were carried out at sites where the ocean environment was benign for MFI: constant water depth and minimal variability of the ocean sound speed profile and the sediment materials and structure over the track of the experiment. For these conditions, the inversions could be carried out assuming that the sound propagation was independent of range. An example of Bayesian inversion with experimental data from the SW06 experiment is discussed here that demonstrates the performance of the method, and reveals the fundamental limitations of MFI in strongly variable ocean environments [40].

The SW06 experimental site is strongly influenced by internal waves, eddies and fronts that are shed from the Gulf Stream that passes offshore along the coast of New Jersey. These features create a highly variable sound speed profile in the ocean, with short time scales of the order of minutes and spatial variability scales of the order of a few km. An example

of the sound speed variability at the site during the experiment is shown in Figure 6. The profiles were obtained from CTD (conductivity, temperature, salinity) measurements from the source ship at stations along the track of the experiment.
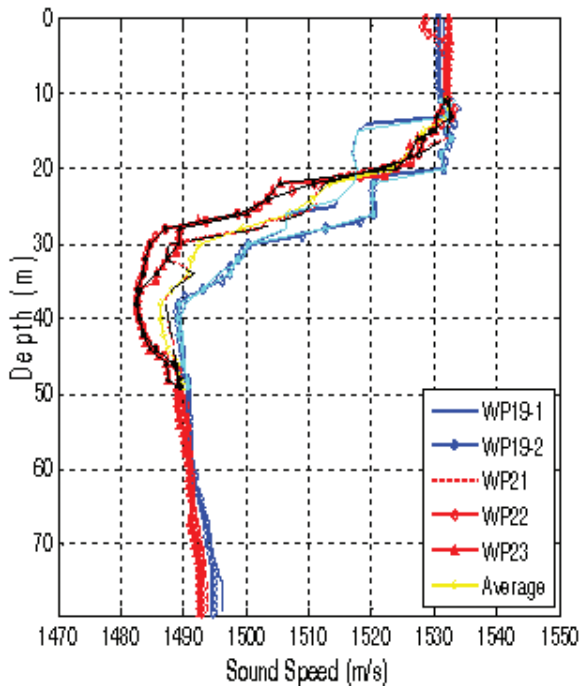

Figure 6. Sound speed profiles measured from CTDs deployed along the track from the SW06 experiment

The data used in the experiment were multiple CW tones transmitted from a ship that held station at a distance of 1 km from a bottom moored vertical line array. The array consisted of 16 hydrophones equal spaced at 3.75 m, with the bottommost sensor about 8.2 m above the sea floor. The water depth was ~79 m over the propagation path. Data from 7 CW tones over the frequency band 53–703 Hz were combined incoherently in the inversion.

The ocean environment in SW06 presented a significant challenge for MFI due to the strong spatial and temporal variability of the sound speed profile in the water over the experimental track. The conventional practice in MFI of using a single measured sound speed profile for the water column was ineffective for inverting the data. A simple demonstration of this problem is obtained from an ambiguity surface calculated for source localisation using one of the measured profiles. The true source location should be at 30 m and 1 km range, but as can be seen in Figure 7, the estimated location is near the ocean bottom and much closer in range. The ambiguity surface was calculated using 7 CW tones that were processed incoherently over frequency. In this case, the use of multiple frequencies was not effective in mitigating the mismatch caused by the unknown variation in the water sound speed profile, since the field could not be properly focussed at the receiver for any of the frequencies.
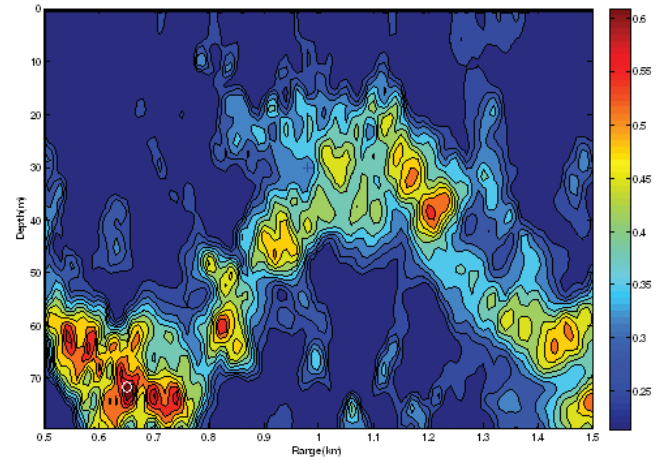

Figure 7. Ambiguity surface for multi-tone CW data from the SW06 experiment

To account for the variability, it was assumed that a single estimated profile would account for the changes in the water sound speed along the propagation path. The profile was modelled by empirical orthogonal functions (EOFs) to account for the observed variability in the profile, and the EOFs were included as unknowns in the inversion. Consequently, a total of 17 parameters were required in the inversion: 4 geometrical parameters of the experimental arrangement (source range and depth, water depth, and array tilt); 4 EOFs for the sound speed profile in the water; and 9 geoacoustic parameters of a single layer model of the bottom in which the sediment was modelled as a gradient layer for the sound speed and density over a halfspace basement (Figure 1). The local environment was assumed to be range independent in the inversion.

The inversion results are presented as marginal probability densities for the model parameters in Figure 8. Sensitive parameters that are well estimated have marginal densities that are tightly focused in a favoured region of the parameter bounds; the marginal densities for parameters for which there is little information in the data are flatter. These shapes are similar to the shapes of the scatter plots from optimization inversions for parameters with similar sensitivities. However, a statistically meaningful measure of the uncertainty can be derived from the Bayesian inference, such as the 95% HPD limits. As seen in the figure, the geometric parameters indicated by the dashed circles were highly sensitive in the inversion, and the estimated values compared very well with independent measurements of the range, source depth and bathymetry from the experiment. The 4 EOFs were also well estimated.

Marginal densities for the layer depth (H), and top and bottom sound speed of the sediment layer, c_{p1} and c_{p2}, respectively and the sound speed in the basement half space, c_{pb}, (shown in the solid circles) were also tightly focused, indicating that these geoacoustic parameters were well estimated. However, the marginal densities for the other geoacoustic parameters were relatively flat, indicating that the data did not contain significant information about them.

The results shown in the figure are typical of those from other matched field inversions: the most sensitive parameters are

generally the sound speeds in the uppermost layers of sediment (within a few wavelengths of the sea floor). A particularly striking result from this inversion is the accurate estimate of sediment thickness. Ground truth chirp sonar surveys revealed a strong sub-bottom reflector at a depth of about 20 m that was ubiquitous over the experimental area. The inversion was also sensitive to a slow sound speed layer within the sediment above the basement reflector. Although the detailed structure within the sediment could not be resolved with these data, the presence of the low speed layer was inferred from the negative gradient of sound speed within the sediment.
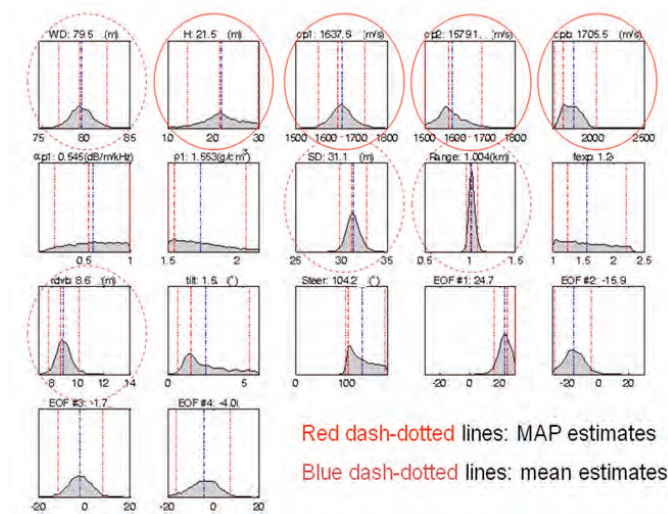
Figure 8. Marginal probability densities for the model parameters inverted from the SW06 data. The vertical dashed lines represent the 95% HPD limits. Red dash-dotted lines are MAP estimates, and blue dash-dotted lines are the mean estimates. The solid and broken circles indicate well estimated geoacoustic and geometric parameters, respectively

Attenuation is interpreted as an intrinsic loss in the sediment, and was modelled in this inversion as frequency dependent, $\alpha_0 (f/f_0)^\beta$, where $f_0 = 1$ kHz. The results indicated that the inversion with data from a range of 1 km was not sensitive to attenuation: the marginal densities for the constant, α_{p1}, the exponent, f_{exp}, were flat. However, the experimental data are affected by other mechanisms that remove energy from the propagation plane, such as scattering. Since the loss accumulates with range, data from greater ranges likely contain more information about attenuation.

Other insight into the estimated model can be obtained from two-dimensional marginal densities. Displays such as shown in Figure 9 for the SW06 data reveal model parameter correlations, and provide added confidence about the quality of the estimated model. From the figure, there is a clear indication of the correlation between water depth (WD) and range, and also water depth and source depth (SD). The correlation between the water depth and first EOF shows the linkage between the waveguide depth and the sound speed profile in focussing the signal at the receiver. A negative sound speed gradient in the sediment layer is revealed in the correlation between the top

and bottom sound speeds of the layer (c_{p1} and c_{p2}). Other pairs of parameters do not show any strong correlation, as would be expected for pairs such as water depth and the thickness of the sediment layer.

Although the inversion was successful in providing accurate estimates of the geoacoustic model, the overall success of the same approach for other data sets at longer ranges was not repeated. The success of the inversion reported here depended on the assumption that the sound speed variation in the water column could be represented by a single profile based on the observed sound speed variations. This assumption was not upheld for data from ranges of 3 km and 5 km from the same experiment. Oceanographic data from moored sensors revealed that internal waves passed through the experimental site when the longer range data were obtained. Knowledge of the full range dependence of the sound speed profile is required for inverting these data.

This example indicates the fundamental weakness of model-based inversions such as MFI. If the environmental variation cannot be modelled sufficiently accurately, the inversion will fail. However, the degree of variability that will allow simple assumptions such as a single profile is not known. And even for simple assumptions, the increased computational load of including additional model parameters as unknowns in the inversion is a significant drawback.

Other challenges in model based inversions

Apart from the issues mentioned above, there are other challenges that need to be addressed in model based inversions. Most of the inversions reported to date have been restricted to low frequencies (< 1 kHz) for which the sea floor and sub-bottom layer interfaces are assumed to be smooth. Inversions at higher frequencies must address rough surface scattering losses in modelling the acoustic field. The impact of shear wave propagation in the bottom has been considered in some inversions, but this issue is generally ignored. Another important issue is the assumption of 2-D sound propagation. In most cases, this assumption is valid. However, in experimental geometries that involve propagation across a sloping sea bottom such as along a continental shelf, 3-D propagation effects must be considered. An example reported by Jiang et al. demonstrated the impact of 3-D sound propagation on MFI at a site in the Florida Straits [41]. In this inversion, the sound refracted along the slope could be removed by spatial filtering since it was propagated in higher order modes with larger propagation angles. Otherwise, a 3-D sound propagation model is required [42].

Ocean sediments are porous media, and there has been significant research effort in developing theories of sound propagation in sediment materials. Among the most well known theories are the Biot theory [43, 44], and the more recent theories based on viscous grain shearing by Buckingham [45-47]. The critical issue for modelling sound propagation is the dispersion of sound speed and attenuation in sediments: experiments show that the frequency dependence of attenuation in sand sediments is non-linear within the low frequency band less than 5 kHz [48]. However in most applications of MFI, sound propagation has been modelled using viscous fluid models or in some cases
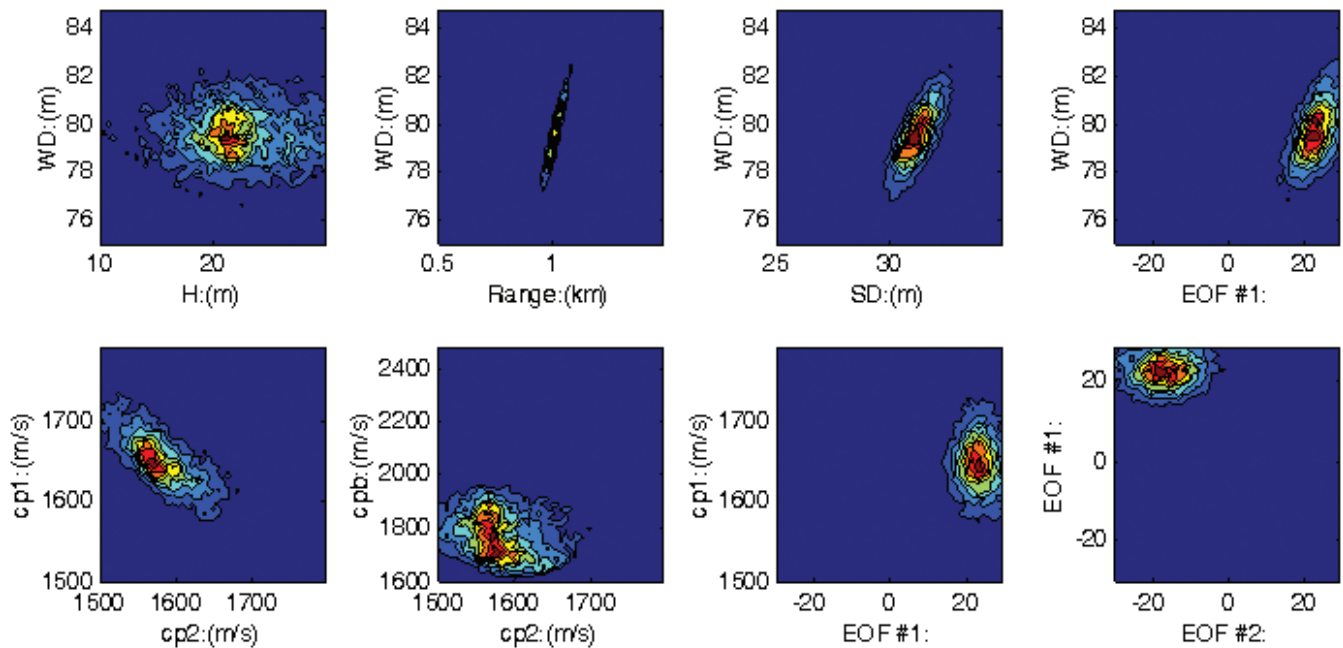
Figure 9. Two-dimensional marginal probability densities for the model parameters inverted from the SW06 data

visco-elastic models, both of which inherently assume linear frequency dependence for attenuation.

The impact of using more appropriate theories of sound propagation in marine sediments has not been examined extensively in MFI. One of the benefits of using the viscous grain shearing theory, for instance, may be in obtaining a more efficient set of model parameters for sampling the PPD. The theory provides analytic expressions for the sound speed, attenuation and density in terms of more fundamental physical parameters (such as porosity, compressional and shear grain contact stress) that are independent [47].

The inversions have generally assumed that the model developed from the prior information is correct. New work by Dettmer et al. [49, 50] has focused on removing the dependence on a specific form for the prior model in Bayesian inversions. Their research has introduced a method for allowing the inversion to select models during the inversion process. The method shows considerable promise, but at increased computational expense. Another approach using particle filters for applications in range dependent environments was implemented by Yardim et al. [51]. In analogy with a Kalman filter, the method tracks the source location and the changing ocean bottom environment.

OTHER APPROACHES FOR GEOACOUSTIC INVERSION

There is no simple remedy to enable model-based approaches such as MFI for conditions in which there is insufficient knowledge of the waveguide environment. A reasonable alternative approach is to use quantities derived from the acoustic field in the inversion, instead of the measured pressure. Although this usually requires special signal processing to extract the observable, there are clear benefits if modelling the observable is not sensitive to variability in ocean waveguide properties. One example is the use of travel time. Jiang et al. [52] reported a Bayesian inversion of relative travel times between sub-bottom and sea floor broadband signal arrivals to estimate sound speed and attenuation in the sediment. The experiment was designed to provide a tomographic sampling of the sediment using multiple source depths and a vertical hydrophone array at very short range. The data (shown in Figure 10 for a single source/receiver pair) are more robust to uncertainty in the water sound speed profile due to the relatively short range (~ 200 m), assuming that the sound speed profile is adequately sampled at the site during the experiment.

The sea bottom reflection coefficient derived from broadband data in an elegant experimental design has been used to invert fine structure of the sediment profile near the sea floor [53, 54]. However, the experimental geometry with a receiver very close to the sea floor requires calculation of reflection of a spherical wave to model the data correctly. Modal dispersion data have also been used in linearised inversions of time-frequency information [55]. This approach has the advantage of using a single receiver since the information is contained in the broad frequency band of the data. However, the technique is somewhat restricted to longer ranges to enable time resolution of the modes.

Perhaps the most novel approaches are those that make use of ambient noise. The use of ambient noise measured on a vertical array as a fathometer has been demonstrated by Siderius et al. [56]. Recently, Quijano extended this approach for geoacoustic inversion using the wind noise measured by the array as the sound source [57, 58]. The method inverts the

broadband reflection coefficient that is estimated from wind noise data on the array. The estimate of reflectivity is self-calibrated, and the reflection coefficient inversion is robust to uncertainty in the water sound speed profile. This is also true for the reflection coefficient inversions of controlled source data as proposed by Holland and Osler [53].
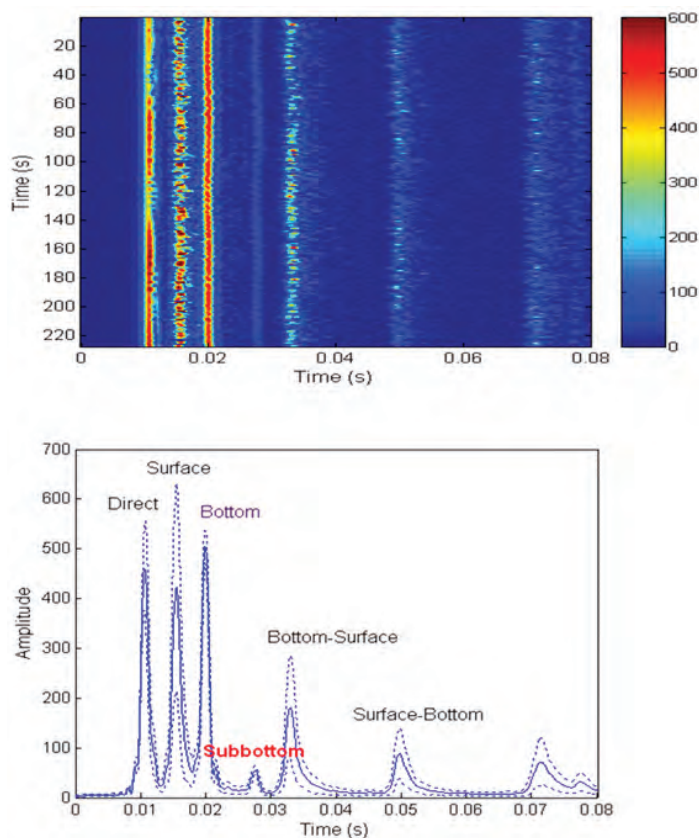

Figure 10. The multipath signal received at short range over a time of about 4 minutes. The top panel shows match filtered multipath signal from a 1-s chirp pulse over the band 1.5-2.5 kHz. The bottom panel shows the relative signal amplitudes over the time interval. Data are from the SW06 experiment

Finally, a promising technique that is robust to uncertainty in both the experimental geometry and the water sound speed profile was reported by Bonnel et al. [59, 60]. The method is based on estimating the modal dispersion from single hydrophone data using a signal processing technique known as warping. Although the use of modal dispersion data for estimating geoacoustic model parameters is not new, warping enables the inversion of relatively short range data for which the modes are not clearly separated in time. Warping transforms the non-linear dispersion relationship in the original time-frequency domain to single tones at frequencies near the Airy frequencies in the warped domain (Figure 11). It is evident from the figure that the range of the light bulb is not sufficiently great to resolve the modes in the original signal. The warping operation is reversible, so that the modes that are resolved in the warped domain can be filtered and transformed back to the original time-frequency space.
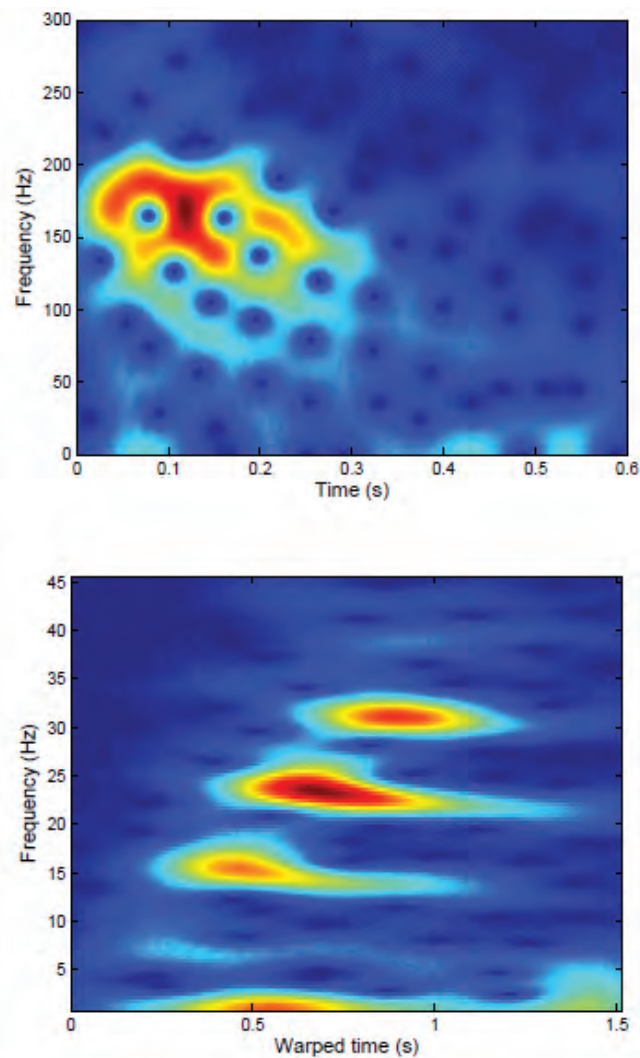

Figure 11. Left panel: original time-frequency dispersion of a light bulb shot deployed at a range of about 7 km in the SW06 experiment; right panel: the same signal transformed in the warped domain. Four modes are resolved at (warped) frequencies between 7 and 30 Hz

SUMMARY

This paper reviewed the development of geoacoustic inversion in ocean acoustics as a statistical inference method. The inversion methods fall into two categories, linear and non-linear. Linear methods have been implemented using relationship between differences in horizontal wave numbers and sound speeds compared to an initial model. Linear methods have the advantage of efficient computational implementation, but the results are sensitive to the initial model. The widely used non-linear technique of matched field inversion was examined to display its advantages and discuss its fundamental limitations. The method is based on matched field processing in which model parameters are estimated by comparing measured data with calculated replicas of the data. The Bayesian formalism for matched field inversion provides the complete solution to the inverse problem: estimates of the model parameter values and statistically valid measures of their uncertainties are derived from the *a posteriori* probability

density. The marginal probabilities derived from the PPD indicate the degree to which the experimental data contain information about the model parameters. However, if there is uncertainty due to variability in the properties of the ocean environment, model-based inversions such as matched field inversion can fail.

New approaches that are robust to uncertain knowledge of the ocean properties and the experimental geometry provide some options for alternative methods for model-based inversion of geoacoustic model parameters. A few of these methods, such as time-frequency analysis of broadband data, reflection coefficient inversion and travel time tomography were briefly discussed.

ACKNOWLEDGEMENTS

REFERENCES

[1] L.M. Brekhovskikh and I.P. Lysanov, *Fundamentals of Ocean Acoustics, 3rd Edition*, Springer, Berlin, 2003

[2] F.B. Jensen, W.A. Kuperman, M.B. Porter and H. Schmidt, *Computational Ocean Acoustics*, American Institute of Physics, Woodbury, New York, 1994

[3] F.B. Jensen, and W.A. Kuperman, "Sound propagation in a wedge shaped ocean with a penetrable bottom", J*ournal of the Acoustical Society of America* **67**, 1564-1566 (1981)

[4] N.R. Chapman, "Modeling ocean-bottom reflection loss measurements with the plane-wave reflection coefficient", *Journal of the Acoustical Society of America* **73**, 1601-1607 (1983)

[5] R.B. Evans and W.M. Carey, "Frequency dependence of sediment attenuation in two low frequency shallow water acoustic experimental data sets", *IEEE Journal of Oceanic Engineering* **23**, 439-447 (1998)

[6] G.V. Frisk, "Inverse methods in ocean bottom acoustics", in *Oceanographic and Geophysical Tomography: Les Houches 1988*, edited by Y. Desuabies, A Tarantola and J. Zinn-Justin, North-Holland, Amsterdam, 1990, pp 439-437

[7] A. Caiti, N.R. Chapman, J-P Hermand and S. Jesus, (editors) *Acoustic Sensing Techniques for the Shallow Water Environment*, Springer, Dordrecht (332 pages), 2006

[8] N.R. Chapman, *Inverse problems in Underwater Acoustics, Handbook of Signal Processing in Acoustics*, D. Havelock, S. Kuwano and M. Vorlander, editors, Springer, New York, 2009, pp. 1723-1736

[9] W. Menke, *Geophysical Data Analysis: Discrete Inverse Theory*, Academic Press, Orlando, 1987

[10] A. Tolstoy, N.R. Chapman and G.E. Brooke, "Workshop '97: Benchmarking for geoacoustic inversion in shallow water", *Journal of Computational Acoustics* **6**, 1–28 (1998)

[11] N.R. Chapman, S.A. Chin-Bing, D. King and R.B. Evans, "Benchmarking geoacoustic inversion methods for range dependent waveguides", *IEEE Journal of Oceanic Engineering* **28**, 320–330 (2003)

[12] G.V. Frisk and J.F. Lynch, "Shallow water waveguide characterization using the Hankel transform", *Journal of the Acoustical Society of America* **76**, 205–211 (1984)

[13] S.D. Rajan, J.F. Lynch and G.V. Frisk, "Perturbative inversion methods for obtaining bottom geoacoustic parameters in shallow water", *Journal of the Acoustical Society of America* **82**, 998–1017 (1987)

[14] K.M. Becker and G.V. Frisk, "Evaluation of an autoregressive spectral estimator for modal wave number estimation in range-dependent shallow water waveguides", *Journal of the Acoustical Society of America* **120**, 1423–1434 (2006)

[15] D.J. Tang, J.N. Moum, J.F. Lynch, P. Abbot, N.R. Chapman, P.H. Dahl, T.F. Duda, G. Gawarkiewicz, S. Glenn, J.A. Goff, H. Graber, J. Kemp, A. Maffei, J.D. Nash and A. Newhall, "Shallow Water '06: A joint acoustic propagation/nonlinear internal wave physics experiment", *Oceanography* **20**(4),156–167 (2007)

[16] M. Ballard, K.M. Becker and J.A. Goff, "Geoacoustic inversion for the New Jersey shelf: three dimensional sediment model", *IEEE Journal of Oceanic Engineering* **35**, 28–42 (2009)

[17] A. Parvulescu, "Matched signal ("M.E.S.S.") processing in the ocean", *Journal of the Acoustical Society of America* **98**, 943-960 (1995)

[18] H. Bucker, "Use of calculated sound fields and matched field processing to locate sound sources in shallow water", *Journal of the Acoustical Society of America* **59**, 368–373 (1976)

[19] A. Tolstoy, *Matched Field Processing for Underwater Acoustics*, World Scientific Publishing, Singapore, 1993

[20] M.D. Collins and W.A. Kuperman, "Focalization: Environmental focusing and source localization", *Journal of the Acoustical Society of America* **91**, 1410–1422 (1991)

[21] A. Basu and L.N. Frazer, "Rapid Determination of the Critical Temperature in Simulated Annealing Inversion", *Science*, 21, September 1990: 1409–1412 (1990)

[22] P. Gerstoft, "Inversion of seismoacoustic data using genetic algorithms and a posteriori probability distributions", *Journal of the Acoustical Society of America* **95**, 770–782 (1994)

[23] M.D. Collins, W.A. Kuperman and H. Schmidt, "Non-linear inversion for ocean bottom properties", *Journal of the Acoustical Society of America* **92**, 2770–2783 (1992)

[24] C.E. Lindsay and N.R. Chapman, "Matched Field Inversion for Geoacoustic Model Parameters Using Adaptive Simulated Annealing", *IEEE Journal of Oceanic Engineering* **18**, 224–231 (1993)

[25] S.E. Dosso, M.J. Wilmut and A-L. Lapinski, "An adaptive-hybrid algorithm for geoacoustic inversion", *IEEE Journal of Oceanic Engineering* **26**, 324–336 (2001)

[26] P. Gerstoft, "Inversion of acoustic data using a combination of genetic algorithms and the Gauss–Newton approach", *Journal of the Acoustical Society of America* **97**, 2181–2190 (1995)

[27] M. Musil, M.J. Wilmut and N.R. Chapman, "A hybrid simplex genetic algorithm for estimating geoacoustic properties using matched field inversion", *IEEE Journal of Oceanic Engineering* **24**, 358–369 (1999)

[28] M.D. Collins and L. Fishman, "Efficient navigation of parameter landscapes", *Journal of the Acoustical Society of America* **98**, 1637–1644 (1995)

[29] G.L.D. D'Spain, J.J. Murray, W.S. Hodgkiss, N.O. Booth and P. Schey, "Mirages in shallow water matched field processing", *Journal of the Acoustical Society of America* **105**, 3245–3265 (1998)

[30] P. Gerstoft and C. Mecklenbrauker, "Ocean acoustic inversion with estimation of a posteriori probability distributions", *Journal of the Acoustical Society of America* **104**, 808–819 (1998)

[31] L. Jaschke and N.R. Chapman, "Matched field inversion of broadband data using the Freeze Bath method", *Journal of the Acoustical Society of America* **106**, 1838–1851 (1999)

[32] S.E. Dosso, "Quantifying uncertainties in geoacoustic inversion I: A fast Gibbs sampler approach", *Journal of the Acoustical Society of America* **111**, 128–142 (2002)

[33] M.K. Sen and P.L. Stoffa, "Bayesian inference, Gibbs sampler and uncertainty estimation in geophysical inversion", *Geophysical Prospecting* **44**, 313–350 (1996)

[34] S.E. Dosso, P.L. Nielsen and M.J. Wilmut, "Data error covariance in matched-field geoacoustic inversion", *Journal of the Acoustical Society of America 119*, 208–219 (2006)

[35] Y-M. Jiang, N.R. Chapman and M. Badiey, "Quantifying the uncertainty of a geoacoustic model for the new jersey shelf by inverting air gun data", *Journal of the Acoustical Society of America* **121**, 1879–1894 (2007)

[36] Z.-H. Michaloupoulou, "Robust multi-tonal matched field inversion: A coherent approach", *Journal of the Acoustical Society of America* **104**, 163–170 (1998)

[37] D.P. Knobles, R.A. Koch, L.A. Thompson, K.C. Focke and P.E. Eisman, "Broadband sound propagation in shallow water and geoacoustic inversion", *Journal of the Acoustical Society of America* **113**, 205–222 (2003)

[38] D.J. Battle, P. Gerstoft, W.S. Hodgkiss, W.A. Kuperman and P.L. Nielsen, "Bayesian model selection applied to self-noise geoacoustic inversion", *Journal of the Acoustical Society of America* **116**, 2043–2056 (2004)

[39] R.A. Koch and D.P. Knobles, "Geoacoustic inversion with ships as sources", *Journal of the Acoustical Society of America* **117**, 626–637 (2005)

[40] Y-M. Jiang and N.R. Chapman, "The impact of ocean sound speed variability on the uncertainty of geoacoustic parameter estimates", *Journal of the Acoustical Society of America* **125**, 2881–2895 (2009)

[41] Y-M. Jiang, N.R. Chapman and H.A. DeFerrari, "Geoacoustic inversion of broadband data by matched beam processing", *Journal of the Acoustical Society of America* **119**, 3707–3716 (2006)

[42] F. Sturm, S. Ivansson, Y-M. Jiang and N.R. Chapman, "Numerical investigation of out-of-plane sound propagation in a shallow water experiment", *Journal of the Acoustical Society of America* **123**, EL155–EL160 (2008)

[43] M.A. Biot, "Theory of propagation of elastic waves in a fluid-saturated porous solid. i. low-frequency range", *Journal of the Acoustical Society of America* **28**, 168–178 (1956)

[44] M.A. Biot, "Generalized theory of acoustic propagation in porous dissipative media", *Journal of the Acoustical Society of America* **34**, 1254–1264 (1962)

[45] M.J. Buckingham, "Theory of acoustic attenuation, dispersion, and pulse propagation in unconsolidated granular materials including marine sediments", *Journal of the Acoustical Society of America* **102**, 2579–2596 (1997)

[46] M.J. Buckingham, "Theory of compressional and transverse wave propagation in consolidated porous media", *Journal of the Acoustical Society of America* **106**, 575–581 (1999)

[47] M.J. Buckingham, "On pore-fluid viscosity and the wave properties of saturated granular materials including marine sediments", *Journal of the Acoustical Society of America* **122**, 1486–1501 (2007)

[48] J.-X. Zhou, X.-Z. Zhang, and D. P. Knobles, "Low-frequency geoacoustic model for the effective properties of sandy seabottoms", *Journal of the Acoustical Society of America* **125**, 2847–2866 (2009)

[49] . Dettmer, S.E. Dosso and C.W. Holland, "Sequential trans-dimensional Monte Carlo for range-dependent geoacoustic inversion", *Journal of the Acoustical Society of America* **129**, 1794–1806 (2011)

[50] J. Dettmer and S.E. Dosso, "Trans-dimensional matched-field geoacoustic inversion with hierarchical error models and interacting Markov chains", *Journal of the Acoustical Society of America* **132**, 2239-2250 (2012)

[51] C. Yardim, P. Gerstoft and W.S. Hodgkiss, "Geoacoustic and source tracking using particle filtering: Experimental results", *Journal of the Acoustical Society of America* **128**, 75–87 (2010)

[52] Y-M. Jiang, N.R. Chapman and P. Gerstoft, "Estimation of marine sediment properties using a hybrid differential evolution method", *IEEE Journal of Oceanic Engineering* **35**, 59–69 (2010)

[53] C.W. Holland and J. Osler, "High-resolution geoacoustic inversion in shallow water: A joint time- and frequency-domain technique", *Journal of the Acoustical Society of America* **107**, 1263–1279 (2000)

[54] C.W. Holland, J. Dettmer and S.E. Dosso, "Remote sensing of sediment density and velocity gradients in the transition layer", *Journal of the Acoustical Society of America* **118**, 163–177 (2005)

[55] G. Potty, J. Miller and J.F. Lynch, "Inversion for sediment geoacoustic properties at the New England Bight", *Journal of the Acoustical Society of America* **114**, 1874–1887 (2003)

[56] M. Siderius, C.H. Harrison and M.B. Porter, "A passive fathometer technique for imaging seabed layering using ambient noise", *Journal of the Acoustical Society of America* **120**, 1315–1323 (2006)

[57] J.E. Quijano, S.E. Dosso, J. Dettmer, M. Siderius, L.M. Zurk and C.H. Harrison, "Bayesian geoacoustic inversion using wind-driven ambient noise", *Journal of the Acoustical Society of America* **131**, 2658–2667 (2012)

[58] J.E. Quijano, S.E. Dosso, J. Dettmer, L.M. Zurk and M. Siderius, "Trans-dimensional geoacoustic inversion of wind-driven ambient noise", *Journal of the Acoustical Society of America* **133**, EL47–EL53 (2012)

[59] J. Bonnel, C. Gervaise, P. Roux, B. Nicolas and J. Mars, "Modal depth function estimation using time-frequency analysis", *Journal of the Acoustical Society of America* **130**, 61–71 (2011)

[60] J. Bonnel and N.R. Chapman, "Geoacoustic inversion in a dispersive waveguide using warping operators", *Journal of the Acoustical Society of America* **130**, EL101–EL107 (2011)

A SEMI-ANALYTICAL MODEL FOR NON-MACH PEAK PRESSURE OF UNDERWATER ACOUSTIC PULSES FROM OFFSHORE PILE DRIVING

Marshall V. Hall

Moya Crescent, Kingsgrove NSW 2208, Australia

marshallhall@optushome.com.au

The equations of motion for the axial and radial displacements in a hammered semi-infinite pile comprise a system of coupled partial differential equations which are solved by taking their Fourier Transforms. The impact generates a pulse of axial and radial vibrations (a bulge) that disperses slightly as it travels down the pile. The damping rate is high at frequencies close to the radial resonance frequencies of the pile. After the bulge arrives at a given depth, the axial displacement increases with time to an asymptote, whereas the radial displacement rapidly rises to a peak and then decays to zero. Although the bulge constitutes a moving sound source, the radiated peak pressure is computed as if it were stationary at a number of depths. The ratio of pressure to fluid particle velocity at the pile wall is obtained by assuming the pile to be in a homogeneous medium. The spectrum of radial displacement, which is subject to radiation loading, is expressed as a closed-form algorithm in terms of the hammer impact velocity, the radius and wall thickness of the pile, and the Poisson ratio, longitudinal sound-speed, and density of the pile material. The radial displacement algorithm is linked to two simple models for sound radiation from a cylinder: near-field from depth-independent vibration, and far-field from depth-dependent vibration. These models are applied to a published case for which radiated peak pressures were measured and computed at a fixed range from a steel pile, using a Finite Element Model. The near-field/ depth-independent model overestimates the peak pressure, since it assumes that the cylinder is of infinite length. The far-field/ depth-dependent model underestimates the observed peak pressure. If a sound source moves supersonically perpendicular to a sound propagation path then coherent multipaths arrive quasi-simultaneously (Mach waves). The first model over-estimates the Mach wave pressure from a finite cylinder, while the second model neglects Mach waves altogether. A non-rigorous method for estimating the Mach wave pressure is described.

INTRODUCTION

Offshore pile driving radiates regular pulses of loud noise underwater, and a substantial amount of data has been presented in the literature on the measured peak pressure of these pulses. The peak pressure at a horizontal range of 10 m can be in the region of 1 atmosphere (100 kPa). Pile driving pulses are "brief, broadband, atonal" and "characterised by a relatively rapid rise from ambient pressure to a maximal pressure value followed by a decay period that may include a period of diminishing, oscillating maximal and minimal pressures" [1]. The frequency of successive pile driving pulses (the blow rate) is usually between 15 and 30 per minute [2]. The individual pulse duration can vary between 15 and 90 ms, and is most likely to lie between 25 and 40 ms [3].

Although the quantity of descriptive data on underwater noise from offshore pile driving is large, there have been few papers that attempt to model the physics of the impact and the consequent sound radiation. It is generally accepted that the major underwater signals originate from radial vibration (bulging) of that portion of the pile that is submerged. Since the bulge travels downward faster than sound travels through water, the first arrival at a hydrophone will originate at a point on the pile a little shallower than itself, and the trailing signal will be due to multipaths from portions of the pile both above and below the originating point. A significant paper [4] reported

the use of a finite-element model of the sound generated by a simple impact hammer. The results were entirely numerical, and their sensitivities to the various input parameters cannot be ascertained by examining the paper. The dominating effect of the simultaneous arrivals of multipaths from the pile (the "Mach wave") was included [4].

There has been significant theoretical work on onshore pile driving, including analytical modelling [5-7]. These and other numerical models were concerned only with axial vibration however, and did not present material that could be significantly applied to radial vibration.

The objective of the present paper is to present a semi-analytical model for the peak pressure of non-Mach radiation, since such a model allows the relative importance of the driving parameters to be estimated. Although the effect of Mach waves is not treated explicitly, the results obtained do suggest a method by which it may be estimated.

ASSUMPTIONS

A pipe pile is modelled as a thin vertical cylindrical shell of an elastic material such as steel. Absorption of sound (conversion to heat) in the material is represented by a small loss factor. The pile is semi-infinite in length. Although other analyses have treated finite lengths and thus include echoes from the pile toe, this aspect is not addressed here. The upper

portion of the pile is in air and finite in length. The remainder is submerged in water of infinite depth. The hammer is a compressible solid vertical cylinder with the same density and Young modulus as the pile. It has a finite mass and therefore length. Reflections from the top of the hammer following impact are however neglected. Since the hammer is compressible, the initial velocity of the pile face is estimated by assuming the interfaces satisfy the principle of momentum conservation.

The hammer strikes the pile instantaneously and uniformly over its face, and does not cause the pile to twist or bend. The ensuing axial and radial displacements will therefore not vary significantly with azimuthal (polar) angle around the pile axis. Only the sound radiated shortly after impact is addressed.

Each of the two external media allows sound waves to radiate from the pile. The effect of the medium on the pile vibration is obtained by assuming the radial velocity of the pile wall generates strain in the external medium, and the consequent stress (pressure) has the same effect on the cylinder as if it were an external pressure applied to a cylinder in-vacuo [8]. The wall vibration is thus subject to feedback.

For a hydrophone at a given horizontal range from the pile and depth beneath the water surface, the problem of determining the pressure waveform from the moment the leading edge of the downward travelling bulge crosses the water surface until it reaches great depth is beyond the scope of the present paper. Instead, it is assumed that the peak pressure occurs a short time (the travel time for the horizontal range) after when the leading edge is at the same depth as the hydrophone. For the purpose of modelling, the bulge is considered to be vibrating at that fixed depth; the vertical motion of the bulge down the pile is neglected. The aperture of the pile that determines the waveform and hence peak pressure is the whole pile beneath the water surface.

The radial displacement algorithm to be produced will be linked to two simple models (near-field and far-field) for sound radiation from a cylinder. Modelling of Mach-wave multipaths that arrive simultaneously due to the supersonic speed of the sound source is included in the near-field model, but neglected in the far-field model.

It is assumed that reflection of underwater sound waves by the water surface has negligible effect on peak pressure. Most pile driving noise spectra have dropped to no more than 10% of their peak by a frequency of around 4 kHz. To replicate such data, sampling with a time resolution of 0.1 ms would suffice. If source and hydrophone are at a horizontal range and depths such that a few samples (say 4) of the direct arrival are taken before the surface reflection arrives then the peak pressure will not be affected by the reflection. This criterion requires a delay of 0.4 ms (which corresponds to a path difference in water of 0.6 m). In this paper, results for peak pressure will be presented only if the path difference between direct arrival and surface reflection is at least 0.6 m.

PILE VIBRATION

Equations of motion in the pile

The problem of a cylindrical shell being struck longitudinally has been modelled analytically only with a view to determining axial stress [5-7]. The similar problem of a solid slender cylindrical rod being struck by an incompressible mass has also been addressed [9, 10]. Although both of these analyses were concerned only with axial vibration, they did present concepts that are useful in analysing the generation of radial waves. In a general analysis of a rod vibrating at given frequency, a solution was obtained for the case in which torsion is absent and the axial and radial vibrations are independent of azimuth angle [9]. Using the boundary condition that the normal and shear stresses on the cylinder's lateral surface are zero, it was shown that for a slender rod the axial propagation speed is given approximately by

$$q_y = \sqrt{Y/\rho_s} \tag{1}$$

where Y and ρ_s are the Young modulus and density of the solid material. For steel, q_y is nominally 5000 m/s (whereas the separate sound and shear waves that occur in a steel block large in all three dimensions have speeds of approximately 5700 and 3100 m/s respectively).

In an analysis of an infinite cylindrical shell in-vacuo subject to an external pressure, equations of motion for each of the three types of vibration (axial, radial and azimuthal) have been presented [8]. Cylindrical axial and radial co-ordinates were used (z and r), and the respective components of displacement were denoted by u and w. It was assumed that the only external loading (p_a) acts normally to the cylindrical surface of the shell and is independent of azimuth. If torsion and bending are neglected, the equations of motion simplify to the following

$$u''(z, t) + w'(z, t)\, v/a - \ddot{u}(z, t)/q_h^2 = 0 \tag{2}$$

$$u'(z, t)\, v/a + w(z, t)/a^2 + \ddot{w}(z, t)/q_h^2 = p_a/\rho_s\, q_h^2\, h \tag{3}$$

where a is the cylinder external radius, h the wall thickness, z is distance along the cylinder axis from an arbitrary position, and t is time. Above each displacement (u or w), apostrophes and dots denote partial differentiation with respect to axial distance and time respectively. In a thin shell, there is no variation with radius. The symbol q_h is defined by

$$q_h = q_y / \sqrt{1 - v^2} \tag{4}$$

in which v is the Poisson ratio of the shell material. The bending rigidity of the shell is characterised by $h^2/12a^2$ [8]. This rigidity is neglected here, and the only term in which h appears in either of the equations of motion is the external loading term.

Initial velocity of pile face

The initial velocity of the pile face is obtained by applying the principle of momentum conservation to the infinitesimal bottom layer of the hammer and the infinitesimal top layer of the pile that are compressed during an infinitesimal time δt following impact [5]. The hammer is assumed to be a solid vertical cylinder made of the same material as the pile, and to have the same radius. The thicknesses of the infinitesimal

layers will both be $q_y \delta t$. Before impact, the total momentum $(v_h \delta M)$ of these two layers is that of the bottom layer of the hammer

$$v_h \delta M = v_h \rho_s \pi a^2 q_y \delta t$$

where v_h is the hammer velocity. After impact both the bottom face of the hammer and the top face of the pile have a common velocity (v_0) and the total momentum will be

$$v_0 \delta M + v_0 \delta m = v_0 \rho_s \pi a^2 q_y \delta t + v_0 \rho_s A q_y \delta t$$

where $A = 2\pi a h$ is the area of the annular pile face. Equating the prior and subsequent momentums yields

$$v_0 = v_h / [1 + 2h/a] \qquad (5)$$

For the [4] case, $a = 0.381$ m, $h = 0.0254$ m and $v_h = 7.6$ m/s; Eq. (5) produces an estimate of 6.7 m/s for v_0.

Initial conditions at impact

Since Eqs. (2) and (3) each have second order time derivatives their solutions will require two initial conditions. It is sufficient for each to specify two variables at one time for all vertical distances (depths) z. The pertinent initial conditions when $t = 0$ are that (a) the axial particle velocity is 0 at all values of z except $z = 0$ where it is v_0; (b) the radial particle velocity is zero for all z; and (c) both axial and radial displacements at $t = 0$ are zero for all z.

Boundary conditions at pile face

Since Eq. (2) also has a second order depth derivative, its solution will need two boundary conditions. It is necessary to provide two specifications of variables at any depths where events occur (the single depth $z = 0$ in the present scenario). It is also necessary that these specifications be applicable at all $t \geq 0$. One boundary condition is that since the pile is semi-infinite in length there will be an outgoing wave (for which the depth of a particular feature of an acoustic wave increases with time) but no incoming wave. If it did not include a term in w, Eq. (2) would be a wave equation in u with phase speed q_h. It will be assumed that the term in w does not cause reflections and that, as applies to the solution of any such wave equation in which z increases with time, the displacement will be a function of $z - q_h t$ as a single variable (rather than of $z + q_h t$). The second boundary condition arises from the mutual equation of motion for the hammer base and pile face (which remain in contact for a semi-infinite pile, since there is no reflection). The hammer compresses the pile face, which in return decelerates the hammer. The longitudinal stress at the pile face equals the product of Young modulus and strain. The strain $(\partial u / \partial z)$ near the pile face is negative since at a fixed time $t > 0$, u decreases monotonically with z to zero at $z = q_h t$. Since the hammer will be decelerated, its equation of motion will be

$$M\ddot{u}(0,t) = AY\partial u(z,t) / \partial z \quad (z = 0) \qquad (6)$$

where M is the hammer mass (axial strain in the hammer is neglected here). Since $u = u(z - q_h t)$ and thus $\frac{\partial u}{\partial z} = -\frac{1}{q_h}\frac{\partial u}{\partial t}$, Eq. (6) becomes

$$\ddot{u}(0,t) = -\Omega \dot{u}(0,t) \qquad (7)$$

in which $\Omega = AY/Mq_h$. Solving Eq. (7) for axial velocity of the pile face, while taking account of the initial value of the axial particle velocity (v_0), yields

$$\dot{u}(0,t) = v_0 \exp(-\Omega t) \ , \ t \geq 0 \qquad (8)$$

Integration of Eq. (8) yields

$$u(0,t) = v_0/\Omega \ [1 - \exp(-\Omega t)] \ , \ t \geq 0 \qquad (9)$$

The pile-face axial displacement asymptotes to v_0/Ω with increasing time.

A note on Fourier Transforms

In succeeding sections, Fourier Transforms (FT) will be taken of displacements and pressures as functions of time. In the mathematical definition of the forward FT, the integrand is the product of the function of time and $\exp(-i\omega t)$, while in the inverse Fourier Transform (IFT) the integrand is the product of the function of frequency and $\exp(+i\omega t)$ ($\omega = 2\pi f$, f being frequency). In recent decades, many publications written by physicists or engineers, including textbooks referred to in this paper, have interchanged these definitions. Since the numerical component of the present work uses routines in the International Mathematics and Statistics Library (IMSL), which conforms to the mathematical definition, that definition is adopted here. This definition is consistent with the assumption that the time dependence of a single-frequency (harmonic) variable is $\exp(+i\omega t)$ rather than $\exp(-i\omega t)$. Fourier Transforms of individual variables (u, w and p) will be denoted by the corresponding capital letters (U, W and P).

Boundary condition at the pile wall

If the pile is submerged in fluid, then Eq. (2) is unaffected but in Eq. (3) p_a changes from pressure applied to a cylinder in-vacuo to pressure exerted on the cylinder by the external compressible medium as a result of the cylinder's vibration (the pile radial vibration induces strain in the external fluid). The basic equation of acoustic motion in the fluid adjacent to the wall is

$$\partial p(r,z,t)/\partial r = -\rho \ddot{w}(z,t) \qquad (10)$$

the FT of which is

$$\partial P(r,z,\omega)/\partial r = \omega^2 \rho W(z,\omega) \qquad (11)$$

In deriving a relation between pressure and vibration at the wall, it will be assumed that the cylinder vibration is a downward travelling wave with an (initially unknown) phase velocity G which may be complex and vary with frequency. For time dependence $\exp(+i\omega t)$ the appropriate dependence on depth is $\exp(-i\omega z/G)$, and the radial vibration FT is expressed as

$$W(z,\omega) = W(0,\omega)\exp(-i\omega z/G) \qquad (12)$$

Because the wave equation is separable in cylindrical co-ordinates, it follows from Eq. (11) that the depth-dependence

of P must be the same as that of W [8], and may be expressed as

$$P(r,z,\omega) = R(r)\exp(-i\omega z/G)$$

Taking the FT of the wave equation in $p(r,z,t)$ produces the Helmholtz equation

$$\nabla^2 P + (\omega^2/c^2)\, P = 0$$

which yields the Bessel equation of order 0 for $R(r)$

$$R'' + R'/r + \xi^2 R = 0 \tag{13}$$

where

$$\xi^2 = \omega^2/c^2 - \omega^2/G^2 \tag{14}$$

Since the Hankel function of the second kind gives the appropriate dependence on range for time dependence $\exp(+i\omega t)$, the solution to this equation is $H_0^{(2)}(\xi r)$. The FT of the radiated pressure at horizontal range r from the cylinder axis is therefore given by

$$P(r,z,\omega) = A(z,\omega)H_0^{(2)}(\xi r) \tag{15}$$

where $A(z,w)$ must be chosen so that the acoustic particle velocity in the fluid adjacent to the cylinder surface equals the wall radial velocity. Using Eq. (15) to obtain $\partial P/\partial r$ yields

$$\partial P(r,w)/\partial r = -A(z,w)\xi H_1^{(2)}(\xi r) \tag{16}$$

Substituting Eqs. (11) and (12) into (16) yields A in terms of W

$$A(z,\omega) = -\rho\omega^2\, W(0,\omega)\exp(-i\omega z/G)/\,\xi H_1^{(2)}(\xi a) \tag{17}$$

hence

$$P(r,z,\omega) = -\rho\omega^2\, W(0,\omega)\exp(-i\omega z/G)\, H_0^{(2)}(\xi r)/\,\xi H_1^{(2)}(\xi a) \tag{18}$$

The FT of the Specific Acoustic Impedance (Z) at the wall ($r = a$) is thus

$$Z(a,\omega) = P(a,z,\omega)/i\omega W(z,\omega) = i\omega\rho H_0^{(2)}(\xi a)/\,\xi H_1^{(2)}(\xi a) \tag{19}$$

As would be expected from Eq. (11), Z is independent of z.

Solving the equations of motion

Equation (2) is an equation of motion in u but includes a term in w', while Eq. (3) is an equation of motion in w that includes a term in u'. In order to allow for effects that may be frequency dependent, these two equations are solved simultaneously by taking the FT of each. Since loading pressure is opposite in sign to radiated pressure, the FT of p_a in Eq. (3) ("P_a") is replaced by $P_a = -i\omega WZ$, and the following equations in U and W are obtained

$$U'' + W'v/a + (\omega^2/q_h^{\,2})\, U = 0 \tag{20}$$

$$vU'/a + W/a^2 - (\omega^2/q_h^2)\, W = -i\omega WZ_n/\rho_s h\; q_h^2 \tag{21}$$

in which the subscript n can have values of 1 or 2, denoting air and water respectively. The available information on $\dot{u}(z,0)$ has not been used in deriving Eqs. (20) or (21); it was instead used in deriving Eq. (9), which will be referred to later. Eq. (21) simplifies to

$$W = -vq_h^2 U'/aS_n^2(q_h) \tag{22}$$

where

$$S_n(q_h) = \sqrt{q_h^2/a^2 - \omega^2 + i\omega\, Z_n/\rho_s h}\quad, n = 1, 2 \tag{23}$$

The feedback to W caused by the pressure it generates in the external fluid is represented by the third term in Eq. (23) which, since it depends on ξ and hence on G, is unknown at this stage.

Axial vibration

Since Z_n does not vary with depth, differentiating Eq. (22) with respect to z and then substituting W' into Eq. (20) will yield

$$U'' + \omega^2/V_n^2(\omega)\, U = 0 \tag{24}$$

where

$$V_n(\omega) = q_h\, S_n(q_y)/S_n(q_h) \tag{25}$$

Since Eq. (24) is a standard Helmholtz equation with a depth-independent coefficient, $V_n(\omega)$ will be the phase velocity of the solution for U.

The next step is to find the appropriate solution to Eq. (24). The general solution is

$$U(z,\omega) = F(\omega)\exp(-i\omega z/V_n) + F_2(\omega)\exp(+i\omega z/V_n) \tag{26}$$

The terms in Eq. (26) correspond to waves travelling in opposite directions along the z axis, and it is necessary to determine which term corresponds to z increasing with time. Since the time dependence is $\exp(+i\omega t)$, the second term would result in u(z,t) depending on $t + z/V_n$, which is inappropriate, as discussed prior to Eq. (6). It follows that $F_2 = 0$.

Since q_y, q_h and Z_n and hence V_n are independent of z (within a given medium), the solution to Eq. (24) may be written as

$$U_n(z,\omega) = F(\omega)\exp(-i\omega z/V_n) \tag{27}$$

By taking the FT of Eq. (9) it can be seen that $F(\omega) = v_0/i\omega(\Omega + i\omega)$.

Radial Vibration

Differentiating Eq. (27) with respect to depth yields

$$U_n'(z,\omega) = -v_0\exp(-i\omega z/V_n)/V_n(\Omega + i\omega) \tag{28}$$

Substituting Eq. (28) into Eq. (22) yields

$$W_n(z,\omega) = \chi\exp(-i\omega z/V_n)/S_n(q_y)\, S_n(q_h)\, (\Omega + i\omega) \tag{29}$$

where

$$\chi = vv_0 q_h/a \qquad (30)$$

On comparing Eq. (29) with Eq. (12) it can be seen that $G = V$ (in the current context, the dependence on medium 'n' is not significant and is suppressed for clarity). The situation is that V is a function of $S(q_y)$ and $S(q_h)$ which in turn are functions of Z and hence of V

$$V = \varphi(V) \qquad (31)$$

where φ is the function represented by Eqs. (25), (23) and (19). Equation (31) is solved by iteration; one starts with a trial solution $V^{[0]}$ and then computes successive approximations [11]

$$V^{[j+1]} = \varphi(V^{[j]}) \; j = 0, 1, 2 \qquad (32)$$

The iteration is terminated at $j = J$ when the ratio $|V^{[J]} - V^{[J-1]}|/|V^{[J]}|$ is sufficiently small. For the current problem, 10^{-6} was found to be suitable as the terminating ratio, and the Fortran "huge" number ($\sim 10^{38}$) was found to be suitable for $V^{[0]}$. J was observed to be 2, 3 or 4.

Spectra of phase velocity and damping rate

For an external medium of air, the iterations $V^{[1]}$ and $V^{[J]}$ are found to be indistinguishable at any frequency. The real part of $V_1(\omega)$ for the [4] case is shown in Figure 1 over frequencies from 0 to 10 kHz. It is q_y at zero frequency, and asymptotes to q_h at high frequency. The two radial resonance frequencies of a cylindrical shell are $q_y/2\pi a$ and $q_h/2\pi a$ [9]. For the [4] case the corresponding resonance frequencies are 2089 and 2183 Hz. Real $\{V_1\}$ is small at the lower resonance, and large at the higher. Thus Real $\{V_1\}$ increases rapidly from a small to a large value as frequency increases (by 4.5%) from the lower resonance to the other.

The damping rate in decibels per metre is given by

$$D = -\omega \; Imag(1/V_1) \; 20/\ln 10 \qquad (33)$$

in which the factor 20/ln10 converts nepers to decibels. The result for the damping rate in air-exposed pile (D_1) for the [4] case is shown in Figure 2, over frequencies from 0 to 10 kHz.
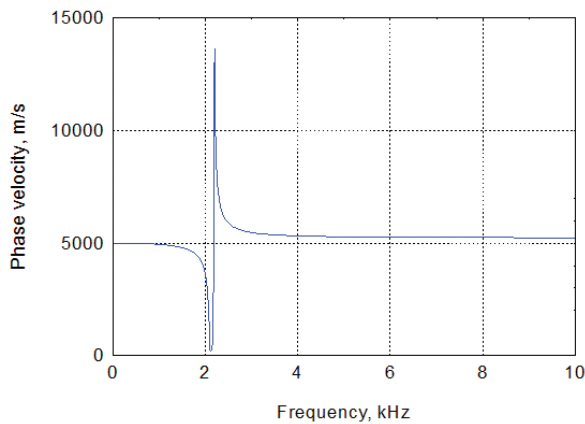
It is small at most frequencies, but large (up to 57 dB/m) at frequencies between the two resonance frequencies.

In water, the real parts that correspond to the iterations $V^{[1]}$ and $V^{[J]}$ are found to be distinguishable in the neighbourhoods of the two frequencies where they have their minimum and maximum values. The initial and final iteration values of Real $\{V_2\}$ for the [4] case are shown in Figure 3. They vary smoothly (but not monotonically) with frequency. Each is q_y at zero frequency, falls to a minimum (around 1% lower than q_y at 1.4 kHz for the [4] case), increases to a maximum (around 3% above q_h at 2.7 kHz for the [4] case), and then asymptotes to q_h as frequency increases further.

In a water medium, the damping rates that correspond to the iterations $V^{[1]}$ and $V^{[J]}$ are found to be distinguishable in the neighbourhood of the frequency where they have their maximum values. The results for the [4] case are shown in Figure 4. Each is zero at zero frequency, and rises to a broad peak at 2.1 kHz. If there were no absorption in the pile, D_2 would asymptote to zero as frequency approaches and passes 10 kHz. The presence of absorption in steel with $Q=500$ [12] causes both D_1 and D_2 to asymptote to a linear increase with frequency (and reach 0.53 dB /m at 50 kHz).

One difference between a shell and solid cylinder is that, as may be seen from Figures 1 and 3, the propagation speed of high-frequency axial vibrations along a shell is higher by a ratio of q_h/q_y. For steel ($v = 0.29$) the high-frequency propagation speed along a thin shell is 4.5% higher than along a solid rod, giving a nominal value of 5225 m/s. The rationale for these behaviours can be seen by considering the three terms in each of the numerator and denominator of Eq. (25), as given in Eq. (23). The constant terms, which are the only terms that differ between numerator and denominator, are respectively q_h^2/a^2 and q_y^2/a^2. At high frequencies, the functions $S_n(q_y)$ and $S_n(q_h)$ will asymptote to a common value (and V will asymptote to q_h) when either the terms in ω^1 exceed the constant terms, or the terms in ω^2 exceed the constant terms. At low frequencies, these functions will approach different values.

Figure 1. Real part of phase velocity in the air-exposed portion of a pile for the [4] case
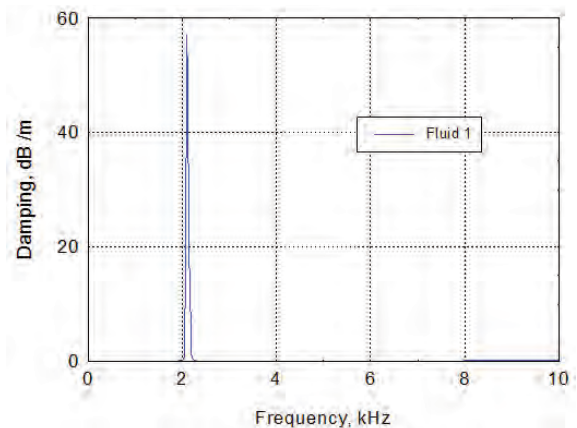

Figure 2. Damping rate in the air-exposed portion of a pile for the [4] case

Damping of shell vibration with axial distance

The cylinder material is modelled with a small loss factor, represented by making the Young modulus complex and assigning to it an imaginary part of Y/Q. Any additional damping must be attributed to the loss of energy through acoustic radiation. It follows from Eqs. (27) and (29) that, at angular frequency ω:

(a) axial and radial phase speeds are both V_n (which approaches q_y as frequency approaches zero in both air and water);

(b) axial and radial damping rates are both $-$ Imag $\{\omega/V_n\}$ nepers per unit depth.

The next step is to compute W_2 at depth z below the water surface, according to:

$$W_2(H,z,w) = \chi \exp(-i\omega H/V_1 - i\omega z/V_2)/S_2(q_y)S_2(q_h)(\Omega + i\omega) \quad (34)$$

where H is the height of the pile face above the water surface. Attenuation of W_2 with increasing H or z is computed automatically due to the positive imaginary parts of V_1 and V_2.

To enhance clarity in distinguishing between depth along the pile and hydrophone depth, the latter will henceforth be denoted by a different symbol (ξ) in any context where they could be different in principle. In view of the assumption that the peak pressure at position (r,ξ) will arrive from that portion of the pile at the same depth (the closest), ξ and z will generally have the same value in the present derivation. For the [4] case, $H = 5.4$ m and the minimum and maximum values of ξ were 4.9 and 10.5 m. The magnitudes of the spectrum $|W_2(H,z,\omega)|$ at both $z = 4.9$ and 10.5 m are shown in Figure 5 (in decibels). Although the spectra were computed with a Nyquist frequency of 50 kHz, the maximum frequency shown is 10 kHz (the results at higher frequencies did not reveal any unexpected features). It can be seen that the high damping in the air-exposed pile between the radial resonance frequencies causes a deep minimum there, and that the spectra decay significantly with depth, especially between 1 and 4 kHz. The results for W that correspond to the iterations $V^{[1]}$ and $V^{[J]}$ are found to be indistinguishable at any frequency.

The IFTs of $W_2(H,z,\omega)$ have been calculated at both $z = 4.9$ and 10.5 m and the magnitudes of the resulting waveforms $|w_2(H,z,t)|$ are shown in Figure 6. The waveforms rise rapidly to peaks of around 170 and 152 μ and then decay quasi-exponentially with a time constant of 3 ms. Compared with the shallower waveform, the deeper waveform is 1 ms later, and its amplitude is 11% smaller.
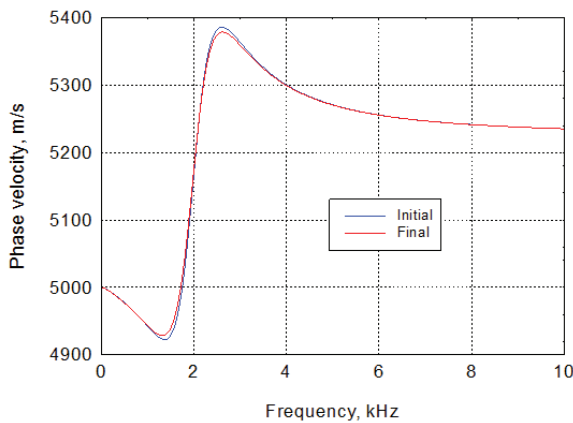
Figure 3. Real part of Phase velocity in the water-exposed portion of a pile for the [4] case: Blue (first iteration); red (final iteration).

Figure 5. Magnitude of the radial displacement spectra at depths in water of 4.9 and 10.5 m for the [4] case

Figure 4. Damping rate in the water-exposed portion of a pile for the [4] case: Blue (first iteration); red (final iteration)

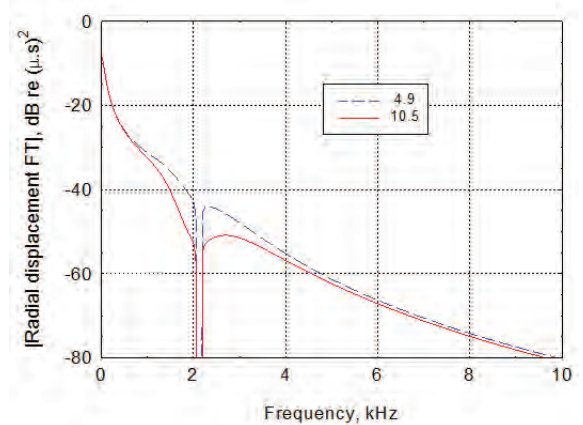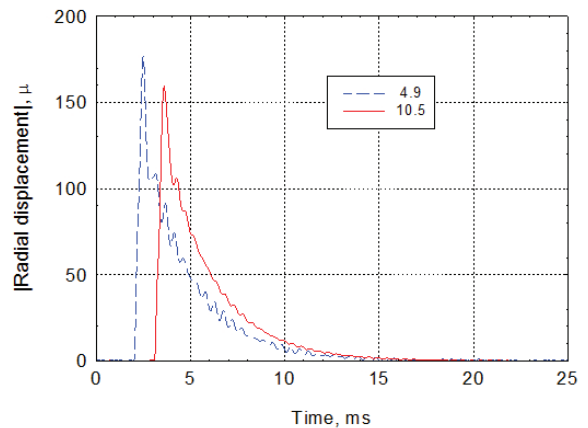Figure 6. Magnitude of the radial displacement waveforms at depths in water of 4.9 and 10.5 m for the [4] case

UNDERWATER RADIATED SOUND PRESSURE

The sound pressure radiated into the surrounding fluid by a vertical cylinder will be computed using two models for acoustic radiation from a vibrating cylinder. The first model assumes that the cylinder vibration is independent of depth, and the second allows for it to vary with depth. Both models assume the external medium to be fluid, homogeneous and unbounded. The sound speed and density of the external medium will be denoted by c and ρ.

Depth-independent cylinder vibration

If an infinite vertical cylinder were to vibrate radially with a depth-independent amplitude, then $V(\omega)$ would be infinite, ξ would become ω/c and $P(r,z,\omega)$ would be given by a simplified version of Eq. (18)

$$P(r,z,\omega) = -\rho c\omega W(0,\omega) \exp(-i\omega z/V) H_0^{(2)}(\omega r/c)/ H_1^{(2)}(\omega a/c) \quad (35)$$

If V were treated consistently as infinite, then the exponential term in Eq. (35) would be unity. Equation (35) would be independent of z and equivalent to that presented by [13] for radiation from an infinite cylinder vibrating uniformly. The exponential term will be retained here however, and Equation (35) will be referred to as the "hybrid Morse" model. For the [4] case, $r = 12$ m, and the magnitudes $|P(12,z,\omega)|$ computed from Eq. (35) are shown in Figure 7. $W(H,z,\omega)$ is again given by Eq. (34) for both $z = 4.9$ and 10.5 m, and $H = 5.4$ m. Since Eq. (35) will give the exact pressure spectrum only if W is independent of depth, these results are approximate; they assume that the cylinder vibrates at all depths with the value computed at z.

The IFTs of $|P(12,z,\omega)|$ have been computed for both $z = 4.9$ and 10.5 m, and the resulting waveforms $|p(12,z,t)|$ are shown in Figure 8. The peak pressure is 160 kPa at 4.9 m and 120 kPa at 10.5 m, a decrease of 25%.

Results have been obtained for the hybrid-Morse peak pressures for hydrophones at a range of 12 m and depths from 1 to 12 m, and are shown in Figure 9. For each of these calculations the source depth was set to the hydrophone depth. The individual data points labelled "Reinhall" are the peaks of the individual waveforms at nine hydrophone depths, as read from Figure 11 in [4]. The Reinhall results increase significantly with depth, whereas the hybrid-Morse pressures decay with depth due to the decay in $W(z,\omega)$, and are also too high. Being too high is to be expected, since this model assumes the cylinder to be infinitely long and vibrating with uniform phase.
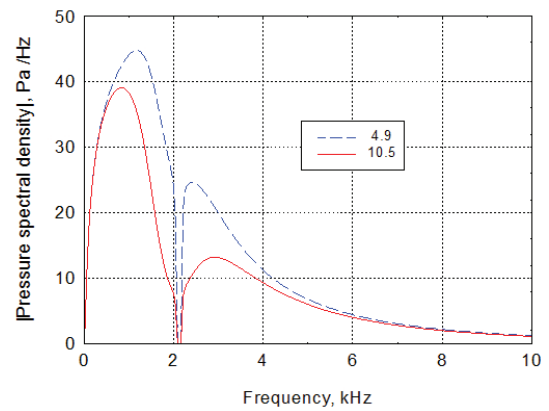
Figure 7. Magnitude of the "hybrid Morse" sound pressure spectra at depths in water of 4.9 and 10.5 m for the [4] case. Obtained by applying the Morse acoustic model to $W(z,\omega)$ as per Eq. (34)
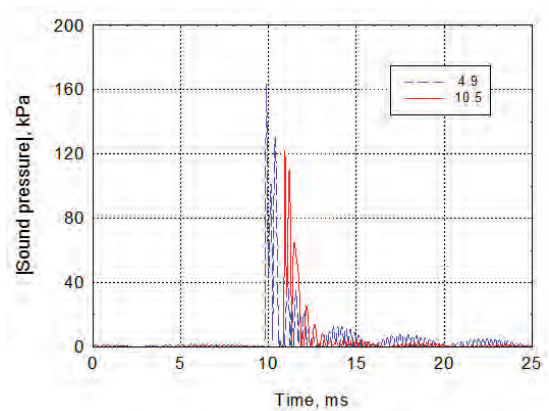

Figure 8. Magnitude of the "hybrid Morse" sound pressure waveforms at depths in water of 4.9 and 10.5 m for the [4] case. Obtained by taking the IFTs of the spectra whose magnitudes are shown in Figure 7
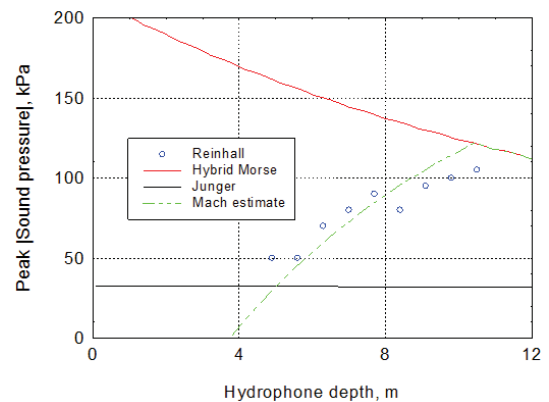

Figure 9. Peak pressure of waveforms computed for hydrophones at a range of 12 m and at depths from 0.1 to 12 m for the [4] case. 'Reinhall' refers to results read from [4], 'Hybrid Morse' refers to IFT of Eq. (35), 'Junger' refers to IFT of Eq. (38), and 'Mach Estimate' refers to Eq. (42)

Depth-dependent cylinder vibration

A method that allows for vibration to vary with distance along a cylinder has been presented by [8]. The derivation of this cylinder vibration model takes the spatial FT of the vibration's depth dependence, and uses the property that the component at each wavenumber is invariant with depth (just as a spectral component of a temporal waveform is invariant with time). The sound pressure component as a function of wavenumber is computed, and for the scenario of no azimuthal dependence, the spatial IFT presented in [8] simplifies (after converting the time dependencies) to

$$P(r,z,\omega) = \omega^2\rho W(0,\omega)\int_{-\infty}^{\infty} H_0^{(2)}(\xi r)\, \tilde{f}(\gamma,\omega)\, \exp(i\gamma z)/2\pi\xi H_1^{(2)}(\xi a)d\gamma$$
(36)

where

$$\xi = \sqrt{k^2 - \gamma^2}$$

$$k = \omega/c$$

γ is axial (depth) wavenumber

$\tilde{f}(\gamma,\omega)$ is the spatial FT of the ratio $W(z,\omega)/W(0,\omega)$ as a function of z

$$\tilde{f}(\gamma,\omega)W(0,\omega) = \int_0^{\infty} W(z,\omega)\, \exp(-i\gamma z)\, dz$$
(37)

It is evident that Eq. (36) cannot cater for a radial displacement $w(z,t)$ that also varies with time due for example to motion of the sound source. A description will be required of $P(r,z,\omega)$ at various depths of the bulge below the pile face, and thus at various times. It will therefore be necessary to re-compute P at each such time.

If r is sufficiently large that the large-argument asymptotic value of the Hankel function can be used for most of the values of ξ in Eq. (36), then an approximate simple expression for the pressure spectrum can be obtained using the method of stationary phase to simplify the integral [8]. An argument of at least 2π makes the approximation reasonable, and since $r = 12$ for the [4] case, this assumption will be reasonable for a minimum k of $2\pi/12$ m^{-1}, which in seawater corresponds to minimum frequency of around 125 Hz. Thus only a very small portion of the spectrum will be rendered in significant error by this approximation. According to [8], Eq. (36) will simplify to

$$P(r,\zeta,\omega) = i\rho\, \exp(-ikr)\omega^2 \tilde{f}(k\cos\theta,\omega)W(0,\omega)/\pi krH_1^{(2)}(ka)$$
(38)

where $\theta = \arctan(r/(\zeta-z))$. Equations (36)-(38) will be referred to as the "Junger" model. If the depth of the leading edge of the bulge (z) is the same as the depth of the hydrophone (ζ) then $\theta = \pi/2$ and the first argument of the spatial FT will be zero. From Eqs. (29) and (37), the spatial FT will be given by

$$\tilde{f}(0,\omega) = \int_0^{\infty} W(z,\omega)\, dz\, /\, W(0,\omega) = V/i\omega$$
(39)

Taking the spatial FT of $W(z,\omega)$ renders P independent of ζ. Computed results for the spectrum $P(12,\omega)$ for the [4] case, with $\tilde{f}(0,\omega)$ given by Eq. (39), are shown in Figure 10. The

peak of the spectrum is about 75% less than those of the hybrid-Morse spectra shown in Figure 7.

The corresponding pressure waveform has been obtained by taking the temporal IFT of Eq. (38), and the result is shown in Figure 11. The peak pressure is 32 kPa, which is around 80% less than the corresponding results in Figure 8. The Junger result is independent of source /hydrophone depth, since this model takes the wavenumber FT along the (infinite) length of the pile, which is independent of depth. It is ironic that a model that caters for depth-dependent cylinder vibration produces a sound pressure that is independent of depth.

The Junger peak pressure of 32 kPa for hydrophones at a range of 12 m is shown (by the horizontal line) in Figure 9. The whole Junger curve is lower than the smallest Reinhall peak pressure.
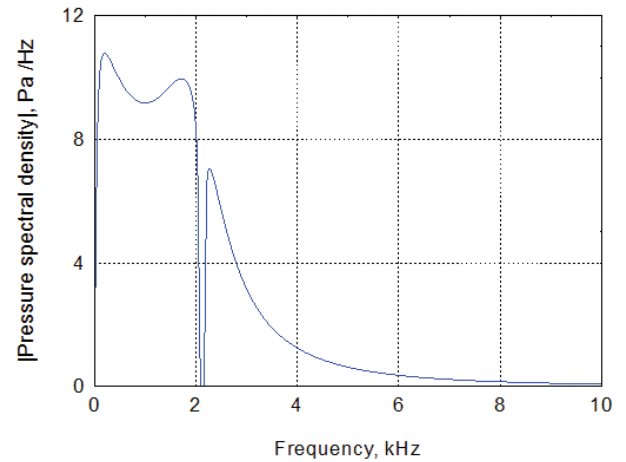
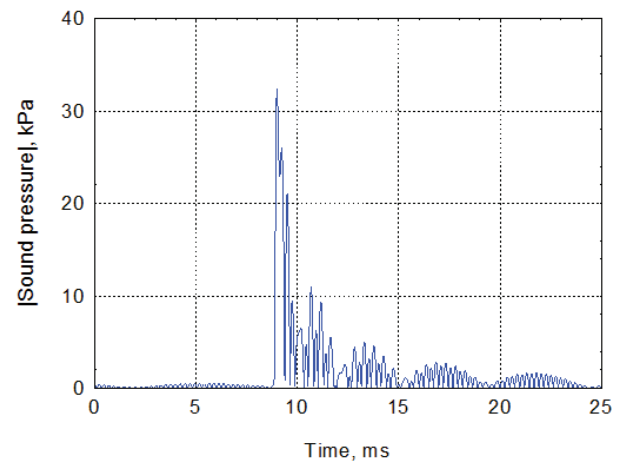Figure 10. Magnitude of the Junger sound pressure spectrum in water for the [4] case

Figure 11. Magnitude of the Junger sound pressure waveform in water for the [4] case. Obtained by taking the IFT of the spectrum whose magnitude is shown in Figure 10

Estimation of Mach-wave pressures

The travel time of a pulse from a water entry at (0,0) to a hydrophone at (r, ξ) will be given by

$$t(r, \zeta) = z/q + \sqrt{(z-\zeta)^2 + r^2/c} \qquad (40)$$

where z is the depth of the bulge on the pile from which the pulse emanates. If $q > c$ then at any ζ this function has a minimum, which occurs at

$$z - \zeta = -r / \sqrt{q^2/c^2 - 1} \qquad (41)$$

In the r - z plane this corresponds to a straight line: at $r = 0$, $z = \zeta$; and $dz/dr = -1/\sqrt{q^2/c^2 - 1}$. If ϕ is the depression angle of this line relative to the horizontal r-axis, then $\tan\phi = dz/dr$ and thus $\sin\phi = c/q$. For the [4] case, $\phi = 17°$. At a given (r, ζ), the first arrival originates from position $(0, z)$ on the pile where z is given by Eq. (41). Successive pulses arrive simultaneously from points both above and below that z. (For the hybrid-Morse model for which q is effectively infinite, $\phi = 0$ and $z = \zeta$.) For source depths (z) from 0.1 to 12.5 m (the seafloor depth in the [4] case), the arrival times at range 12 m and five hydrophone depths from 4.9 to 10.5 m are shown in Figure 12. At a hydrophone depth of 7.7 m for example, the first pulse arrived at 10.3 s and originated from a depth of 4.0 m (at $r = 12$ m, Eq. (41) gives -3.7 m for $z - \zeta$).

The feature of the curves in Figure 12 that is relevant to simultaneous arrivals is the region around the minimum. For $\zeta = 7.7$ m for example, the arrival time is 10.7 s for a pulse from the surface, decreases to 10.3 at the minimum ($z = 4.0$), and then increases and attains its surface value at $z = 7.6$ m; this arrival will be referred to as the "surface-coincident" arrival. Pulses that emanated from the pile at both $z = 0$ and $z = 7.6$ m arrived simultaneously at (12,7.7), and the continuum of pulses that emanated at intervening depths all arrived within a time span of 0.4 s.

The results for source depth of both the first and surface-coincident arrivals have been computed for the [4] case and are shown as functions of hydrophone depth in Figure 13. The curves are exactly linear and quasi-linear respectively, and extrapolate to $\zeta = 3.7$ m at $z = 0$, in accordance with Eq. (41). Thus for $\zeta \leq 3.7$ m, simultaneous arrivals would not occur at a range of 12 m (although they would at a shorter range).
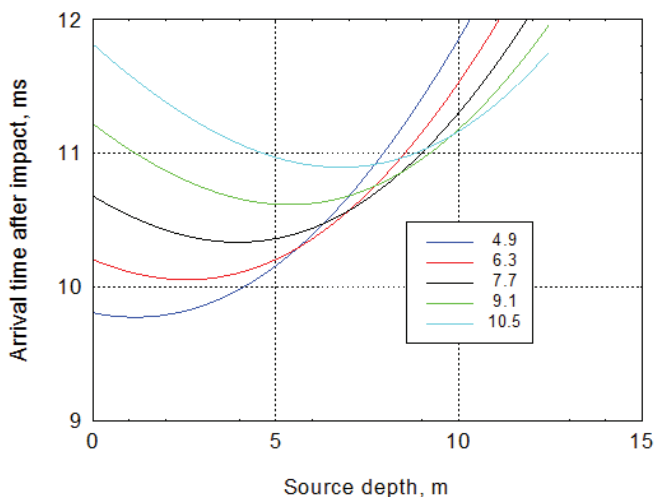
Since there is little variation in arrival time for source depths between zero and the surface-coincident depth (Zsc), it will be hypothesised that the Mach-wave pressure is due to an equivalent finite uniform (virtual) cylinder with length equal to Zsc. The formula postulated as an estimate of the Mach-wave pressure is

$$p\,Mach(\zeta) = p\,Morse(\zeta) \times Zsc(\zeta)/D\,, \;\; Zsc \leq D \qquad (42)$$

$$p\,Mach(\zeta) = p\,Morse\,(\zeta), \qquad Zsc > D$$

where D is the seafloor depth. The results are shown in Figure 9, and are seen to be a reasonable estimate of the results reported by [4].

CONCLUSIONS

A model of the vibration of a cylindrical shell struck by a hammer has been derived with some rigour. The model includes coupling of the axial and radial vibration. It has been used to predict peak pressure of the pulse radiated into water by linking with both a "hybrid Morse" infinite cylinder and a "Junger" depth-dependent cylinder. In the first case, the predicted peak pressure is higher than reported results of an accurate Finite-Element model [4]; this is attributed to the quasi-uniform cylinder being infinite in length. The FE peak pressures increased from 50 to 100 kPa as the hydrophone depth increased from 5 to 11 m, whereas the hybrid-Morse pressure decreased from 160 to 120 kPa over the same interval. In the second case, the predicted peak pressure is constant at 32 kPa. An ad-hoc hypothesis, that the pressure is given by the product of the hybrid-Morse pressure and the ratio of hydrophone depth to seafloor depth, yields a reasonable result for the particular case that was tested.
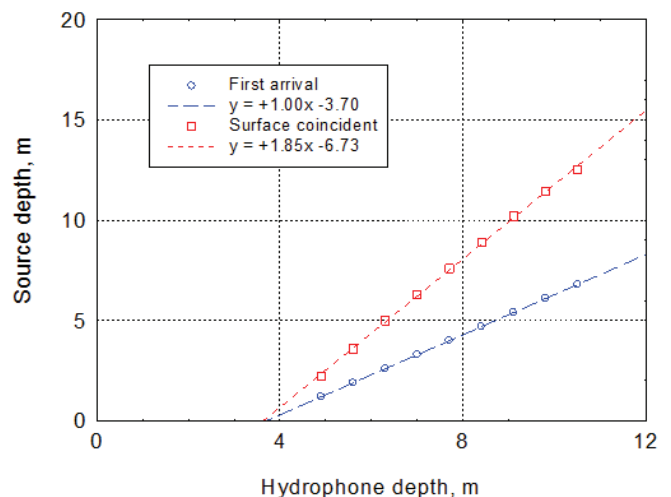

Figure 12. Arrival times at range 12 m as a function of source depth on a pile. Hydrophone depths range from 4.9 to 10.5 m in steps of 1.4 m, as indicated in the legend

Figure 13. Source depths of both the first (Z_1) and surface-coincident arrivals (Zsc) as functions of hydrophone depth

ACKNOWLEDGMENT

REFERENCES

[1] B.L. Southall, A.E. Bowles, W.T. Ellison, J.J. Finneran, R.L. Gentry, C.R. Greene Jr., D. Kastak, D.R. Ketten, J.H. Miller, P.E. Nachtigall, W.J. Richardson, J.A. Thomas, and P.L. Tyack, "Marine mammal noise exposure criteria: initial scientific recommendations", *Aquatic Mammals* **33**, 411-521 (2007)

[2] R. Matuschek and K. Betke, "Measurements of construction noise during pile driving of offshore research platforms and wind farms", *Proceedings of the NAG/DAGA 2009 International Conference on Acoustics*, Rotterdam, The Netherlands, 23-26 March 2009, pp. 262-265

[3] T.J. Carlson and M.A. Weiland, *Dynamic Pile Driving and Pile Driving Underwater Impulsive Sound*, final report, Battelle–Pacific Northwest Division, Richland, Washington, 2007

[4] P.G. Reinhall and P.H. Dahl, "Underwater Mach wave radiation from impact pile driving: Theory and observation", *Journal of the Acoustical Society of America* **130**, 1209-1216 (2011)

[5] D.V. Isaacs, "Reinforced concrete pile formulae", *The Journal of the Institution of Engineers Australia, Transactions of the Institution* **3**, 305-323 (1931)

[6] V.H. Glanville, G. Grime, E.N. Fox and W.W. Davies, *An investigation of the stresses in reinforced concrete piles during driving*, Technical Paper No. 20, Building Research, Department of Scientific and Industrial Research, London, 1938

[7] B. Hansen and H. Denver, *Wave equation analysis of a pile – an analytic model*, Technical Report No. 17, Danish Geotechnical Institute, 1984. Available at www.geoteknisk.dk/media/5392/geo.technical.report.no.17.pdf

[8] M.C. Junger and D. Feit, *Sound, Structures, and Their Interaction* (second edition), Acoustical Society of America, New York, 1993

[9] A.E.H. Love, *A treatise on the mathematical theory of elasticity* (fourth edition), Dover Publications, New York, 1944

[10] S.P. Timoshenko and J.N. Goodier, *Theory of elasticity* (third edition), McGraw-Hill Kogakusha Ltd, Tokyo, 1970

[11] G.A. Korn and T.M. Korn, *Mathematical Handbook for scientists and engineers* (second edition), McGraw-Hill Book Company, New York, 1968

[12] J.S. Sastry and M.L. Munjal, "Response of a multi-layered infinite cylinder to a plane wave excitation by means of transfer matrices", *Journal of Sound and Vibration* **209**, 99-121 (1998)

[13] P.M. Morse and K.U. Ingard, *Theoretical Acoustics*, McGraw-Hill Book Company, New York, 1968

Inter-Noise 2014

MELBOURNE AUSTRALIA 16-19 NOVEMBER 2014

The Australian Acoustical Society will be hosting Inter-Noise 2014 in Melbourne, from 16-19 November 2014. The congress venue is the Melbourne Convention and Exhibition Centre which is superbly located on the banks of the Yarra River, just a short stroll from the central business district. Papers will cover all aspects of noise control, with additional workshops and an extensive equipment exhibition to support the technical program. The congress theme is *Improving the world through noise control*.

Key Dates
The dates for Inter-Noise 2014 are:
Abstract submission deadline: 10 May 2014
Paper submission deadline: 25 July 2014
Early Bird Registration by: 25 July 2014

Registration Fees
The registration fees have been set as:

Delegate	$840	$720 (early bird)
Student	$320	$255 (early bird)
Accompanying person	$140	

The registration fee will cover entrance to the opening and closing ceremonies, distinguished lectures, all technical sessions and the exhibition, as well as a book of abstracts and a CD containing the full papers.

The Congress organisers have included a light lunch as well as morning and afternoon tea or coffee as part of the registration fee. These refreshments will be provided in the vicinity of the technical exhibition which will be held in the Main Foyer.

The Congress Banquet is not included in the registration fee.

Technical Program
After the welcome and opening ceremony on Sunday 16 November, the following three days will involve up to 12 parallel sessions covering all fields of noise control. Major areas will include Community and Environmental Noise, Building Acoustics, Transport Noise and Vibration, Human Response to Noise, Effects of Low Frequencies and Underwater Noise.

A series of distinguished lectures will cover topics such as:
- Acoustic virtual sources
- Wind turbine noise
- Active noise control
- Aircraft noise
- Soundscapes

Organising and Technical Committee
- Congress President: Dr Norm Broner
- Technical Program Chair: Adjunct Professor Charles Don
- Technical Program Co-Chair: Adjunct Professor John Davy
- Technical Program Advisor: Mrs Marion Burgess
- Proceedings Editor: Mr Terry McMinn
- Sponsorship and Exhibition Manager: Dr Norm Broner
- Congress Treasurer: Ms Dianne Williams
- Social Program Chair: Mr Geoff Barnes
- Congress Secretariat: Ms Liz Dowsett

Further details are available on the congress website
www.internoise2014.org

METHODS TO CLASSIFY OR GROUP LARGE SETS OF SIMILAR UNDERWATER SIGNALS

L. J. Hamilton

Defence Science & Technology Organisation (DSTO), 13 Garden St, Eveleigh, NSW 2015
Les.hamilton@dsto.defence.gov.au

Three methods of classifying large sets of acoustic signals are briefly discussed. The purpose of the discussion is to broadcast the existence and summary details of the methods to a wider audience. Large implies that hundreds of signals to several tens of thousands of signals may be detected. The signals of interest are broadly Gaussian, Rayleigh, or sinusoidal in shape, and of finite duration, such as seabed echoes and beaked whale chirps. The classification methods are (1) feature analysis, (2) direct statistical clustering of signals treated as single-valued curves, and (3) matched filtering with use of normalisations and kurtosis of the cross-correlation function output of the matched filter. Method (1) has been used for many years in several fields of science. It is suitable for many applications, but classifies on proxies, not the actual signals, which may lead to loss or distortion of information. Method (2) is a post processing operation suitable for signals with well defined signal to noise ratio which can be well aligned in time. Although simple in concept, it is a recent innovation, as it was apparently not previously realised that it could be done. A suitable clustering algorithm can classify signals into groups or sets where each set has a different average shape from the other sets, and can also classify signals forming quasi-continuums, such as those which can be viewed as morphing from one shape to another. Method (3) is suitable for detection and classification of stereotypical signals (those with strongly repeating waveform or signal shape), including weak signals in noisy backgrounds. In the usual application of matched filtering, classification is made solely on the un-normalised amplitude of the cross-correlation function. A novel extension of method (3) is to provide a confidence estimate for the classification through the kurtosis of the normalised autocorrelation function. The kurtosis is observed to be related to the degree of signal distortion or malformation relative to the template signal. When incoming signals of the same type vary in energy and degree of distortion or malformation, this scheme greatly outperforms standard matched filtering.

INTRODUCTION

Underwater acoustics may detect and classify inputs received by hydrophones over time intervals which can yield high numbers of received signals. Detection and processing may be carried out in real-time or executed as a post-processing activity. For example, real-time monitoring of offshore sites may be carried out to determine the presence of marine mammals, and to find to which species they belong.

The first step in signal processing is signal detection, often in the presence of noise or unwanted signals. The signals of interest to the present paper are broadly Gaussian, Rayleigh, or sinusoidal in shape and of finite duration (for examples see Figures 1 and 2). A second step is signal pre-processing or conditioning, where acoustic propagation effects and removal of artefacts caused by the measuring system are allowed for. The present paper does not specifically deal with these topics. It assumes signal pre-conditioning, and is instead concerned with the problem of classifying preprocessed received signals into groups with similar properties, particularly shape. When received signal types are very different from each other in one or more properties this is not necessarily a difficult problem. Problems can arise if, for example, signal shapes morph smoothly from one shape to another. This situation arises in the classification of seabed echoes stimulated by echosounders, or other active sonar types, when seabed properties along a transect change smoothly from one type to another, and consequently so do the echo shapes. Classification methods

discussed are (1) feature analysis, (2) unsupervised statistical clustering applied directly to single-valued curves, and (3) matched filtering with normalisations and use of kurtosis as a classification parameter. These are versatile and relatively routine signal processing methods, suitable for a wide range of detection and classification applications. However, the direct clustering method for classification of signals is a recent innovation which is not widely known. Nor perhaps is an appreciation of the need for normalisation in matched filtering, or the fact that there is more useful information from the output of matched filtering than an amplitude.

THREE METHODS FOR CLASSIFICATION OF UNDERWATER SIGNALS

Method 1 – Classification through feature detection (reduction of a signal to a set of proxy parameters) and statistical clustering

When detection of any signal at all is important then the exceedance of a threshold value for a single parameter, such as signal to noise ratio, may be sufficient to decide a signal has been received. In the more general case of classification, rather than detection, two or more parameters may be required to decide that a particular type of signal has been received. Feature detection classifies on time and/or frequency domain properties of signals such as peak height, peak position relative to the start of the signal, duration, kurtosis, skewness, Fourier and wavelet transform coefficients, fractal dimension, and

time domain or spectral moments. In cases when it is not known which proxies are optimal for classification, such as when these may vary in time or space, hundreds of proxies may be formed [1]. Formation of proxies may require curve fitting, application of assumed models of signal shape or signal formation, and specification of user criteria such as what height, width, and separation define peaks. Multimodal signals can cause complications for feature detection. In post processing the features or proxies (m in number) may be subject to Principal Components Analysis (PCA) to reduce them to n independent or orthogonal principal components ($n < m$). The principal components are combinations of the features which best describe a particular data set in terms of the variance. The actual number of components used for classification is typically chosen to account for 95% or more of the variance of the data set [1]. However, three components are often used, and the remainder discarded, so as to enable visualisation in a pseudo three-dimensional space as point data. The relation of the principal components to echo properties or to physical processes may not be known, but a visual assessment of the distribution of the proxy points is used to discover any trends or distribution patterns which can be used to segment the point distribution into classes. Automatic segmentation of the three dimensional point data can be made by statistical clustering, simulated annealing, or simple segmentation into voxels (a voxel is a volume element in three dimensional space, analogous to a pixel or picture element in two dimensions). Examples of feature detection followed by PCA and simulated annealing or clustering may be found in [1] where these techniques are applied to seabed echoes based on proxies calculated in time and frequency domains.

Statistical Clustering

Statistical clustering views the n proxy components (or the n parameters) as coordinates in an n-dimensional space. Each set of coordinates identifies an n-dimensional point in the space. The function of clustering is to automatically find if points form discrete groups (clusters) which can be used as classes. This process begins by finding which points are close together and which are far apart. In a general framework, distances between any two points are calculated by measures such as the Minkowski distance:

$$\left(\sum_{i=1}^{n} |x_i - y_i|^p \right)^{1/p} \qquad (1)$$

where $p >= 1$, and x_i and y_i are vectors with the same number of elements (n in the present notation). The extended or n-dimensional Euclidian metric is given for $p = 2$, and the n-dimensional Manhattan metric for $p = 1$. Other metrics, such as entropy, may be suitable for some data sets. Points are assigned to trial groups or clusters, and in an iteration process are then moved to other clusters if this improves a global cost function. The statistical clustering algorithm employed in the present work is the CLARA (Clustering LARge Applications) algorithm of [2], described in the next section.
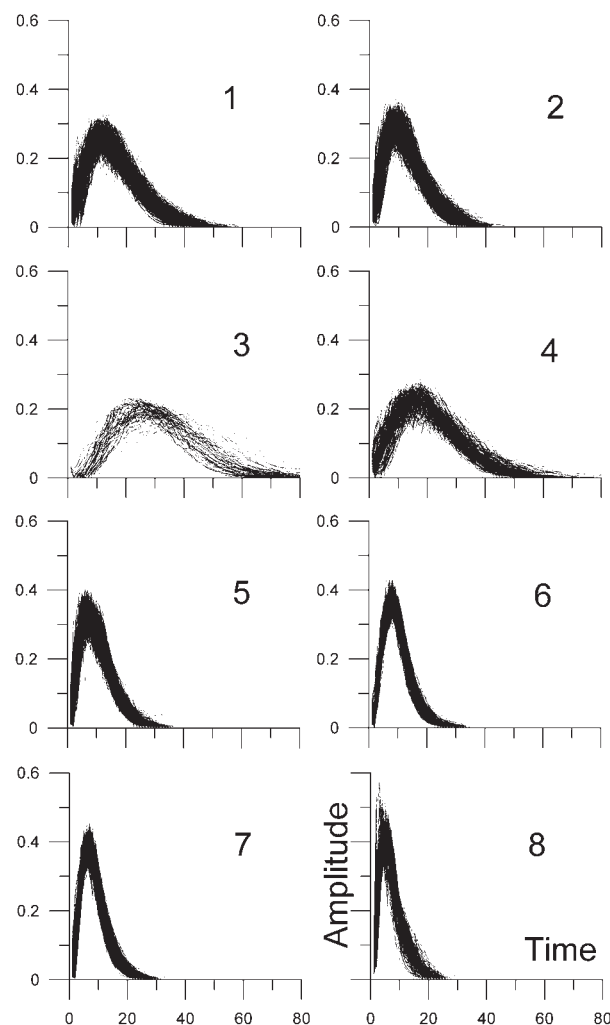

Figure 1. Statistical clustering of seabed echoes (clusters of single-valued curves) from Sydney Harbour into eight groups. Each group or cluster has a different basic shape from other groups, and all groups have relatively narrow dispersion or spread about a well defined central tendency (see Figure 2 for central tendency of the clusters).
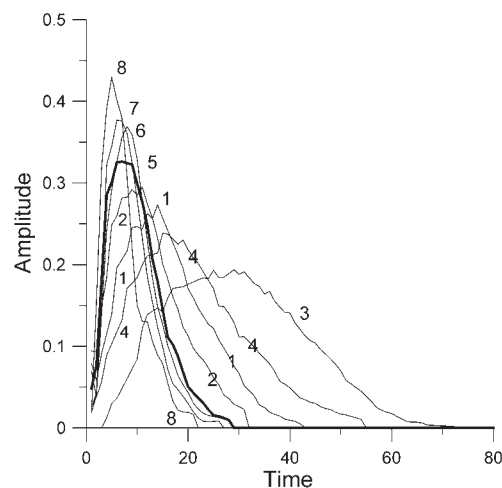

Figure 2. Medoids (central tendencies) of the eight clusters of Figure 1.

Method 2 – Classification through direct statistical clustering of signals treated as geometrical objects

The pseudo-Gaussian (Figures 1, 2) and sinusoidal signals of interest to the present paper can be described as single-valued curves. These have only one ordinate value for each abscissa value, whereas a multi-valued curve such as a circle has two for all but two points of its span. The classification of single-valued curves by description or reduction to features (Method 1) has been the orthodoxy for some decades in many scientific fields. Feature analysis has been used for example in geology to classify cumulative grain size curves, in underwater acoustics to classify seabed echoes, and in oceanography to classify wind-wave spectra. It has been demonstrated that a different approach is possible [3-5]. The signals in each of these cases form single-valued curves which can be regarded as discrete geometrical objects. Single-valued curves can be directly grouped or classed using suitable clustering algorithms. This approach is model free, and requires no curve fitting or selection and calculation of proxies. The actual curves are used, and data are not distorted or lost before analysis begins.

The CLARA algorithm of [2] has been demonstrated to be suitable for clustering of curves [3-5], although it was not designed for this activity. For a description of the CLARA algorithm see [2] and remarks in [5]. The CLARA algorithm is intended to cluster a minimum of 100 objects. A sister algorithm called PAM (Partitioning Around Medoids) can be used for less than 100 objects [2]. When clustering curves, the objective is that each cluster contains curves of similar shape, and that each group has a different basic curve shape than other groups. A distance metric, e.g. the multi-dimensional Euclidian or Manhattan distances referred to earlier, is used to decide whether curves are similar or dissimilar in properties. For CLARA, each curve in the entire data set is assigned to one (and only one) of the groups. Alternatively, fuzzy clustering algorithms assign probabilities of membership of an object to all clusters. The individual curve most closely approximating the central tendency of a cluster is termed a medoid [2]. A combination of non-standardisation of parameters and Manhattan distance metric was found to produce best results for curves. Alternatively, standardisation allows identification of outlier curves and of sets of curves most different from others [3]. A feature of CLARA demonstrated by [3-5] is that it can successfully partition a set of similarly shaped curves forming a quasi-continuum in their space. As an example, seabed echoes may form a quasi-continuum when seabed properties change gradually from one place to another, rather than jumping from one type to a completely different type. Another useful characteristic of CLARA is that clusters appear independent of data numbers. Clusters holding very small numbers of curves can be formed in classification of large data sets if they are geometrically different from other curves, providing a sufficient number of clusters is requested [3,4]. Another advantage of CLARA is that results do not depend on the order that objects are input to it, unlike K-means algorithms [2].

Estimation of the number of classes present in a data set is discussed in [3,5]. Companion algorithms to the clustering provide a quasi-independent estimate of the number of clusters. For CLARA this estimate is termed the Silhouette Coefficient. However, [3] recommends that users form from 2 clusters upwards (for example, 2, 3, 5, 8, 10, 20, …) until no more useful results are obtained for the particular data set being examined. Data exploration is an essential part of any examination of large data sets, and it is usually better to request many clusters, rather than a few. If discrete clusters do exist in a data set then CLARA and the Silhouette Coefficient will find them, but further information may be revealed by forming more clusters than recommended [3,5]. The effectiveness of the clustering can be checked by (1) examination of overplots of cluster medoids (the central tendencies of the clusters), and (2) examination of overplots of the curves forming each cluster for uniformity of properties (shape, location, central tendency, and spread). Figures 1 and 2 provide examples of medoids and their parent clusters.

Many clustering algorithms require too much processing power, computer memory, or processing time to be tenable for analysis of large data sets. Software program CLARA overcomes data size and processing time limitations by coupling statistical sampling and clustering techniques. The algorithm first clusters several sets of randomly chosen subsamples (for example, 5 sets with 200 objects in each for a data set with a total of 900 objects), then uses the particular subsampling returning best results to cluster the entire data set. This provides a fast algorithm suitable for processing of large data sets, at the possible expense of accuracy. However, the scheme has proved robust. The present author has used CLARA to cluster about 45,000 objects, and divide and conquer schemes can be used to increase this figure. It is also noted [3] that CLARA can be used to very quickly examine large data sets when the number of randomly chosen samples placed into the data sets is initially made very small. Running CLARA in this fashion provides a quick-look facility for data examinations, which can also be used to quickly estimate the number of clusters necessary to discover the structure in a data set.

Example of clustering of curves

An example is provided by classification of seabed echoes received by an echosounder [5]. Echoes are first compensated for acoustic propagation losses, corrected for artefacts caused by sampling effects, and are then normalised to unit energy. Normalisation removes relative amplitude information between signals, but this can be retained if necessary. The artefacts are caused by sampling the echo at fixed times instead of times corresponding to a set of particular incident angles on the seabed [6]. More samples are received for some particular angular range as depth increases, even if seabed type remains the same. Echoes received at different depths from the same seabed type are dilated or compressed relative to some reference depth, and this effect must be removed for comparisons of echo shapes to be meaningful (see [1] for more details). Figure 1 shows clusters and Figure 2 shows cluster medoids for a data set of seabed echoes from Sydney Harbour. The medoids generally morph from high amplitude, short duration signals to low amplitude, long duration signals. The longer duration signals are received from rougher or softer surfaces (muds) than the shorter duration, higher peaked echoes (which are from sands).

Discrete clusters do not exist for this data set, but the CLARA algorithm is able to sensibly partition the curves. For data sets such as this the clusters can be mapped to geographical space to provide a segmentation of seabed properties according to the seabed acoustic response stimulated by the echosounder. If this provides spatially coherent patterns then in principle only a few seabed samples need be taken to label or classify the seabed types indicated by the acoustics. A similar procedure can be carried out for multibeam sonar backscatter response curves [7], as an alternative to feature extraction and image processing methods. In both cases, because the actual backscatter response curve is used, geographical mappings of seabed areas with similar and dissimilar responses indicated by the clustering are standalone mappings which in themselves do not require validation. The same cannot be said when proxies are used. Some seabed samples or video must be taken if labels describing the physical or biological properties of the seabed classes are required.

Underwater signals are also used for purposes other than detection and classification of targets (including the seabed). For example, see [8] for statistical clustering of profiles of water current speeds with depth obtained from an Acoustic Doppler Current Profiler in the Changjiang estuary, Shanghai.
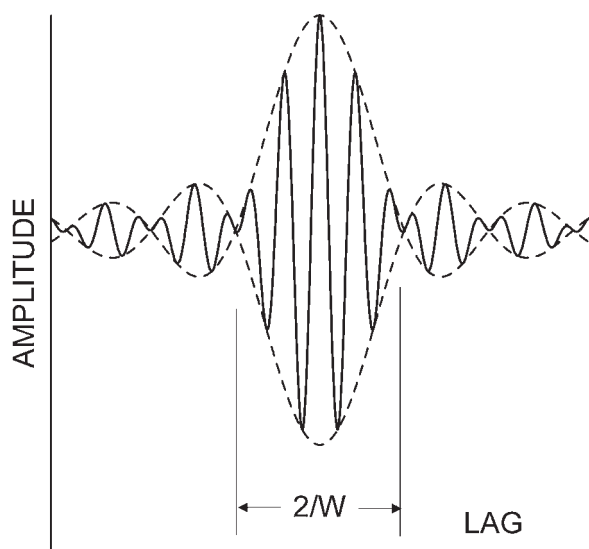
Figure 3. The autocorrelation function for a chirp signal, approximated as a sinc function. W=bandwidth (Hz) of the chirp.

Method 3 – Matched Filtering

Matched filtering cross-correlates one or more signal templates with time series to detect particular signals with known waveforms. This yields a sinc type cross-correlation function (Figure 3). The template is used as a sliding time window, and the exceeding of some threshold in peak amplitude of the resulting cross-correlation functions is used to indicate a detection. This operation can be performed in near real-time or in post processing. A major advantage of matched filtering is that it is very efficient at detecting signals buried in noise (e.g. [9]). It can also be used to detect signals overlapping in time.

If signals originally identical in waveform and source strength are received from very different distances, their received amplitudes and energies may vary greatly. If the propagation distances and paths are unknown, then compensation for spreading, scattering, and absorption losses can not be made, and genuine signals may be erroneously rejected by matched filtering. To overcome this [10] normalised the template signals and detected signals to unit energy. After normalisation of the detected signal, the cross-correlations were recalculated. It was observed that incoming signals, including spikes, which were partially correlated with a template could have a cross-correlation function of high peak amplitude, giving an erroneous classification. This spurious effect was reduced by searching for spikes and very short signals, and also by normalising the cross-correlation peak amplitude and kurtosis by the corresponding template parameters of the autocorrelation function.

Two examples of amplitude normalised autocorrelation functions for marine mammal chirp templates are shown in Figure 4. Their shapes are similar, but the peak of one function is noticeably broader than the other. The kurtosis parameter was found to be able to quantify this difference in shape very well, so much so that it could be used as the primary measure of the reliability of the detection. Kurtosis was observed to be related to the degree of distortion or malformation of the detected waveform compared to its template. Through the normalisations and use of kurtosis a low-amplitude well-formed signal scores higher than a distorted high amplitude signal. In this scheme the degree of distortion of the waveform is most important to the classification, not the signal to noise ratio of the detected signal.
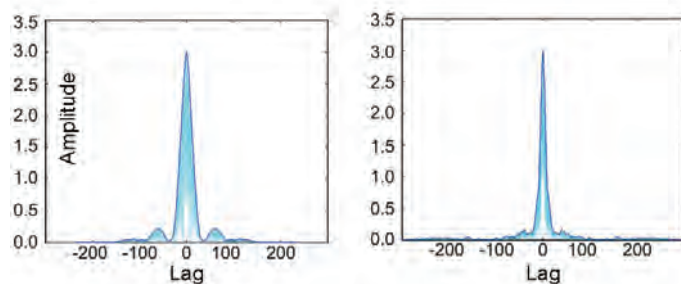

Figure 4. Two examples of amplitude normalised autocorrelation functions for marine mammal vocalisations. Note the different peak widths, which can be differentiated by the kurtosis parameter.

Example of matched filtering including allowance for ambiguity

The matched filtering scheme with normalisations and use of kurtosis as the primary detection parameter was applied by [10] to classification of the chirp vocalisations of beaked whales (Ziphiidae), a family of toothed whale or odontocete. Chirps are oscillating signals for which the frequency increases or decreases with time (Figures 5 and 6).
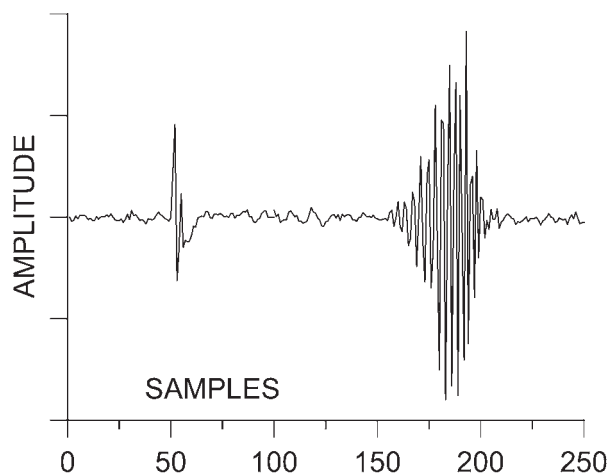
Figure 5. Examples of two stereotypical whale vocalisations from the digital library of the Marine Biological Library, Woods Hole Oceanographic Institute (www.mblwhoilibrary.org). The right hand waveform is a probable Blainville's beaked whale (*Mesoplodon densirostris*) chirp. Note the relative differences in duration of the two waveforms.
(Filename Set3_A1_042705_CH11_H11_A0300_0330.WAV,
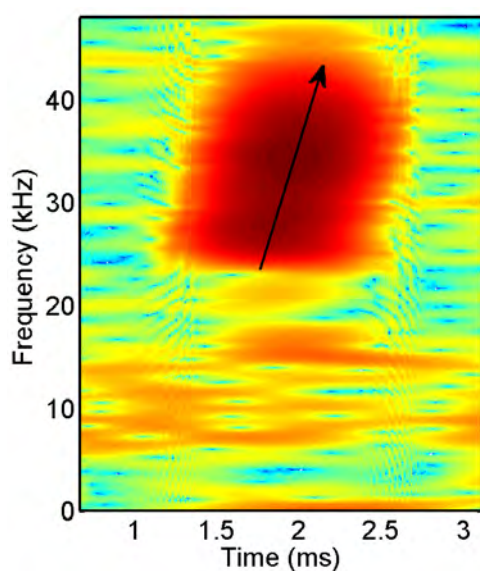Time 11:14.0500 to 11:14.0534).

Figure 6. Spectrogram of a chirp with frequency upsweep. For the waveform (a Blainville's beaked whale chirp) see Figure 5.

A further processing step was necessary to obtain reliable detections, as a property of chirp signals can result in detection ambiguity, even though chirp waveforms may have very obvious time domain differences. The autocorrelation function of a chirp is approximately a cosine modulated by a sinc function (Figure 3). The width between the primary nulls of the sinc function is 2/W, where W is the chirp bandwidth (Hz). The frequency of the cosine is the median frequency of the chirp [9,11]. Chirps with similar bandwidth will produce sinc envelopes with similar widths between the primary nulls, regardless of chirp duration or centre frequency. Chirps with similar median frequencies and similar bandwidth have

similar autocorrelation functions, including phase, regardless of marked differences in durations or number of cycles of waveform. This matched filtering ambiguity must be resolved by other information on the signal. Simple time or frequency domain rules suffice for some cases. For example, beaked whale chirps have much longer signal durations than the click sounds and chirps of other odontocetes such as the false killer whale (*Pseudorca crassidens*) vocalisations which caused ambiguity. Simple duration criteria were used to separate possible Ziphiids and non-Ziphiids before the final classification step.

The scheme was largely self-verifying in that the number of detections of a particular beaked whale species for some particular confidence level over some particular length of time plateaued as the initial matched filter amplitude criterion specifying a detection was decreased. In contrast, the number of detections for standard matched filtering methods, when used without additional rules, kept increasing without apparent limit (Figure 7). The normalised scheme also produced very few false detections for higher confidence values.
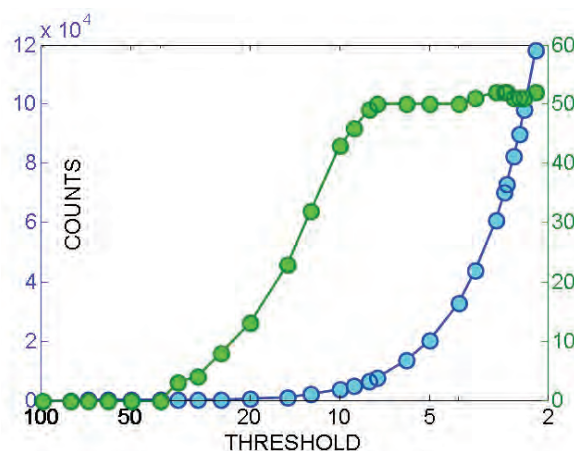
Figure 7. Number of detections as a function of detection threshold for the normalised two parameter matched filtering scheme (green circles) compared to standard matched filtering (blue circles). Note the different ordinate scales. The normalised scheme plateaus at 50 detections as the standard scheme rises to 120,000 detections.

DISCUSSION

Three methods have been briefly discussed for classification of underwater signals. These are (1) feature analysis, (2) direct statistical clustering of signals treated as single-valued curves, and (3) matched filtering with normalisations. Method (1) is simple and is suitable for many applications, but classifies on proxies, not the actual signal, and may lose or distort information. Method (2) is a post processing operation suitable for signals with well defined signal to noise ratio which can be well aligned in time. A suitable clustering algorithm can classify sets of signals where each set has a different average shape from the other sets, and can also classify signals forming quasi-continuums, such as signals which can be viewed as morphing from one shape to another. Method (3) is suitable for stereotypical signals with strongly repeating shape, and is very

good at detecting such signals in noisy backgrounds.

In order to apply clustering directly to signals of different durations the signals must have well defined start points or be able to be well aligned in time. For signals such as seabed echoes alignment should not be made by echo peak, because the peak position is determined largely by the interaction of the acoustic wavelength and seabed roughness, and does not occur at some fixed interval after initial contact of the output echosounder pulse with the seabed (see Figure 2). For seabed echoes it is usually possible to automatically determine robust start points by simple amplitude criteria [5]. However, the criteria are a function of echosounder make and model, since they depend on the shape of the output pulse.

Cross-correlation is generally sufficient to align and detect highly stereotyped signals. It is not necessary to be able to find well defined start points for them, and weak and noisy signals may be detected and aligned. However, identical signals of the same source strength received from different and unknown ranges will produce different cross-correlation amplitudes. Unless normalisation of some kind is used this negates the use of matched filtering for signal classification. Incoming signals of unwanted type which are partially correlated with the desired signal in the time domain may also cause erroneous classification. Matched filters are very efficient at detection of signals, including signals buried in noise, but not necessarily at discrimination. If matched filter banks are to be effective, then users must check and allow for ambiguity between templates, and must also be aware of the other factors which may lead to ambiguity in classification.

REFERENCES

[1] J.M. Preston, "Acoustic classification of seaweed and sediment with depth-compensated vertical echoes", *Proceedings of OCEANS 2006*, Boston, USA, 18-21 September 2006

[2] L. Kaufman and P.J. Rousseeuw, *Finding groups in data: An introduction to cluster analysis*, John Wiley, New York, 1990

[3] L.J. Hamilton, "Clustering of cumulative grain size distribution curves for shallow-marine samples with software program CLARA", *Australian Journal of Earth Sciences* **54**, 503-519 (2007)

[4] L.J. Hamilton, "Characterising spectral sea wave conditions with statistical clustering of actual spectra", *Applied Ocean Research* **32**(3), 332-342 (2010)

[5] L.J. Hamilton, "Acoustic seabed classification for echosounders through direct statistical clustering of seabed echoes", *Continental Shelf Research* **31**, 2000-2011 (2011)

[6] D.A. Caughey and R.L. Kirlin, "Blind deconvolution of echosounder envelopes", *Proceedings of the IEEE International Conference on Acoustics, Speech and Signal Processing Conference* (ICASSP'96), 6, 3149-3152 (1996)

[7] L.J. Hamilton and I. Parnum, "Seabed segmentation from unsupervised statistical clustering of entire multibeam sonar backscatter curves", *Continental Shelf Research* **31**(2), 138-148 (2011)

[8] Z. Cao, X.H. Wang, W. Guan, L.J. Hamilton, Q. Chen, D. Zhu, "Observations of nepheloid layers in the Yangtze estuary, China, through phase corrupted Acoustic Doppler Current Profiler speeds", *Marine Technology Society Journal* **46**(4), 60-70 (2012)

[9] A. Hein, *Processing of SAR data: fundamentals, signal processing, interferometry*, Springer-Verlag, Berlin, New York, 2004

[10] L.J. Hamilton and J. Cleary, "Automatic detection of beaked whale calls in long acoustic time series from the Coral Sea", *Proceedings of OCEANS 2010*, Sydney, Australia, 24-27 May 2010

[11] C. de Moustier, *Fourth Asia-Pacific coastal multibeam sonar training course*, Cairns, Australia, 14-19 August 2000

AAS Research Grants
WE NEED YOUR INPUT

One of the objectives of the AAS is to promote and advance acoustics in all its branches and to facilitate the exchange of information and ideas in relation thereto. Another objective is to encourage research and the publication of new developments relating to acoustics. This AAS project aims to activate these two objectives.

A special committee of the AAS Federal Council was formed at the last AAS Conference in Fremantle to look at research grants. The committee members are Matthew Stead (Chair, SA), Luke Zoontjens (WA), Matt Terlich (QLD), Neil Gross (NSW), Geoff Barnes (Vic), Norm Broner (President), Peter Heinze (Past President) and Tracy Gowen (AA and NSW).

One outcome from the committee is a survey to seek YOUR input on the proposal for research grants and to identify priority research areas.

The survey will be open to the end of April and can be accessed at: http://www.surveymonkey.com/s/9DNB6M6.

It is proposed that funding would need to be at least equally matched from other sources as identified in any proposal.

Additional information and selection criteria for applications will be released after the survey results are analysed.

For additional questions please email the AAS General Secretary Richard Booker or contact Matthew Stead at matthew.stead@resonateacoustics.com

THE SOUNDS OF FISH OFF CAPE NATURALISTE, WESTERN AUSTRALIA

Miles Parsons, Robert McCauley and Frank Thomas
Centre for Marine Science and Technology, Curtin University, WA 6845, Australia
m.parsons@cmst.curtin.edu.au

Fish calls and choruses contribute considerable energy to the underwater soundscapes of Western Australia's waters. There are many fish species of social and economic importance which could be the source of these sounds. For example, the Western Australian dhufish (*Glaucosoma hebraicum*), which is endemic to the coast, has been shown to produce sound when captured. To investigate how much this species contributes to ambient noise levels, loggers were deployed between December, 2011 and February, 2012 at numerous locations around Cape Naturaliste in Western Australia, where some of the largest numbers of *G. hebraicum* are reported. Recordings taken near the site of the HMAS Swan wreck between 2009 and 2010 were also examined. Five fish choruses have been described centred at approximately 0.5, 1, 2 and >2 kHz (two choruses at >2 kHz). Many individual fish calls were detected at various locations around the Cape, particularly in the frequency ranges between 100 and 900 Hz. The acoustic characteristics of these calls are described, as well as the contribution of fish calls and choruses to the local soundscapes. The calls most similar to the previously reported *G. hebraicum* calls have been identified.

INTRODUCTION

Around Australia numerous species of fish produce sound, individually, in small groups or as part of a chorus [1-5]. A chorus is formed when sounds from individual callers overlap, with a significant increase above background levels (>3 dB re 1 µPa) for prolonged periods, using an equipment averaging time of one second [2]. A discontinuous chorus accounts for calls which do not overlap, but are frequent enough to raise time averaged noise levels over one minute, rather than one second [3]. Acoustic characteristics of fish calls can be species-specific, or even individually characteristic, such as call spectral peak frequency (typically defined by a combination of the resonant frequency of a fish's swimbladder, the tension of muscles that vibrate the swimbladder to produce sound and/or the damping of the swimbladder wall), modulation frequency (defined by the rate at which a swimbladder is "pulsed" by the associated muscles) and the rate at which calls are produced [4, 5]. These vocalizations often have associated behavioural functions and can provide insights into the ecology of the fish [6-13]. Indeed, once a species' characteristic calling rates and source levels have been identified it is possible to monitor the relative and theoretically absolute abundance of the fish contributing to a chorus [4, 14, 15].

An increasing number of socially and economically important fish have been studied to confirm if they are soniferous [16, 17]. The use of passive acoustic recording of calls as a complementary data source to monitor vocal aggregations is becoming of increasing benefit to biologists and managers [15, 17-19]. For example, the endemic Western Australian dhufish (*Glaucosoma hebraicum*), an iconic and highly prized species, is notoriously shy, inhabiting reefs and caves to depths of 200 m and, in general, is observed as single fish or sometimes groups of small numbers, often involving a harem of several females to one or two males [20, 21]. While comparatively little is known about the spawning behaviour of the species, catch reports and biological sampling have shown that significant numbers of *G. hebraicum* aggregate each year to spawn in waters around Cape Naturaliste, in the state"s southwest, between December and February [22]. A recent study has been investigating the use of passive acoustics as a means of detecting *G. hebraicum* and confirmed the species as soniferous [16]. Trains of swim bladder pulse driven calls were recorded from captured individuals in 14 m of water, with spectral peak frequencies of 150-160 Hz and pulse repetition frequency of approximately 10 Hz [16]. Whether *G. hebraicum* produce sound during natural behaviour is unknown, though the complex social structure of schools and nocturnal activity suggest that acoustic communication may be a viable alternative to visual cues for this species [21].

The aim of this study was to record and identify sounds in waters where *G. hebraicum* reportedly spawn and investigate whether sounds with similar characteristics to those of *G. hebraicum* were detected. This paper describes some of the fish choruses and calls detected in waters off Cape Naturaliste between December, 2011 and February, 2012.

METHODS

Autonomous underwater sea-noise loggers, developed by the Centre for Marine Science and Technology and the Defence Science and Technology Organisation, were deployed to the seabed in waters around Cape Naturaliste at various times between 2008 and 2012 (Figure 1). Recordings were taken using a calibrated, omni-directional, HTI 90-U or 96-min hydrophone (HighTech Inc., MS, USA). Sampling schedules, deployment periods and approximate locations for these deployments can be found in Table 1. Each system was

calibrated with a white noise generator at -90 dB re 1 V²/Hz and data analysed using the CHaracterisation Of Recorded Underwater Sound (CHORUS) Matlab toolbox, written at the Centre for Marine Science and Technology (CMST). Spectrograms were produced with a 1024 point Hanning window at a frequency resolution of either 1 or 10 Hz.
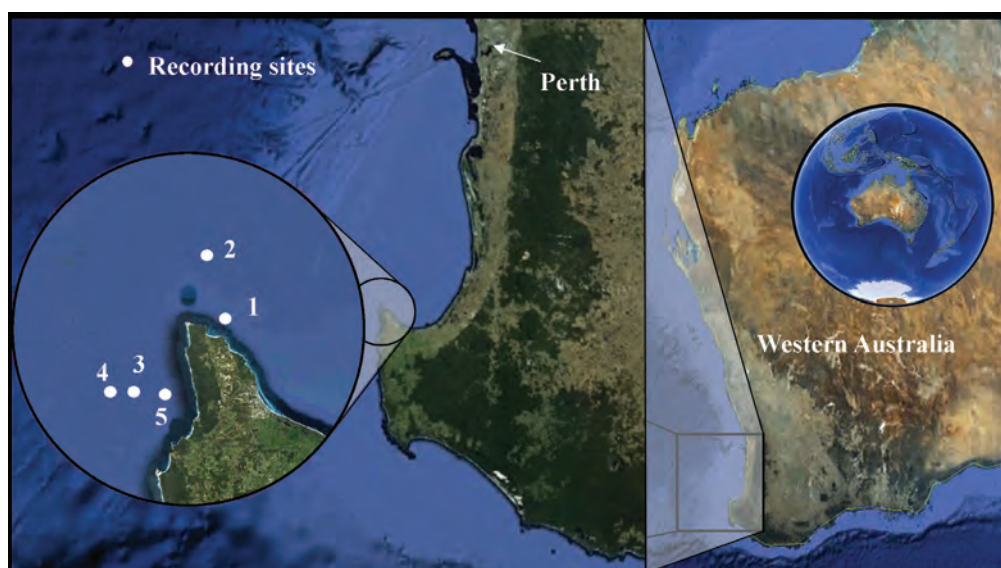

Figure 1. Map of southwest Australia with expanded inset of Cape Naturaliste and local waters. Approximate locations of deployed loggers shown by white circles (1: near the wreck of the HMAS Swan, 2: Geographe Bay logger, 3: Offshore logger A, 4: Offshore logger B, 5: Inshore Logger). Image source: Google earth 14/7/12

Table 1. Deployment periods and schedules of underwater noise loggers between 2008 and 2012

Deployment location	Depth (m)	Start date	End date	Sample rate	Low frequency roll-off	Anti-aliasing filter	Sampling schedule
1:HMAS Swan	26	21/12/08	15/03/09	6 kHz	8 kHz	2.8 kHz	780 s every 900 s
	26	23/11/09	26/07/10	6 kHz	8 kHz	2.8 kHz	780 s every 900 s
2: Geographe Bay logger	29	13/12/10	26/01/11	8 kHz	8 kHz	2.8 kHz	700 s every 900 s
3: Offshore logger A	41	21/12/11	26/02/12	11 kHz	8 kHz	5 kHz	540 s every 660 s
4: Offshore logger B	57	21/12/11	26/02/12	11 kHz	8 kHz	2.8 kHz	540 s every 660 s
5: Inshore logger	37	08/02/11	12/02/11	6 kHz	8 kHz	2.8 kHz	700 s every 900 s

RESULTS

Numerous fish calls and choruses were recorded at the various logger sites around Cape Naturaliste. Sounds from individual callers or small groups of fish were typically in the frequency band of 100 to 900 Hz, while five predominant choruses that were detected were centred at approximately 0.5, 1, 2 and >2 kHz (two types of chorus were detected >2 kHz).

Choruses

Five types of recorded choruses are described here. The first four were recorded at the site near the HMAS Swan wreck between January and March, 2009. Over a two week period the four choruses were present on the same days (Figure 2),

illustrating that there was often overlap in frequency and temporal bands of each chorus.

The first chorus (Figure 2a, black ellipse and 2b) was centred at approximately 500 Hz and lasted approximately 1 hour each day, beginning approximately an hour before sunset at 18:30 and comprising few callers (estimated at between 5 and 10 calling fish).

The second chorus (Figure 2a, orange ellipse and 2c) began before the first finished, around the time of sunset, and lasted 1 to 1.5 hours. This chorus comprised series of short "pops", likely generated by either a click or a single pulse of a swim bladder, centred around 1 kHz (Figure 2c, waveform).

The third and fourth choruses (Figure 2a, green and yellow

ellipses, respectively) were both centred above 2 kHz (the sampling frequency of 6 kHz restricted the identification of the upper frequency limit of the chorus). The first of these two choruses began in the evening, after sunset, prior to the end of the 1 kHz centred chorus (Figure 2a, green ellipse) and lasted approximately 2 hours. The second occurred in the morning, lasting up to 2 hours either side of sunrise (Figure 2a, yellow ellipse). Both of these choruses comprised sounds centred above 2 kHz, with all energy above 1 kHz, similar to those of the planktivorous fish described by McCauley [5].

An example of the fifth type of chorus (Figure 3) was recorded at the Inshore logger (5), in 40 m of water. The chorus began

quickly, with many fish calling shortly after sunset, but ended as the calls slowly diffused, with odd callers sometimes continuing for several hours into the night. This chorus comprised calls of pulse trains centred between 2 and 2.2 kHz in frequency. While pulse repetition rate was high, so was the damping of the swim bladder, thus the calls were audibly detected as a series of knocks. These pulse trains ranged considerably in pulse number (48 ±12, n = 50, min = 12, max =71) and duration (1.971 ±0.493 s, min = 1.112, max = 2.9523), often containing upwards of 50 pulses (Figure 3c). This type of chorus was also detected on recordings from the two loggers located further west of Cape Naturaliste (Figure 1) in January and February.
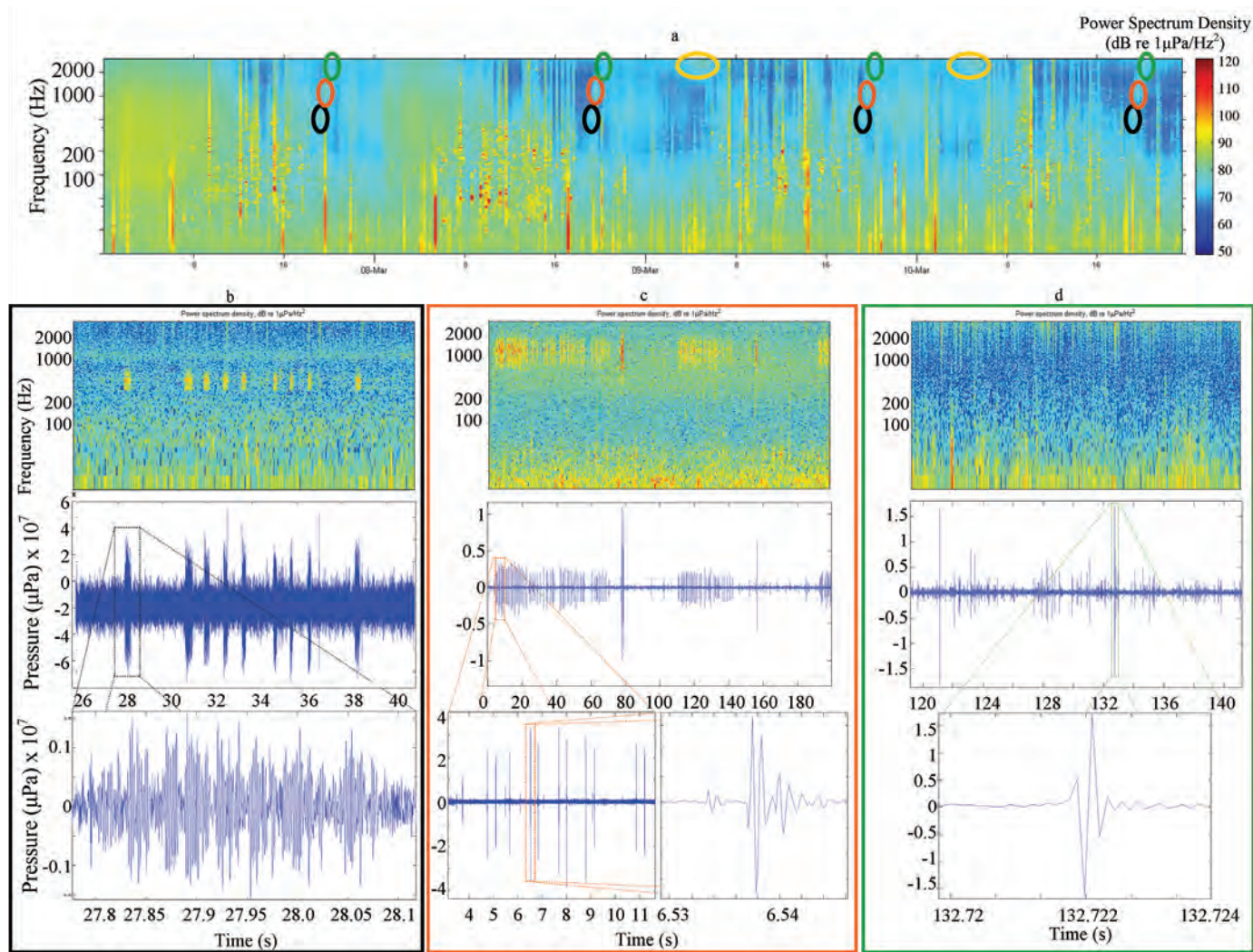
Figure 2. Spectrogram of four days of acoustic recording in Geographe Bay (a). Magnified examples spectrograms and waveforms for four types of recorded calls contributing to each chorus centred around 500 Hz (2a black ellipse and 2b), 1000 Hz (2a orange ellipse and 2c) and greater than 2000 Hz (2a green and yellow ellipses and 2d). Points of interest are explained in the text
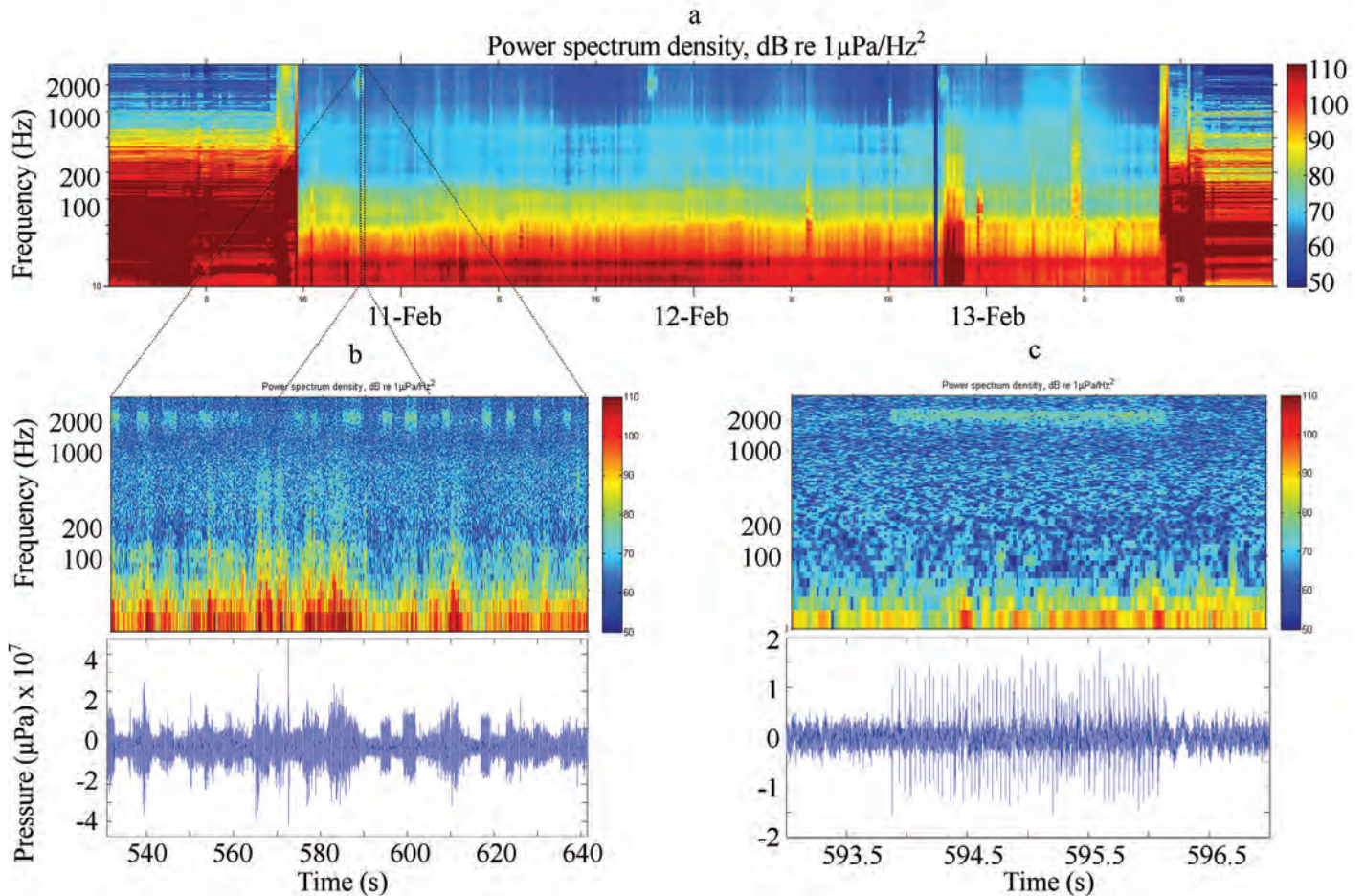
Figure 3. Spectrograms and waveforms of a chorus recorded in waters around the Inshore Logger (Figure 1 Point 5), Western Australia, in 40 m of water. Innumerate calls over the 2-2.2 kHz band (b) where each call comprised a pulse train of often >50 pulses (c) audibly detected as a series of knocks

Individual fish calls

Several types of individual fish calls were recorded. These calls were few in number and did not build to constitute a chorus. In each case the calls were most likely emitted by a single fish or few individuals. In general, the majority of energy within these calls was between 100 and 900 Hz (Figure 4). Four common examples of those calls are described here.

The first call type (Figure 4a, n = 11 calls) comprised 7.55 ± 2.70 pulses (min = 3, max = 12) at spectral peak frequency of 521 ±53 Hz and pulse repetition frequency of 42 ±11 Hz.

The second type (Figure 4b, n = 2) comprised a train of 19 ±2 pulses. The spectral peak frequency over the call was 198 ±27 Hz, however, throughout the call the spectral peaks rose and then fell (Figure 4b, spectrogram) due, in part, to the decrease (129 Hz to 87 Hz) and then increase in pulse repetition frequency (87 to 105 Hz) during the call (Figure 4b).

The third type of call (Figure 4c, n = 53) was a series of pulse sets (up to 4 pulses within a set) of spectral peak frequency of 857 ±46 Hz (min = 741, max = 979), at a pulse repetition frequency of 9.1 ±1.8 Hz.

A fourth type of call was categorised from recordings taken between December, 2011 and February, 2012. Offshore logger B, deployed approximately 6 n.m. west of Cape Naturaliste (Figure 1) recorded many fish calls (Figure 5b).

Of 75 analysed calls the mean spectral peak frequency was 239 ± 37 Hz (min = 86, max = 297) with pulse repetition frequency of 8.3 ± 3.2 Hz (min = 4.2, max = 14.7). The logger also recorded an increase in sound pressure levels (SPLs) between 50 and 200 Hz for prolonged periods. The most notable of these periods was between the 29th December and the 4th January, a period when anecdotal evidence from recreational fishers suggested significant numbers of *G. hebraicum* were caught in the surrounding area.

Individual fish calls of characteristics similar to those of mulloway [4, 23, 24] were also detected during recordings, as well as numerous other biological sounds. For brevity these have not been described here.

DISCUSSION

This study has highlighted numerous different types of fish choruses and calls around the Cape Naturaliste region of Western Australia. The choruses displayed distinct differences in frequency content, likely due to the size of fish and/or mechanism of sound production, providing a means of discrimination between species for the intended recipients of the calls [3-5].

The species producing the choruses presented here are currently unknown. However, the first chorus, centred around
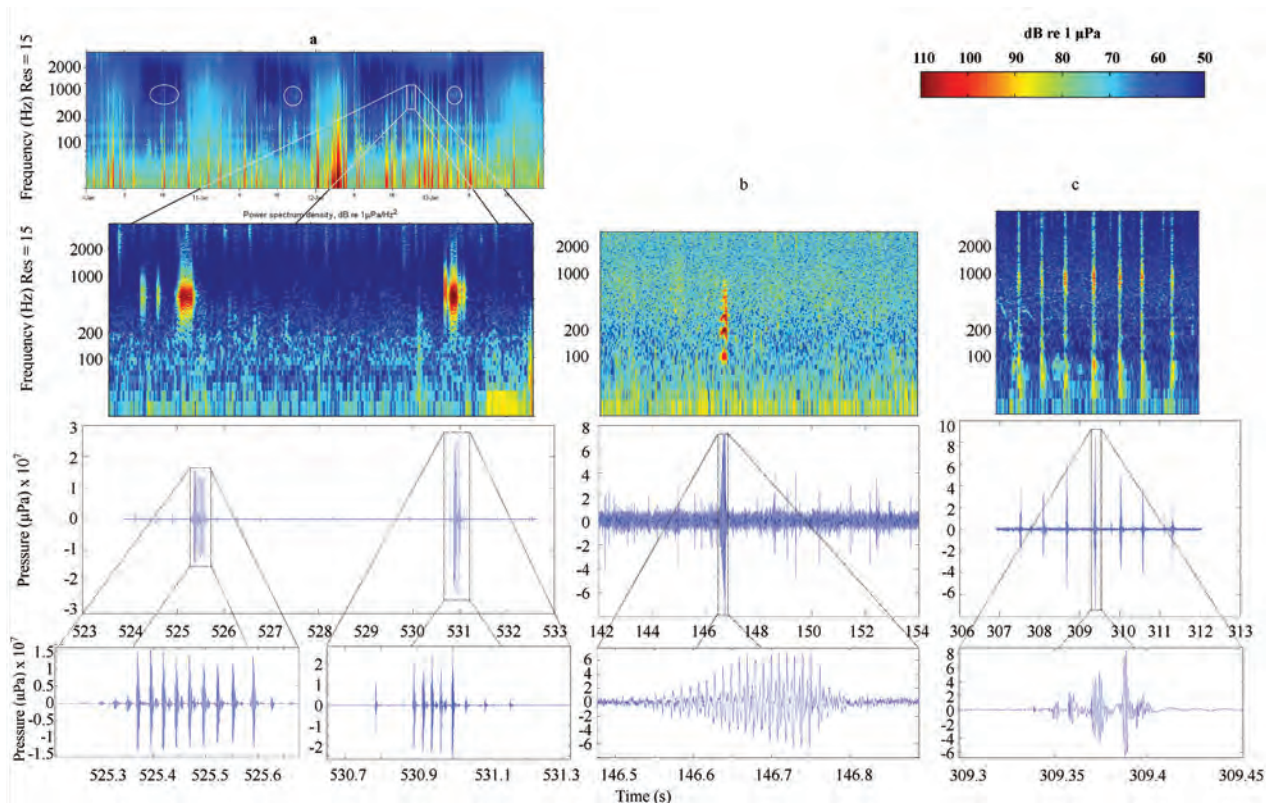
Figure 4. (a) Spectrogram of 4 days recording in Geographe Bay with a magnified spectrogram of 10 s at approximately 20:00 hrs on the 12th January, 2011. Waveforms of two recorded calls are shown with swimbladder pulses magnified. Circles in the top spectrogram highlight periods at dawn and dusk when similar calls were observed. (b and c) Spectrogram and waveform of unidentified calls recorded on 10th December 2010 at approximately 10:15 and 11:15 in Geographe Bay.
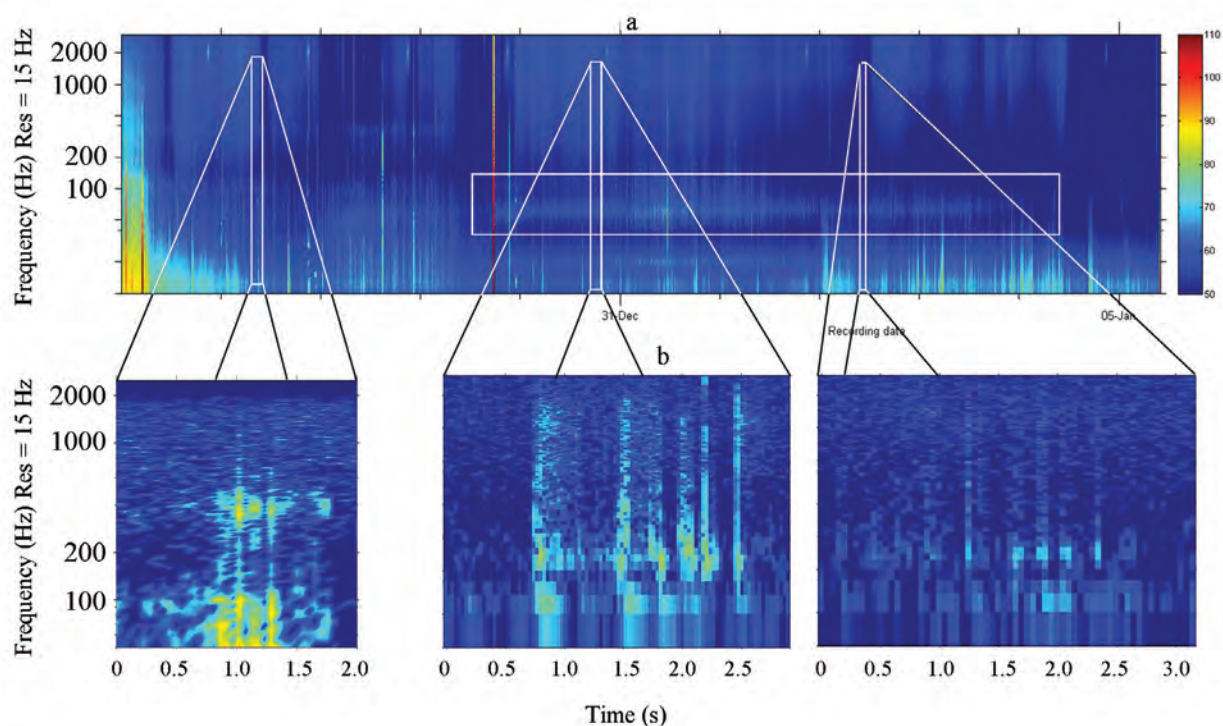

Figure 5. Spectrogram from 10 days recording in waters west of Cape Naturaliste (a). Spectrograms of a example sound with similar characteristics to *G. hebraicum* calls (b) and increase SPLs during a period when significant numbers of *G. hebraicum* were capture in the area and this period is within the known spawning season of *G. hebraicum* (highlighted by horizontal rectangular white box)

500 Hz is of similar frequency band to those of weakfish (*Cynoscion regalis*), for fish ranging between 25 and 35 cm [25]. Thus a species of similar size and possessing a swimbladder is suggested to be the source of these sounds. The frequency band and duration of "pops" in the second chorus are similar to that of urchin noises, which produce sound between 700 and 1500 Hz [26], which could be a possible source of this chorus. The third "evening" chorus is typical of small planktivorous fish reported by McCauley [3, 5] and are likely to also be the source of the fourth "dawn" chorus. The fifth chorus comprised calls produced via long trains of swimbladder driven pulses. While the source of this chorus has not been determined calls of similar spectral peak and modulation frequencies have been reported at other recordings sites around Australia [3, 5] and observed by the authors at other locations around the world.

The choruses recorded in this study provide significant information on at least four different aggregations of fish. While there was temporal overlap at the start and beginning of the choruses detected here there were discrete differences in the timing of the peak of calling. This implies that the calling fish use not only frequency, but also time to discriminate between choruses, similar to that found on the northwest shelf [5]. Parsons [4] and McCauley [3] described how environmental drivers such as temperature, salinity and lunar phase can affect the timing and caller numbers in a fish chorus. Although assessment of the long-term timing of the southwest choruses has not been documented and would require substantially longer datasets than those presented here, the variable presence of the choruses suggest different external drivers affect each of the aggregations and requires examination. This type of monitoring of long-term variations in fish chorus levels is the subject of a future CMST study.

The individual calls recorded displayed distinct differences in spectral peak and modulation frequencies. The duration of each call type also varied significantly, not only from other individual call types, but also the calls that contributed to the five chorus types. The fourth type of call was centred between 200 and 300 Hz with pulse repetition frequency of 8.3 ± 3.2 Hz and was most similar to the calls of the *G. hebraicum* reported by Parsons et al. [16] at approximately 154 ± 45 Hz and 10 Hz spectral peak and pulse repetition frequencies, respectively. While the difference in peak frequency between the call type here and reported *G. hebraicum* calls is noted, Parsons et al. [16] recorded the *G. hebraicum* calls at depths of less than 14 m. The recordings in this study were taken at depths of between 27 and 57 m. Increased pressure with depth reduces the size of an uncompensated swim bladder and therefore increases the resonant frequency (and therefore spectral peak frequency in individual pulses) of a call [27]. Some fish species secrete a gas into the swim bladder to compensate for the additional pressure and therefore maintain swim bladder size and call frequency [3]. It is currently unknown whether *G. hebraicum* maintain buoyancy via secretion of gas into the swim bladder, although their susceptibility to barotrauma [28] would suggest that the species possess little control over swim bladder volume. At the depths recordings were in this study it is unknown whether a *G. hebraicum* call spectral peak frequency would increase and, if so, by how much. The

pulse repetition frequency of the fourth call type was the most similar to the reported *G. hebraicum* calls of those recorded here and, combined with the spectral peak frequencies, it is suggested that this is the most the likely call type to have been emitted by *G. hebraicum*. It should be noted, however, that it is not inconceivable that spawning *G. hebraicum* at 40 m depth emit calls of elevated peak frequency and/or increase the pulse repetition rate. Haddock (*Melanogrammus aeglefinus*), and Atlantic cod (*Gadus morhua*) for example, emit calls at a range of pulse repetition frequencies [29, 30] during different behaviour.

The increase in sound pressure levels between 50 and 200 Hz in the Offshore Logger A recordings between the 29th December and 5th January were due to short pulsed sounds, often of the fourth call type. This period coincided with a time when anecdotal evidence from fishers suggested the largest number of *G. hebraicum* were caught in the area (author, unpublished data). Whether the *G. hebraicum* are responsible for this increase is unknown and is the subject of further study.

ACKNOWLEDGEMENTS

REFERENCES

[1] L.J. Kelly, D.J. Kewley and A.S. Burgess, "A biological chorus in deep water northwest of Australia", *Journal of the Acoustical Society of America* **77**(2), 508-511 (1985)

[2] D.H. Cato, "Marine biological choruses observed in tropical waters near Australia", *Journal of the Acoustical Society of America* **63**(4), 736-43, (1978)

[3] R.D. McCauley, *Biological sea noise in northern Australia: Patterns of fish calling*, PhD Thesis, James Cook University, Australia, 2001

[4] M.J.G. Parsons, Passive acoustic techniques for monitoring fish aggregations, In *An investigation into active and passive acoustic techniques to study aggregating fish species*, PhD Thesis, Curtin University, Australia, 2010

[5] R.D. McCauley, "Fish choruses from the Kimberley, seasonal and lunar links as determined by long-term sea-noise monitoring", *Proceedings of Acoustics 2012 Fremantle*, Fremantle, Western Australia, 21-13 November 2012

[6] H.K. Mok and R.G. Gilmore, "Analysis of sound production in estuarine aggregations of *Pogonias cromis, Bardiella chrysoura*, and *Cynoscion nebulosus* (Sciaenidae)", *Bulletin of the Institute of Zoology Academia Sinica* (Taipei) **22**, 157-86 (1983)

[7] H.E. Winn, *The biological significance of fish sounds in WN Tavolga* (ed.), Marine Bioacoustics, vol. 2, Pergamon Press, Sydney, 1964

[8] F. Engen, and I. Folstad, "Cod courtship song: a song at the expense of dance?", *Canadian Journal of Zoology* **77**, 542-550 (1999)

[9] A.D. Hawkins, "The use of passive acoustics to identify a haddock spawning area", *An International Workshop on the Applications of Passive Acoustics in Fisheries, Massachusetts Institute of Technology*, Cambridge, MA. pp. 43-47, 2002

[10] J.P. Lagardere and A. Mariani, "Spawning sounds in the meagre *Argyrosomus regius* recorded in the Gironde Estuary, France", *Journal of Fish Biology* **69**, 1697-1702 (2006)

[11] P.S. Lobel and P. Macchi, "Spawning sounds of the damselfish *Dascyllus albisella* (Pomacentridae), and relationship to male size", *Bioacoustics* **6**, 187-98 (1995)

[12] A.A.J. Myrberg and J.Y. Spires, "Sound discrimination by the bicolour damselfish (*Eupomacentrus Partitus*)", *Journal of Experimental Biology* **57**, 727-735 (1972)

[13] A.A.J. Myrberg, S.J. Ha and M.J. Shamblott, "The sounds of bicolor damselfish (*Pomacentrus partitus*): predictors of body size and a spectral basis for individual recognition and assessment", *Journal of the Acoustical Society of America* **94**, 3067-70 (1993)

[14] J.J. Luczkovich, M.W. Sprague, S.E. Johnson and C. Pullinger, "Delimiting spawning areas of weakfish *Cynoscion regalis* (family sciaenidae) in Pamlico Sound, North Carolina using passive hydroacoustic surveys", *Bioacoustics* **10**, 143-60 (2000)

[15] M.W. Sprague and J.J. Luczkovich, "Modeling fish aggregation sounds in very shallow water to estimate numbers of calling fish in aggregations", *Proceedings of Meetings on Acoustics*, **12**, (2012)

[16] M.J.G. Parsons, P. Lewis, L. Longbottom, R.D. McCauley and D. Fairclough, "Dhu they, or don"t they: A study of sound production by three fish species of commercial and recreational fishing importance in Western Australia", *Proceedings of Acoustics 2012 Fremantle*, Fremantle, Western Australia, 21-13 November 2012

[17] R.A. Rountree, R.G. Gilmore, C.A. Goudey, A.D. Hawkins, J.J. Luczkovich and D.A. Mann, "Listening to fish: applications of passive acoustics to fisheries science", *Fisheries* **31**, 433-446 (2008)

[18] J.J. Luczkovich, D.A. Mann and R.A. Rountree, "Passive acoustics as a tool in fisheries science", *Transations of the American Fisheries Society* **137**, 533-541 (2008)

[19] J.J. Luczkovich, R.C. Pullinger, S.E. Johnson and M.W. Sprague, "Identifying sciaenid critical spawning habitats by the use of passive acoustics", *Transactions of the American Fisheries Society* **137**, 576-605 (2008)

[20] B. Hutchins, and R. Swainston. *Sea Fishes of Southern Australia. Complete Field Guide for Anglers and Divers*. Swainston Publishing. 180 pp. (1986)

[21] M.C. Mackie, R.D. McCauley, R.H. Gill and D.J Gaughan, *Management and monitoring of fish spawning aggregations within the west coast bio-region of Western Australia*, Fisheries Research and Development Corporation, Perth, 2009

[22] D. Fairclough, E. Lai, C. Bruce, N. Moore and C. Syers, "West Coast Demersal Scalefish Fishery Status Report. In: *State of the Fisheries and Aquatic Resources Report 2010/11*", (eds W J Fletcher & K Santoro). Department of Fisheries, Western Australia, pp. 96-103 (2011)

[23] M.J.G. Parsons, R.D. McCauley, M.C. Mackie and A.J. Duncan, "In situ source levels of mulloway (*Argyrosomus japonicus*) calls", *Journal of the Acoustical Society of America* **132**(5), 3559-68 (2012)

[24] M.J.G. Parsons, R.D. McCauley, M. Mackie, P.J. Siwabessy and A.J. Duncan, "Localisation of individual mulloway (*Argyrosomus japonicus*) within a spawning aggregation and their behaviour throughout a diel spawning period", *ICES Journal of Marine Science* **66**, 1007-14 (2009)

[25] M.A. Connaughton, M.H. Taylor and M.L. Fine "Effects of fish size and temperature on weakfish disturbance calls: Implications for the mechanism of sound generation", *The Journal of Experimental Biology* **203**, 1503-1512 (2000)

[26] C.A. Radford, A.G. JeVs, C.T. Tindle and J.C. Montgomery, "Resonating sea urchin skeletons create coastal choruses", *Marine Ecology Progress Series* **362**, 37-43 (2008)

[27] J.E. Simmonds and D.M. MacLennan, *Fisheries Acoustics, Theory and Practice*, 2nd edition, Blackwell Science, Oxford, 2005

[28] J. St John, and C.J. Syers, "Mortality of the demersal West Australian dhufish, *Glaucosoma hebraicum* (Richardson 1845) following catch and release: The influence of capture depth, venting and hook type", *Fisheries Research* **76**, 106-116 (2005)

[29] J. Nilsson, Acoustic behaviour of spawning cod (*Gadus morhua*), Candidatus scientiarum Thesis, University of Bergen, Norway, 2004

[30] A.D. Hawkins, and M.C.P. Amorim, "Spawning sounds of the male haddock, *Melanogrammus aeglefinus*", *Environmental Biology of Fishes* **59**, 29-41 (2000)
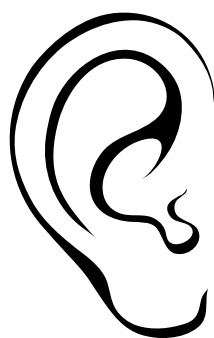
SEABED MULTI-BEAM BACKSCATTER MAPPING OF THE AUSTRALIAN CONTINENTAL MARGIN

Rudy J. Kloser and Gordon Keith

CSIRO Wealth from Oceans Flagship, Marine and Atmospheric Research, GPO Box 1538, Hobart, Tasmania 7001, Australia
rudy.kloser@csiro.au

A multi-beam sonar (MBS) has been used to map Australia's continental margin seabed from the marine national facility vessel Southern Surveyor on opportunistic transit and research voyages since 2004 with 0.35 M km^2 mapped. The MBS data are used to infer key ecological features based on bathymetry (e.g. seamounts, canyons, terraces, banks and deep reefs) and backscatter data for ecological hard (consolidated, e.g. rock for attachment of fauna) and soft (unconsolidated, e.g. mud for burrowing fauna) substrate. Seabed consolidation inference is consistent with a seabed scattering model. To consistently infer ecological significant hard and soft substrate from the backscatter data requires minimisation of errors due to changing absorption (~2 dB) with temperature and depth, calibration drift, changes in pulse length and estimates of area insonified due to seabed slope (<8 dB). Area insonified corrections were required for both across and along-ship slopes. Highest corrections were needed for along-ship slopes in canyon regions and large incidence angles (>60°). A data collection and processing framework is described that works towards a national backscatter mapping program for environmental seabed mapping. Data collected and automated processing for depth, sound absorption and area insonified at level 2 of a possible 5 level data processing hierarchy is available for viewing at http://www.marine.csiro.au/geoserver.

INTRODUCTION

Australia's continental margin, defined here from ~100 m to 1500 m, is a narrow strip characterised by high productivity and diversity of the mega epifauna [1]. This area also supports major ecological and economic (fishing, oil and gas) resources, is poorly understood yet heavily exploited in parts. A simple first step to assist management of this region is to map the spatial scales of the types of terrain and key components of the biotic assemblages to define marine habitat patches and key ecological bathymetric features (e.g. canyons, seamounts and deep reefs) and ecological significant hard and soft substrate type. Ecological hard (consolidated) terrain is potential habitat for attached fauna whilst ecological soft (unconsolidated) terrain is potential habitat for burrowing and soft sediment fauna [2]. Mapping with multi-beam sonars (MBS) is attractive as they can provide both high resolution bathymetry and from the backscatter, data to infer seabed type.

A MBS provides detailed bathymetry along the line of the vessel's track with swath widths of 2 to 5 times water depth and produces detailed acoustic backscatter maps of the seabed. Methods to process and interpret the data from MBS have been evolving. The processing of depth data, removing errors caused by ray bending, platform motion, fish schools, bottom detection method and noise have been developed (e.g. [3-5]). Advances are also being made in the processing and understanding of seabed backscatter from multi-beam instruments (e.g. [6-9]).

In-situ backscatter calibration of these instruments is not always possible but advances are being made [10]. For large instruments, relative calibrations are the normal procedure and data from reference sites can be used to calibrate and cross validate the measurements between beams [8]. A consistent methodology for interpretation of seabed backscatter is complicated by the facts that the mean echo and its statistics change with incidence angle for a given seafloor type (roughness and hardness), and that the sampling volume and area resolution of the instrument change with depth and incidence angle. Therefore, several core methods applied separately or in combination are used to analyse the acoustic backscatter based on seabed backscatter models, backscatter statistics and phenomenological characteristics in the data at various spatial scales [9, 11].

A backscatter processing method that minimises between beam instrument and calibration errors and maximise the spatial resolution, references the backscatter to a particular incidence angle (BS$_{ref}$) is adopted here [2, 12]. This method removes the effect of incidence angle on the backscatter response and results in a loss of information near normal incidence but has the advantage of better spatial resolution [2]. Near normal incidence the rate of change of backscatter with incidence angle provides information of seabed type if the seabed is homogeneous across that scale [13]. Interpretation of BS$_{ref}$ for a simplified question of consolidated or unconsolidated sediment that is ecologically significant suggests relative errors less than +/- 2 dB [2] are necessary. To achieve this for large scale data collections requires correction of instrument biases and drift as well as absorption and incidence angle corrections. Instrument biases can be difficult to remove without detailed calibration (but see [12]). In this work we outline a national collection of backscatter from a Kongsberg EM300 MBS instrument mounted on the 65 m marine national facility vessel Southern Surveyor. We nest our collection and processing method into 5 levels being:

Level 1. Raw data collected from the instrument with at sea user adjustments.

Level 2. Automated depth cleaning, consistent backscatter corrections for absorption and incidence angle area estimates for a locally derived slope vector. Referencing the backscatter to an incidence angle of 40° (BS_{40}) to provide a user product.

Level 3. Detailed bathymetric data cleaning for adjusting locally derived slope vector and updating absorption and incidence angle area corrections. Detailed backscatter data cleaning to remove aeration, noise and instrument setting errors.

Level 4. Calibration of the instrument, adjusting for between beam errors and instrument calibration drift using reference sites through a range of temperatures and depths.

Level 5. Detailed absolute calibration at regular intervals.

This paper focuses on level 2 processing where we describe sound absorption and incidence angle area corrections for the locally derived slope at a continental scale.

METHODS

Multi-beam mapping

Bathymetric and backscatter data were collected on opportunistic transit and research voyages using a Kongsberg EM300 multi-beam sonar operating at nominally 31.5 kHz with 135, 1° by 1°, beams on the national marine research vessel Southern Surveyor since 2004 (Figure 1). The mills cross transducers for the MBS were located on a gondola attached 1 m below the keel of the vessel to reduce interference from bubble sweep down (aeration).
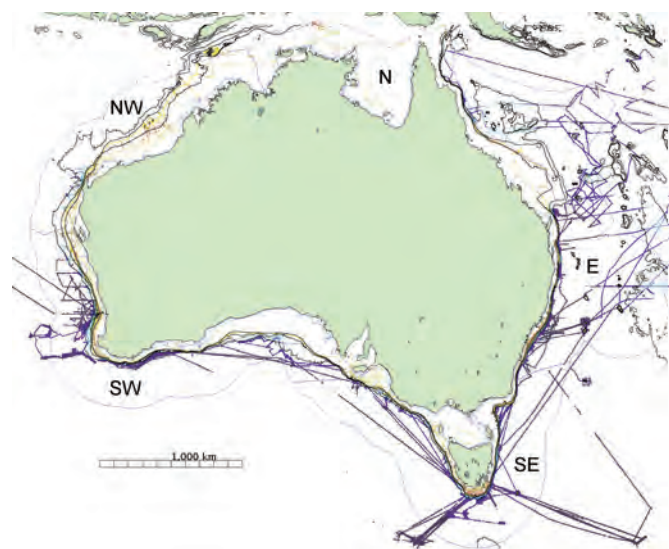
Figure 1. Data collected from the EM300 multi-beam sonar from research and transit voyages from the marine national facility vessel Southern Surveyor since 2004. Blue lines are the large marine domains of North West (NW), North (N), East (E), South East (SE) and South West (SW) with black lines at the 200 m, 700 m and 1500 m depth contours

During research voyages a dedicated MBS operator would monitor the instrument to check settings and update with the appropriate sound velocity and absorption files derived from the temperature profiles using expendable bathy thermographs (XBTs) or temperature and salinity profiles from a conductivity temperature depth probe (CTD) in the region. During transit voyages data were collected using standard settings with minimal human intervention and default sound velocity and absorption profiles. The default operation mode of the EM300 MBS was to set the beam operation into equi-distance mode where the beams were positioned to insonify the seafloor at equal distance assuming a flat seabed from the average depth. The pulse length was set depending on the depth mode as outlined in Table 1.

Table 1. Frequency and pulse length (PL) of the EM300 for incidence angles for the commonly used different operating modes, M, and emitted angle sectors, S

M	PL ms	S	Emitted Angles (θ_{ie})	Transmit Frequency kHz
1	0.7	3	-75 to -47.5 to 47.5 to 75	31.5, 33. 30
2	2	3	-75 to -47.5 to 47.5 to 75	31.5, 33. 30
3	5	9	-75 to -53.7 to -37.05 to -24.75 to -11.4 to 11.55 to 24.5 to 36.6 to 52 to 75	31, 32.5, 34. 32, 33.5, 30.5, 33, 31.5, 30

Processing of the data was done in the following order for the level 2 output where we focus on steps c. and d., the absorption and insonified area backscatter corrections for the target depth range of 150 to 1500 m:

a. Collection of data at sea

b. Correction of depth data for statistical outliers and adjusting to a locally sourced or derived sound velocity profile.

c. Correction of backscatter values to the locally sourced or derived absorption profile and corrected range data.

d. Correction of the estimated area insonified at the seabed incidence angle based on derived along-ship and across-ship slopes.

Processing methods

The acoustic depth data were corrected for sound speed errors, outlier identification and vessel-induced motion artefacts following standard procedures using MB system's software [14]. Anomalous backscatter data were evident when there were inconsistent measured depths due to aeration under the hull of the vessel. These values were excluded from further computations based on the level of processing. For level 2 processing, backscatter data were removed for anomalous depth data only. The backscatter as calculated by the MBS at the centre of each beam was georeferenced based on the edited bathymetry and referenced as an incidence angle to the seabed by the locally derived slope as outlined below. Absorption

corrections were as outlined below. No corrections for transmit and receive beam pattern errors (± 2 dB) were done for this data set at level 2 processing.

Based on software developed by Caress et al. [14] the acoustic backscatter was referenced to a seabed incidence angle of 40°, $BS_{40°}(\theta_i)$, by calculating the mean incidence angle profile $\overline{BS(\theta_i)}$ for 1000 ping bins and subtracting it from the instantaneous backscatter $BS(\theta_i)$ then referencing to the mean backscatter at 40° incidence $\overline{BS(\theta_{40°})}$ where [2]

$$BS_{40°}(\theta_i) = BS(\theta_i) - \overline{BS(\theta_i)} + \overline{BS(\theta_{40°})} \text{ dB} \quad (1)$$

The length of the 1000 ping average assuming a 10 knot steaming speed varies with depth being approximately 5 n.miles, 10 n.miles and 15 n.miles in length at 200 m, 1000 m and 1500 m depths respectively. For pings which sit between the mid-point of two bins the correction is interpolated in time between the two bin averages. The $BS(\theta_{40°})$ data were "despeckled" using a 3 beams x 3 pings boxcar median low-passed filter and gridded data with overlapping tracks were weighted by incidence angle, acknowledging that inner and outer incidence angles are subject to greater variation and error respectively (Table 2). Note that this weighting only occurs when there is data from more than one incidence angle within a grid location placing more weight on data from incidence angles with less statistical variability and or susceptance to noise [2, 15]. The referenced seabed incidence angle of 40° was chosen based on both experimental and model evidence for improved discrimination across substrate types whilst minimising potential errors due to, noise, statistical variation and compensation for absorption and area insonified estimates [2].

Table 2. Weighting of overlapping incidence angle data used for gridding to suppress centre beam normal incidence variability and noise in outer beams at large angles of incidence

Angle (deg.)	0	14.9	15	45	60	80
Weight	0.1	0.1	0.8	1.0	0.2	0.1

Absorption error correction

The real time EM300 algorithms calculate a bottom backscattering strength, BS, following the sonar equation [16]. The BS is calculated from the received echo level (EL), transmitter source level (SL), the two-way transmission loss (2TL) and the logarithm of the resolvable area $A(\theta_{ie})$ on a flat seabed at emitted incident angle, θ_{ie}, where

$$BS(\theta_{ie}) = EL(\theta_{ie}) - SL(\theta_{ie}) + 2TL(\theta_{ie}) - 10\log_{10}A(\theta_{ie}) \text{ dB} \quad (2)$$

where $2TL = 40\log R + 2\alpha R$, for range, R (m), and absorption, α (dB km^{-1}). The error in measured seabed backscatter as a function of depth (D), incidence angle (θ_{ie}) on a flat horizontal seafloor due to the difference in the applied, $\propto_\alpha$, and derived, $\propto_d$ absorption is,

$$Error_\propto = \frac{2D}{\cos\theta}(\propto_\alpha - \propto_d) \text{ dB} \quad (3)$$

The sensitivity of EM300 backscatter measurements to absorption estimates is explored using both the Francois and Garrison (F&G) [17] and the Doonan [18] equations at a reference incidence angle of 40° assuming a flat horizontal seabed. The main difference between F&G and Doonan equations is the estimation of the relaxation frequency for magnesium sulphate. In the frequency range 10 to 120 kHz the absorption due to magnesium sulphate is the dominant factor [17].

When using the EM300 multi-beam the frequency at a given incidence angle changes depending on the mode (Table 1). It is assumed that the EM300 internal algorithms correct for the variation of absorption across frequencies and that the EM300 reference frequency is 31.5 kHz. Estimates of absorption at depth when no temperature and salinity profile was available was done using the temperature and salinity profiles derived by inference based on the satellite altimetry, SST, and all available subsurface information interpolated within a 0.18 degree grid scale [19].

Corrections for incidence angle

Corrections for the area insonified were required for both the along-ship and across-ship directions. The real time EM300 MBS area only approximates the area for across-ship slopes and this will be in error for rugged terrain or noisy real time bathymetric data. Therefore the EM300 applied area compensation that is derived assuming the nearest range is normal incidence was removed [16].

Area compensation was then applied based on two criteria. Firstly, calculating the locally derived slope in the across-ship direction, $Ø_{y_i}$, at the centre of each beam, i, based on the corrected per ping depth data using the automated depth corrections. Secondly, calculating the locally derived slope in the along-ship, $Ø_{x_i}$, and across-ship direction based on a topographic grid of 50 m. The grid size was selected based on the target depth range (200 m to 700 m) for the mapping and a need to smooth the slope estimates from high local deviations due to potentially incorrect bathymetry. For small beamwidths as used in MBS the area, A_i, insonified at the centre part of each beam, i, for an emitted angle, θ_{ei}, was approximated by the minimum of the area estimated near normal incidence, A_{ni}, and oblique incidence A_{oi}

$$A_{ni} = \frac{\psi_y l_x R}{\cos(\theta_{ei} - \phi_y)} \quad (4)$$

$$A_{oi} = \frac{c\tau l_x}{2\sin(\theta_{ei} - \phi_y)} \quad (5)$$

where ψ_x is the -3dB beam-width (radians) in the along-ship direction, for sound speed, c ms^{-1}, range, R m, and pulse length, τ ms. The insonified length, l_{xi}, at the centre of each beam, i, in the along-ship direction, was approximated as the minimum of near normal incidence length, l_{nx} m, and oblique incidence, l_{ox} m

$$l_{nx} = \frac{\psi_x R}{2\cos(\phi_x)} \quad (6)$$

$$l_{ox} = \frac{c\tau}{2\sin(\phi_x)} \tag{7}$$

where ψ_x is the -3dB beam-width (radians) in the across-ship direction [20]. This estimate of insonified area as a rectangle is an approximation and yields a less than 0.6 dB error [21].

Seabed Model

The APL-UW [22] seabed scattering model combines the most dominant dimensionless seabed scattering mechanisms of homogeneous sediment volume scattering coefficient $S_v(\theta)$ and surface roughness coefficient $S_s(\theta)$ as a superposition of incoherent scatter to estimate the seabed backscattering strength $S_b(\theta)$, where:

$$S_b(\theta) = 10log_{10}[S_s(\theta) + S_v(\theta)] \text{ dB} \tag{8}$$

$S_b(\theta)$ was calculated for seabed incidence angles, θ, of 0° to 80° at transmitted frequency of 31.5 kHz and geoacoustic properties of 6 seabed types derived from a synthesis of historic physical seabed samples (table 3.2, [22]).

RESULTS

Since 2004, 0.35 M km^2 of seabed in Australia's five marine domains has been mapped with the MBS, representing 6% of the total. Within the target seabed depth range of 100 m to 1500 m and 200 m to 700 m, 11% and 18% of the seabed has been mapped respectively. This low amount of seabed mapping is mainly due to the wide slope regions in the North West, South West and East bio-regions. In the South East region where the slope is narrow, 75% of the 200 to 700 m seabed has been mapped and 37% in the 100 to 1500 m depth range (Table 3).

Table 3. Area in 1000 km^2 of Australia's five marine domains (Figure 1) and the associated targeted areas of the continental margin from 100 m to 1500 m and 200 m to 700 m. The area mapped in 1000 km^2 and the proportion of the total in each marine bioregion since 2004 from opportunistic transit and research voyages are given

Area 1000 km^2	Marine Bio-Region					
	East	North	North West	South East	South West	Total
Total	2026	626	1068	1157	1292	6168
100 m to 1500 m	502	45	399	86	208	1239
200 m to 700 m	109	4	129	16	45	303
Mapped area total	120	7	29	88	109	352
100 m to 1500 m	39	1	24	32	44	140
200 m to 700 m	12	0	13	12	16	54
Proportion mapped total	5.9%	1.1%	2.7%	7.6%	8.4%	5.7%
100 m to 1500 m	7.8%	2.3%	5.9%	37.4%	21.1%	11.3%
200 m to 700 m	11.1%	0.0%	10.0%	75.0%	36.0%	17.7%

Absorption correction

At the example depth of 400 m, 10° C, 31.5 kHz, 35 salinity and 7.8 pH, the measured absorption is 7 dB km^{-1} and 6.5 dB km^{-1} for the F&G and Doonan equations respectively. There is a potential 0.5 dB uncertainty in the absorption estimate between the two absorption equations for those reference conditions (Figure 2). The absorption coefficient is sensitive to input parameters of temperature, depth, frequency and salinity (Figure 2). The exact nature of this sensitivity needs to be explored for expected ranges of these parameters and the effect on the integrated absorption at depth. The effect of pH on the measured absorption is significantly less than the other parameters and is not shown.

The change in the measured backscatter at 1500 m water depth when the backscatter is referenced to 40° incidence angle for errors in absorption of 0.5, 1 and 1.5 dB km^{-1} is 2 dB, 3.9 dB and 5.8 dB respectively (Figure 3).
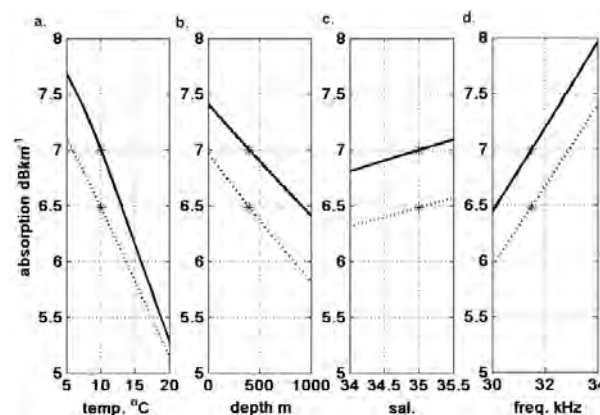
Figure 2. Variation of absorption using the F&G (solid line) and Doonan (dashed line) equations for variations in (a) temperature, (b) depth, (c) salinity and (d) frequency. The absorption at the example depth, 400 m, temperature, 10°C, salinity, 35, and frequency 31.5 kHz is noted with an asterisk *
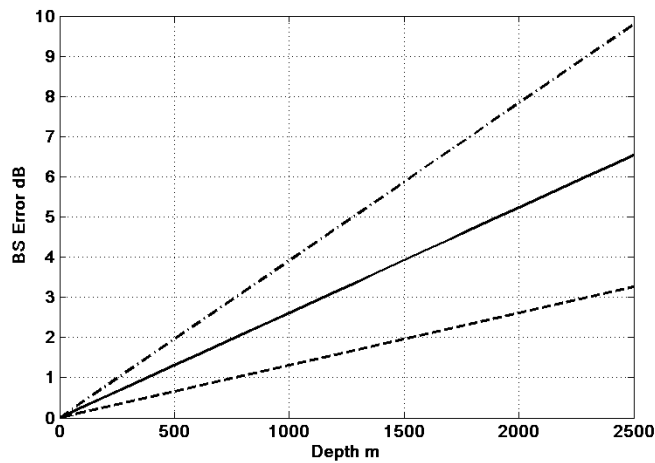
Figure 3. Error in measured backscatter referenced to 40° incidence angle for absorption error of 0.5 (dashed), 1.0 (solid) and 1.5 (dot-dashed) dB km^{-1}
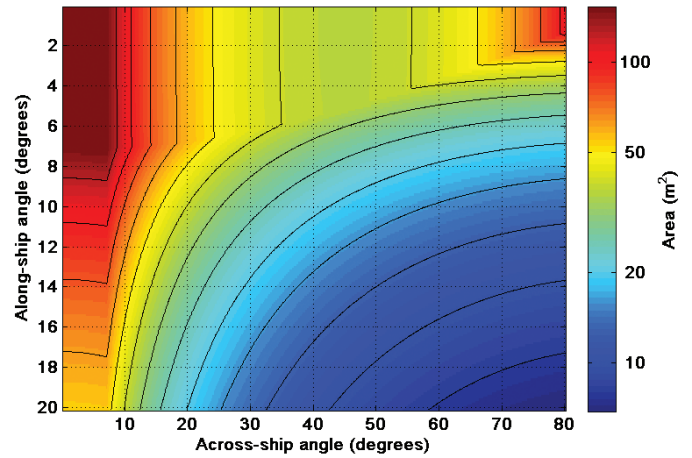

Figure 4. The variation in the area insonified ($10\log_{10}A(\theta_{ei})$) based on equations (4) to (7) at a depth of 700 m and pulse length of 2 ms for across-ship seabed incidence angles of 0° to 80° and along-ship seabed incidence angles of 0° to 20°. Contour intervals are at 1 dB
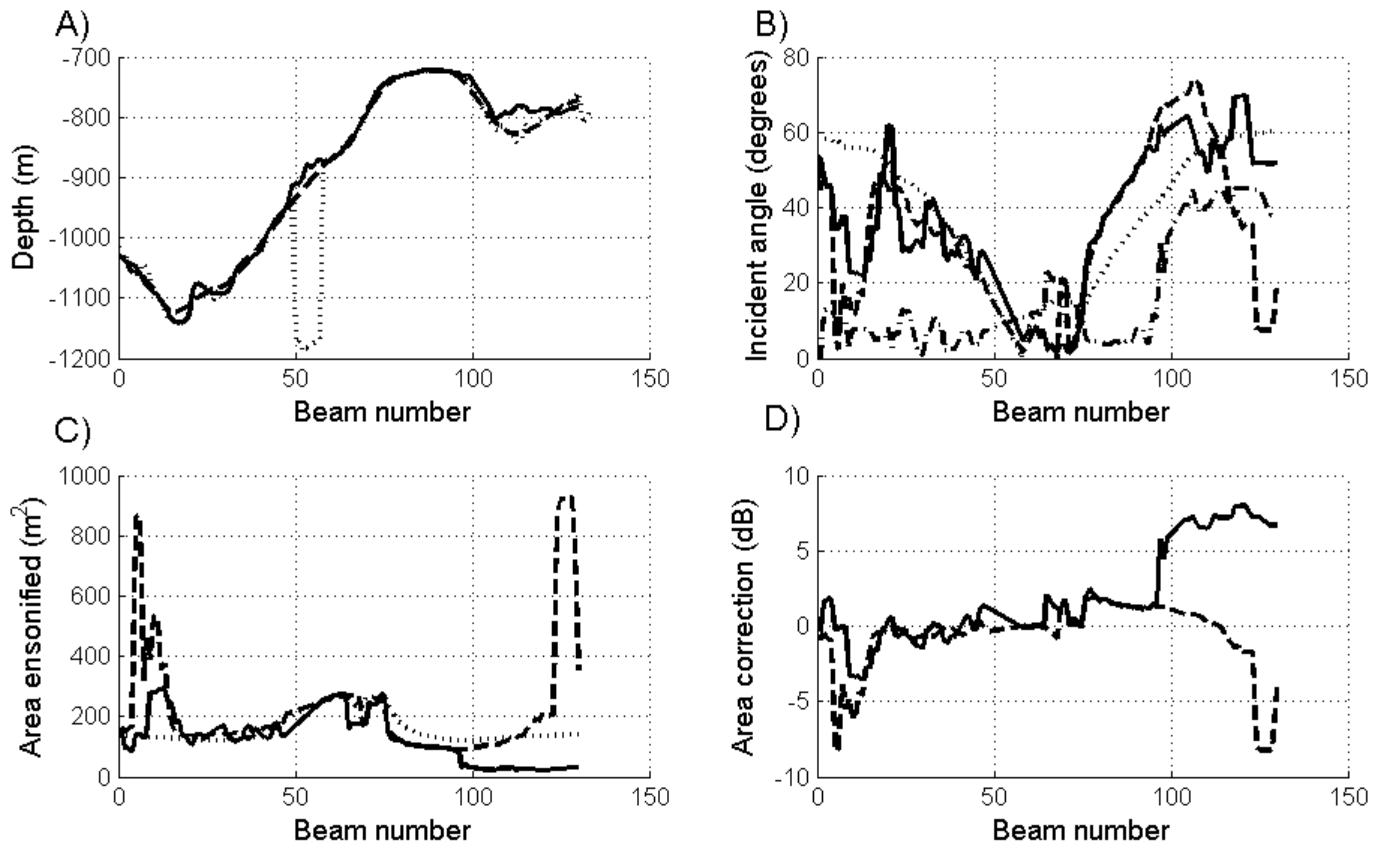

Figure 5. Example of the correction in backscatter for one EM300 ping referenced to the beam number through a canyon feature for a) bathymetry, b) the estimated seabed incidence angle, c) estimated area insonified for each beam and d) the error between the different area estimates. The dotted lines indicate values derived from the real time EM300 instrument algorithms, dashed lines are derived using only the across-ship bathymetry and slope corrections, solid lines are the values from the bathymetry and slope corrections using the topology grid and the dot-dashed line is the along-ship slope estimate

Corrections for incidence angle

The correction of the area insonified will be variable depending on the difference in the assumed and derived across-ship and along-ship seabed incidence angle. The greatest variation is for large seabed incidence angles and along-ship slopes (Figure 4). For the EM300 operating at 2 ms pulse length and an along-ship slope of 10° the backscatter error at 700 m depth is < 1 dB or as high as 5 dB at 0° and 60° incidence respectively (Figure 4).

The correction to the seabed backscatter is most apparent in complex terrain where high across-ship and along-ship slopes are encountered (Figure 5). Figure 5a shows the beam number corrections that are required to the bathymetry data using the ping based and topographic grid based methods. Based on the bathymetric corrections the seabed incidence angle for each beam can be calculated (Figure 5b). In this example there are differences between the applied and derived across-ship incidence angles of 55°. In the along-ship direction the derived seabed slope is a maximum of 45°. The difference in the applied and derived area insonified changes markedly depending on the incidence angle used (Figure 5c). Backscatter corrections in this complex topography varies between +8 to -8 dB for the different incidence angle approaches (Figure 5d). The backscatter area correction that includes both across-ship and along-ship seabed incidence angles should be more precise.

Removal of the incidence angle relationship is done after the corrections for bathymetry and adjustments to the seabed backscatter for absorption, seabed incidence angle and area. An empirically derived 1000 ping average is applied to the data where the average backscatter to seabed incidence angle is derived and a low pass filter applied (Figure 6).

Model seabed backscatter

The expected dynamic range of seabed backscatter at 31.5 kHz for consolidated (rough rock) and unconsolidated sediment (clay) at a seabed incidence angle of 40° is -6 dB to -28 dB based on the APL94 model [22] (Figure 7). In this instance consolidated seabed is characterised as -6 to -15 dB and unconsolidated -18 to -28 dB at 40° incidence angle. The transition zone between the definition of consolidated and unconsolidated is 3dB and accuracy in the estimated backscatter of 1-2 dB is required to minimise misclassification errors. This model of seabed types highlights the improved discrimination of the reference seabed incidence angle of 40° and is consistent with previous model estimates and measurements using a similar instrument at a higher frequency (Kloser et al. 2010).
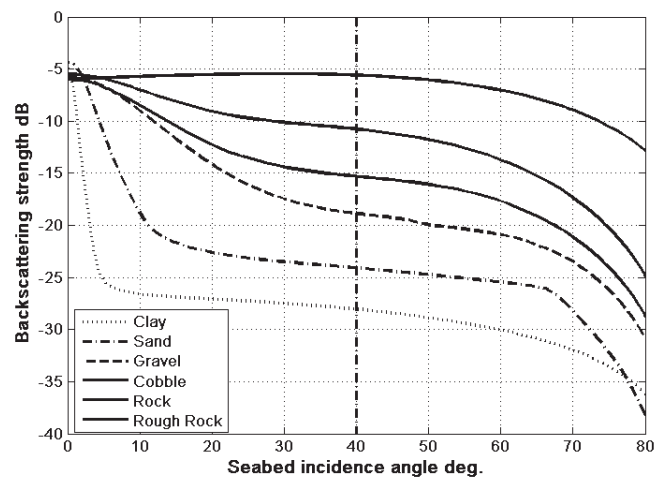
Figure 7. Estimated seabed backscatter at 31.5 kHz based on the APL94 [22] seabed model for consolidated (cobble, rock and rough rock) and unconsolidated (gravel, sand and clay) seabed assuming geoacoustic parameters as outlined in table 3.2 of APL94 [22]. The reference seabed incidence angle of 40° is highlighted

DISCUSSION

In this paper we have outlined a seabed backscatter mapping program based on opportunistic transit and research voyages of the marine national facility vessel Southern Surveyor since 2004. Based on this opportunistic sampling 100% coverage of the wide upper slope regions in the North West, and East marine bioregions has not been possible with less than 11% mapped in the 200-700 m range. For these regions alternative sampling strategies should be considered to provide representative coverage. In the South East region, systematic sampling has meant that 75% of the 200-700 m depth range is mapped. The processing of the data has been nested in a 5 level scale and only level 2 processing to minimise errors due to incorrect sound absorption and area compensation has been discussed here. The objective of distinguishing consolidated from unconsolidated sediments is reported to require relative measurement accuracies of better than 2 dB for a 100 kHz MBS [2]. This error requirement is consistent with the scattering model predictions at 31.5 kHz where the differentiation of consolidated and unconsolidated material is ~3 dB [22].

Figure 6. EM300 backscatter for a vessel track at ~ 200 m depth for (a) raw, (b) backscatter referenced to 1000 ping average at 40° incidence angle to the seabed, (c) after low pass filtering. Dynamic range is -20 dB dark and -40 dB light. The inserts highlight the effects of the median 3 beams by 3 pings box car filter on the backscatter

Corrections for incorrect sound absorptions are required given the large temperature range experienced from Australia's tropics to temperate regions. A consistent method has been applied when processing data from transit voyages where no direct temperature and salinity profile of the region is available. This method should reduce relative measurement errors. What remains uncertain is which of the F&G and Doonan absorption equations are more correct. For fisheries research the Doonan equation at 38 kHz is recommended based on a statistical reanalysis of historic data [18]. There is an approximate 0.5 dB difference between these two equations that can increase to errors of 3 dB at 2500 m. To resolve which equation is more appropriate will require new experiments in appropriate temperature, salinity and depth ranges.

Significant corrections for the area insonified were necessary to correct for across-ship and along-ship slopes. The real time EM300 algorithms to estimate the area insonified can be in significant error when the estimated bathymetry is incorrect. This is due to the assumption in the real time EM300 algorithms that the shortest range signal is derived from normal incidence. Corrections for both across and along slope are required which is most pronounced in canyon systems of highly variable topography. Errors of +8 to -8 dB can be observed in the data set. It is normal practice to map out a region with a MBS perpendicular to the overall slope therefore minimising along-ship slope errors. In canyon and seamount systems this is not always possible and backscatter corrections using the topology are required. The magnitude of predicted errors for along-ship slopes was highest in the outer beams (incidence angles >60°). At 700 m depth the predicted error in backscatter for a 10° along-ship slope was 5 dB at 70° incidence angle (Figure 4). The predicted errors for estimating the area insonified are themselves subject to errors. Estimating the local along-ship and across-ship slopes relies on good bathymetry. To remove noise it is necessary to smooth the slope over a number of points that may or may not be consistent with the insonified area at all incidence angles. We have assumed that the area insonified can be treated as a rectangle and not an ellipse by integrating the transmit and receive beam patterns ([6, 21]). For narrow beams this error has been shown to be less than 0.6 dB but can be significantly higher near normal incidence and for wider beams [21]. Further, the exact area insonified will be related to the seabed materials the detailed transmit and received beam patterns and the processing methods internal to the MBS at each incidence angle [6, 8].

Despite all the uncertainties expressed above there is a consistent large difference in seabed backscatter between consolidated and unconsolidated seabed that is readily detected using this method and a given MBS instrument within a specified region and appropriate seafloor sampling [2, 23]. There is commonly a greater than 7 dB difference at 40° incidence angle between unconsolidated sand and consolidated rock substrate. This large relative difference is easily detected with a MBS at the time of mapping. Greater uncertainty in classification of seabed types arises in fine scale differences between substrate types and moving between instruments, depths, regions and over time. This highlights the need to establish reference seabed sites over various depths which can be mapped (with MBS, video and physical samplers) at regular intervals (potentially annually) around the continental margin. These reference sites would not only ensure appropriate calibration and classification of the seabed backscatter data but also monitor natural and human induced changes to the seabed [23]. In this study, seabed sites close to major ports have been opportunistically remapped. Based on the processing method outlined here these sites will be used to evaluate instrument measurement variability and substrate discrimination resolution. It that way it should be possible to associate an error estimate to the backscatter value to guide usage and future needs for mapping.

The overarching goal of the mapping program was to maximise the transit times on the Marine National Facility (MNF) vessel Southern Surveyor and the EM300 MBS at minimal cost. In this work we have nested the data collection into a 5 level processing method and due to cost only processed to level 2 with largely automated processing (http://www.marine.csiro.au/geoserver). At level 2 processing a user can determine where mapping has occurred and know that a consistent processing method has been applied for the absorption, area insonified and the effect of incidence angle. Estimates of consolidated and unconsolidated sediments can then be done as outlined in Kloser et al. [2]. At level 2 processing artefacts in the data remain as no visual analysis has been done to remove aeration and incorrect instrument settings. Depending on how the data is to be used it will be necessary to process the data to level 4 for consistent relative estimates and level 5 for absolute backscatter estimates. As part of a national mapping data set we recommend the data is processed to levels 4 and 5.
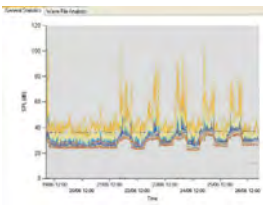
ACKNOWLEDGEMENTS

REFERENCES

[1] A. Williams, N.J. Bax, R.J. Kloser, F. Althaus, B. Barker and G. Keith, "Australia's deep-water reserve network: Implications of false homogeneity for classifying abiotic surrogates of biodiversity", *ICES Journal of Marine Science* **66**(1), 214-224 (2009)

[2] R.J. Kloser, J.D. Penrose and A.J. Butler, "Multi-beam backscatter measurements used to infer seabed habitats", *Continental Shelf Research* **30**, 1772-1782 (2010)

[3] N.C. Mitchell, "Processing and analysis of Simrad multibeam sonar data", *Marine Geophysical Researches* **18**(6), 729-739 (1996)

[4] B.R. Calder and L.A. Mayer, "Automatic processing of high-rate, high-density multibeam echosounder data", *Geochemistry Geophysics Geosystems* **4**, 1-22 (2003)

[5] G. Canepa, O. Bergem and N.G. Pace, "A new algorithm for automatic processing of bathymetric data", *IEEE Journal of Oceanic Engineering* **28** (1), 62-77 (2003)

[6] C. de Moustier, "Beyond bathymetry: Mapping acoustic backscattering from the deep seafloor with Sea Beam", *Journal of the Acoustical Society of America* **79**(2), 316-331 (1986)

[7] J.E.H. Clarke, L.A. Mayer, N.C. Mitchell, A. Godin and G. Costello, "Processing and interpretation of 95 kHz backscatter data from shallow-water multibeam sonars", *Proceedings of Oceans '93*, 437-442 (1993)

[8] L. Hellequin, J. M. Boucher and X. Lurton, "Processing of high-frequency multibeam echo sounder data for seafloor characterisation", *IEEE Journal of Oceanic Engineering* **28**(1), 78-89 (2003)

[9] C.J. Brown and P. Blondel, "Developments in the application of multibeam sonar backscatter for seafloor habitat mapping", *Applied Acoustics* **70**(10), 1242-1247 (2009)

[10] K.G. Foote, D.Z. Chu, T.R. Hammar, K.C. Baldwin, L.A. Mayer, L.C. Hufnagle and J.M. Jech, "Protocols for calibrating multibeam sonar", *Journal of the Acoustical Society of America* **117**(4), 2013-2027 (2005)

[11] D.R. Jackson and M.D. Richardson, *High-frequency seafloor acoustics*, Springer, New York, 2007

[12] G. Lamarche, X. Lurton, A.L. Verdier and J.M. Augustin, "Quantitative characterisation of seafloor substrate and bedforms using advanced processing of multibeam backscatter-Application to Cook Strait, New Zealand", *Continental Shelf Research* **31**(2), 93-109 (2011)

[13] L. Fonseca, C. Brown, B. Calder, L. Mayer and Y. Rzhanov, "Angular range analysis of acoustic themes from Stanton Banks Ireland: A link between visual interpretation and multibeam echosounder angular signatures", *Applied Acoustics* **70**(10), 1298-1304 (2009)

[14] D.W. Caress, S.E. Spitzak and D.N. Chayes, "Software for multibeam sonars. New software for processing data from side-scan-capable multibeam sonars facilitates determining seafloor characteristics", *Sea Technology* **37**(5), 54-57 (1996)

[15] A.N. Gavrilov and I.M. Parnum, "Fluctuations of seafloor backscatter data from multibeam sonar systems", *IEEE Journal of Oceanic Engineering* **35**(2), 209-219 (2010)

[16] E. Hammerstad, "Multibeam echo sounder for EEZ mapping", *Proceedings of Oceans '97*, **2**, 1255-1259 (1997)

[17] R.E. Francois and G.R. Garrison, "Sound absorption based on ocean measurements. Part II: Boric acid contribution and equation for total absorption", *Journal of the Acoustical Society of America* **72**(6), 1879-1890 (1982)

[18] I.J. Doonan, R.F. Coombs and S. McClatchie, "The absorption of sound in seawater in relation to the estimation of deep-water fish biomass", *ICES Journal of Marine Science* **60**(5), 1047-1055 (2003)

[19] K.R. Ridgway, R.C. Coleman, R.J. Bailey and P. Sutton, "Decadal variability of East Australian Current transport inferred from repeated high-density XBT transects, a CTD survey and satellite altimetry", *Journal of Geophysical Research-Oceans* **113**(C8), 18 (2008)

[20] C. Demoustier and D. Alexandrou, "Angular-dependence of 12 kHz seafloor acoustic backscatter", *Journal of the Acoustical Society of America* **90**(1), 522-531 (1991)

[21] R. J. Kloser, *Seabed biotope characterisation based on acoustic sensing*, PhD Thesis, Curtin University of Technology, Australia, 2007

[22] Applied Physics Laboratory, *High frequency ocean environmental acoustic model handbook,* Technical Report APL-UW TR 9407, 1994

[23] R. J. Kloser, A. Williams and A. J. Butler, "Exploratory Surveys of Seabed Habitats in Australia's Deep Ocean using Remote Sensing – Needs and Realities in Todd, B.J., and Greene, H.G., eds., Mapping the Seafloor for Habitat Characterisation:" *Geological Association of Canada*, Special Paper 47, 93-110 (2007)

AN ANALYSIS OF GLIDER DATA AS AN INPUT TO A SONAR RANGE DEPENDENT ACOUSTIC PERFORMANCE PREDICTION MODEL

Janice Sendt

Thales Underwater Systems, Thales Australia, 274 Victoria Road, Rydalmere NSW 2116 Australia

Janice.sendt@thalesgroup.com.au

This paper describes an initial assessment of the role of glider data as an input into a sonar nowcast acoustic detection range prediction model. It includes an analysis of the temporal and spatial variability of the water column data measured by a glider in shallow Australian waters. The area covered by the data includes a region where there is a known persistent frontal feature. The glider data verified that a persistent front was present in the data.

INTRODUCTION

One of the difficulties in underwater nowcast predictions for sonar acoustic detection ranges has often been the paucity of available water column data which can also have a very inhomogeneous distribution in both space and time. Ideally the acoustic calculation should consist of at least one or a number of sound velocity profiles (SVPs) across the required distance which gives a true representation of the variation in sound. Historically, the measured sound speed at a given location has either been calculated from measured temperature and salinity profiles or directly measured with a speed of sound sensor. Depending on the gradient within the SVP, sound may propagated well in the water column or be dissipated at either of the boundaries.

A number of papers compare calculated transmission loss with at sea measurements in Australian waters [1,2]. The collecting of the necessary data within the time scale required for these calculations has been an expensive logistic exercise requiring support equipment in the form of aircraft or support vessels collecting SVPs across the required range and bearing/s.

For an operational system it has not been practical to expect access to this level of data collection on a regular ongoing basis, instead for nowcast sonar range predictions it has been the practice to use an insitu bathy drop (this contains a temperature probe which measures the profile and is supplemented with climatology data to characterise the water column). This situation changed about four years ago with the increasing availability of 3D gridded water column oceanographic data sets produced on an hourly basis [3].

An obvious source of water column data which has recently become available is from autonomous gliders. These have the ability to measure the water column ahead of a vessel, albeit slowly and to provide this data in a reasonably short time period. In addition, there can be multiple gliders concurrently collecting data so that many bearings can be covered simultaneously.

Autonomous gliders follow an up and down sawtooth profile through the water column sampling the water column for temperature and salinity approximately every 5 seconds.

As the glider is driven by variable buoyancy it travels at approximately 1 km/hour (see Figure 1).

Initial data assessment

The data was collected by Defence Science and Technology Organisation (DSTO) using two Slocum gliders over five days from 11th - 15th July 2011 at the top end of the Capricorn channel in the southern Great Barrier Reef area [4]. Figure 2 plots the route of the two gliders, named, glider "k85" which traversed further from the coast than glider "k90". Cape Clinton is the nearest coastal feature spanning from 22.55°S to 22.65°S. The CTD probe fitted to the glider is Sea-Bird 41CP.

The Temperature-Salinity (T-S) diagram of all the data points for both gliders is shown in Figure 3. The features displayed in these plots differ due to the different glider routes with glider k85 traversing deeper water than glider k90. The maximum temperature was recorded by the k85 which was slightly less than 21°C compared to glider k90 which recorded a maximum temperature 0.05°C lower. The salinity range is greater for k85 than k90.
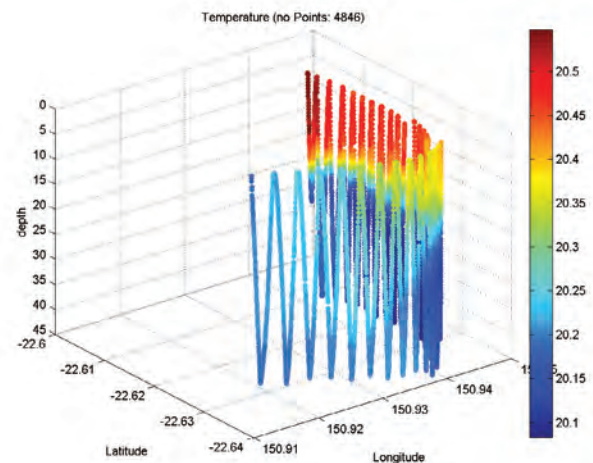

Figure 1. Raw temperature glider data showing the sawtooth profiles as a function of depth. Temperature measured in degrees Celsius and depth in metres
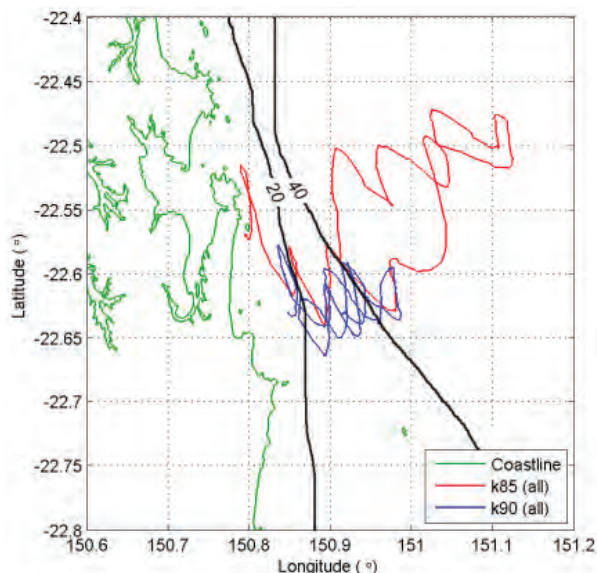
Figure 2. Route taken by the two gliders over a three day period starting late 11th July 2011. Depth contours are in metres

There are obvious differences in the features between the two glider T-S plots which could be due to the time of measurement and/or the location. When the glider data was reviewed in hourly time increments it became apparent that a parcel of cold water was traversed by glider k90 on the early morning of the 15th July. The maximum surface temperature was then reduced by 0.8°C in a 2 hour time period (see Figure 4). The second glider traversed the same area 8 hours later and the temperature profile exhibited similar changes symptomatic of a sustained front. For the salinity profile, there is a delay of some two hours after the temperature reaches its lowest value at 11 hours transit when the salinity values which have initially increased, then stabilise to a small range of values between surface and maximum glider depth. This is indicative of a well mixed water column. Thus the complexity of the two temperature/ salinity curves shown in Figure 3 is partially due

to the overlaying of two parcels of water, one with a maximum temperature slightly below 21°C and the second with a maximum temperature at approximately 19.7°C.

Ocean Currents

Previous studies conducted in the area of the Southern Great Barrier Reef based on satellite thermal imaging have concluded that there is a persistent frontal feature, called the Clinton Cape front, caused by the impact of the change in coastal orientation on a northward moving, well-developed boundary current [5]. This front was described as a mushroom shaped jet of cold water starting from the coast, and extending eastward 245 km. Along the coast line the width of the root was 85 km and tapered at the throat to 18 km before expanding at the head to 105 km. An earlier reference found that the front was smaller, extending out 100 km [6]. The jet temperature was generally 1° to 2°C cooler than the surrounding water. It is hypothesised that the routes of both gliders crossed this frontal boundary. As there is no open source high resolution satellite sea surface temperature (SST) imagery for this time and area this cannot be independently verified. It is also assumed that waters within the jet are well mixed based on the T-S diagrams.

The boundary delineation where the temperature values become constant for the entire water column depth can be estimated by viewing the T-S diagrams which have been clustered into three different types, typical examples are shown in Figures 5 to 7. Figure 8 plots the different T-S types on the glider routes. Figure 5 shows that the water column was generally well mixed in the bathymetry range of 0–20 m and in deeper water during the start of glider "k89" transit when it was between 22.5°S and 22.55°S. Generally, as the water depth increased the T-S diagram showed a greater range of temperature and salinity values and the resulting plot varied from a curve as shown in Figure 6 to a rotated L or hook shape over a small temperature and salinity range. In the 41-60m water depth the T-S data often included a hysteresis as shown in Figure 7 which is a 3D temperature salinity depth diagram. The data in this figure shows that the T-S hysteresis is due to the salinity measurements. There are two possible causes for the hysteresis: firstly, it may be due to
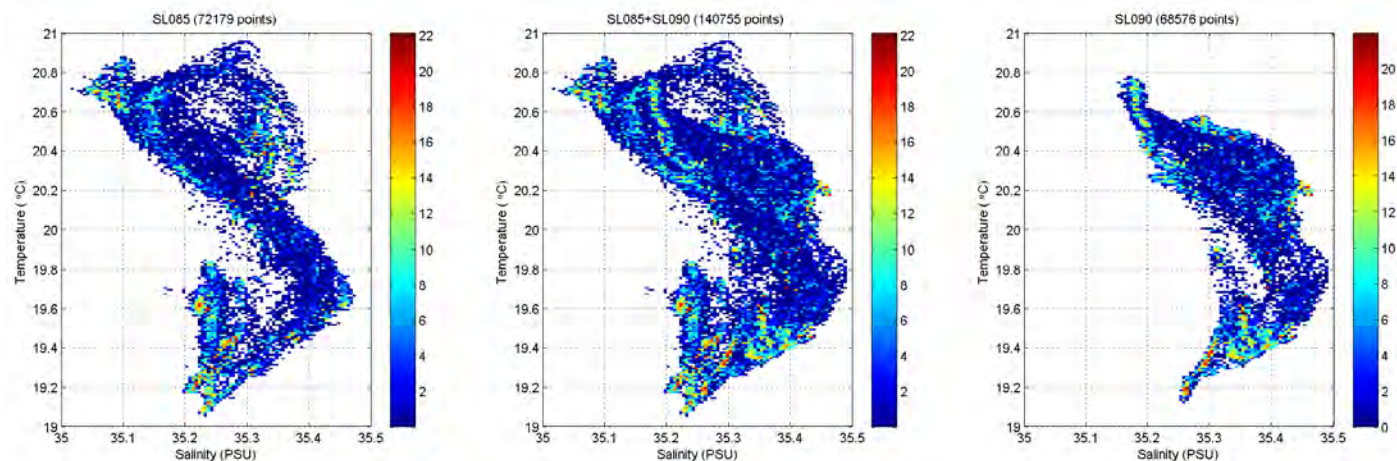

Figure 3. Temperature Salinity diagram for the two gliders. The colour intensity scale shows the number of points which recorded each temperature salinity pair

different sensor measurement latency times during the downcast/upcast cycle or secondly, it may reflect an actual water column event. There are no independent measurements to clarify this. If the cause is due to a latency issue then either a correction needs to be applied to the salinity measurement or some of the data is excluded in the speed of sound calculation.

Tidal Analysis

This area of the Great Barrier Reef is noted for its macro tidal ranges [7]. Table 1 shows the tidal information for 3 days of the trial. During the time of the significant change in the T-S plots, the night of Thursday 14th and Friday 15th morning the tidal heights were at a maximum due to the new moon as indicated by the open circle next to the "Friday 15" caption.

Middleton [10] notes that the surface temperature increases from the coast across the shelf and the salinity decreases across the shelf. This is in agreement with the data presented in Figure 9. Both of these findings are supported by the data for the eastward leg from location 22.55°S 150.9°E where the maximum surface temperature was 20.1°C with a steady increase until 22.5°S 151.1°E where the maximum surface temperature was 20.8°C. After this time, the glider apparently moved away from the cool water jet and the maximum surface temperature remained stable down to location 22.6°S 151°E.
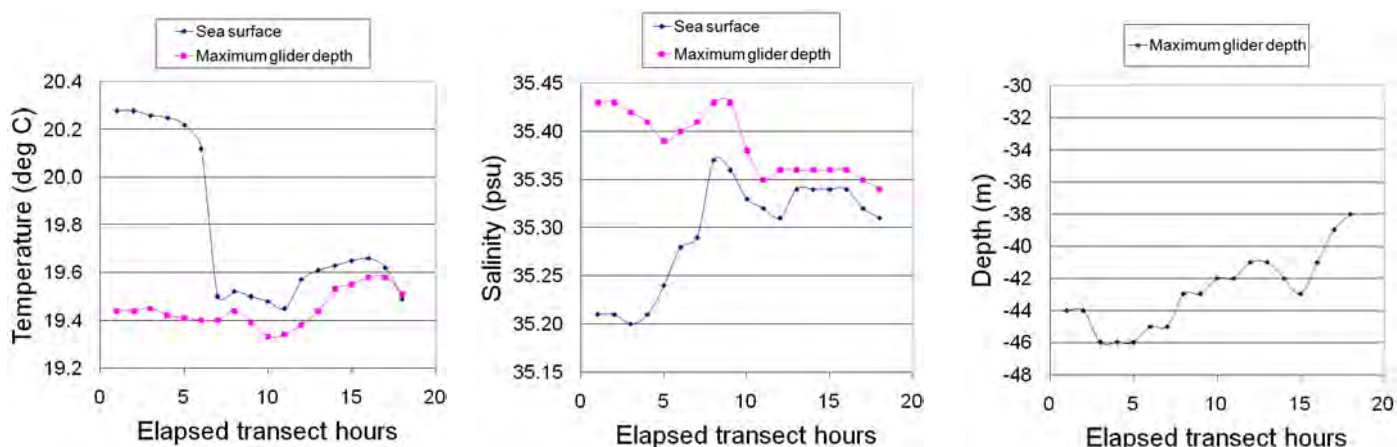
Figure 4. Temperature, salinity and maximum glider depth during a 20 hour transit time for glider "k90"
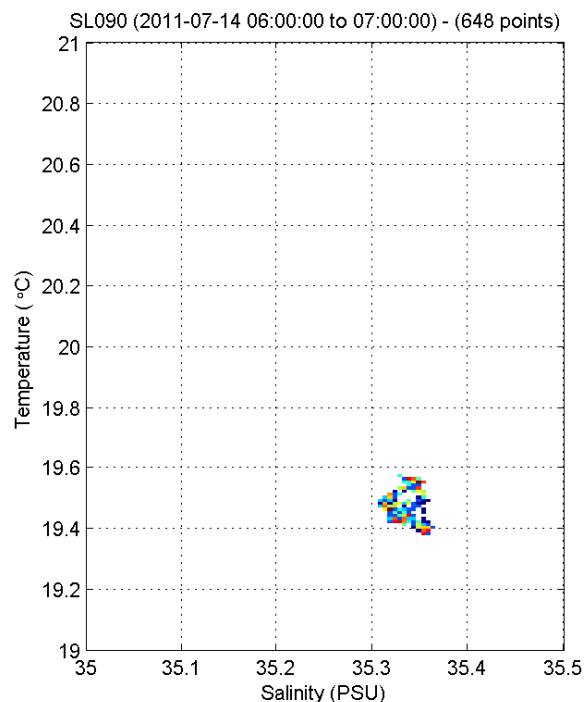
Figure 5. T-S diagram of well mixed water based on 1 hour of data. The colour intensity scale shows the number of points which recorded each temperature salinity pair
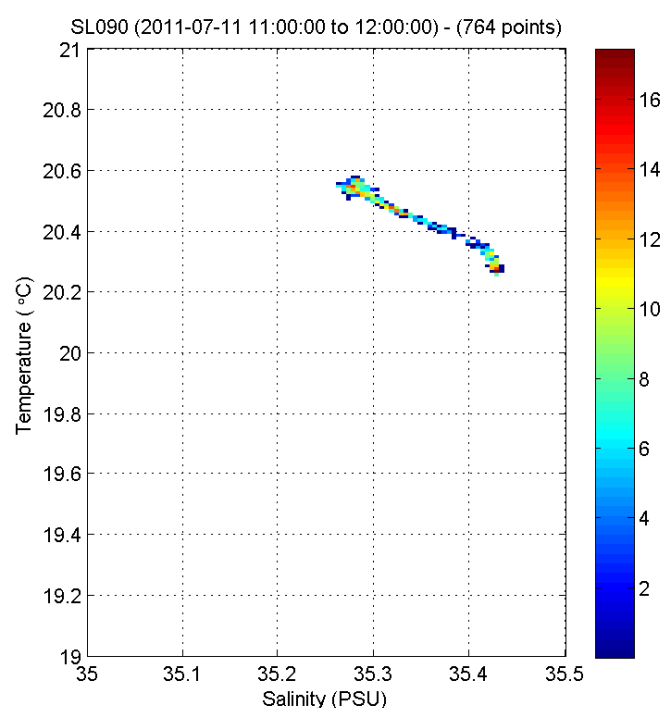
Figure 6. T-S diagram for water column with a vertical gradient in properties based on 1 hour of data. The colour intensity scale shows the number of points which recorded each temperature salinity pair. Water depth is 50 metres

Table 1. Local tidal information. Height is in metres (extracted from [8])

Port Alma - Times and Heights of High and Low Waters
July - 2011

(Peaked Island, add 3 minutes for approximate tide times)

Wednesday 13		Thursday 14		○ Friday 15	
Time	Height	Time	Height	Time	Height
0209	0.98	0255	0.87	0336	0.82
0744	4.19	0829	4.27	0909	4.32
1408	0.87	1451	0.81	1529	0.80
2027	5.25	2107	5.29	2143	5.26
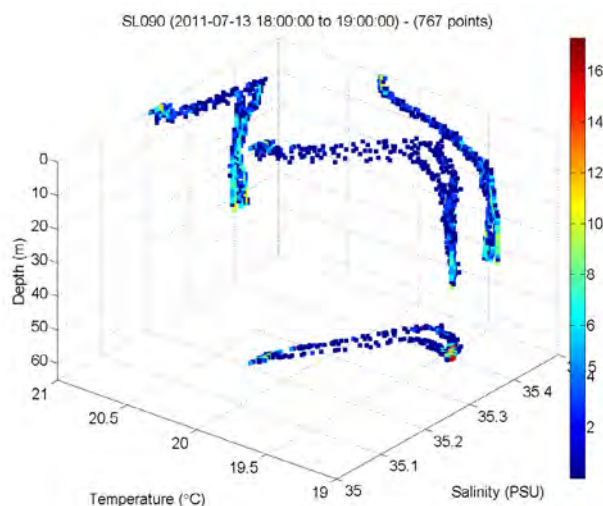
Figure 7. 3D Temperature Salinity Water Depth diagram for 1 hour of data which displayed hysteresis. The colour intensity scale shows the number of points which recorded each temperature salinity pair
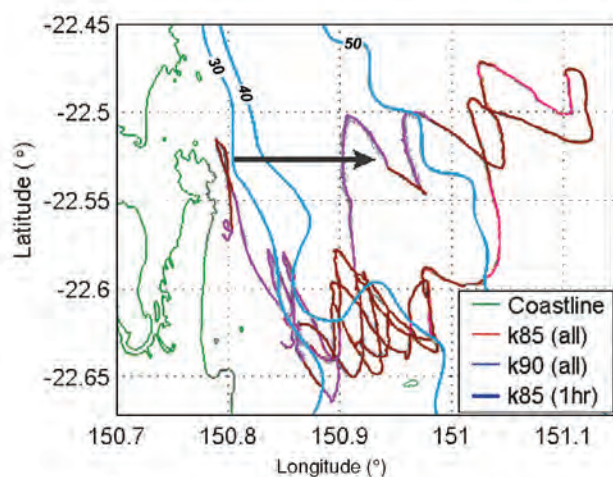
Figure 8. Cluster analysis of the T-S data based on 1 hour sampling. The arrows indicate the reported current flow. The purple overlay of the routes indicate the possible southern edge of a cold water jet and is based on T-S diagrams which are similar to Figure 5. The brown route overlay is for locations where the T-S diagram is similar to Figure 6. The pink route overlay is for locations where the T-S diagram is similar to Figure 7
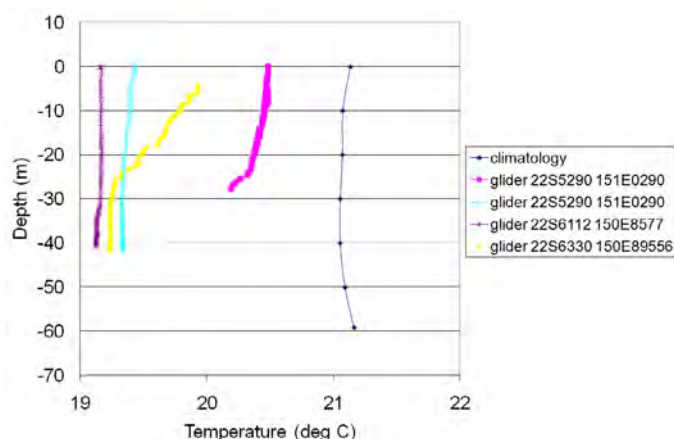

Figure 9. Comparison between the temperature profiles recorded at different glider locations against climatology database [9]

Consecutive glider up and down casts

A 7.5 km northerly route starting from approximately 150.9°E 22.6°S and ending at approximately 150.9°E 22.5°S was chosen (see Figure 8). The T-S characteristics of this route are of well mixed water similar to those given in Figure 5. Figures 10 and 11 show the raw temperature and salinity concatenated, contiguous, upcasts profiles as a function of depth. The average distance travelled and the elapsed time from the start of the route for each upcast is given in Figure 12. The jump in distance between cycle 5 and 6 in Figure 12 is assumed to be due to a GPS adjustment and the range along the route would need to be reduced accordingly.

Although the temperature and salinity ranges are small for each of the plots, there is evidence of the dynamics of the water column present in Figures 10 and 11. For example, there is a parcel of warm water present near the surface in Figure 10 from cycle 6-8. The salinity plot (Figure 11) shows an evolution from slight stratification at cycle 1 to well mixed from cycle 9 onwards.
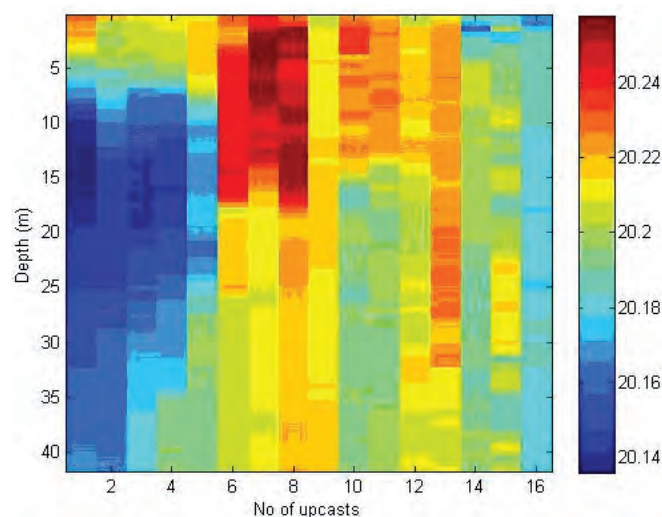

Figure 10. Sequence of contiguous upcast temperature profiles (°C) as a function of depth
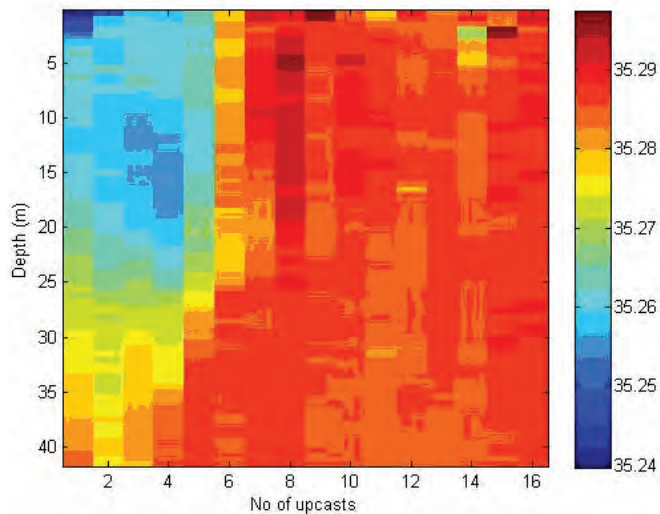
Figure 11. Sequence of contiguous upcast salinity profiles (psu) as a function of depth
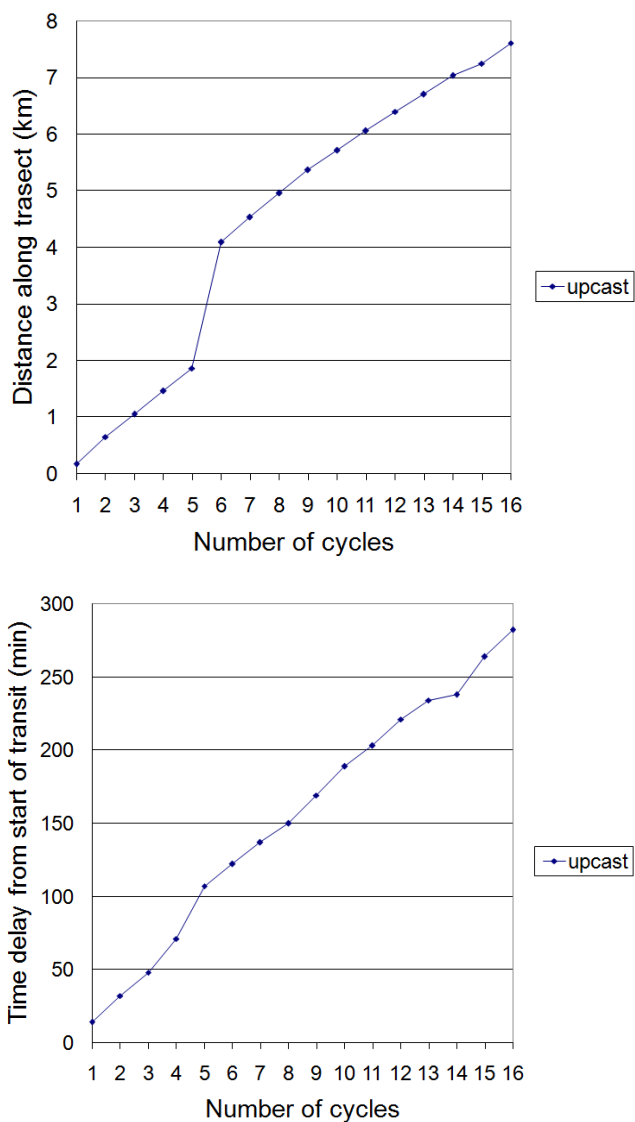

Figure 12. Distance and time delay along upcast route

The temperature and salinity profiles have been converted into sound speed profiles for five ranges from the start of the transect as indicated in Figure 13. Although, the temperature and salinity ranges for this route are small, the resulting sound velocity profiles are noticeably different, particularly in the first 5 to 10 metres. As the glider moved along the route, for a 3 hour period and 2 km distance, the sound velocity profile became primarily dependent on depth due to the well mixed water for the entire water column. The mechanism for the mixing could be tidal or due to the Clinton Cape jet or both. Measurements across at least two tidal cycles along the same track would assist in assessing the relative contribution of each mixing mechanism.
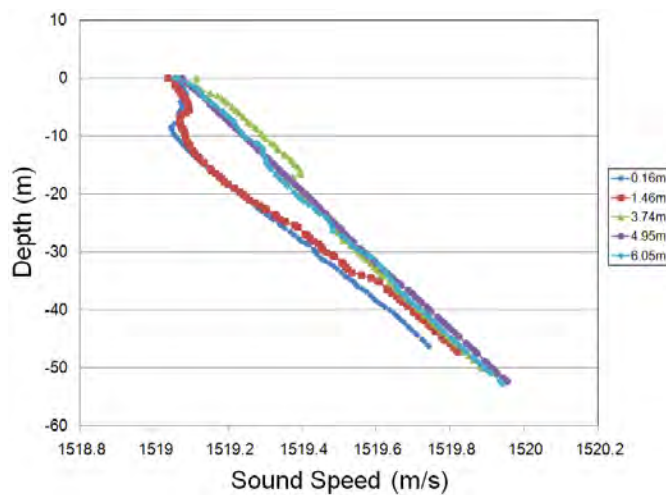

Figure 13. Sound speed profiles based on concatenated upcast glider measurements using the raw ranges given in Figure 11

Figure 14 shows the full sequence of contiguous sound speed profiles using the salinity and temperature data for the full water depth given in Figures 10 and 11. The profiles show the upward refracting sound velocity profiles are a constant feature of the track with some small variations near the surface. Figure 15 shows sound velocity profiles at an easterly point in the route.
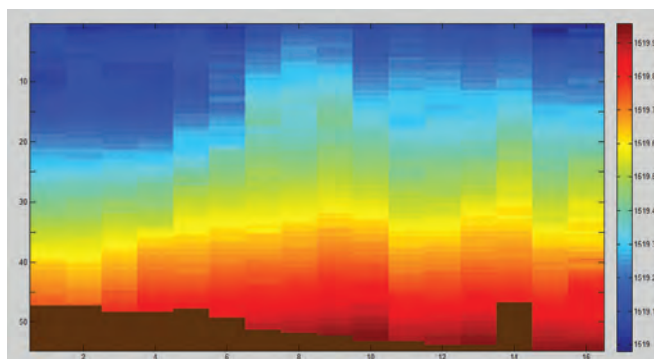

Figure 14. Sound speed profiles based on concatenated upcast glider measurements using the raw ranges given in Figure 12
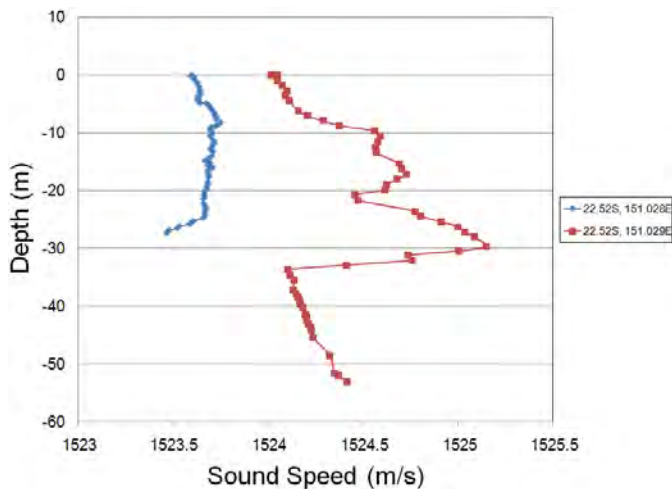
Figure 15. Up cast sound speed profiles at an easterly point of the route

DISCUSSION

The goal of this preliminary study was to look at the suitability of glider data as an input for nowcast range dependent acoustic transmission loss calculations. The conclusion reached based on the dynamic datasets reviewed is that if one uses this data directly to calculate sound speed profiles then a number of caveats would need to be applied. In the first instance there is the issue of the salinity hysteresis to be resolved. In the second instance, the profiles need to be aligned in time for the different upcast/downcast time delays noting that the data has the finest time resolution in depth compared to the coarser and variable time resolution in range. In the third instance, the location of the measurement may require a correction due to GPS adjustments. Finally, there is the need to include the differences between individual upcast/downcast. A solution to the latter issue is to separate the data into two sets or to average the upcasts and downcasts. One set would consist of upcasts and the other down casts. These could each be used to predict the transmission loss and detection range. This may result in different detection ranges being calculated and the concept of "range of ranges" (i.e. a number of possible ranges based on the dynamics of the water column) needs to be invoked for the detection range calculations.

Rather than directly using the glider data after applying suitable corrections, a more preferred approach is to use it in conjunction with a priori knowledge or as an input into a local regional oceanographic model. As indicated in this study, the general location of oceanographic features, such as the northward moving boundary current and the Cape Clinton jet can be given as existing knowledge. The role of the glider data could be to refine this information for nowcast predictions. In particular, the glider data can be used to infer greater detail, such as steric height (steric height anomaly is the difference between the height of a given water column and the height of an ideal 0°C, 35 psu salinity column,), which could supplement existing satellite observations. The given set of glider data has a limited lifetime which can be extended with the inclusion of an afternoon effect model (which calculates the effect of the warming of the top of the ocean), but at the expense of requiring a number of additional inputs such as wet and dry air temperature. The use of the afternoon effect model can also allow the glider data to be aligned to a particular instant in time. The concept of "range of ranges" is also suitable in this context as a means of including the variability of the measured parameters in the range prediction result.

ACKNOWLEDGEMENTS

REFERENCES

[1] A.D. Jones, J.S. Sendt, Z. Yong Zhang, P.A. Clarke and J.R. Exelby, "Optimisation of transmission predictions for a sonar performance model for shallow oceans regions", *Proceedings of Acoustics 2002*, Adelaide, Australia, 13-15 November 2002

[2] A.D Jones, J.S. Sendt, Z. Yong Zhang, P.A. Clarke and A. Maggi, "Modelling the acoustic reflection loss at the rough ocean surface", *Proceedings of Acoustics 2009*, Adelaide, Australia, 23-25 November 2009

[3] BLUElink ocean forecasting for Australia's future, http://www. csiro.au/en/Organisation-Structure/Flagships/Wealth-from-Oceans-Flagship/BLUElink-Brochure.aspx (last accessed 20 March 2013)

[4] P.N. Jackson and A.D. Jones, "Slocum gliders deployed by the Defence Science and Technology Organisation (DSTO) in the Coral Sea in July 2011 (DSTO_T11_20110711 and DSTO_MadmaxTest2011_20110711)", Defence Science and Technology Organisation (DSTO), 2012

[5] D.M. Burrage, C.R. Steinberg, W.J. Skirving and J.A. Kleypas, "Mesoscale circulation features of the Great Barrier Reef region inferred from NOAA satellite imagery", *Remote Sensing of Environment* **56**, 21-41 (1996)

[6] J.A. Kleypas and D.M .Burrage, "Satellite observations of circulation in the southern Great Barrier Reef, Australia", *International Journal of Remote Sensing* **15**, 2051-63 (1994)

[7] The Tides of Australia, *www.abs.gov.au › ABS Home › Statistics*

[8] Bureau of Meteorology, Tide Predictions for Queensland, http://www.bom.gov.au/oceanography/tides/MAPS/gbr. shtml#map (last accessed 20 March 2013)

[9] CSIRO Atlas of Regional Seas (CARS 2000), www.marine.csiro. au/~dunn/eez_data/atlas.html (last accessed 20 March 2013)

[10] J.H. Middleton, P. Coutis, D.A. Griffin, A. Macks, A. McTaggart, M.A. Merrified and G.J. Nippard, "Circulation and water mass characteristics of the southern Great Barrier Reef", *Australian Journal of Marine Freshwater Research* **45**, 1-18 (1994)

MODELLING ACOUSTIC TRANSMISSION LOSS DUE TO SEA ICE COVER

Polly Alexander[1,2], **Alec Duncan**[3], **Neil Bose**[1] **and Daniel Smith**[2]

[1]**Australian Maritime College, University of Tasmania, Maritime Way, Launceston, TAS 7248, Australia**
[2]**Intelligent Sensing and Systems Laboratory, CSIRO ICT Centre, Hobart, TAS, 7000, Australia**
[3]**CMST Curtin University, Kent Street, Bentley, Perth, WA, 6102, Australia**
pollyalexander@gmail.com

The propagation of underwater acoustic signals in polar regions is dominated by an upward refracting sound speed environment and the presence of a dynamic highly variable ice canopy. This paper provides an overview of the acoustic properties of sea ice and assesses the influence of ice canopy and water column properties on acoustic transmission loss for propagation within 20 km of a sound source at 20 m depth. The influence of the ice canopy is assessed first as a perfectly flat surface, and then as a statistically rough surface. A Monte Carlo method is used for the inclusion of ice deformation and roughness. This involves the creation of sets of synthetic ice profiles based on a given sea ice thickness distribution, followed by statistical methods for combining the output of individually evaluated ice realisations. The experimental situation being considered in the framing of this problem is that of an Autonomous Underwater Vehicle (AUV) operating within 50 m of the surface. This scenario is associated with a frequency band of interest of 9-12 kHz and a horizontal range of interest up to 20 km. The situation has been evaluated for a set of typical ice statistics using Ray and Beam acoustic propagation techniques. The sound speed profile (based on real data) results in a strong defocussing of direct path signals at ranges from 9-20 km and depths shallower than 50 m. This reduction in the signal strength of the direct path creates areas where the influence of surface reflected paths becomes significant. The inclusion of a perfectly flat ice layer reduces the transmission loss between 9-20 km by 15-50 dB. When the ice layer is included as a rough surface layer the results show a boost to signal strength of up to 8 dB in the small areas of maximum defocussing. Sea ice is a strongly time and space varying sea surface and exists in areas where defocussing of the direct path due to the sound speed profile reduces the range of direct path dominated transmission. This work presents methods for including a statistically relevant rough surface through a technique for generation of sets of surfaces based on ice deformation statistics. It outlines methods for including ice in acoustic modelling tools and demonstrates the influence of one set of ice statistics on transmission loss.

INTRODUCTION

Accurate sea ice volumes and under ice biology measurements are important inputs to global ocean climate and ecosystem models, and key indicators to monitor for change. With a heightened focus on climate science and change there is an increasing importance in measuring and monitoring what is happening under the ice covered oceans of the Arctic and Antarctic [1]. With advances in Autonomous Underwater Vehicle (AUV) capability the use of this technology in the ice environment is becoming more frequent [2–4]. AUVs operating in an open ocean environment use underwater acoustic communication for non safety-critical information and rely on their ability to surface and establish radio or satellite communication for critical situations such as navigation error or mission failure. In an under ice environment there is a far greater reliance on underwater communication as surfacing is no longer an option. Understanding and modelling acoustic propagation in an under ice environment is a key component in increasing safety and reliability in these deployments.

Typical Sound Speed Profiles (SSPs) in the Arctic and Antarctic produce an upward refracting sound environment, creating a sound channel that is continuously reflecting off the top ocean boundary, usually an ice layer. Variations in the top few hundred metres of the sound speed profile can create a defocussing of the direct path signal at ranges of 9-20 km. This defocussing creates a situation where the surface reflected paths provide a greater contribution to the received signal than would otherwise be experienced at such short ranges. To model propagation in this environment requires both the ability to create a realistic model of ice and the capability to incorporate the ice model within a framework for predicting acoustic propagation and transmission loss. The ice layer in a sea ice environment is a complex system made up of different ice types, ice thicknesses, roughness, and areas of ice deformation and ridging [5, 6]. This ice covered environment is highly variable with location, season and weather conditions. The presence of this spatially and temporally changing ice layer creates a large variation in the reliability of acoustic propagation.

There are two main parts to including an ice layer in an acoustic model. The first is consideration of the material properties of the ice layer in order to include the ice as an acoustic medium, and the second is the inclusion of randomly shaped and sized perturbations caused by sea ice ridging. Once the ice is included in the acoustic model there is then the question of what propagation modelling technique is most appropriate. There are five main techniques used in modelling underwater acoustic propagation. Ray theory, Normal Mode, Multipath Expansion, Wavenumber Integration (WI) or fast

field, and Parabolic Equation (PE) [7]. Etter [7] reviews and summarises modelling and simulation techniques reported up to 2001. For higher frequency work ray tracing provides the fastest solution with a minor compromise in accuracy [8]. The Acoustics Toolbox [9] is an open source modelling tool that provides a selection of environment and propagation modelling tools within the one software framework. The BELLHOP program is a Fortran ray and beam forming code that is part of the Acoustics Toolbox [9].

This paper reviews these two main parts of including an ice layer and investigates and reports on a method for including a variably ridged layer. Techniques for creating simulated ice cover from sea ice statistics are discussed and a case study involving a typical set of ice statistics is evaluated using BELLHOP. This work considers the influence of including an ice layer in short range acoustic modelling and compares direct path results with flat ice and the results of the presented technique for including statistically rough ice, for a frequency of 10 kHz a range of 20 km and receiver depths shallower than 50 m. Ray tracing is used as the most computationally feasible propagation model for this frequency and range scenario.

Background

There has been significant research into under ice sound propagation in the Arctic since the 1960s. This is due to the disputed nature of borders in this area, defence prerogatives, the potential for natural resources, and the capability for long range propagation. The consequence of this is a body of research investigating the influence of an ice canopy on acoustic propagation at both low and high frequencies. Low frequencies have the potential for long range propagation, whereas high frequency signals undergo greater scattering and attenuation losses both in the sea water and due to the roughness dimensions of the ice and the frequency dependence of its attenuation [10–12]. For high frequencies (>15 kHz) the report by the Applied Physics Laboratory, University of Washington [13] provides a comprehensive section on acoustics in the Arctic. For low frequency there are many investigations into long range propagation that examine low frequency interaction with ice [10, 11, 14].

Compared to many of the long range propagation scenarios considered in the Arctic, communication systems for AUV deployment require relatively high frequencies (9-12 kHz) and short ranges (<100 km). Typical underwater acoustic modems operate between 8-13 kHz, with some modems reporting frequency ranges of 3-30 kHz [15].

SEA ICE

The formation of sea ice is dictated by the weather (meteorological) and water (hydrographical) conditions at the time of formation and through its life cycle. These conditions control the temperature, salinity, density and crystal structure of the ice as it is formed, and as the ice grows in thickness the different layers tell the story of the conditions under which it was created [16]. A large amount of sea ice is formed and decays within a single winter, summer cycle and is referred to as first year ice. In a typical growth scenario, sea ice first forms as slush from the collection of ice crystals in open water.

It then consolidates into small distinct plates, or pancake ice, these combine to make larger floes that are further influenced by environmental conditions and deformed to create a ridged ice environment. This process means that sea ice is a range and time varying surface layer, in both thickness, roughness and material properties.

Jezek et al. [17] describe the impact on the acoustic properties of sea ice due to the change in surface texture at different growth stages. They separate this into three states: slush, growing, and consolidated ice. The growing stage involves the formation of pure ice dendrites, a crystal that forms with a tree like form [18], that acts as a skeletal layer on the ice surface collecting salty brine pockets. Consolidated ice is where the ice has formed a solid bottom surface and the slush stage is where there is only slush ice on the surface. Throughout these stages of growth the ice becomes a better acoustic reflector with slush ice attenuating a signal ten times more than growing ice which itself attenuates a signal five times more than consolidated ice (reported for high frequency near normal incidence) [17, 19].

The two main methods of mechanical ice thickening are ridging and rafting of ice floes. Sea ice ridging is formed by the shearing and compression of ice floes pressing out ice blocks below and on the surface of the ice [20]. Rafting of ice is where one ice floe is pushed on top of another pushing the bottom floe into the water. Shear ridging creates small chunks of ice with a ground up appearance while both pressure ridging and rafting create a collection of more discrete blocks of different shapes, sizes and orientations [13]. These mechanical forces create features, with the air-ice surface features referred to as sails, and the ice-water surface features referred to as ice keels. These forces are not symmetric and the ridge sails undergo significantly different weathering than keels. While this weathering is not symmetric there is correlation between top and bottom geometries that can be used to estimate bottom roughness from surface features [11, 21]. As sea ice undergoes its many deformations the underside becomes a continuously rough surface in which the exact definition of any distinctive feature, as opposed to the other roughness of the surface, varies [22].

Material properties of sea ice

As ice supports both shear and compressional acoustic propagation it can be modelled as an elastic medium. The temperature and salinity profiles of an ice layer control the density and the porosity of the ice which then dictates the elastic properties and the reflection loss of acoustic waves interacting with the ice [13, 23]. Ice porosity and ice sheet thickness are reported to have the largest influence on the acoustic properties of the ice [24] with salinity and temperature variation within the ice having less effect [12]. If the shear velocity is less than the speed of sound in water, a vertically polarised shear velocity, as reported by Kuperman and Schmidt [25] occurs, at which point the air-ice boundary also becomes significant to the model. Hunkins [26] measured and analysed shear and compressional waves within an ice sheet. The shear waves are understood to interfere with compressional waves and the acoustic field in the water close to the ice boundary [8, p443]. McCammon and

McDaniel show that the elastic properties of the ice play an important role in attenuation of a plane wave on an ice surface at both high and low frequencies [12].

A more complex ice model is used by McCammon and McDaniel [12] who model ice as a multi-layered elastic solid bounded on both sides by a fluid half space, and Yew [24] who models it as a 'transversely isotropic brine saturated porous medium'. Modelling ice as a multi-layered medium allows for the inclusion of a skeletal growth layer and surface snow as well as variability with the ice itself. The acoustical properties to describe an ice layer can either be found through specific experiments to measure the sound velocities in the ice or through processing of temperature and salinity measurements.

A method for calculation of the acoustic parameters from temperature and salinity is summarized in the report by the Applied Physics Laboratory [13]. It summarises the process of calculating density and porosity from temperature and salinity then provides equations to compute compressional speed, shear speed and bulk moduli, and gives an approximation for attenuation as a function of frequency and temperature [12].

An ideal model to include the material properties of sea ice could take as input the properties of the ice and supply information to a propagation model such that it can calculate reflection effects. An appropriate description of ice for a model could consists of a combination of the following:

- the acoustic properties of the ice: ice density (ρ), compressional wave speed and attenuation (C_p, A_p), shear wave speed and attenuation (C_s, A_s)

- the physical properties of the ice: temperature, salinity, air/ice temperature, ice growth stage

- the morphological properties of the ice: thickness, ice-water roughness, ice-air roughness, ridging statistics

from which a model would calculate or estimate the reflection losses and phase change with incident angle.

Sea ice as a rough surface

As sea ice undergoes many deformations the underside becomes a continuously rough surface. A view of this roughness in the Antarctic sea ice pack taken by a Remotely Operated Vehicle (ROV) is show in Fig. 1 to illustrate some of the shapes that are possible. Sea ice thickness is often described using a histogram of an ice thicknesses descriptor over the area being considered [5, 27]. Depending on the scale of roughness being investigated descriptors used for variation in the ice surface are: thickness; draft; and keel size. Ice draft is the measurement of ice depth/thickness measured from the water freeboard. Ice feature count and thickness histograms form amplitude distribution functions for a discrete area of sea ice, and can be described by a Probability Density Function (PDF) and spatial power spectrum.

Sea ice density and rafting impacts are such that sea ice is much deeper below the surface than it is tall above the surface which results in an asymmetric thickness PDF with a long positive tail. This is even more the case when considering the PDF of ice draft with the freeboard an upper limit in one direction and the potential for deep keel features creating

Figure 1. View of Antarctic sea ice from below taken by a ROV. This picture illustrates the roughness of the surface. Photo courtesy of the Australian Antarctic Divsion ROV team

large extremes in ice draft depth. Depending on the ice environment the thickness/draft PDF may also contain multiple peaks representative of different ice types, areas of different mean thickness, or age within the one profile [28].

One way of describing the roughness from this information is by characterising the shape of the histogram and fitting it to a known distribution. Previous work characterising the distribution of the sea ice features has not provided a single solution with Gaussian, Gamma, Poisson, Rayleigh, a combination of multiple log normals, and power spectrum descriptions being suggested.

Simulated sea ice

Simulation of ice profiles based on measured or predicted sea ice statistics allows the translation of ice thickness or roughness statistics to acoustic propagation and transmission loss statistics. This translation can be achieved through Monte Carlo simulation or generation of larger, keel feature statistics, such as that suggested by Diachok [21]. Simulation from ice statistics also creates an interface for using output from global climate models that include representations of sea ice for given locations and times to predict an acoustic environment that has not been sampled.

There are two techniques in the literature for creating simulated sea ice draft profiles. The first provided by Hughes [28], uses a combination of log-normal distributions to describe and generate ice profiles. The second proposed by Goff [29] using a covariance model and a gamma based PDF description.

Goff [29] describes the sea ice draft distribution using the following descriptors:

- Mean ice draft t_0
- Normalised skewness μ_3^n
- Characteristic length λ_θ
- RMS variation H
- Fractal dimension D

Hughes [28] specifies the sea ice draft as a combination of seven log-normal curves each described by:

- Individual contribution to the total PDF
- Mean of the log of the individual peak
- Standard deviation of the individual peak

Hughes provides a more complex description of the ice amplitude distribution by including different peaks for different ice types within the one sample area. The multi modal representation of this technique would give it a strong advantage if the ice region being considered covered areas of distinctly different ice types. It reports a very accurate fit to reported ice draft data from different experimental data sets.

Goff's technique provides an approximation of the ice draft amplitude variability as a gamma PDF. The Gamma PDF provides a good model of the asymmetric, long tailed nature of the ice draft measurements, but only includes one peak. The use of a single, standard PDF for ice draft makes this approach easier to implement, but less robust to areas of different ice types, compared with the multi peaked approximation of Hughes.

METHODS

A test case has been implemented to demonstrate this method for including simulated rough ice in the Acoustics Toolbox and to evaluate the influence of including ice on transmission loss for one scenario.

The roughness and depth of each ice realisation was included using an altimetry file that specified the depth of the water ice boundary with range. The Goff method for ice simulation was implemented to create a set of altimetry files for a set of ice descriptors. Goff's technique is selected to evaluate the difference between including a single ice type and including flat ice. Two of the sets of ice statistics described in Goff [29] are shown in Table 1 to show the variation in statistics with ice type. Figure 2 shows simulated ice profiles for these two sets of ice statistics paired with normalized histograms of the deviation from the mean draft. This shows the large amount of surface roughness generated by this technique, the conformity of the simulated profile to the gamma distributions they are based on and the variability between two different sets of ice descriptive statistics. Three instances of each ice statistic are displayed to show the variability within this random sampling. The ice statistics from the first line of this table describing the what is refereed to as 'typical' ice conditions are used in this case study. The generated profiles were processed into altimetry files with 1 m horizontal resolution, that were then entered into the Acoustics Toolbox environment specification and used in the calculation of ray path and transmission loss by BELLHOP. For this typical ice case 25 synthetic ice profiles of 20 km length were created using the Goff technique described in the *Simulated sea ice* section.

The acoustic properties of the ice were included through the specification of a reflection coefficient file that provided a look up table of reflection amplitude and phase change as a function of incidence angle. For this case study the ice layer was modelled as an air backed layer using the acoustic properties of ice approximated by Jensen et al. [8] as: compressional speed 3500 m/s; shear speed 1800 m/s; density 890 kg/m^3; compressional attenuation 0.4 dB/λ_p; and sheer attenuation 1.0 dB/λ_s and a thickness of 2.7 m corresponding to the mean ice draft of the typical ice conditions described by Goff. These two layers were specified as input to the *bounce* program, that is part of the Acoustics Toolbox, which computes the

Table 1. Ice morphology statistics from test cases presented in Goff [29]. Ice is described by mean ice draft (t_0), normalised skewness (μ_3^n), characteristic length (λ_θ), RMS variation (H), and fractal dimension (D)

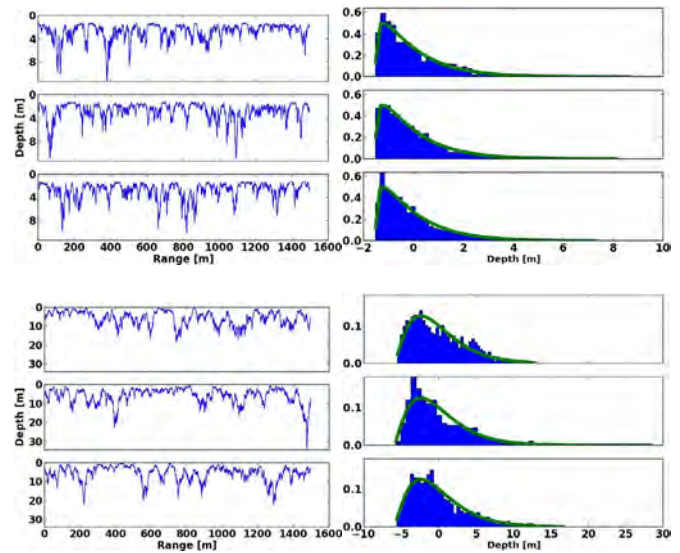|	t_0 [m]	μ_3^n	λ_θ[m]	H [m]	D
Typical Ice					
1	2.76	1.81	40.5	1.38	1.37
Large RMS variation and Low Skewness					
2	4.52	1.27	63.8	3.84	1.26

Figure 2. A random selection of simulated ice drafts with histograms of deviation from mean ice thickness and the probability density functions they are based on. Ice statistics used are those described in Goff [29] and are shown in Table 1. The top figure is based on what are identified as typical ice conditions in the field location reported by Goff and the bottom is for an ice type identified as an area of large RMS and low skewness ice

combined reflection coefficient for a stack of media for a given frequency. The reflection coefficient for 10 kHz generated using this technique is shown in Fig. 3.

The Acoustics Toolbox environment was set up with input parameters shown in Table 2. The Sound Speed Profile (SSP) used was based on the down cast of a Conductivity Temperature Depth (CTD) cast taken in Antarctica on November 22nd 2010 at Latitude 64°35 South, Longitude 81°57 East. The data from the CTD cast were combined using the formula presented by Medwin [30] for sound speed shown in Eq. (1) where T is temperature in °C, S is salinity in practical salinity units (p.s.u.), and z is water depth in metres.

$$C(T,S,z) = 1449.2 + 4.6T - 0.055T^2 + 0.00029T^3 \\ + (1.34 - 0.010T)(S-35) + 0.016z \tag{1}$$

For the cast depth of 600 m used here this formula provides sufficient accuracy [31]. The calculated sound speed for the full cast with the raw temperature and salinity data is shown in Fig. 4. In the case study only the down cast was used and the SSP was extrapolated to the full 2 km depth assuming

minimal change in salinity and temperature beyond the depth of the cast.

Monte Carlo methods work on the principle of combining the output of many instances, randomly sampled from an input distribution, to produce an output representative of the input space. In this case, simulated ice draft profiles are created using a statistical distribution of the ice. The acoustic field is calculated individually for each simulated draft and the combined outputs provides a statistical representation of the acoustic field for that ice sample space. BELLHOP was run individually for each simulated profile to produce an incoherent pressure field p_i. These fields were then combined as an incoherent average as described in Eq. (2).

$$p_{RMS} = \sqrt{\frac{\sum_{i=0}^{N} |p_i|^2}{N}} \qquad (2)$$

The average transmission loss was then calculated using Eq. (3).

$$TL_{avg} = -20 \log_{10}(p_{RMS}) \qquad (3)$$

Two reference case incoherent pressure fields were also calculated. The first, p_{dp}, including the direct path only by removing beams on surface interaction, and the second, p_{flat}, using a flat ice case with an ice boundary at a constant 2.7 m. The differences diagrams in the results section are evaluated as a difference between two fields in decibels using Eq. (4).

$$Rel = 20 \log_{10}\left(\frac{p_1}{p_2}\right) \qquad (4)$$

RESULTS AND DISCUSSION

The increase in sound speed with depth evident in Fig. 4 results in sound being refracted upwards towards the sea surface. However, the marked departure of the profile from a straight line results in this refraction being non-uniform, producing strong focusing of sound at some ranges and defocussing at others. In particular there is strong defocussing near the sea surface at ranges between nine and twenty kilometres. This result can be seen in the direct-path only transmission loss and ray trace plots shown in Fig. 5.

The inclusion of a flat ice layer using the method specified above produces a consistent acoustic field with much lower transmission loss beyond 9 km than if only the direct path is included. The transmission loss and ray tracing results for the flat ice case are shown in Fig. 6. The transmission loss for the flat ice case is similar to what would be expected for an open water surface. This can be explained by evaluating the grazing angles of the rays that are interacting with the surface as shown in Fig. 7. This figure shows that almost all the surface interactions take place with a grazing angle less than 10 °. Figure 3, showing the reflection coefficient for an air-backed layer of ice 2.7 m thick at 10 kHz, shows only minimal reduction in the magnitude of the reflection coefficient for these small angles, explaining the near open water result.
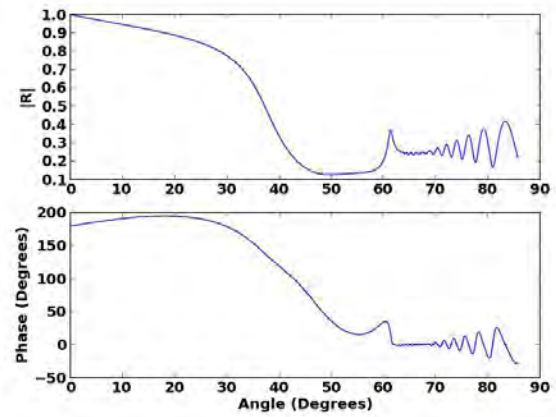

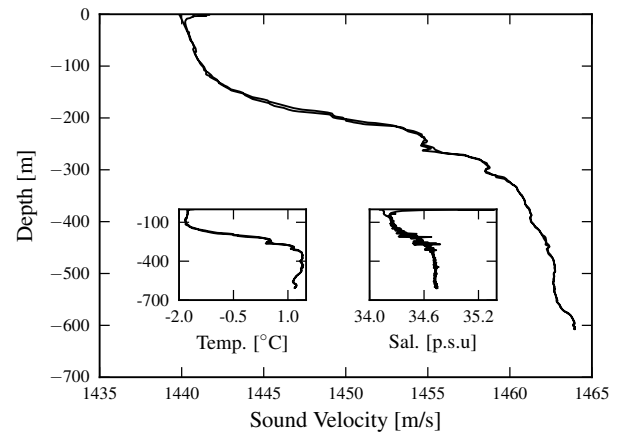Figure 3. Reflection coefficient for combined medium: water, 2.7 m of ice, air at 10 kHz

Figure 4. Sound speed profile measured in the Antarctic Ocean with temperature and salinity shown as inset figures. Values from the down cast were extrapolated to the 2 km depth for use in the case study presented in this paper

Table 2. BELLHOP Inputs

| Parameter	Value
Environment	
Frequency	10 kHz
Range	20 km
Environment depth	2.0 km
Transmission loss	Incoherent
Bottom surface	Water matched
Source	
Source depth	20 m
Beam type	Gaussian
Start Angle (from horizontal)	-20 °
End Angle (from horizontal)	20 °
No. beams	10,000
Receivers	
Number horizontal	200
Number vertical	100
Max receiver depth	50 m
Max receiver range	20 km
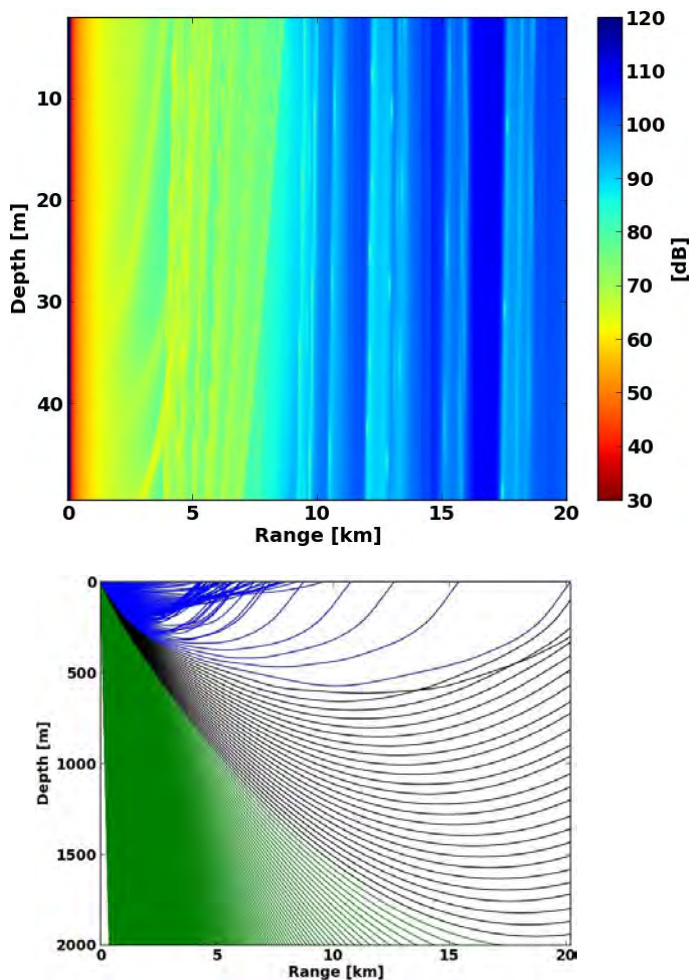
Figure 5. Direct Path only transmission loss for the top 50 m of interest and a ray trace for the full 2 km depth. Red rays touch top and bottom surfaces, green bottom only, blue surface only and black neither surface

The difference between the direct path only and the inclusion of a flat ice layer can be seen in Fig. 8 which shows the difference as calculated by Eq. (4) with p_1 being the flat ice pressure field and p_2 being the direct path only pressure field. This difference representation highlights the defocussing of the direct path only transmission loss and suggests that in the presence of flat ice the received signal strength would be much higher than if considering only the sound that reaches the receiver without interacting with any boundaries.

Results calculated using the Monte Carlo method for the case of deformed sea ice show significantly less surface reflected contribution. The results of the averaged pressure field from the Monte Carlo simulation are shown in Fig. 9. This result shows some filling in of the defocussed band at 17 km but the difference is only 8 dB, as opposed to 42 dB for the flat ice case.

The difference between this rough ice surface realisation and the direct path as calculated by Eq. (4) with p_1 being the ridged ice pressure field and p_2 being the direct path only pressure field is shown in Fig. 10. The reason for this reduction of the signal with the inclusion of the rough surface is clearly seen in Fig. 11 which shows the ray trace for a single rough ice instance with
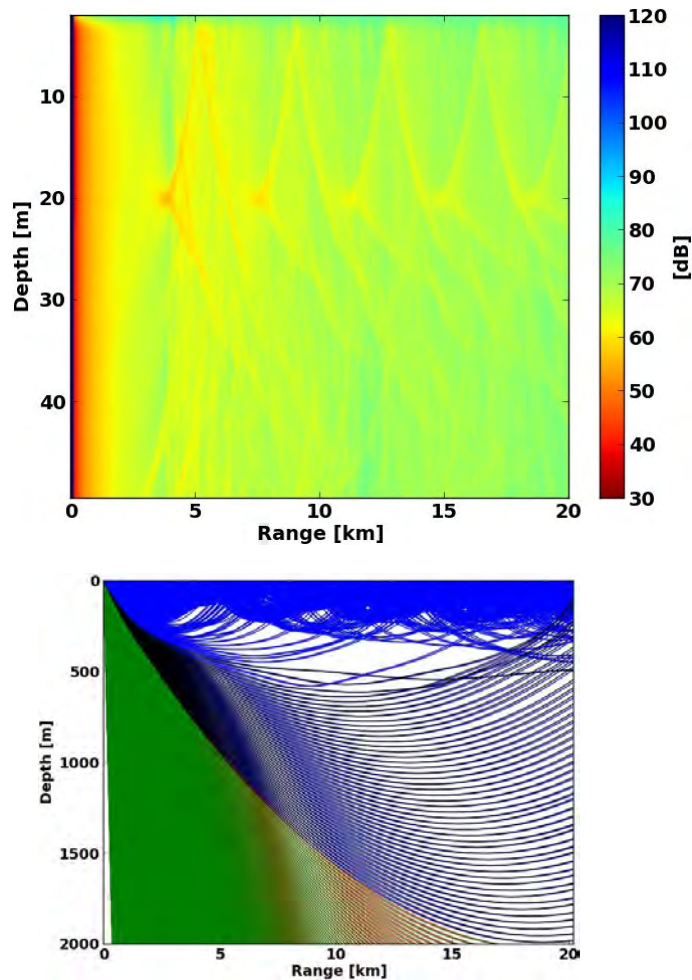

Figure 6. Transmission loss and ray trace for a flat ice surface. The flat ice surface uses compressional speed 3500 m/s; shear speed 1800 m/s; density 890 kg/m^3; compressional attenuation 0.4 dB/λ_p; and sheer attenuation 1.0 dB/λ_s and a thickness of 2.7 m corresponding to the mean ice draft thickness. Red rays touch top and bottom surfaces, green bottom only, blue surface only and black neither surface

increasing scale. This figure illustrates the majority of surface interacting rays being reflected down or back rather than along a forward propagating path as was the case with the flat ice scenario.

Approximations and assumptions

The acoustic parameters and ice roughness statistics used in the test case were approximations from the literature. As discussed in sections *Material properties of sea ice* and *Sea ice as a rough surface* it would be more realistic to calculate these values for the expected temperature, salinity, density, thickness and deformation statistics for the area being evaluated. These can be predicted from global climate models or are available in data sets from previous field studies.

In the Antarctic or Arctic sea ice pack there is unlikely to be 20 km ice surfaces of the one ice type. This single ice type test case is provided to show the impact of being able to include both flat and rough ice in acoustic transmission estimates. Future work could involve a more realistic combination
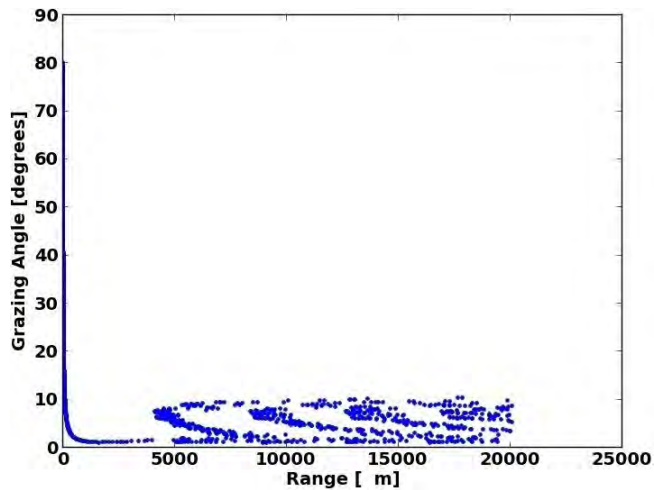
Figure 7. Grazing angles for rays interacting with the flat ice surface
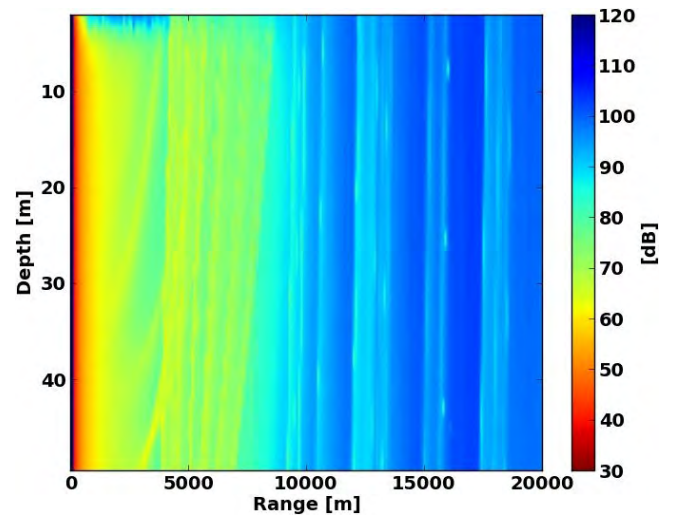

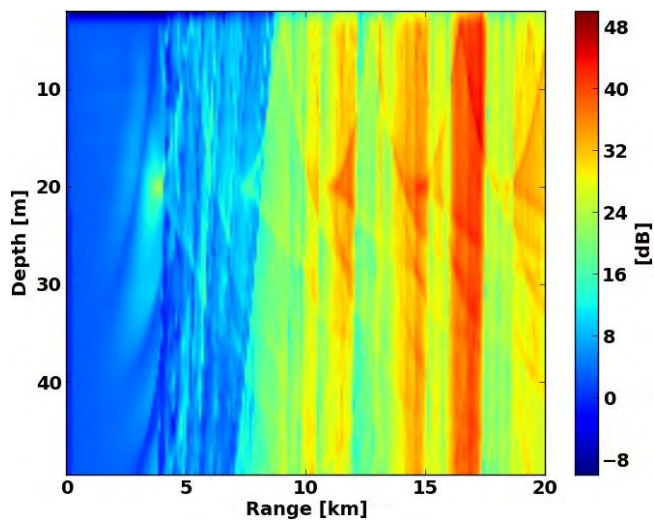Figure 9. Monte carlo rough surface average transmission loss

Figure 8. Difference in decibels between the estimated received fields when representing the surface as a flat ice sheet and direct path only. The difference is calculated by Eq. (4) with p_1 being the flat ice pressure field and p_2 being the direct path only pressure field
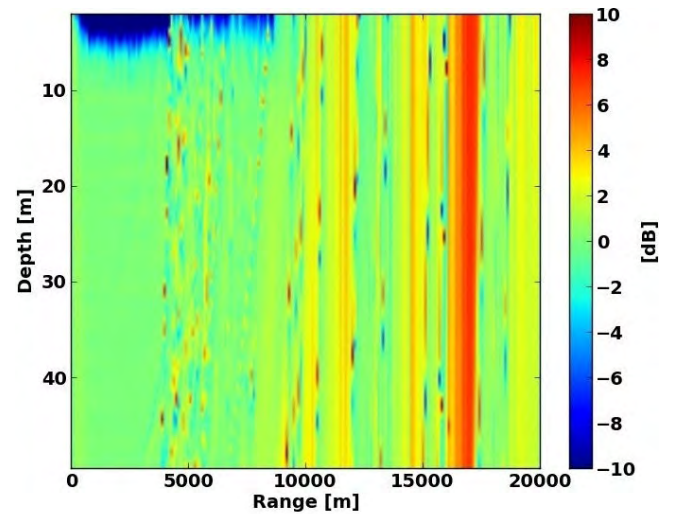

Figure 10. Difference in decibels between representing the surface as a rough ice canopy and direct path only

of different ice types in anticipated autonomous vehicle deployment areas. The location of the source relative to flat ice, open water, or rough ice could have a large influence on the range of effective signal detection.

This treatment of sea ice is only considering it as a two dimensional profile while real sea ice has a third dimension. Future work could compare the validity of this two dimensional approximation and assess the requirement for full three dimensional modelling.

The case study shown uses a simplification of the reflection coefficient based on a single ice thickness. This assumes the top side of the ice is exactly following the bottom surface of the ice to maintain a uniform width, which is not a physically realistic assumption. To assess this assumption the reflection coefficient was calculated at 10 kHz for a range of different ice thicknesses and the results of this are shown in Fig. 12. As can be seen in Fig. 12 for ice thicknesses over 0.3 m there is little change in

the magnitude of the reflection coefficient with ice thickness for grazing angles up to 35 °. What is missing from this reflection coefficient is the consideration of the influence of having a snow or water backed layer, which could be added in a more complex simulation.

The case study does not consider the signal returned by bottom reflection but this could easily be included if the scenario demanded it.

A limitation of using ray tracing is that scattering angles depend solely on the local ice slope and diffraction effects are ignored. It is therefore only considered valid at roughness scales (both horizontal and vertical) much larger than the acoustic wavelength. For a 10 kHz signal in a 1440 m/s water sound speed the wavelength is 14 cm. Future work could involve the division of the ice roughness into wavelength relative large and small features. The influence of smaller features could be included using the Rayleigh roughness parameter and larger scale features included using the altimetry file as detailed here.
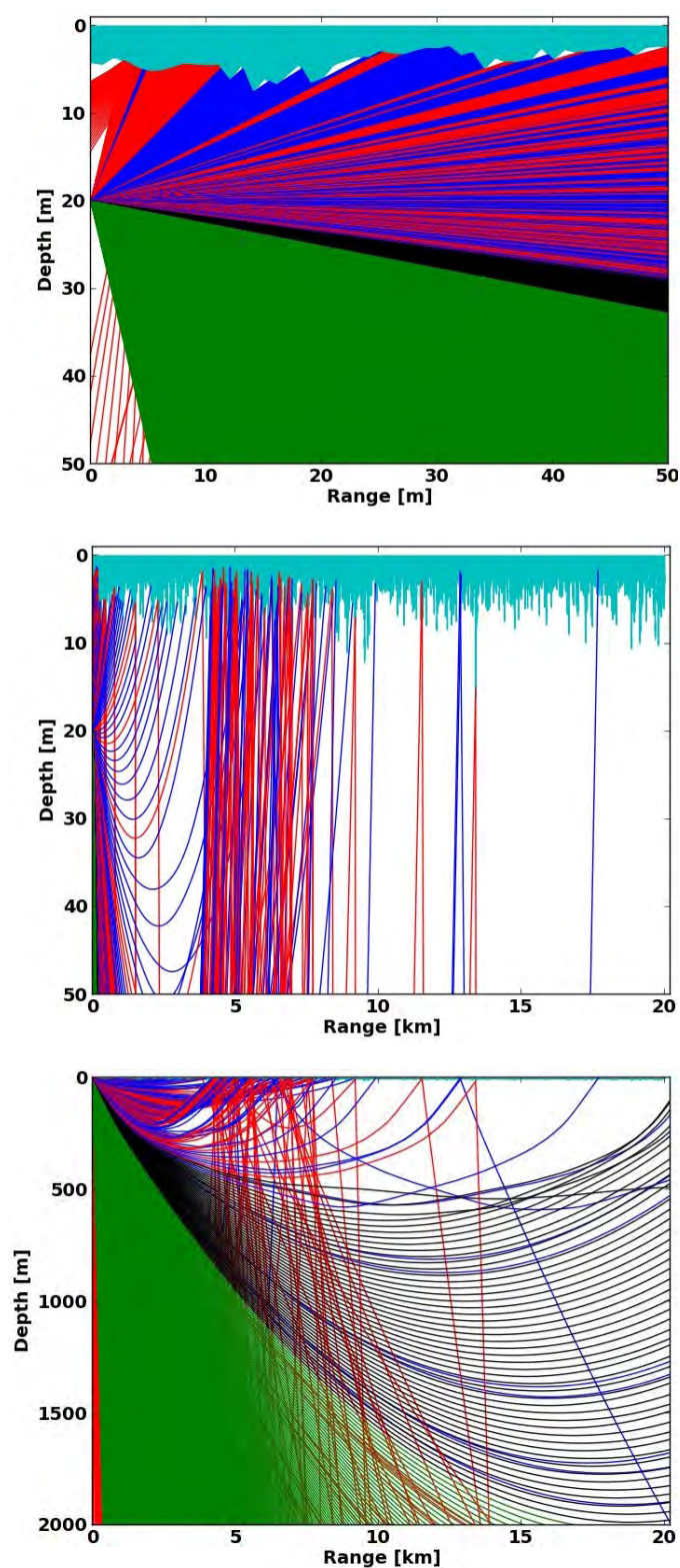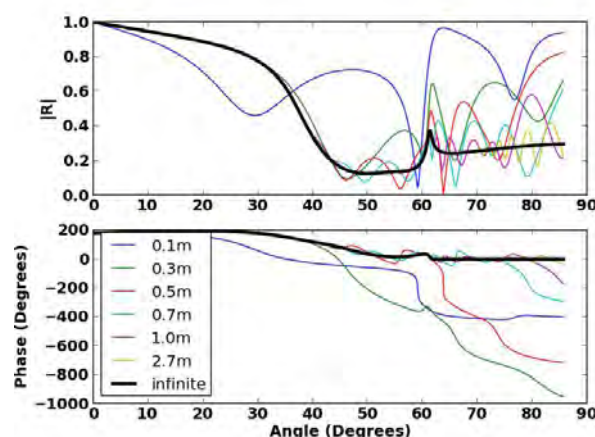
Figure 12. Reflection coefficient at 10 kHz for combined medium: water, ice, air with varying ice thickness

CONCLUSIONS

This paper presents a method, referred to as the Monte Carlo Method, for generating acoustic field information based on a set of simulated ice draft profiles. This has been done with the aim of providing a detailed prediction of an under ice sound environment to support autonomous vehicle deployment reliant on acoustic communications.

It was found that certain polar sound speed profiles, such as the one presented in this case study, create a strong defocussing in the direct path. While it might be expected that surface reflection would have little influence at these shorter, 20 km ranges, this reduction in the strength of the direct path creates a situation where the surface reflected paths dominate the total acoustic field.

Inclusion of a rough sea surface using the Monte Carlo method greatly reduced the contribution of ice surface reflected paths. There was a slight increase of approximately 8 dB over the direct path only case in the defocussed areas, but overall the transmission loss estimate for rough ice was closer to the direct path only case than the flat ice surface case.

If the simulated ice profiles are considered representative of the ice in a given region and season then the Monte Carlo method provides a representative estimation of the acoustic field based on situations that could be encountered. The statistical nature of this approach provides a tool for risk management for autonomous vehicle deployment where worst, best and mean cases for signal propagation could be evaluated. By including the simulated ice profiles directly the Monte Carlo approach can be used with different methods of generating simulated ice. This allows acoustic simulation in ice areas to use all the information available about the expected ice conditions when predicting transmission loss, expected signal range and risk areas.

In real sea ice conditions the surface consists of patches of heavily deformed ice, gently sloping rafted ice, growing ice, and open water. This work shows the significance of being able to include a model of the ice surface in acoustic transmission loss estimates and suggests further work considering more detailed and accurate measures for undertaking this inclusion.

Figure 11. Ray traces for a single instance of a rough canopy shown at three different scales. The three scales are given to provide a complete picture of the rays interacting with the ice surface. Red rays touch top and bottom surfaces, green bottom only, blue surface only and black neither surface

REFERENCES

[1] P. Wadhams, "Sea ice", In J.H. Steel, K.K. Turekian and S. Thorpe, editors, *Encyclopedia of Ocean Sciences*, volume 1, chapter Sea Ice, pages 141–158. Academic Press, Oxford, 2nd edition, 2009

[2] P. Wadhams and M.J. Doble, "Digital terrain mapping of the underside of sea ice from a small AUV", *Geophysical Research Letters* **35**(1), 1–6 (2008)

[3] M. Jakuba, C. Roman, H. Singh, C. Murphy, C. Kunz, C. Willis and T. Sato, "Long-Baseline Acoustic Navigation for Under-Ice AUV Operations", *Journal of Field Robotics* **25**(11-12), 861–879 (2008)

[4] C. Kaminski, T. Crees and J. Ferguson, "12 days under ice an historic AUV deployment in the Canadian High Arctic", *Proceedings of Autonomous Underwater Vehicles*, pages 1–11, Monterey, CA, 2010

[5] A.P. Worby, C.A. Geiger, M.J. Paget, M.L. van Woert, S.F. Ackley and T.L. DeLiberty, "Thickness distribution of Antarctic sea ice", *Journal of Geophysical Research* **113**(C5), 1–14 (2008)

[6] N. Untersteiner, editor, *The Geophysics of Sea Ice*, Springer, New York, 1st edition, 1987

[7] P. Etter, "Recent advances in underwater acoustic modelling and simulation", *Journal of Sound and Vibration* **240**, 351–383 (2001)

[8] F.B. Jensen, W.A. Kuperman, M.B. Porter and H. Schmidt, *Computational ocean acoustics*, Springer, London, 2011

[9] M.B. Porter, Acoustic Toolbox, `http://oalib.hlsresearch.com/Modes/AcousticsToolbox/`

[10] H. Kutschale, "Arctic hydroacoustics", *Proceedings of the U.S. Naval Arctic Research Laboratory Dedication Symposium* **22**(3), 246–264 (1969)

[11] A.N. Gavrilov and P.N. Mikhalevsky, "Low-frequency acoustic propagation loss in the Arctic Ocean: Results of the Arctic climate observations using underwater sound experiment", *Journal of the Acoustical Society of America* **119**(6), 3694–3706 (2006)

[12] D. McCammon and S. McDaniel, "The influence of the physical properties of ice on reflectivity", *Journal of the Acoustical Society of America* **77**(2), 499–507 (1985)

[13] Applied Physics Laboratory, *APL-UW High-frequency ocean environmental acoustic models handbook*, Technical report, University of Washington, Seattle, Washington, 1994

[14] E.Y.T. Kuo, "Low-frequency acoustic wave-scattering phenomena under ice cover", *IEEE Journal of Oceanic Engineering* **15**(4), 361–372 (1990)

[15] L. Freitag, M. Grund and S. Singh, "The WHOI micro-modem: An acoustic communications and navigation system for multiple platforms", *IEEE Proceedings of Oceans 2005*, pages 1–7, Washington D.C, 2005

[16] H. Eicken, "From the microscopic, to the macroscopic, to the regional scale: growth, microstructure and properties of sea ice", In D.N. Thomas and G.S. Dieckmann, editors, *Sea Ice: An introduction to its Physics, Chemisty, Biology and Geology*, chapter 2. Wiley-Blackwell, 2003

[17] K.C. Jezek, T.K. Stanton and A.J. Gow, "Influence of environmental conditions on acoustical properties of sea ice", *Journal of the Acoustical Society of America* **88**, 1903–1912 (1990)

[18] T.K. Stanton, "Acoustical reflection and scattering from the underside of laboratory grown sea ice: Measurements and predictions", *Journal of the Acoustical Society of America* **80**(5), 1486–1494 (1986)

[19] G.R. Garrison, "Acoustic reflections from arctic ice at 15-300 kHz", *Journal of the Acoustical Society of America* **90**(2), 973–984 (1991)

[20] A. Marchenko and A. Makshtas, "A dynamic model of ice ridge buildup", *Cold Regions Science and Technology* **41**(3), 175–188 (2005)

[21] O.I. Diachok, "Effects of sea-ice ridges on sound propagation in the Arctic Ocean", *Journal of the Acoustical Society of America* **59**(5), 1110–1120 (1976)

[22] D. Rothrock and S. Thorndike, "Geometric properties of the underside of sea ice", *Journal of Geophysical Research* **85**(C7), 3955–3963 (1980)

[23] S.D. Rajan, "Determination of compressional wave and shear wave speed profiles in sea ice by crosshole tomography Theory and experiment", *Journal of the Acoustical Society of America* **93**(2), 721–738 (1993)

[24] C. Yew, "A study of reflection and refraction of waves at the interface of water and porous sea ice", *Journal of the Acoustical Society of America* **82**, 342–353 (1987)

[25] W.A. Kuperman and H. Schmidt, "Rough surface elastic wave scattering in a horizontally stratified ocean", *Journal of the Acoustical Society of America* **79**, 1767–1777 (1986)

[26] K. Hunkins, "Seismic studies of sea ice", *Journal of Geophysical Research* **65**(10), 3459–3472 (1960)

[27] R.H. Bourke and R.P. Garrett, "Sea ice thickness distribution in the Arctic ocean", *Cold Regions Science and Technology* **13**, 259–280 (1987)

[28] B.A. Hughes, "On the use of lognormal statistics to simulate one-and two-dimensional under-ice draft profiles", *Journal of Geophysical Research* **96**, 101–111 (1991)

[29] J.A. Goff, "Quantitative analysis of sea ice draft, 1, Methods for stochastic modeling", *Journal of Geophysical Research Oceans* **100**, 6993–7004 (1995)

[30] H. Medwin, "Speed of sound in water: A simple equation for realistic parameters", *Journal of the Acoustical Society of America* **58**(6), 1318–1319 (1975)

[31] X. Lurton, *An Introduction to Underwater Acoustics: Principles and Applications*, Springer, Chichester, UK, 2002

A STUDY OF THE BEHAVIOURAL RESPONSE OF WHALES TO THE NOISE OF SEISMIC AIR GUNS: DESIGN, METHODS AND PROGRESS

Douglas H. Cato[1], Michael J. Noad[2], Rebecca A. Dunlop[2], Robert D. McCauley[3], Nicholas J. Gales[5], Chandra P. Salgado Kent[3], Hendrik Kniest[5], David Paton[6], K. Curt S. Jenner[7], John Noad[2], Amos L. Maggi[3], Iain M. Parnum[3] and Alec J. Duncan[3]

[1]Maritime Operations Division, Defence Science and Technology Organisation, Sydney, NSW and University of Sydney, NSW

[2]Cetacean Ecology and Acoustics Laboratory, School of Veterinary Science, University of Queensland, Gatton, QLD

[3]Centre for Marine Science and Technology, Curtin University of Technology, Perth, WA

[4]Australian Marine Mammal Centre, Australian Antarctic Division, Kingston, TAS

[5]University of Newcastle, Newcastle, NSW

[6]Blue Planet Marine, Canberra, ACT

[7]Centre for Whale Research, WA

The concern about the effects of the noise of human activities on marine mammals, particularly whales, has led to a substantial amount of research but there is still much that is not understood, particularly in terms of the behavioural responses to noise and the longer term biological consequences of these responses. There are many challenges in conducting experiments that adequately assess behavioural reactions of whales to noise. These include the need to obtain an adequate sample size with the necessary controls and to measure the range of variables likely to affect the observed response. Analysis is also complex. Well designed experiments are complex and logistically difficult, and thus expensive. This paper discusses the challenges involved and how these are being met in a major series of experiments in Australian waters on the response of humpback whales to the noise of seismic airgun arrays. The project is known as BRAHSS (Behavioural Response of Australian Humpback whales to Seismic Surveys) and aims to provide the information that will allow seismic surveys to be conducted efficiently with minimal impact on whales. It also includes a study of the response to ramp-up in sound level which is widely used at the start of operations, but for which there is little information to show that it is effective. BRAHSS also aims to infer the longer term biological significance of the responses from the results and the knowledge of normal behaviour. The results are expected to have relevance to other sources and species.

INTRODUCTION

For many years, there has been widespread concern about the effects of the noise of human activities on marine mammals, particularly whales. This has led to a substantial amount of research and, as a result, far better understanding of the effects. In spite of this, there is still much that is not understood, particularly in terms of the behavioural responses to noise and the longer term biological consequences of these responses. Behaviour of whales is difficult to study because the whales spend so much time submerged and out of sight. Whales normally show a range of behaviours, so determining whether a behavioural action is in response to noise exposure or just part of normal activity is difficult. It is generally recognised by scientists and regulators, that a behavioural reaction to noise may not in itself be a problem if there is no significant longer term effect. The concern is about changes that have longer term biological significance in that they affect the life functions (such as feeding, breeding), vital rates (e.g. birth rate) and ultimately, the health of the population [1]. There is limited knowledge of these aspects of whale biology which makes it particularly difficult to infer the longer term effects of responses to noise.

In the meantime, regulatory measures have been imposed by many governments aimed at minimising the impacts from human activities at sea. These generally require activities to be managed according to certain guidelines and various mitigation measures to be employed. The limitations in the scientific knowledge on which these measures are based, however, means that there is significant uncertainty about the effectiveness of the guidelines and mitigation. Managing this uncertainty usually results in greater limitations on activities than might be the case with better knowledge, without necessarily providing adequate protection of whales. Hence we need not only to improve our understanding of the impact of noise but also to assess the effectiveness of management and mitigation, and to develop methods that provide adequate protection of whales while allowing human activities at sea to continue.

A widespread mitigation measure for activities that produce high noise levels is to start with a relatively low source level and build up to the normal operational source level over a period of time, typically 20 to 30 min. The idea is that this will alert the whales and they will move away from the source, thus reducing their exposure level when the full sound output is reached. This is usually called "ramp-up" or "soft start," but

experimental evidence to show that this is effective is lacking.

This paper discusses how we are approaching these challenges in a project known as BRAHSS (Behavioural Response of Australian Humpback whales to Seismic Surveys). Although it addresses the response of humpback whales to the noise of seismic air gun arrays, it is expected that the experimental design will allow the results to be more generally applicable to other types of high level sources and to other species. It aims to reduce the uncertainty in evaluating the impacts on whales of noise from human activities by assessing the response of whales to various sizes of air gun arrays up to a full commercial array. BRAHSS also aims to determine how the whales react to ramp-up or soft start used at the start of surveys, and how effective this is as a mitigation measure. It involves a series of four major experiments at sea off the east and west coasts of Australia. This paper describes the overall plan of BRAHSS, the experimental design, the approach to analysis and the experiments conducted so far.

The study of the effects of noise on whales is interdisciplinary, covering a range of the biological and physical sciences. Animal behaviour, mammal hearing and auditory perception, population dynamics, marine mammal biology, ocean acoustic propagation, ambient sea noise, sound generation and signal detection are some of the disciplines that need to be drawn on. The investigators involved also need to be very experienced in conducting studies with whales at sea and in underwater acoustic measurements. The approach to experimental studies in biology and physics are different, and these need to be merged in any experimental study. For example, physicists tend to have limited understanding of the significance of individual variation of animals and the need to sample a number of individuals as well as including controls in the experimental design. Biologists tend to have limited understanding of the processes and significance of errors of physical measurements. The BRAHSS team includes experts from the range of disciplines required, and with the experience in working with whales at sea in behavioural and acoustic studies.

APPROACHES TO MANAGEMENT AND MITIGATION OF IMPACTS OF NOISE

There are various levels of impact of noise on whales. Although it has been stated that physiological effects are possible for whales exposed to very high noise levels (as when very close to a high level source), there is little evidence of this in practice for sources other than explosions, where the shock wave can cause trauma and death [2]. It is apparent, however, that temporary threshold shift (TTS) in hearing sensitivity is possible for a range of sources and conditions, based on what is known about the noise exposure levels required to induce TTS and the expected noise exposure in the ocean. TTS results in a short term reduction in hearing sensitivity and is not harmful unless it occurs regularly for long periods of time. TTS in humans and laboratory mammals has been extensively studied [3] and there have been a number of experimental studies with small whales (e.g. dolphins) and seals in captivity (reviewed in ref. 4). These show a consistency across a wide range of taxa when compared in terms of the estimated sound levels in the cochlea or inner ear, where auditory sensing occurs, for the onset of TTS. The level required to cause permanent hearing loss (permanent threshold shift or PTS) from short term exposure is substantially higher than the exposure to produce TTS. In an extensive review of effects of noise on marine mammals to develop a set of noise criteria, including information about hearing in other mammals, Southall et al. [4] chose the level to cause 40 dB of TTS as the criterion for onset of PTS as a result of the exposure. They noted that this was very conservative. The very high noise levels likely to cause permanent hearing damage from short term exposure to noise would require a whale to be so close to a source that it would occur rarely in practice.

An approach taken in managing noise impact is to design procedures that limit exposure to levels below those likely to cause TTS, thus providing a substantial safety margin against permanent hearing damage (see for example the Australian Seismic Guidelines and the background paper to these [5]). Management requires observations of whales in the vicinity of the source vessel and subsequent shut down of the source, or reduction in source level, when whales come within a prescribed distance, based on avoiding TTS.

Behavioural responses of whales to noise can occur at much lower levels and thus at significantly greater distances than high level effects such as TTS. For example, humpback whales have been found to react to playback of tones even when received levels are close to those of background noise [6]. It might be said that if a whale can hear a source there is the potential for it to react. Behavioural effects are therefore more difficult to manage because they can occur at large distances.

Generally, however, it is accepted by scientists and regulators that the behavioural responses of concern are those that are likely to have longer term biological consequences. Such responses are usually referred to as being "biologically significant". For example, if a whale showed a reaction that lasted for a short period but then resumed normal activities soon after, this would not be considered to be biologically significant. Some examples of biologically significant effects are a long-term decrease in the size of a population, fragmenting an existing population, adversely affecting habitat critical to the survival of a species, or disruption of the breeding cycle of a population. The Australian Government has published a set of guidelines under the Environment Protection and Biodiversity Conservation Act 1999 (EPBC 1999) to assist in determining what is a significant impact [7].

Determining what responses are biologically significant for whales is very difficult. A working group of experts under the auspices of the National Research Council of the National Academies of the USA examined this in depth to determine how responses to noise may result in biologically significant effects [1]. They produced a framework of a model known as PCAD (Population Consequences of Acoustic Disturbance) that linked the initial noise exposure in steps through to effects at population level, however there is little information available on some of the steps required.

BRAHSS EXPERIMENTAL APPROACH

Factors affecting behavioural responses

Biological systems are far more complicated than physical systems and the deterministic approach of the physical sciences

has limited effectiveness in biological experimentation. Individual animals of the same population vary in their characteristics. Consequently, their responses to a stimulus, whether it is exposure to noise in the ocean or application of a new drug in medical trials, generally vary significantly between individuals. Many of the factors affecting this variation may not be known. The well established experimental protocol to deal with this involves the use of a large number of individuals (the sample). The results of the experiment can then be expressed in terms of a statistical distribution of individual responses which is assumed to be representative of the whole population. In addition, the experiments are conducted without the stimulus but otherwise identical in every way possible. These are referred to as the "controls". Assessment of the response involves a statistical comparison of the response distributions for the stimulus with those for the controls. The terminology used comes from testing medical treatments: the stimulus is usually referred to as the "treatment" and usually there will be an attempt to obtain a dose response, i.e. a relationship between the response and the level of dose (which may be the received level in noise exposure).

In terms of noise exposure, high sound level impacts, such as TTS, can be closely related to received sound levels and durations [3], even though there is likely to be significant individual variation. Behavioural responses, on the other hand, are likely to be affected by many other factors. The reception of the sound may be predominantly what alerts the whale but whether it reacts may not be simply related to the received sound level. The acoustical characteristics of the received noise, e.g. spectral shape (distribution of energy across the frequency band), may also be a significant factor, but there is a range of non acoustic factors that may also be important. If, for example, whales react in order to avoid the source, the response may depend on how close the source is and which way the source is moving relative to the whale. Cows with calves are more likely to be sensitive to anthropogenic noise than males and thus more likely to react (especially if they interpret the noise as a threat). The amount of behavioural interaction between individuals at the time of exposure may also affect the response. Whales that are preoccupied with close interaction may not react as readily as whales that are not. Such interaction would include acoustic communication as well as other physical interaction, and responses may include changes in vocalisations. The presence of other sources of noise such as boats or ships may also have an effect. Ambient noise levels in the ocean vary over a range of at least 20 dB [8, 9], so the received level at which a noise source is detectable will also vary by 20 dB. Hence, attempts to relate responses simply to received levels may give results that depend on the ambient noise level at the time.

The fact that we can identify a range of variables that are likely to affect the response allows us to build these into the BRAHSS experimental design. The aim is to obtain a dose response, not just in terms of the received noise level but also in terms of these other factors discussed above. In the process, we expect to determine which of these likely factors are of most significance in the response. Understanding response to noise exposure in terms of the main factors affecting the results will allow more effective management and mitigation measures to be designed than might be the case with simply confining the study to dependence on received level.

Any experiment at sea is difficult. The ocean is a hostile and unforgiving environment. Studies of the effects of noise on whales are particularly complicated and expensive. The logistic difficulties of studying whales limit the amount of observations that can be made and thus the sample size that can be obtained in experiments for reasonable cost. The need to obtain an adequate statistical sample has to be balanced against the cost. Some studies have produced results that are inconclusive because the sample size was found to be too small to provide statistically significant results.

In order to determine the sample size required in the BRAHSS experiments, we conducted a statistical power analysis of a previous experiment in which tones and humpback whale social sounds had been played back to humpback whales at the east coast site [6]. From this we were able to determine the sample size required for a high likelihood that, if there were real responses, these would be apparent as statistically significant results in the analysis. We have chosen a sample size of 15 for each treatment and for each control, which provides an adequate amount based on the power analysis [10].

Australian humpback whales

Of the many species of whales in the Australian region, the best studied and the one most likely to be exposed to seismic and other anthropogenic sources is the humpback whale. These migrate annually between their feeding grounds in the Southern Ocean and the breeding grounds in shallow tropical waters, within the Great Barrier Reef on the east coast and the Northwest Shelf on the west coast [11, 12]. During their migrations, they pass along the east and west coast lines for thousands of kilometres. These are two separate populations, and the latest estimates of population sizes (with 95% confidence intervals in brackets) are 14,520 (12,780 – 16,500) for the east coast in 2010 [13] and 21,750 (17,550 – 43,000) [14] and 26,100 (20,150 – 33,270) [15] both for the west coast in 2008. These are likely to be significantly larger now if the long-term increases of between 10 and 11% has been sustained. There is substantial information on many aspects of life history and biology such as birth rate and age to maturity obtained from the examinations of thousands of individuals of these populations at whaling stations during the 1952 to 1963 whaling period [11]. There have been many studies of the acoustics and behaviour for both east and west coast populations and some studies of response to playback, for example references 6, 10, 16 – 25. Thus we have a wealth of information on normal behaviour (i.e. in the absence of air gun sounds) and the use of sound by the whales to put the observed responses in the context of normal behaviour. An advantage of working with migrating whales is that new whales come past each day, so there is little chance of including the same individual twice in an experiment.

Considerations of the source used in the experiments

A seismic survey involves the towing of a large array of air gun sources which are fired at regular intervals. Each source produces an impulsive sound when compressed air within the

air gun is released into the water. This is a very efficient type of source, generally monopole in nature. The bubble produced oscillates with decaying amplitude following the first impulse. The air guns in the array are spatially separated and fired coherently to direct the energy downwards but a significant amount also radiates near horizontally, i.e. towards a distant receiver. In order to understand the responses of whales to air guns sources and the effectiveness of ramp-up, the project includes exposure to a range of sources from a single small air gun of 20 cu in (cubic inch) capacity (typical of the smallest used in surveys) to progressively larger sources of multiple air guns up to a full seismic array (several thousand cubic inches). Such a range of exposures helps avoid pseudoreplication in the nature of the stimulus [26] (where we decrease the risk that behaviours observed are only in response to one particular size or type of air gun array) and also allows us to understand how whales react to the components of ramp-up. This led to the design of a small array with four stages of ramp-up (four radiated levels).

Ramp-up at the beginning of a seismic survey typically starts with the smallest air gun only, and then additional air guns are added in steps up to the full array over a period of 20 – 30 min. Typical arrays contain tens of air guns, so there may be many steps. Considerable analysis went into the design of the array used for four stages of ramp-up. Firstly this involved analysis of the ramp-up used in surveys and then modelling of the horizontal sound field produced [27]. It was apparent that there is significant variation in ramp-up used in surveys in terms of the time between steps in radiated level and the increase in level at each step. Usually there are many steps over the 20 – 30 min of ramp-up and this means that the increase in level at each step is less than 3 dB, though there are some exceptions.

The ability of mammals to detect differences in sound level (i.e. to perceive differences in loudness), is known as loudness discrimination. For humans, the minimum detectable change in level, measured by presenting successive sounds alternating between two levels, varies from about 0.5 to 3 dB for most data [28]. Since the changes in level of the near horizontally radiated sound between ramp-up steps are generally within this range or not much larger, they may be too low to be noticed by a mammal. We do not have measurements of the ability of humpback whales to discriminate differences in level, though their sounds have frequency and temporal ranges that are of the same order as those of humans (as opposed to dolphin sounds, for example, where these ranges are much different). If the discrimination ability of humpback whales is similar to that of humans, they would be unlikely to notice the increase in received level typically used in ramp-up. While we may not have this information for humpback whales, there is no reason to suggest that their discrimination ability should differ significantly from that of other mammals so that they would notice such small increases in sound level. For the above reasons, we chose to design an array that would produce an increase in level of nominally 6 dB per step of ramp-up, since the expectation is that this would be sufficient for a mammal to take notice. An array design was developed using a physics based numerical model to predict the sound output that included the effects of interactions between the acoustic pressure field and the oscillation of the airgun bubbles. The resulting array has four stages or three steps in level. The final experiment will use a full seismic array, with ramp-up for that array.

Although seismic arrays are phased to direct most of the energy downwards, there was no need for this in the experimental array. Indeed it is better to avoid any directionality in the radiated sound because that would introduce another variable. Our modelling showed that there is directionality in the horizontal direction from a full array, but the rate of variation in the horizontal plane is small enough that a whale would not experience significant variability in received level as the bearing of the array changes.

The design required six air guns displaced horizontally on the perimeter of a rectangle 2 m (in tow direction) by 1.3m (across tow direction). The air gun capacities and positions are given in Table 1. Air gun combinations provided the four stages: 20, 60, 140 and 440 cu in.

Table 1. Air gun capacities and positions in the array relative to a point at the array centre (x is negative to the rear or aft of centre and y is negative to the left)

Air gun capacity (cu in)	x position (in tow direction) re array centre (m)	y position (across tow) re array centre (m)
20	0	-0.65
40	0	+0.65
40	-1.11	-0.65
40	-1.11	+0.65
150	+1.11	-0.65
150	+1.11	+0.65

Because the air gun signal is impulsive, measurements are usually made in terms of the integral of the acoustic pressure squared over the duration of the pulse. In the far field, this is proportional to the received acoustic energy (just as the mean square pressure is proportional to acoustic intensity). This is referred to as the Sound Exposure Level (*SEL*) and is defined by

$$SEL = 10\log(\int_{t_1}^{t_2} p^2 dt) \qquad (1)$$

where p is the received acoustic pressure and the time period t_1 to t_2 covers the duration of the received impulse. Equation (1) could apply to the full bandwidth of the signal, or to finer frequencies bands.

THE BRAHSS EXPERIMENTS

Plan of experiments

There are four major experiments in the BRAHSS project over the period 2010 to 2014. Each occurs in September and October during the southbound migration of humpback whales from the breeding grounds in tropical waters to the Antarctic feeding grounds. Behaviour differs between the northbound and southbound migrations, but in order to obtain an adequate sample size, we had to limit the experiments to

the same migration. The southbound migration was chosen because it includes new born calves which are likely to be more susceptible to acoustic disturbance than juvenile or adult whales. Also, southward migrating whales show a wider range of behaviours.

The first two experiments have been completed near Peregian Beach on the southern coast of Queensland. The whales migrate close to shore here allowing land based observations including fine tracking of whales with theodolites. The Peregian site provides high resolution observations, but it is not feasible for a full seismic array to operate there because of the proximity of the coast. The remaining two experiments will be off Western Australia and will be further off shore allowing the use of a full array, but too far offshore for land-based observations. The advantage of using two sites is that it involves two largely separate populations of whales and two different environments. This allows us to generalise the results more than we could using the results from only one site and population. Importantly, the acoustic propagation at the two sites is different so that the relationship between received noise level and distance from the source differs between the two sites. Both distance to the source and received level may be important in whale responses and this allows us to separate the effects. The program of experiments is:

- Experiment #1, 2010: East coast using a single 20 cu in air gun.

- Experiment #2, 2011: East coast using four stages of ramp-up and a "hard start," and completion of the 20 cu in air gun trials.

- Experiment #3, 2013: West coast: repeating aspects of the east coast experiments.

- Experiment #4, 2014: West coast: fully operational commercial array with ramp-up.

The hard start used stage 3 of the ramp-up (140 cu in), theoretically 12 dB in level above that of the 20 cu in air gun. This is an alternative mitigation to ramp-up. The idea is that using a higher level is more likely to get the whales' attention and the hope is that they are more likely to move away. While this is not generally used, we included it in our experiments to help provide material to understand how effective ramp-up is and how this might be improved.

Trials with the 20 cu in air gun involved towing the air gun on two paths, one from south to north into the migration and one from west to east across the migration. This allowed us to test the effect of two tow paths. Although the migrating whales are moving in a general southbound direction, there is a lot of meandering. For the ramp-up and hard start, the array was towed from west to east.

Experiment #3, off the west coast, is intended to match aspects of Experiment #2 off Queensland to allow us to compare the effects on the results of whale population and the environment (e.g. propagation). Because of the greater distance from shore, it will not be possible to make shore base observations such as theodolite tracking and operations will be entirely boat based. Off Peregian, focal follow observations were done both from shore and from small boats, allowing a comparison of the effectiveness of both. The moored acoustic array will not be used off the west coast because of the greater

distance from shore. The moored loggers will be deployed in a way that will allow acoustic tracking during analysis after the experiments. They will include methods of synchronising the timing between loggers (e.g. by use of pingers) to allow source localisation in later analysis

Experimental design

The BRAHSS experimental design follows the "before, during and after" (BDA) method in which the treatment (noise exposure or control) occurs in the "during" phase, whereas there is no treatment in the "before" and "after" phases. Each phase lasts for 1 h (except for ramp-up for which the treatment lasts only 30 min). Observations of whale behaviour are conducted for all phases, thus allowing a comparison between the phases. The air gun array is towed for the "during" phase but the vessel and array are effectively stationary during the "before" and "after" phases. In the "exposure" treatments, the air guns are fired in the "during" phase at 11 s intervals while being towed at 4 knots (7.4 km/h). In control treatments, the air guns are towed in the "during" phase at the same speed, but are not fired. There are also observations of whale behaviour and the other variables when the source vessel is absent to provide a control for the presence of the vessel. The number of controls are planned to equal the number of treatments with the air guns operating.

Behavioural observations and measurements

Experiments #1 and #2 have been completed successfully off Peregian Beach. The study site is shown in Figure 1. Activities were coordinated from a base station in an apartment building at the southern end of Peregian beach (Figure 1). The following describes the observations platforms in Experiment #2 which were similar to those of Experiment #1 with some additions (though treatments were different, as shown above). More than 70 people were on site for the experiment, including the project team, staff hired for the experiment and volunteer scientists.

The air gun vessel, *RV Whale Song*, a 24 m ship, was operated out of Mooloolaba to the south of the site. It also provided a platform 8 m above the water for observations of whales in the vicinity of the vessel, both to collect data on responses and to provide information required to ensure that no whale came within the exclusion zones for start up or operation of the array. The exclusion zone was part of the mitigation procedures which were based on the avoidance of TTS, in accordance with the same criteria as used in the Australian seismic guidelines [5].

Observations of whale behaviour were made from land by three teams (two "focal follow" and one "scan") on Emu Mt. (Figure 1) and two "focal follow" teams in an apartment building (Costa Nova), about 12 km to the north of Emu Mt. Binoculars were used to record all behaviours and theodolites were used to track the whale movements.

"Focal follow" observations involved the teams focussing on one group of whales and following it for the entire time it was in the study area, recording all behaviours and whale positions. The "scan" team attempted to record behaviours and positions of all whale groups passing through the study area, but there were too many groups to get the detail of observations
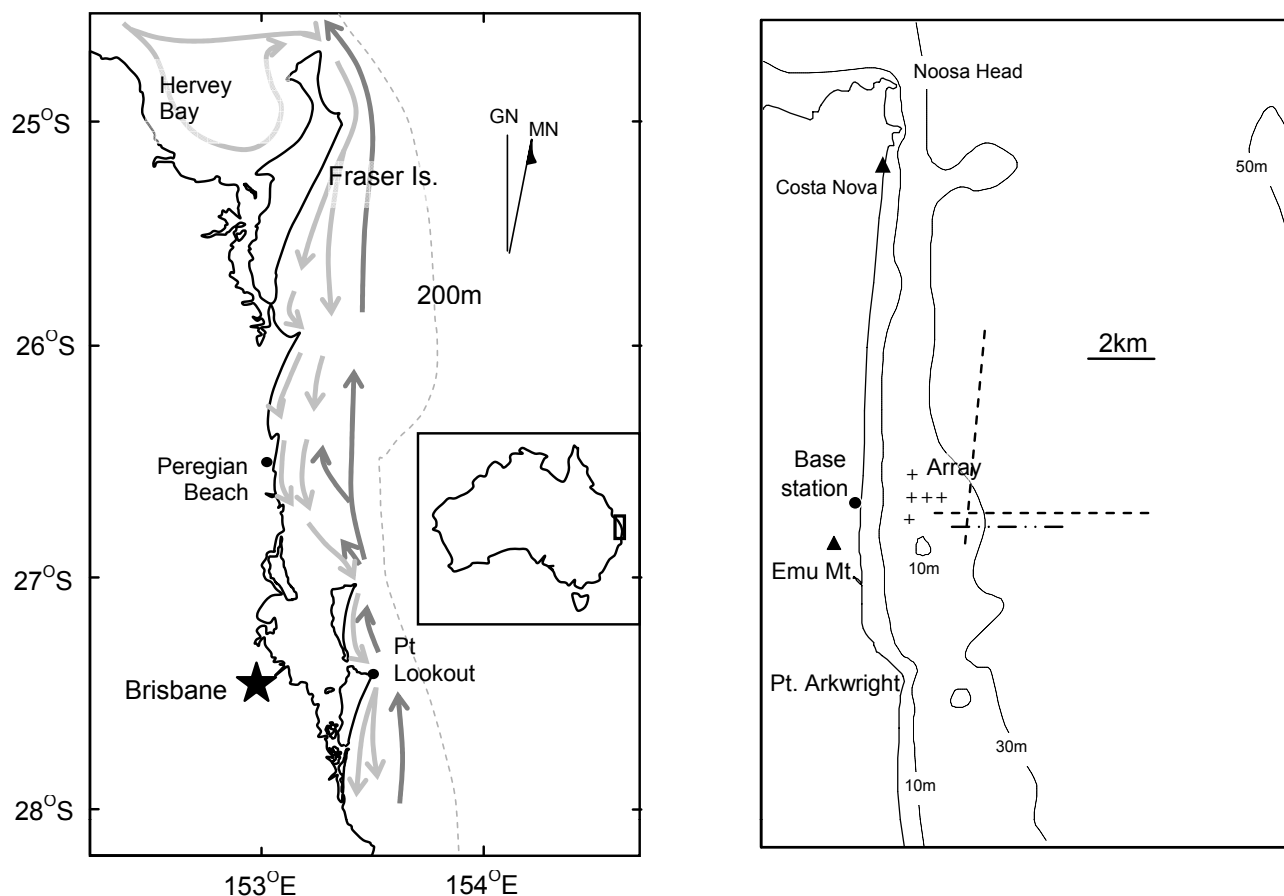
Figure 1. Location of the east coast study site at Peregian Beach. Left: south-eastern Queensland showing Peregian relative to Brisbane and the migratory routes of the humpback whales, with the 200 m depth contour. Right: detail of the Peregian study site with the southern theodolite station (Emu Mt.), the northern theodolite station (Costa Nova), and the five hydrophone buoys (shown as +) that made up the acoustic array. The 10 m, 30 m and 50 m depth contours are also shown. The 20 cu in eastward and northward and the hard start 140 cu in air gun array tow-paths are shown as regular dashed lines while the ramp-up tow-path is shown as a shorter dash and dot line. GN and MN are geodetic and magnetic north respectively

obtained by focal follow methods. Two or three focal follow samples were obtained for each trial and these provided the observations for the analysis of response (a trial is one treatment with the set of before, during and after observations). "Scan" or "Ad lib." observations provided the context for the focal follow groups such as interaction between individuals.

The two focal follow stations at the northern site located whales as they came past Noosa Heads and into the northern part of the study area. Groups of whales were chosen for focal follow and tracked until they reached the southern limits of the northern field of view. By then, the southern focal follow teams had detected the groups and so continued to follow them as they moved south until they reached the limits of the study area.

All observer teams used laptop computers to record the theodolite data directly and to input observational data. VADAR software, developed for this purpose [29], controlled the data input and calculated the position of each whale from the theodolite bearing and vertical angle. The VADAR display showed a map of whale tracks, annotated with behaviours.

Angles from compass-reticule binoculars were also used to obtain a less accurate position. VADAR also allowed the collection of whale behavioural observations without a corresponding position. The laptops were linked by internet to a VADAR computer at the base station.

Three small boats were also used for focal follow observations, each following the selected whale group at a discreet distance as it travelled through the area. Dtags [30] were deployed from the boats on a small number of the focal group whales for the duration of a trial. These tags, from the Woods Hole Oceanographic Institution, record the sound received by a hydrophone in the tag, depth and 3D movements of the whale (using magnetometers and accelerometers), allowing a detailed picture of the diving behaviour and movements underwater to be obtained. The tags are held on by suction cups and attached to the back of a whale using a long pole. Dtags were attached prior to the "before" phase of a trial and were programmed to stay on the whale usually for about four hours, thus covering the duration of the trial. Dtagged whales were always focally followed and continued to be followed until the tag detached,

whereupon it was retrieved, and the data later downloaded from it. The small-boat teams recovered the tags after each trial and also obtained biopsies of focal follow whales where possible.

Acoustic measurements

We aimed to characterise the sound field throughout the study area so that the sound received by each whale during a trial could be determined. We had multiple acoustic recording systems deployed throughout the area. Received level measurements provided the data to develop an empirical propagation loss model which can be used to interpolate the sound field between acoustic recording systems. Acoustic propagation in the ocean is very variable. Although there are a number of propagation models that can be used to predict propagation in an area, they need input of environmental variables, particularly acoustic properties of the bottom in shallow water. Since the experiments are in shallow water and there is limited information about the bottom, measurement of propagation loss is important.

Moored acoustic loggers

Four Curtin CMST-DSTO[1] sea noise loggers were deployed in the study region over the period of the experiments to record the signals from the air gun array, whale vocalisations and ambient sea noise. The loggers were set weighted on the seabed with a ground line attached to an acoustic release with sub-surface floats. Four loggers were used, each deployed for a few days at a time. They were then recovered, the data downloaded, and then redeployed, some in the same position, others in new positions. A total of 23 positions (not shown in Figure 1) were sampled in the two experiments. Each logger had a sampling rate of 4 kHz and the incoming signal was split with consecutive bytes having 20 dB difference in gain in order to avoid any overloading from air gun array signals (i.e. two channels were recorded with 20 dB difference in gain settings). All loggers used Massa TR1025C hydrophones and data were recorded in 16 bit digital format.

Moored hydrophone array.

An array of five hydrophone buoys was moored off Peregian Beach. The buoys were arranged in a T-shape (Figure 1) with separation of adjacent buoys being about 750 m. Each buoy was moored by rope to an anchor and the hydrophone (High Tech Inc. HTI-96-MIN) was attached near the bottom of the rope, so that it did not move much as the buoy above swung around the mooring in the wind and seas. The cable from the hydrophone ran up the anchor rope to the buoy where it was connected to a preamplifier and then to a wideband sonobuoy FM transmitter in the buoy. The frequency response was within 3 dB over the frequency range of 50 Hz to 10 kHz.

The signals from the buoys were received by a Yagi antenna mounted on the base station ashore and connected to a four-channel type 8101 sonobuoy receiver and a single channel custom-built sonobuoy receiver. The outputs of these receivers were split, the signals sent to two desktop computers. One desktop computer with *Ishmael* software [31] recorded

the data to an external hard drive. The second computer used *Ishmael* software to track vocalising whales from the acoustic arrival time differences between hydrophone pairs and these locations were also exported into VADAR. Hence the VADAR plots showed visually and acoustically derived whale tracks, annotated with behaviour, along with tracks of the source and other vessels. The displays were updated in close to real time. VADAR also calculated the cumulative sound exposure of each whale that came close to the air gun array and the array was shut down when the *SEL* reached 183 dB re 1 $\mu Pa^2 s$, the criterion for the onset of TTS used in the Australian Seismic Guidelines [5] which is consistent with the value chosen in reference 4.

Whale tracks determined from visual observations are not expected to correlate with those determined acoustically, except in broad terms. Visual observations are limited to the times when the whale is at the surface but acoustic positions can only be determined when the vocalising whale is submerged. As the vocalising whale approaches the surface, the interference between the source and its out of phase surface image results in increasing cancellation with the result that the received acoustic signal fades out. However, comparison of the visual and acoustic tracks provides identification of which of the visually tracked whales is vocalising, information which is important in understanding the behaviour. The acoustic tracks provide information about the movements of the singer while submerged.

Drifting recording systems

Two drifting hydrophone buoys were also used. Each of these had a vertical array of four hydrophones (High Tech Inc. HTI-96-MIN) set at depths of 5, 10, 15 and 20 m. These recorded to an on-board 4-channel Sound Devices 744T digital recorder. They were deployed from the small vessels during focal follows at the start of each exposure or "during" phase and collected later in the day. These systems provided samples of the sound field as a function of depth in the water column as well as the received level near the focal follow whales. The system response was within 3 dB from 40 Hz to 16 kHz.

Statistical modelling

Statistical analysis is using generalized linear mixed models (GLMM) incorporating fixed effects, covariates and random effects. These are generated using the statistical software package 'R' (R Foundation for Statistical Computing). This analysis follows closely that used for previous playback experiments on the east coast. Behavioural response variables from the focal follow data include measures of course and speed, measures associated with dive profile, rates of various surface behaviours, and vocalisation parameters.

Behavioural responses are being modelled using GLMMs with appropriate choice of link and distribution functions (depending on the distribution of the response variable). Fixed effects (those which are determined by the experimenter), include exposure (exposed/non-exposed), treatment (single air gun, multiple air guns, ramp-up, full array and controls), tow-

---

[1] CMST: Centre for Marine Science and Technology. DSTO: Defence Science and Technology Organisation.

path, experimental period (before, during and after exposure) and social context (group composition, group social behaviour, nearest singing whale and nearest neighbour). Covariates (other variables that might affect the results) including array proximity, array movement, received level and background noise, will be incorporated as additive and/or interactive effects.

Random effects are those where the effects are assumed to be randomly selected from an infinite population of possible effects, in this case, the selection of the groups that form the sample. The variance from this 'random effect' is also included in the model. The use of a mixed model also allows the incorporation of the variance associated with using more than one observation per experimental unit, i.e. where multiple measurements are taken on a single subject (a repeated measures design). The sequence of behaviour of the focal followed groups falls into this category. Even though the behaviour of a group may change as the external conditions change, different observations are not independent because it is the same group and behaviour at any time may depend on an earlier behaviour.

Generated models will be compared using likelihood ratio tests and AIC (Akaike Information Criterion) scores to assess which model (i.e. combination of fixed factors) best explain the data. Multivariate analysis methods may also be used, which will incorporate a number of response variables into the model and therefore determine the multivariate response.

The final result is expected to be a dose response in which the dose depends on multiple variables, in addition to the received noise exposure level.

PROGRESS

The first two experiments were completed successfully and more than 140 focal follows were obtained exceeding the target sample size, each with a large number of observations leading to almost 200,000 lines of data. The processing of the data into a form suitable for analysis is now largely complete for both Experiment #1 and #2. This involved the cataloguing of data, the reconciliation between platforms, stringent quality control and the generation of meaningful metrics of behaviour. The data were then exported from VADAR into Excel spreadsheets which were subject to more quality control procedures before being appended into one complete data spreadsheet for each experiment. This has proved to be a substantial task because of the large number of variables and observation and measurement platforms. We are now moving into the statistical modelling stage and some preliminary modelling has been done to check the integrity of the processed data.

Some preliminary measurements of the sound levels received from the air gun array for each stage relative to that of stage 1 (20 cu in air gun) in Experiment #2 are given in Table 2. These were made during four test runs. One stage of ramp-up was fired throughout each run, with the array towed either towards the north or the south at a distance of 6 km to the west of the receiving hydrophone. A run was about 1.2 km in length, centred on the point of closest approach to the hydrophone. Corrections have been made for the broad band propagation loss differences due to variations in the distance between the

array and the receiver over the runs.

The air gun singals were recorded on an M-Audio MicroTrack digital recorder from a High Tech Inc. HTI-96-MIN hydrophone suspended over the side of a small boat. At least 10 samples of each stage were measured. The source level of the 20 cu in air gun was measured in Experiment #1 much closer to the array, and found to be 200 dB re 1 $\mu Pa^2 s$. The measurements have not yet been corrected for differences in the propagation loss between each stage due to frequency dependence of the propagation (larger array capacities tend to have more energy at lower frequencies). Frequency dependent propagation is likely to vary the relative difference in level between stages as a function of distance. This may explain some of the difference between the theoretical and measured differences between stages.

Table 2. Measurements of sound levels of the stages of the air gun array relative to the level of stage 1, as received at a distance of about 6 km to the east of the array. For each air gun stage, the results are the average of 10 or more samples taken over the duration of the test for that stage. The levels were measured over the frequency band 20 Hz to 10 kHz (most of the energy was between 50 Hz and 1 kHz). "St Dev" is the standard deviation (calculated from the decibel values) of the difference in level between each stage and stage 1 over the sample. The results may change slightly after correction for transmission loss

Stage	SEL re stage 1 (dB) measured	SEL re stage 1 (dB) as designed	St Dev (dB)
2	4.0	6	1.1
3	12.6	12	1.2
4	16.1	18	1.1

In Experiment #1, the 20 cu in air gun was towed along two paths one to the north and one to the east through part of the study area, while the moored acoustic loggers were deployed at a total of 11 different positions. This provided propagation loss measurements over many paths between the source and the receivers. The results showed that while the received level as a function of distance was generally consistent throughout the area, there were significant patches where the propagation was anomalous, showing a much larger decrease in level with increasing distance than observed over the rest of the area. These would have significantly affected sound exposure of whales over or beyond the patches. Consequently, a sea bed survey was conducted in the second Experiment #2 and this showed exposed rock in the patches of anomalous propagation loss.

Three sonar units, underwater video transects and grab samples were used to survey patches of the sea bed where the 2010 measurements of propagation loss had shown anomalously high loss. The purpose was to determine the nature of the sea bed to improve the empirical model of propagation loss for the area. Four sea bed types were identified [32]: (1) sand, both flat and with small ripples, (2) shelly sand which appeared as large sand waves with shell deposits in the troughs, (3) shell with reef platform found at the edges of exposed reef, and (4) exposed reef platforms. The exposed reef platform correlated

in space with the measured high transmission loss types and provided a map of areas of anomalous propagation.

SUMMARY

BRAHSS is a multidisciplinary behavioural response study involving four major experiments in Australian waters in which humpback whales are exposed to various levels of noise from seismic air gun arrays. The experiments are logistically complicated. In Experiment #2, there were nine separate behavioural observation platforms and seven acoustic recording systems, providing measurements of a wide range of variables likely to affect the response of whales to the noise exposure. Experiments #1 and #2 have been completed successfully off the east coast, obtaining an adequate sample size for the observations of response. Experiments #3 and #4 will be off the west coast in 2013 and 2014 respectively.

Such a comprehensive project results in a substantial amount of data and consequently, substantial effort is required to consolidate the data, to coordinate observations between platforms and for quality control. Statistical modelling is now in progress.

The acoustic measurements show the importance of measuring propagation in behavioural response experiments. Without that, we would not be aware of the high loss patches and would not be able to allow for the rapid decline in received level at whales over or beyond these patches relative to the source, leading to significantly increased uncertainty in the results.

REFERENCES

[1] National Research Council (NRC), *Marine mammal populations and ocean noise: Determining when noise causes biologically significant effects*, National Academies Press, Washington DC, 2005

[2] W.J. Richardson, C.R. Greene Jr, C.I. Malme and D.H. Thomson, *Marine Mammals and Noise*, Academic, San Diego, 1995

[3] K.D. Kryter, *The effects of noise on man*, Academic Press, New York, 1970

[4] B.L. Southall, A.E. Bowles, W.T. Ellison, J.J. Finneran, R.L. Gentry, C.R. Greene, Jr, D. Kastak, D.R. Ketten, J.H. Miller, P.E. Nachtigall, W.J. Richardson, J.A. Thomas and P.L. Tyack, "Marine mammal noise exposure criteria: Initial scientific recommendations", *Aquatic Mammals 33*, 411-521 (2007)

[5] Department of Environment, Water Heritage and the Arts (Australia), *EPBC Act Policy Statement 2.1 – Interaction between offshore seismic exploration and whales* and back ground paper, 2008 http://www.environment.gov.au/epbc/publications/seismic.html

[6] R.A. Dunlop, M.J. Noad, D.H Cato, E. Kniest, P. Miller, J.N. Smith and M.D. Stokes, "Multivariate analysis of behavioural response experiments in humpback whales (Megaptera novaeangliae)", *Journal of Experimental Biology* **216**, 759-770 (2013)

[7] Department of Environment, Water Heritage and the Arts (Australia), *Matters of National Environmental Significance: Significant impact guidelines 1.1*, Environment Protection and Biodiversity Conservation Act 1999, 2009 http://www.environment.gov.au/epbc/publications/pubs/nes-guidelines.pdf

[8] G. M. Wenz, "Acoustic ambient noise in the ocean: spectra and sources", *Journal of the Acoustical Society of America* **34**, 1936-1956 (1962)

[9] D.H. Cato, "Ambient sea noise in Australian waters," *Proceedings of the Fifth International Congress on Sound and Vibration*, Adelaide, 1997, pp. 2813-2818

[10] R.A. Dunlop, M.J. Noad and D.H. Cato, "Behavioural-response studies: problems with statistical power." In *Effects of Noise on Aquatic Life*, eds. A.N. Popper and A. Hawkins, Springer, New York, pp. 293-297, 2012

[11] R.G. Chittleborough, "Dynamics of two populations of the humpback whale, *Megaptera novaeangliae* (Borowski)", *Australian Journal of Marine and Freshwater Research* **16**, 33-128 (1965)

[12] W.H. Dawbin, "The seasonal migratory cycle of humpback whales", *Whales, Dolphins and Porpoises*, eds. K.S. Norris, University of California Press, Berkeley & Los Angeles, pp. 145-70, 1966

[13] M.J. Noad, R.A. Dunlop, D. Paton and H. Kniest, "Abundance estimates of the east Australian humpback whale population: 2010 survey and update," Paper to the International Whaling Commission Scientific Committee, Tromsø, Norway, 30 May - 11 June 2011, SC/63/SH22

[14] S.L. Hedley, J.L. Bannister and R.A. Dunlop, "Group IV Humpback Whales: Abundance estimates from aerial and land-based surveys off Shark Bay, Western Australia, 2008" Paper to the International Whaling Commission, SC/61/SH23, 2009

[15] C.P. Salgado Kent, K.C.S. Jenner, M. Jenner, P. Bouchet and E. Rexstad "Southern Hemisphere Breeding Stock D humpback whale population estimates from North West Cape, Western Australia", *Journal of Cetacean Research and. Management* **12**(1), 29-38, (2012)

[16] R. Paterson and P. Paterson, "The status of the recovering stock of humpback whales *Megaptera novaeangliae* in east Australian waters", *Biological Conservation* **47**, 33-48, (1989)

[17] D.H. Cato, "Songs of humpback whales: the Australian perspective", *Memoirs of the Queensland Museum* **30**(2), 278-290 (1991)

[18] R.D. McCauley, M-N.M Jenner, K.C.S. Jenner, K.A. McCabe and J. Murdoch, "The response of humpback whales (Megaptera novaeangliae) to offshore seismic survey noise: Preliminary results of observations about a working seismic vessel and experimental exposures", *APPEA (Australian Petroleum Production and Exploration Association) Journal* **38**(1), 692-707 (1998)

[19] M.J. Noad, D.H. Cato, M.M. Bryden, M-N. Jenner and K.C.S. Jenner, "Cultural revolution in whale songs", *Nature* **408**(6812), 537 (2000)

[20] K.C.S. Jenner, M-N.M. Jenner and K.A. McCabe, "Geographical and temporal movements of humpback whales in Western Australian waters", *APPEA (Australian Petroleum Production and Exploration Association) Journal* **41**, 749-765 (2001)

[21] R.D. McCauley, J. Fewtrell, A.J Duncan, K.C.S Jenner, M-N. Jenner, J.D. Penrose, R.I.T. Prince, A. Adhitya, J. Murdoch, and K. McCabe, "Marine seismic surveys: analysis and propagation of air-gun signals; and effects of exposure on humpback whales, sea turtles, fishes and squid". In (Anon) *Environmental implications of offshore oil and gas development in Australia: further research*. Australian Petroleum Production Exploration Association, Canberra, pp. 364-521, 2003 http://www.cmst.curtin.edu.au/publicat/index.html#2000

[22] M.J. Noad and D.H. Cato, "Swimming speeds of singing and non-singing humpback whales during migration", *Marine Mammal Science* **23**(3), 481-495 (2007)

[23] R.A. Dunlop, M.J. Noad, D.H. Cato and D. Stokes,. "The social vocalization repertoire of east Australian migrating humpback whales (Megaptera novaeangliae)", *Journal of the Acoustical Society of America* **122**(5), 2893-2905 (2007)

[24] J.N. Smith, R.A. Dunlop, A.W. Goldizen and M.J. Noad, "Songs of male humpback whales (Megaptera novaeangliae) are involved in intersexual interactions", *Animal Behaviour* **76**, 467-477 (2008)

[25] R.A. Dunlop, D.H. Cato and M.J. Noad, "Your attention please: increasing ambient noise levels elicits a change in communication behaviour in humpback whales (*Megaptera novaeangliae*)", *Proceedings of the Royal Society of London B* **277**, 2521–2529 (2010)

[26] P.K. McGregor, "Playback experiments: design and analysis", *Acta Ethology* **3**, 3-8 (2000)

[27] A.L. Maggi, A.J. Duncan and D.H. Cato, *Airgun Array Ramp-Up Modelling Study*, Curtin University, Centre for Marine Science and Technology, Project CMST 843, Report number: 2010-67, December 2010

[28] B. Scharf, "Loudness" in *Encyclopedia of Acoustics*, edited by M.J. Crocker, John Wiley & Sons, New York, 1997, Vol. 3, Chapter 118, pp. 1481-1495

[29] H. Kniest, VADAR: Visual and Acoustics Detection and Ranging, http://www.cyclops-tracker.com/

[30] M.P. Johnson, and P.L. Tyack, "A digital acoustic recording tag for measuring the response of wild marine mammals to sound", *IEEE Journal of Oceanic Engineering* **28** 3-12 (2003)

[31] D.K. Mellinger, *Ishmael 1.0 User's Guide*, NOAA Technical Memorandum OAR PMEL-120, 2001

[32] I.M. Parnum, *Seafloor characterisation of the east coast experiment site used for the behavioural response of Australian humpback whales to seismic surveys project*, Curtin University, Centre for Marine Science and Technology CMST report 841, January 2012

Inter-Noise 2014

MELBOURNE AUSTRALIA 16-19 NOVEMBER 2014

The Australian Acoustical Society will be hosting Inter-Noise 2014 in Melbourne, from 16-19 November 2014. The congress venue is the Melbourne Convention and Exhibition Centre which is superbly located on the banks of the Yarra River, just a short stroll from the central business district. Papers will cover all aspects of noise control, with additional workshops and an extensive equipment exhibition to support the technical program. The congress theme is *Improving the world through noise control*.

Key Dates
The dates for Inter-Noise 2014 are:
Abstract submission deadline: 10 May 2014
Paper submission deadline: 25 July 2014
Early Bird Registration by: 25 July 2014

Registration Fees
The registration fees have been set as:

Delegate	$840	$720 (early bird)
Student	$320	$255 (early bird)
Accompanying person	$140	

The registration fee will cover entrance to the opening and closing ceremonies, distinguished lectures, all technical sessions and the exhibition, as well as a book of abstracts and a CD containing the full papers.

The Congress organisers have included a light lunch as well as morning and afternoon tea or coffee as part of the registration fee. These refreshments will be provided in the vicinity of the technical exhibition which will be held in the Main Foyer.

The Congress Banquet is not included in the registration fee.

Technical Program
After the welcome and opening ceremony on Sunday 16 November, the following three days will involve up to 12 parallel sessions covering all fields of noise control. Major areas will include Community and Environmental Noise, Building Acoustics, Transport Noise and Vibration, Human Response to Noise, Effects of Low Frequencies and Underwater Noise.

A series of distinguished lectures will cover topics such as:
- Acoustic virtual sources
- Wind turbine noise
- Active noise control
- Aircraft noise
- Soundscapes

Organising and Technical Committee
- Congress President: Dr Norm Broner
- Technical Program Chair: Adjunct Professor Charles Don
- Technical Program Co-Chair: Adjunct Professor John Davy
- Technical Program Advisor: Mrs Marion Burgess
- Proceedings Editor: Mr Terry McMinn
- Sponsorship and Exhibition Manager: Dr Norm Broner
- Congress Treasurer: Ms Dianne Williams
- Social Program Chair: Mr Geoff Barnes
- Congress Secretariat: Ms Liz Dowsett

Further details are available on the congress website
www.internoise2014.org

PROPAGATION OF WIDEBAND SIGNALS IN SHALLOW WATER IN THE PRESENCE OF MESO-SCALE HORIZONTAL STRATIFICATION

Boris Katsnelson[1], Andrey Malykhin[2] and Alexandr Tckhoidze[1]
[1]School of Marine Sciences, University of Haifa, 31905, Israel
[2]Physics Department of Voronezh University, Voronezh, 394006, Russia
katz@phys.vsu.ru

In the paper examples of an oceanic waveguide with parameters varying in the horizontal plane are considered: an area of coastal wedge, (slopes and canyons), an area of varying water layer properties - in the presence of nonlinear internal waves and a temperature front. In these cases there is significant horizontal refraction or redistribution of the sound field in the horizontal plane. Due to waveguide dispersion (dependence of modal propagation constants on frequency) the refraction index in the horizontal plane depends on frequency also, and it is possible to observe different spatial and temporal variations of the sound signal similar to those in a two dimensional medium with frequency and spatial dispersion. This can be manifested as a non-stationary interference pattern, arrival time variations, and/or variations of spectra. These effects can be used to solve different inverse problems especially by using horizontal and vertical line arrays.

INTRODUCTION

In most publications concerned with sound propagation in shallow water authors have concentrated on the vertical variability of the temperature field, and discussed a simple model of how that variability arises. This vertical structure is the most important feature of the shallow water column, as the water column and bottom are approximately horizontally stratified (comprised of vertically stacked layers) over the propagation scales of interest, which reach to about 50 km in shallow water. However, horizontal stratification is a broad-brush first approximation only, and in many shallow water scenarios there is appreciable sound speed variability in the horizontal direction, as well as in the vertical. Perhaps the strongest horizontal variability in shallow water is due to shallow water fronts and bathymetry variations, mainly in areas of the coastal wedge and nonlinear internal waves. In this paper we consider just three types of horizontal variability.

TEMPERATURE FRONT

Figure 1 shows the configuration of the Polar front in the Barents Sea [1]. The temperature variation is non-uniform in depth: as a rule, it is concentrated in the vicinity of the thermocline.

Aforementioned temperature variations are accompanied by a change in the sound speed profile, which is most pronounced across the front. In the vicinity of the thermocline, the sound speed drop across the front can reach 15–20 m/s within a distance of several hundreds of metres. Such a difference corresponds to a substantial horizontal sound speed gradient, which persists over a rather large area. More detailed information on the temperature front is presented in Figure 2: it shows a sequence of sound speed profiles when passing from one side of the temperature front to another in a region of the

Barents Sea within a zone of about 500 m in length where the temperature variations are most pronounced [1,2].
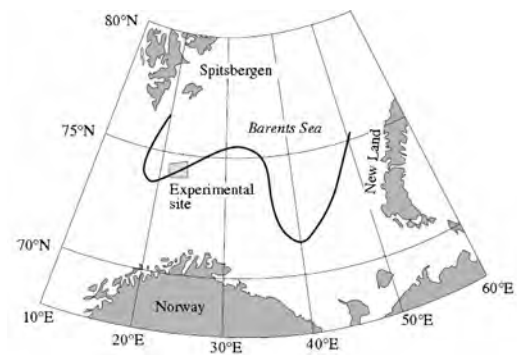
Figure 1. Temperature front (Barents Sea Polar front)
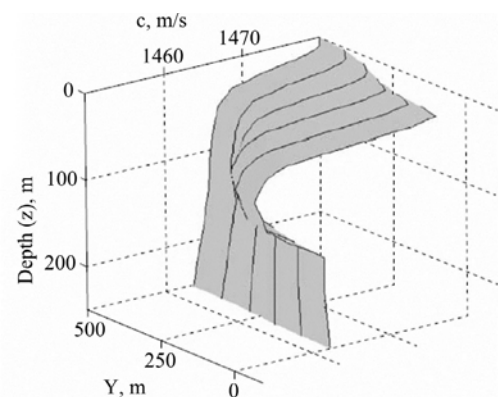
Figure 2. Sequence of sound speed profiles in the vicinity of the temperature front. The nearest and farthest profiles correspond to the colder Arctic Current and the North-Atlantic Current, respectively

Under the influence of such a gradient, the oceanic medium becomes acoustically anisotropic, and a number of effects arise in the course of sound propagation through it. In particular, space–time fluctuations of the sound field due to the modes coupling in the region where the acoustic path crossed the Polar front of the Barents Sea were considered in [1,2]. Another effect that can considerably change the sound field is the horizontal refraction, which manifests itself when the acoustic path is approximately parallel to the TF. The approach of horizontal rays and vertical modes can be applied to such a phenomenon. Such a study can reveal a number of spatial and frequency–time effects that, in principle, can be experimentally observed by using a vertical hydrophone array. In this sense, the influence of the temperature front on the sound field is similar to that of soliton-like internal waves (or internal solitons (IS)) [3], although the horizontal gradients of the sound speed in the TF are 2–5 times lower than those in the IS, and the velocities of the TF are much smaller than those of the IS.

Let us consider the space–frequency features of the sound field propagating in a shallow-water sound channel with a temperature front. The oceanic medium is represented as a three-dimensional underwater waveguide in the Cartesian coordinate system where the (X,Y) plane coincides with the sea surface and the Z axis is directed vertically downwards. The waveguide is formed by the water layer $0 \leq z \leq H$ with density $\rho(x,y,z) = \rho_0(z) + \delta\rho(y,z)$ and a sound speed profile $c(x,y,z) = c_0(\rho) + \delta c(y,z)$, where $\rho_0(z)$ and $c_0(z)$ correspond to the profiles of density and sound speed on one side of the TF. In our case, δc and $\delta\rho$ characterise the variations of the acoustic parameters under the influence of the TF. The latter is considered to be plane and parallel to the X axis. The bottom is assumed to be homogeneous, liquid, and absorbing with density ρ_1, sound speed c_1 and absorption coefficient α. Here, the TF is modelled in such a way that, on average, the temperature (and the sound speed as well) at $y > 0$ is higher than that at $y < 0$ (see Figure 2). Correspondingly, the horizontal rays leaving the source at $y < 0$ will be refracted in the same direction (Figure 3). In other words, our statement of the problem corresponds to the situation where, at the receiving array positioned in the zone of intersection of horizontal rays, a complicated structure will be observed as the result of interference of the direct horizontal ray with a set of horizontal rays deflected by the temperature gradient and corresponding to different horizontal angles at the source and different vertical modes. The particular characteristic of the horizontal refraction is that the horizontal rays corresponding to different frequencies and different vertical modes propagate along different trajectories, and, consequently, the intensity of the sound field at the reception point may depend on the frequency and the ordinal number of the detected mode

First of all, one can estimate the distance from the source and the temperature front, or, in other words, the position of the zone where one can expect the intersection of the direct and refracted horizontal rays and, hence, the manifestations of the aforementioned phenomena. Specifically, such a zone that is closest to the source is determined by the maximum admissible departure angle β of the horizontal ray that returns to the region $y < 0$ after its refraction in the zone of the temperature front. In the simplest case, the estimate is as follows [5]:
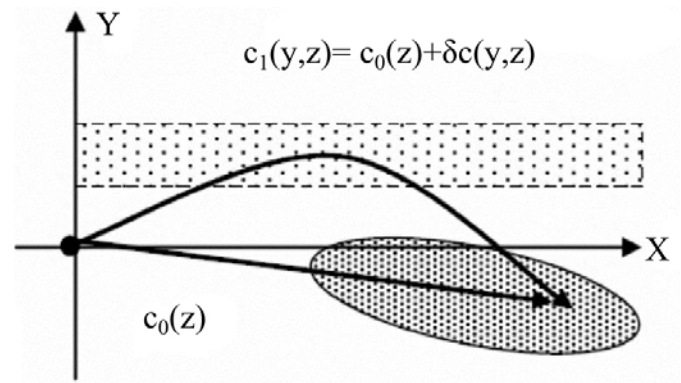

Figure 3. Schematic diagram of the horizontal refraction in the region near the temperature front. The shaded area is the zone of probable enhancement of the sound field due to horizontal refraction. The dashed strip approximately indicates the transition layer

$$\beta \approx \sqrt{2\frac{h_t}{H}\frac{\delta c}{c}} \tag{1}$$

where h_t is the thickness of the thermocline. For the Barents Sea [1], $H \sim 230$ m, $h_t \sim 70$–90 m, $\delta c \sim 15$–20 m/s, and, hence, $\beta \approx 6$–8×10^{-2}. This means that, if the source is at a distance of 600–800 m from the temperature front with a thickness of about 500 m, the effects of horizontal refraction manifest themselves at the receiver that is at a distance of about 20 km along the temperature front.

INTERNAL WAVES

Intense internal waves (IWs) are known to cause substantial perturbation of the low-frequency sound field. The well-known study [4] reports on measuring the fluctuations of the sound field over a horizontal array in the presence of IWs with the propagation path passing at a small (about 10°) angle to the wave fronts of a train of intense IWs moving along the coastline. It was experimentally established that the amplitude fluctuations of the sound field correlated with the fluctuations of the water layer influenced by IWs. Data from numerical simulation allow one to assume the adiabatic mechanism of interaction between the IWs and the sound field: the intensity variations are caused by local changes in the waveguide parameters. A detailed study of fluctuations of the sound field under the influence of IWs was also performed in the SWARM'95 experiment [6] for different orientations of the acoustic path with vertical receiving arrays used for mode filtering. Publications [7-9] devoted to analysing the data of the SWARM'95 experiment show that, when the acoustic path is approximately parallel to the wave front of the IW train, intensity fluctuations can be rather substantial because of the influence of horizontal refraction. A theoretical analysis and estimation of intensity fluctuations were presented in [9] in the framework of a ray approximation in the horizontal plane. There, in terms of horizontal rays, the mechanism of intensity fluctuations was explained by changes in the ray density (the cross-section of the ray tube). In this case, the estimates of intensity variations can be obtained by assuming the

horizontal rays to be approximately straight with perturbations of the phase front being neglected. On the other hand, in the presence of appreciable horizontal refraction, the objective of the study is to consider the fluctuations of the directions of sound propagation in the horizontal plane (the fluctuations of the phase front in a more general formulation). For instance, an experiment measuring the fluctuations of the direction of sound propagation in the horizontal plane was carried out in the Barents Sea [10]. There, a horizontal hydrophone array was used to study the fluctuations in the phase distribution with characteristic periods starting from several tens of minutes, which, according to the authors, correspond to the typical periods of IWs.

In the present paper we estimate the variations of the sound-field phase front under the effect of a train of intense internal waves crossing the acoustic path and consider the possibility of experimental observation of such variations.

An illustration of the influence of internal waves on sound propagation is shown in Figure 4 where there is a 3D shallow-water sound channel with IWs. The ocean medium is represented as an underwater waveguide in the XYZ coordinate system, where the XY plane coincides with the sea surface and the Z axis is oriented vertically downwards. The waveguide is formed by a water layer $0 \leq z \leq H$ with a density $\rho(z)$ and a sound speed profile $c(x,y,z) = c_0(z) + \delta c(x,y,z,T)$, where $c_0(z)$ corresponds to the equilibrium stratification of the layer and $\delta c(x,y,z,T)$ characterises the changes of the acoustic properties of the layer under the influence of IWs. The latter quantity depends on both coordinates and time T (we make a difference between the "slow" time T that characterises the variability in δc and "quick" time t, determining sound field variability)
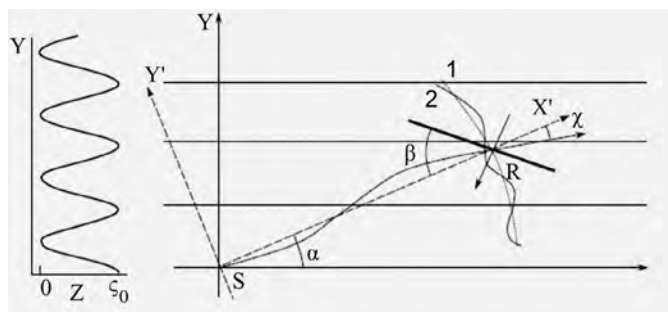
Figure 4. The XY coordinate system is related to IWs, the $X'Y'$ coordinate system is determined by the direction of the acoustic path, α is the angle between the path and the wave front of IWs, β is the angle between the path and the array, and γ is the angle of horizontal refraction. At the left, the position of the IW envelope is shown at the instant $T = 0$. The (1) dotted and (2) solid curves show the wave front without and with IWs, respectively

Let us consider an IW train with an approximately rectilinear wave front that is parallel to the X axis and with an envelope depending on the y coordinate and with an amplitude ζ_0. This train propagates along the Y axis with a speed v. The sound source S is located at the origin of coordinates in the horizontal plane $x = y = 0$ at a depth $z = z_1$. The transmitted signal is received at the observation point $R(x,y,z)$ by a horizontal array (usually $z = H$). The initial position of the IW envelope at $T = 0$

is such that the IW's maximum is at the source at the zero shift of the train, $vT = 0$ (the envelope with amplitude ζ_0 is shown in the left-hand part of Figure 4). Because of the slow propagation of the IW train, the characteristics of the sound field will depend on the position of the train, or on time T, in a parametric manner. For brevity, we do not write this dependence in an explicit form.

COASTAL WEDGE

In the ocean, coastal slope regions are of primary importance for both practical purposes and research, including acoustic studies. A typical coastal slope region has the form of a wedge with the angle between the sea surface and the bottom reaching ~0.005–0.01rad; this region extends for several tens of kilometres (or more) from the coast to the shelf edge, where the sea depth is about 200–350 m. Beyond this line, the sea depth begins to increase steeply (the continental slope). In the theoretical studies of sound propagation, the coastal slope is usually described by a wedge shaped model region with a constant velocity of sound and with ideally or non ideally reflecting boundaries [11-14]. The solution to the problem of the field in an ideal wedge can be constructed by using, e.g. imaginary sources, in analogy with the well known Pekeris model; in this case, the imaginary sources are positioned in a circle [11, 14]. In some papers the field in the wedge is constructed in a cylindrical coordinate system (the z axis coincides with the edge of the wedge) based on modes depending on angle ϑ in the vertical plane. A somewhat different approach is possible in the case of a smooth dependence of the sea depth on the distance to the coast (a small slope), when the wedge-shaped region can be considered as a waveguide with varying depth and, in terms of the depth dependent field expansion in modes, the field can be described in the adiabatic approximation (ignoring the mode coupling). In the two-dimensional version of the problem, where the field only varies in the vertical plane, one of the main features of sound propagation up the slope is the appearance of the critical cross section for a mode of a fixed number at a fixed frequency with decreasing depth and the reflection of this mode; or, the transformation of the mode into a leaky one and, hence, its escape into the bottom at a certain distance from the edge, this distance being different for different modes and frequencies [15]. The three-dimensional problem was considered in studies of the horizontal refraction of the acoustic field in a coastal slope region in both experimental (laboratory experiments [16] and full-scale experiments in a coastal slope region [17]) and theoretical investigations. In the latter, the field behaviour was described in terms of vertical modes and horizontal rays or numerically [18] by a parabolic equation (see references in [18]). For the ideal wedge model, the ray equations in the horizontal plane have analytic solutions describing the position and shape of rays and caustics in the form of hyperbolas [19]. In the case of a wedge with ideally reflecting surfaces, two rays (the direct ray and the refracted) arrive at each of the points of the horizontal plane, and the corresponding interference pattern is formed. We note that, for a more realistic model (a non-ideal bottom and/or a coordinate dependent sound velocity), the field pattern is more complicated, especially with allowance for the dependence of the refractive index of horizontal rays

on frequency and vertical mode number. Sound propagation in the horizontal plane is similar to the propagation in an inhomogeneous dispersive medium with similar features for narrowband and broadband signals. A similar situation occurs to that in the vicinity of the temperature front [5].
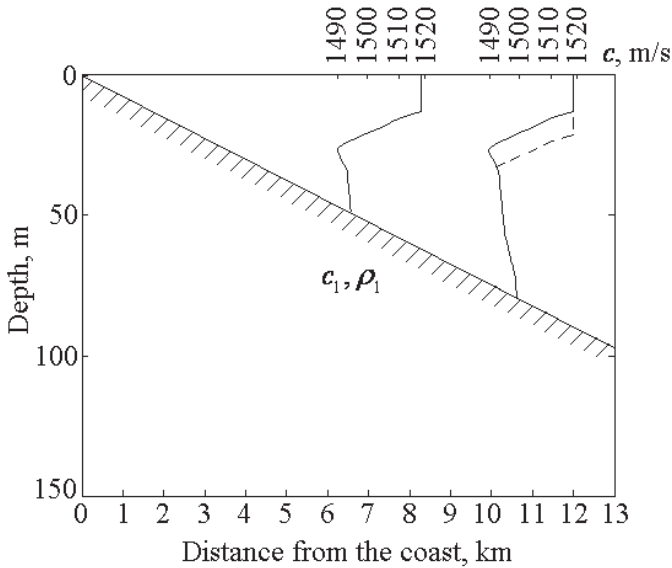

Figure 5. Bathymetry and sound velocity profiles for the waveguide model under study. The dashed line shows the perturbed sound velocity profile under mesoscale perturbation

THEORY OF THE SOUND FIELD IN A HORIZONTALLY STRATIFIED WAVEGUIDE

The complex sound field amplitude of a point source characterised by spectrum $S(\omega)$ and positioned at a point with the coordinates is sought in the form

$$P(\vec{r},z,t) = 2\int_0^\infty \sum_l P_l(\vec{r},\omega)\psi_l(\vec{r},z;\omega)e^{-i\omega t}d\omega \qquad (2)$$

Here, $\psi_l(\vec{r},z;\omega)$ is the eigenfunction with the number l; it is determined by the Sturm–Liouville problem and includes the dependence on $\vec{r}$ (or (x, y)) as a parameter; and in addition, depends on frequency. The quantity $P_l(\vec{r},\omega)$ which depends on the horizontal coordinates, the sound frequency, and the source coordinates, can be called the spectral mode amplitude.

We denote the corresponding eigenvalue (the longitudinal wavenumber) by $q_l(\vec{r},\omega)$. For the value $P_l(\vec{r},\omega)$ neglecting mode coupling we can get the two dimensional Helmholtz equation:

$$\nabla^2_\perp P_l(\vec{r},\omega) + q^2_l(\vec{r},\omega)P_l(\vec{r},\omega) = 0 \qquad (3)$$

where $\nabla^2_\perp = \frac{\partial^2}{\partial x^2} + \frac{\partial^2}{\partial y^2}$ is the Laplace operator in the horizontal plane.

Instead of the eigenvalue $q_l(\vec{r},\omega)$, which determines the space and time dependences of the wavenumber for sound propagation in the horizontal plane, we introduce the corresponding mode refractive index $n_l(\vec{r},\omega)=q_l(\vec{r},\omega)/q_1^0$ where q_1^0 is the eigenvalue of the transverse Sturm–Liouville

problem; this eigenvalue corresponds to the cross section at a certain fixed point, e.g., at the point of the source position. We note that, in the region lying between the source and the coast ($y<y_s$), the wavenumber is $q_l < q_1^0$ and ($n_l(\vec{r},\omega) <1$). For a real situation, the latter index differs little from unity $n_l(\vec{r},\omega) <1-\delta n_l$, $|\delta n_l|<<1$.

Figures 6 and 7 show the value of the increment for our models of temperature front and wedge as a function of the distance to the front and to the edge of the wedge for different frequencies and mode numbers. One can see that, in the region $y<y_s$, the increment increases with an increase in the mode number and with a decrease in frequency; i.e., the refractive index increases with increasing frequency.

The frequency dependence of the refractive index makes the two-dimensional propagation medium a dispersive one (Eq. (3)). For such a medium, the evolution of the sound signal in time is determined by Eq. (2). If the spectrum of the emitted signal is sufficiently narrow, we can ignore the frequency dependence (which is sufficiently smooth) of the eigen functions within this spectrum; then, we factor out the eigen functions from under the integral in Eq. (2) at the central frequency ω_0 of the source spectrum. In this case, the signal amplitude takes the form

$$P(\vec{r},z,t) = 2\sum_l \psi_l(\vec{r},z;\omega_0)\int_0^\infty P_l(\vec{r},\omega)e^{-i\omega t}d\omega = \sum_l \psi_l(\vec{r},z;\omega_0)P_l(\vec{r},t) \qquad (4)$$

where the quantity $P_l(\vec{r},t)$ can be interpreted as the pulse amplitude of the lth mode. As usual for space-time ray approximation we find

$$P_l(\vec{r},t) = A_l(\vec{r},t)e^{i\Theta_l(\vec{r},t)} \qquad (5)$$

where phase (eikonal) depending on coordinates and time can be found by different ways [19, 20]. Examples of variations in refractive index in the horizontal plane for a wedge and temperature front are shown in Figures 6 and 7.
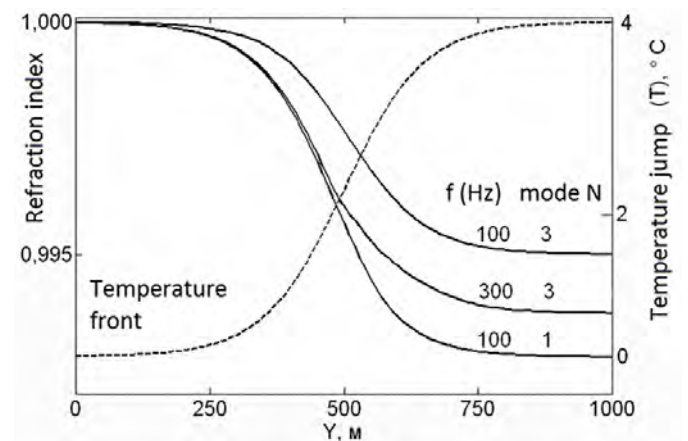

Figure 6. Dependence of the refractive index of the horizontal rays on the Y coordinate for some frequencies and mode numbers in the region of the temperature gradient. The dashed curve indicates the variation of temperature at some depth in the thermocline region across the temperature front
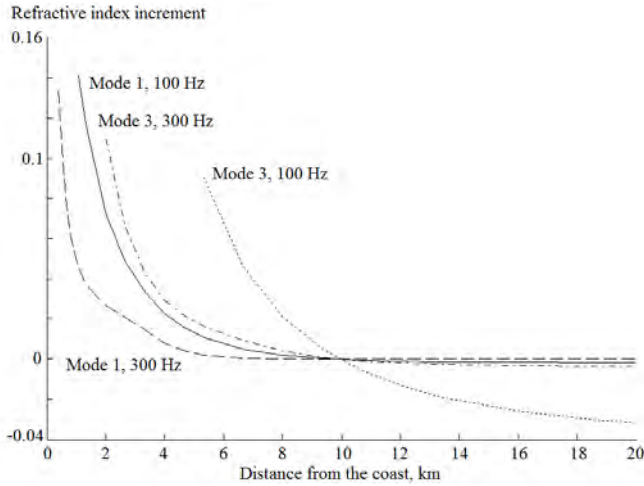
Figure 7. Dependence of the refractive index increment on the distance to the edge of the wedge for different modes and frequencies (the values are indicated in the plot)

STRUCTURE OF HORIZONTAL RAY PATTERN

If we take all the values $0 < t < \infty$, the corresponding curve will determine the spatial horizontal rays. Figure 8 shows examples of horizontal rays in the area of the temperature front. In Figure 9 we can see pattern of horizontal rays in the area of the coastal wedge for a frequency of 100 Hz, which corresponds to the first mode. In the plot, the multipath region can be distinguished. Its shape resembles a sector, so that, in what follows, we use the term "multipath sector" (MS). When the receiver is located in the MS, one should observe the interference of the direct and reflected fields of the corresponding modes if the overlapping of signals arriving over different ray paths takes place or if signal doubling occurs with a certain time interval in the case of pulse arrival time measurements. The interference pattern is rather complicated because of the presence of regions where only one mode (the first) propagates or only two modes propagate (e.g., the first and second modes), and so on. The lower boundary of the sector, i.e., the boundary closest to the coast, represents the caustics (envelope) for the horizontal rays corresponding to a given mode and a given frequency, and the upper (limiting) horizontal ray indicates the MS boundary farthest from the coast.

The positions of the boundaries can be estimated on the basis of a three-dimensional ray consideration with the use of the Brillouin (vertical) grazing angle β_l for the lth mode. The upper limiting ray path in the horizontal plane, or the horizontal launch angle of the boundary ray, which is denoted by $\overline{\chi}_l$ (see Figure 9(a)) and determines the aforementioned ray path, is governed by the parameters of the bottom or, more precisely, by the angle of total internal reflection from the bottom.

As the ray propagates from the source, both the horizontal angle and the Brillouin angle of the given mode (the vertical grazing angle with respect to the bottom) β_l vary (Figure 9(b)). In other words, during propagation up the slope the channel narrows, and the angle decreases, whereas the vertical grazing

angle β_l, which depends on the local depth of the channel, increases and, at a certain instant, may become identical to the angle of total internal reflection from the bottom which depends on c_l. In this case, the direct ray penetrates to the bottom and the reflected (or refracted) ray is absent. The corresponding horizontal ray launch angle (see Figure 9(a)) is determined as follows. The local eigenvalue corresponding to total internal reflection, or the related bottom grazing angle of the Brillouin ray belonging to the lth mode is determined by the expression $\cos \overline{\beta}_l = \overline{q}_l / k = c(\overline{H}) / c_l$ where $\overline{H}$ is the sea depth at the turning point. This yields the refractive index at the turning point for the horizontal boundary ray: $n_l = \overline{q}_l / q_l^0 = k_1 / q_l^0$ where $k_1 = \omega / c_l$ and the horizontal angle χ_l at the turning point is zero. Then $\overline{\chi}_l$ is determined by the relation $\cos \overline{\chi}_l = k_1 / q_l^0$. The corresponding boundary ray path is shown in Figure 9(a). Now, we estimate the coordinates of the ray turning point $(\overline{x}_l, \overline{y}_l)$, which approximately coincides with the vertex of the MS under the assumption that the sound velocity in the wedge is constant. In this case, the horizontal ray paths and ray caustics have the form of hyperbolas [5], whose equations are obtained in an analytic form. Using these results, for the coordinates of the vertex of the hyperbola corresponding to the boundary ray, we derive

$$\overline{x}_l = y_0 \frac{\sin \overline{\chi}_l \cos \overline{\chi}_l \cos^2 \beta_l^0}{1 - \cos^2 \overline{\chi}_l \cos^2 \beta_l^0} = y_0 \frac{k_1 \sqrt{(q_l^0)^2 - k_1^2}}{k^2 - k_1^2}$$

$$\overline{y}_l = y_0 \frac{\sin \beta_l^0}{\sqrt{1 - \cos^2 \overline{\chi}_l \cos^2 \beta_l^0}} = y_0 \frac{\sqrt{k^2 - (q_l^0)^2}}{\sqrt{k^2 - k_1^2}} \quad (6)$$

For our bottom model (the parameters are given above), we can assume that, in the denominator of Eq. (10), $q_l^0 \sim k$; then, we have $\overline{x}_l \, y_0 k_1 / \sqrt{k^2 - k_1^2} \sim 2y_0 \sim 20$ km. We see that $\overline{x}_l$ weakly depends on both mode number and frequency. The coordinate $\overline{y}_l$ exhibits a more pronounced dependence on the mode number, as well as on frequency. For example, for the second mode at a frequency of 100 Hz, from Eq. (10) we obtain $\overline{y}_l \sim 0.5$, $y_0 \sim 5$ km. In general, the straight line $y = \overline{y}_l$ determines the boundary beyond which the lth mode does not propagate (at the given frequency).
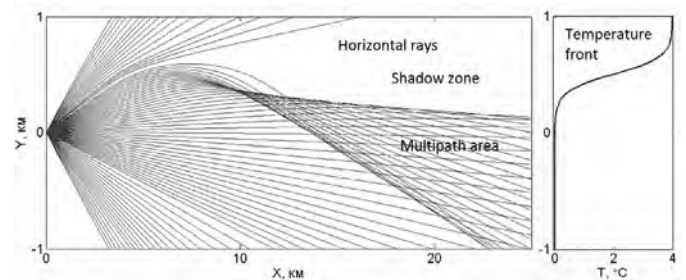

Figure 8. Ray pattern calculated by using the method of vertical modes and horizontal rays with the corresponding temperature distribution at some depth (at the right) in the vicinity of the temperature front for the first vertical mode at a frequency of 300 Hz
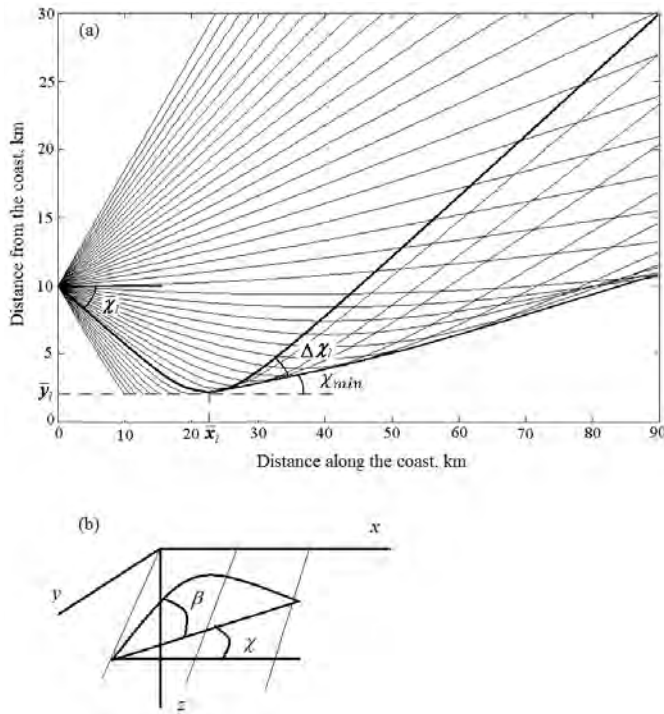
Figure 9. (a) Horizontal ray pattern for the first vertical mode at a frequency of 100 Hz; the solid lines indicate the MS. (b) The vertical and horizontal angles for a three-dimensional ray

One can see that the numerically calculated position of the MS vertex approximately coincides with the coordinates determined above. If we assume that, for our wedge model, the caustic approximately coincides with the asymptote of the corresponding hyperbola (the caustic for the case of a constant velocity), the slope of this asymptote is $\tan \beta_l^0$ i.e. its angle with the x axis is β_l^0. This angle noticeably increases with increasing mode number. The asymptote of the "upper" horizontal boundary ray has the slope $dy / dx = \sqrt{k^2 - k_1^2} / k_1$ which, in the framework of the simple model, is the same for different modes and frequencies and only depends on the sound velocities in water and in the bottom. In the case under consideration, the aforementioned estimate yields a slope of ~0.53 or an angle $\overline{\chi}_l \sim 30°$, which approximately coincides with the numerical results represented in Figure 9(a). In Figure 9(a), the direction of the lower boundary is determined by the angle $\chi_{\min}$, which in our case approximately coincides with β_l^0; for the first mode at a frequency of 100 Hz, this angle is $\chi_{\min} \sim 5°-6°$. The vertex angle of the sector is estimated as $\Delta\chi_l \sim \overline{\chi}_l - \chi_{\min}$ and decreases with the mode number. We note that, as the mode number increases and the frequency decreases, the increment of the horizontal refractive index δn_l increases and the MS shifts toward greater depths. In this case, the characteristic spatial dimensions of the region vary (the transverse size of the MS at a distance of ~30 km makes about 2–4 km). As the frequency increases, the angle $\chi_{\min}$ decreases (tends to zero) and the lower boundary of the MS shifts toward the coast for all of the modes.

TIME-FREQUENCY DIAGRAM AND WIDEBAND PULSE PROPAGATION

The eikonal (the phase) taken at a certain point of the horizontal plane is determined by the phase velocity and the corresponding integral along the horizontal ray from the point of radiation to the point of reception (observation):

$$\Theta_l (M,t) = \int_{R_{0M}} q_l(x,y)ds \tag{7}$$

The characteristic features of the pulse arrival time are illustrated in Figure 10, where, together with the horizontal ray pattern for the first and third modes at a frequency of 200 Hz, one can see lines lying in the horizontal plane, which correspond to a constant arrival time $t = 45$s for signals propagating along the respective ray paths. The regions are denoted as follows: (I) the shadow zone for all modes, (II) the multipath region for the first mode and the shadow zone for the third mode, (III) the multipath region for the first and the third modes, and (IV) the region of only the direct ray paths of these modes. One can see that, in the multipath regions, for each of the modes, there are two curves $t_l(x,y) = $ const corresponding to the direct and reflected signals. The signal propagating over the direct ray path goes farther within a fixed time interval as compared to the ray arriving over the reflected ray path. In other words, for a fixed point in the multipath region, the direct signal usually arrives earlier than the reflected signal; the difference decreases with decreasing distance to the caustics where the direct and reflected rays coincide. The time of signal propagation over the ray path (which is an important observation characteristic) is determined by the integral along the ray path

$$t_l (\omega) = \int_{R_{0M}} \frac{ds}{v_l^{gr} (x,y;\omega)} \tag{8}$$

where $v_l^{gr} (x,y;\omega)$ is the group velocity of the lth mode, depending on coordinates along ray path. Comparing the arrival times at the reception point for different modes, we see that, in the absence of horizontal refraction (for the direct horizontal rays), a "conventional" order of mode arrivals is observed: the lower modes are usually characterized by a higher group velocity, and their travel time is shorter. For the reflected signals in region III, a different order of mode arrivals takes place. This change in arrival order is related to the fact that, despite the higher group velocity of mode 1, as compared to mode 3, the difference in the lengths of the respective ray paths is such that the order of arrival is changed. In particular (see Figure 10), for the direct signal, the first mode arrives before the third mode (in regions III and IV), whereas, for the reflected signals (region III), the third mode arrives before the first one.

Let us consider in more detail the signal arrival time at the observation point, which may fall within the MS. First of all we remark that arrival times can be different for different horizontal rays coming to the receiver. Typical values of arrival times are shown in Figure 11 for a temperature front. Experimental observation of this effect was published in [21] for a moving front of internal waves.

Next we consider arrival times, as a function of frequency for different vertical modes (Figure 12). The corresponding

pattern is called the frequency–time diagram and is often plotted in theoretical considerations and on the basis of experimental data [22]. This pattern reveals the shapes of the dispersion curves for individual modes and is used for solving various problems [23]. The position of the observation point used in our calculations is shown in Figure 10 (its approximate coordinates are $x = 50$ km, $y = 4.5$ km). From Figure 12 one can see that, for frequencies $\omega < \omega_1$ where $\omega_1 = 100$Hz, the receiver falls within the shadow zone for all of the modes. As the lower boundary of the MS shifts toward the x axis and the receiver falls within the caustic for the first mode; here $\omega = \omega_1$, the direct and reflected rays coincide and the corresponding signals arrive simultaneously. With a further increase in frequency $\omega > \omega_1$ the lower boundary of the MS shifts further and falls within the MS for the first mode (still remaining in the shadow zone for the second mode); in this case, two signals are observed with the interval between the first mode arrivals over the direct and reflected ray paths increasing with frequency (the characteristic time between the direct and reflected signal arrivals is ~0.5 s). This corresponds to zone II in Figure 10. As the frequency increases, the signal travel time decreases for the direct ray (the group velocity increases with frequency) and increases for the reflected ray (because of the predominant increase in the ray path length). When the frequency reaches the value $\omega = \omega_2 \approx 250$Hz, the second mode appears at the observation point and the situation is reproduced. For a fixed mode number, as the frequency increases further, the observation point may fall outside the multipath region (we denote the corresponding frequency value as $\omega = \overline{\omega}_l$) and, in this case, only one signal arrives at the observation point. Note that the specific values of ω_l and $\overline{\omega}_l$ depend (in addition to the dependence on the waveguide parameters and the mode number) on the position of the observation point in the horizontal plane. The situation where the observation point falls outside the MS is only possible when this point lies in a relatively narrow region near the upper boundary (see Figure 9). Such a frequency–time diagram can be plotted in an experiment with the use of broadband signals (a frequency band of about 50–500 Hz). It is also possible to consider the spectral features of the signal and, in particular, the spectrum of the received signal as a function of the receiver position. These features are determined by the frequency dependence of the horizontal ray paths.

Let's consider propagation of the wideband pulse. In the presence of horizontal stratification due to the frequency dependence of the refractive index in the horizontal plane each Fourier component of the pulse will propagate along a different trajectory joining source and receiver. In the Figure 13(a) two horizontal rays, corresponding to frequencies of 100 and 300 Hz are shown in the vicinity of the temperature front (refractive index is shown in the Figure 13(b)). It means, first of all, that the frequency spectrum of the received signal will be different in comparison with what would be received in the absence of horizontal refraction, due to a different phase shift for each Fourier component. Next, for different trajectories (Fourier components) we have different directions of wave vectors (tangent to horizontal rays) in the horizontal plane both at the locations of the source and receivers. For example in the
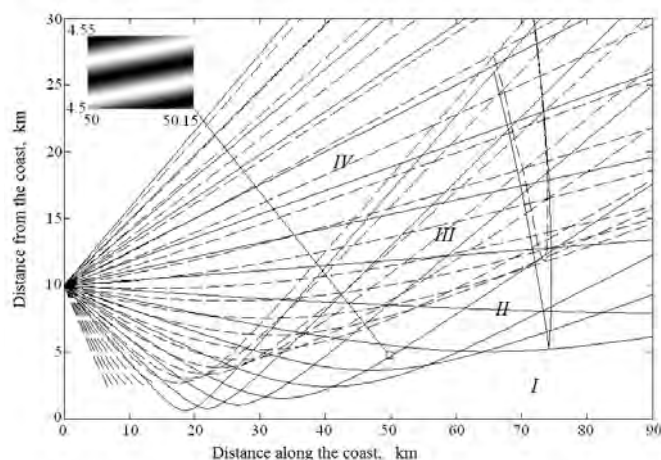
Figure 10. Set of horizontal rays for the first (the solid lines) and fourth (the dashed lines) vertical modes. The frequency is 200 Hz. The lines lying in the horizontal plane and corresponding to a signal arrival time of 45s are indicated. The inset shows the interference pattern formed in the horizontal plane segment near the point indicated in the plot.
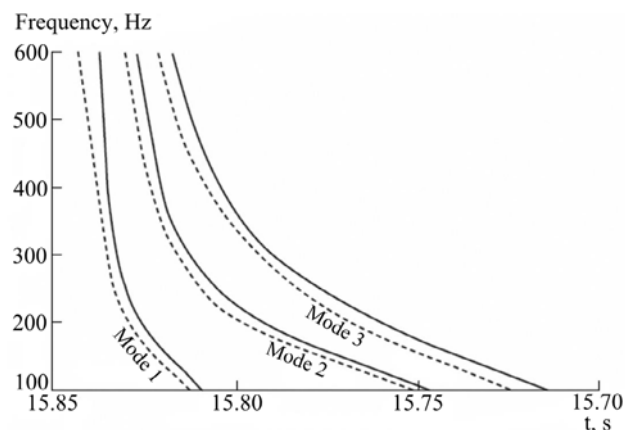

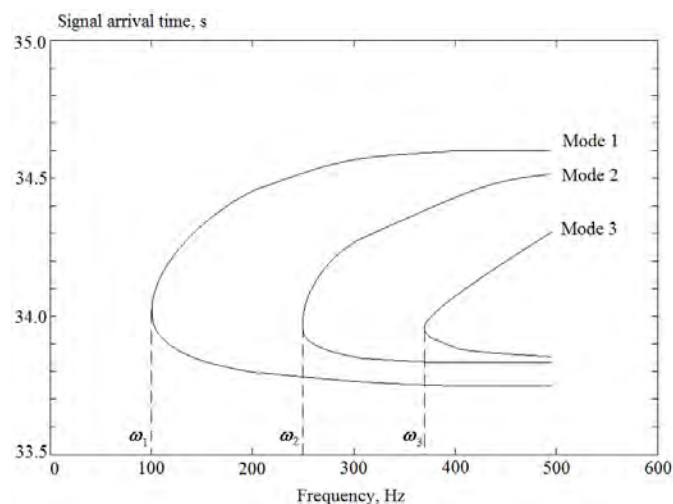Figure 11. Arrival times for horizontal rays reflected from temperature front

Figure 12. Frequency–time curves for three modes. The numbers are indicated in the plot.

situation corresponding to Figure 13 angles between mentioned vectors at the source are about 3°, and at the receiver ~ 2°. In other words we can say that for the sound field near the receiver there is a dependence $\vec{q}_l = \vec{q}_l(\omega)$, that is similar to a medium with spatial dispersion. One of the consequences of this with broadband signals will be spatial modulation of the interference pattern across the direction of propagation and different directions of group and phase velocities.

An example of the interference pattern formed by the beam containing two frequencies, 100 and 300 Hz, in the vicinity of the receiver (Figure 13) is shown in Figure 14(b). We see that in comparison with Figure 14(a) (absence of frequency dependence for horizontal rays) there is spatial modulation of the interference pattern in the y-direction. The scale of this modulation can be estimated as $\Lambda \sim 2\pi/|\Delta\vec{q}|$, where $\Delta\vec{q}$ is the difference between wave vectors, corresponding to frequencies in the beam. We see that in the Figure 14(b) the scale of variability in the y-direction is a few hundreds of metres, in accordance with the angle between vectors for 100 and 300 Hz.
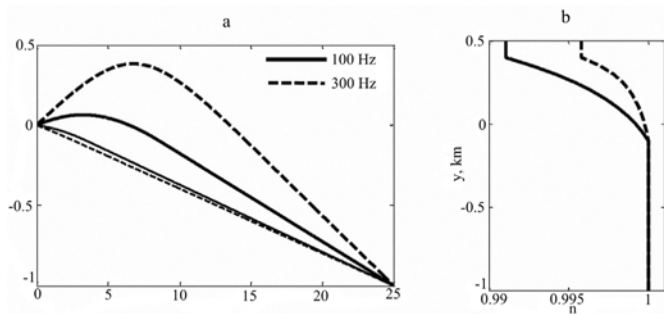
Figure 13. (a) - Horizontal rays (vertical mode 1), frequencies 100 and 300 Hz (direct and reflected from the front). (b) - refractive index n in the horizontal plane for mentioned frequencies
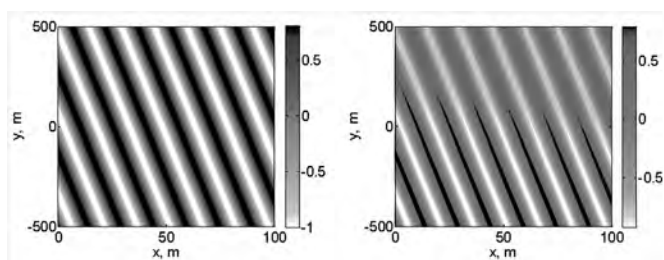
Figure 14. Interference pattern in the vicinity of the receiver neglecting frequency dependence of horizontal rays (left panel) and taking into account frequency dependence

CONCLUSION

We can conclude that the existence of anisotropic meso-scale perturbations can lead to different acoustical effects, such as redistribution of the sound field in the horizontal plane, variation of the spectrum of the signal and a change of temporal shape of a received pulse. Next, due to the frequency dependence of the trajectory of horizontal rays it is possible to observe effects similar to spatial dispersion in sound propagation. All these effects occur in situations considered in the paper, however different spatial scales of coastal wedge (for example) and nonlinear internal waves produce different values of acoustical parameters: horizontal angles, arrival times, interference pattern in the horizontal plane. This implies that to observe these effects it is necessary to take different distances between source and receivers as well as distances from wave fronts and coast lines. It is also necessary to use vertical and horizontal line arrays, allowing different sorts of filtering to be carried out.

REFERENCES

[1]   G. Jin, J.F. Lynch, C.S. Chiu and J.H. Miller, "A theoretical and simulation study of acoustic normal mode coupling effects due to the Barents sea Polar Front, with applications to acoustic tomography and matched-field processing", *Journal of the Acoustical Society of America* **100**(1), 193-205 (1996)

[2]   J.F. Lynch, G. Jin, R. Pawlowicz, D. Ray, A.J. Plueddemann, C.S. Chiu, J.H. Miller, R.H. Bourke, A.R. Parsons and R. Muench, "Acoustic travel-time perturbations due to shallow-water internal waves and internal tides in the Barents Sea Polar front: Theory and experiment", *Journal of the Acoustical Society of America* **99**(2), 803-821 (1996)

[3]   B.G. Katsnelson, A.Y. Malykhin and A.V. Tskhoidze, "Rearrangement of the horizontal space–time structure of the sound field in shallow water in the presence of moving internal waves", *Acoustical Physics* **57**(3), 368-374 (2011)

[4]   D. Rubenstein and M.N. Brill, "Acoustic variability due to internal waves and surface waves in shallow water", in *Ocean Variability and Acoustics Propagation*, eds. J. Potter and A. Warn-Varnas, Kluwer Academic, 1991, pp. 215-228

[5]   B.G. Katsnelson, J.F. Lynch and A.V. Tskhoidze, "Space–frequency distribution of sound field intensity in the vicinity of the temperature front in shallow water", *Acoustical Physics* **53**(5), 611-617 (2007)

[6]   J.R. Apel, M. Badiey, C.S. Chiu, S. Finette, R.H. Headrick. J. Kemp, J.F. Lynch, A. Newhall, M. H. Orr, B. H. Pasewark, D. Tielberger, A. Turgut, K. von der Heydt and S.N. Wolf, "An overview of the 1995 SWARM shallow-water internal wave acoustic scattering experiment", *IEEE Journal of Oceanic Engineering* **22**, 465-500 (1997)

[7]   M. Badiey, Y. Mu, J.F. Lynch, J.R. Apel and S.N. Wolf, "Temporal and azimuthal dependence of sound propagation in shallow water with internal waves", *IEEE Journal of Oceanic Engineering* **27**(1), 117-129 (2002)

[8]   M. Badiey, B.G. Katsnelson, J.F. Lynch, S.A. Pereselkov and W.L. Siegmann, "Measurement and modeling of three-dimensional sound intensity variations due to shallow-water internal waves", *Journal of the Acoustical Society of America* **117**(2), 613-625 (2005)

[9]   M. Badiey, B.G. Katsnelson, J.F. Lynch and S. Pereselkov, "Frequency dependence and intensity fluctuations due to shallow water internal waves", *Journal of the Acoustical Society of America* **122**(2), 747-760 (2007)

[10]   A.Y. Shmelev, A.A. Migulin and V.G. Petnikov, "Horizontal refraction of low-frequency acoustic waves in the Barents Sea stationary acoustic track experiment", *Journal of the Acoustical Society of America* **92**(2), 1003-1007 (1992)

[11] G.B. Deane and M.J. Buckingham, "An analysis of the three-dimensional sound field in a penetrable wedge with a stratified fluid or elastic basement", *Journal of the Acoustical Society of America* **93**(3), 1319-1328 (1993)

[12] F.B. Jensen and W.A. Kuperman, "Sound propagation in a wedge-shaped ocean with a penetrable bottom", *Journal of the Acoustical Society of America* **67**(5), 1564-1566 (1980)

[13] A.D. Pierce, "Guided mode disappearance during upslope propagation in variable depth shallow water overlying a fluid bottom", *Journal of the Acoustical Society of America* **72**(2), 523-531 (1982)

[14] E.K. Westwood, "Broadband modeling of the three-dimensional penetrable wedge", *Journal of the Acoustical Society of America* **92**(4), 2212-2222 (1992)

[15] M.J. Buckingham, "Theory of three-dimensional acoustic propagation in a wedgelike ocean with a penetrable bottom", *Journal of the Acoustical Society of America* **81**(2), 198-210 (1987)

[16] C.T. Tindle, H. Hobaek and T.G. Muir, "Downslope propagation of normal modes in a shallow water wedge", *Journal of the Acoustical Society of America* **81**(2), 275-286 (1987)

[17] R. Doolittle, A. Tolstoy and M. Buckingham, "Experimental confirmation of horizontal refraction of cw acoustic radiation from a point source in a wedge-shaped ocean environment", *Journal of the Acoustical Society of America* **83**(6), 2117-2125 (1988)

[18] F. Sturm, "Numerical study of broadband sound pulse propagation in three-dimensional oceanic waveguides", *Journal of the Acoustical Society of America* **117**(3), 1058-1079 (2005)

[19] L.M. Brekhovskikh and Y.P. Lysanov, *Fundamentals of ocean acoustics*, Springer-Verlag, New York, 2003

[20] Y.A. Kravtsov and Y.I. Orlov, *Geometrical optics of inhomogeneous media*, Springer, Berlin, 1990

[21] M. Badiey, B. Katsnelson, Y-T Lin and J. Lynch, "Acoustic multipath arrivals in the horizontal plane due to approaching nonlinear internal waves", *Journal of the Acoustical Society of America* **129**(4), EL141-147 (2011)

[22] C. Chen, J.H. Miller, G.F. Bourdreaux-Bartels, G.R. Potty and C.J. Lazauski, "Time-frequency representations for wideband acoustic signals in shallow water", *Proceedings of Oceans 2003*, **5**, pp. 2903–2907, September 2003

[23] M. Lopatka, G. Le Touzé, B. Nicolas, X. Cristol, J.I. Mars and D. Fattaccioli, "Underwater broadband source localization based on modal filtering and features extraction", *EURASIP Journal on Advances in Signal Processing*, 2010:304103 (2010)
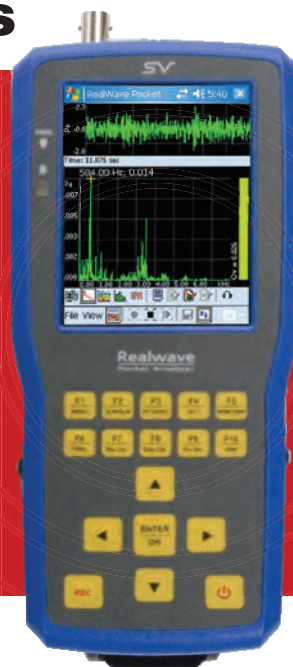
QUANTIFYING THE ACOUSTIC PACKING DENSITY OF FISH SCHOOLS WITH A MULTI-BEAM SONAR

Miles J.G. Parsons, Iain M. Parnum and Robert D. McCauley
Centre for Marine Science and Technology, Curtin University, WA 6845, Australia

Multi-beam (swath) sonar systems provide the capability to ensonify an entire aggregation of fish in a single pass. However, estimation of abundance and discrimination between species via the use of target strength are considerably more complex than using traditional echosounders, because they ensonify targets at a much wider range of incidence angles. The beam pattern and along beam resolution of multi-beam swaths can produce individual sample volumes that are of similar magnitude to an individual fish (particularly for large fish, say >1m in length). If individual fish can be resolved, (either as a single fish within a sample, or as multiple contiguous samples that delineate a single fish), and if one assumes that this situation applies to the whole school, acoustic packing density can be determined by dividing the volume of the school by the number of detected acoustic targets. This estimate is proportional to the actual packing density of the fish, defined as the number of fish per unit volume of water. Acoustic backscatter of fish from a number of schools comprising different species were collected off Perth, in 2005 and 2007, using a Reson Seabat 8125 and 7125 respectively. Nearest neighbour distances of between 1 and 3 body lengths were observed and packing density of acoustic targets showed distinct variation between some species. However, schools of the same species also displayed different acoustic packing densities at different stages of their growth and development. Such differences were more difficult to observe in schools of fewer fish because the variations in packing density had less impact on the overall volume of the smaller schools associated with fewer fish. Therefore discrimination between species was only deemed possible when surveying two species of different sized fish at the same time. Video ground truth data is recommended to confirm species composition whatever the type of school observed.

INTRODUCTION

Multi-beam sonar (MBS) systems have been traditionally used to acquire bathymetric data for mapping purposes. As such, they were developed to produce a swath of wide angle perpendicular to the vessel track (typically upwards of 120°), narrow angle in the alongtrack direction (typically in the order of 0.5-1.5°), and to store only the data from depths near to the seafloor. The MBS beam geometry results in sampling of a very wide, but thin slice of the water column (Figure 1), providing fine-scale information of the seafloor.

Over the last twenty or so years MBS systems have been increasingly employed to map mid-water schools of fish in deeper and deeper waters [1-7]. The capability of MBS to ensonify an entire aggregation or school in a single pass saves considerable time and money, and improves reliability of data by reducing the possible movement of the school [8-10]. These aggregations can be visualised in three dimensions (Figure 1, red and yellow objects, representing schools of two different fish species) and the volume (or area) occupied by the fish can be compared if successive transects are conducted (Figure 2). However, the considerable increase in the amount of data to be stored from the seafloor only to include that for the entire water column, required data processing speeds which have only been achievable with recent advances in data processing and storage techniques. The time taken for the sonar to process the water-column backscatter is one of the limiting factors for the maximum ping rate a system can provide. If the pings are

too far apart then the system may not detect in-water targets that are present between two consecutive pings (Figure 1) [7-10]. Recent MBS systems have improved such that even in waters of >100 m depth a ping rate may be achieved which can significantly reduce the unsampled space between pings [11].
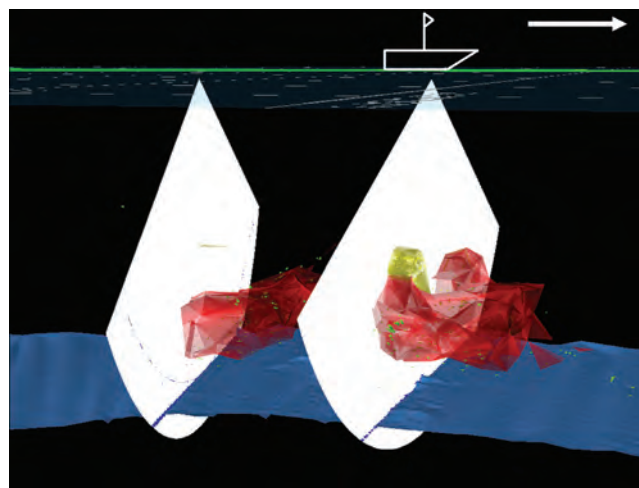

Figure 1. A visualisation of multi-beam sonar 'pings' 7 and 36 (white wedges) from an acoustic transect (green line) over a sandy seafloor (blue surface) and two schools of fish (represented by the yellow and red objects), conducted with a Reson 8125. Note that if consecutive pings are far apart then a target sitting between them may not be ensonified and therefore not detected
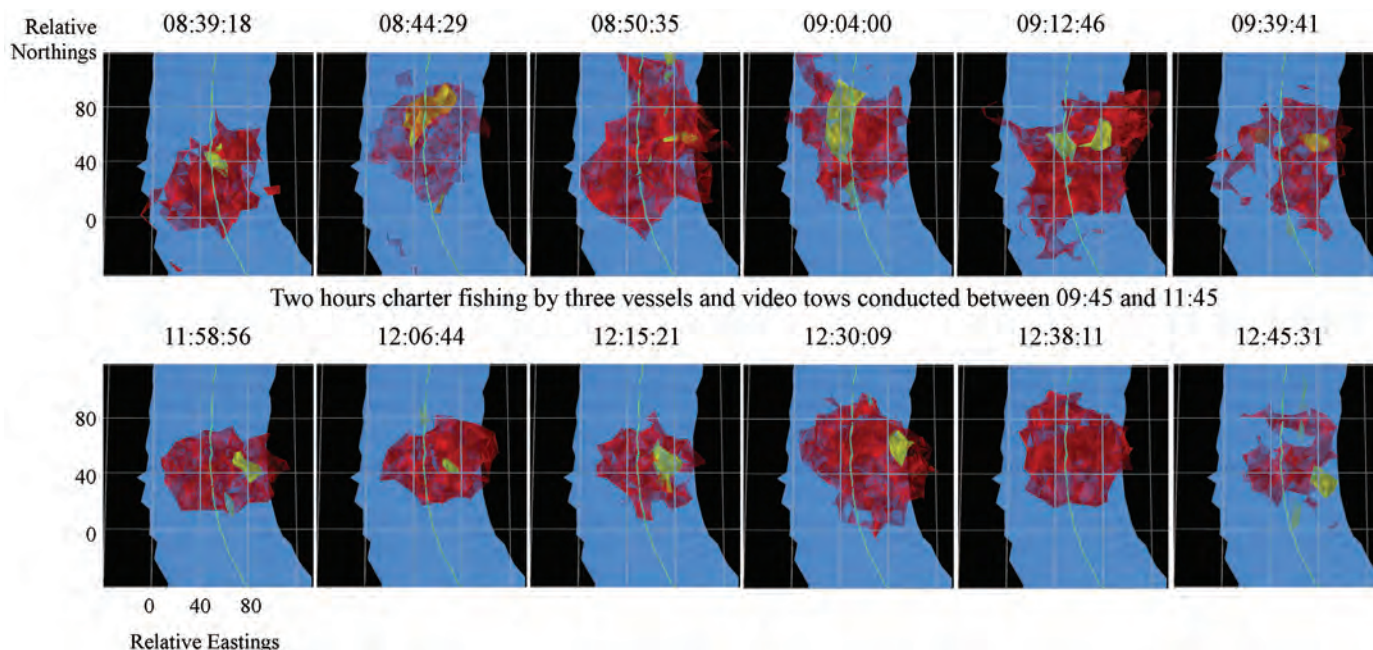
Figure 2. Plan views of two sets of six transects over a school of *S. hippos* (red object) and *P. dentex* (yellow object) above the seafloor (blue surface), separated by two hours of fishing and video tows

As acoustic targets are detected across the MBS swath the variation in angle of incidence between sonar and target is considerably greater than that within a single- or split-beam sonar. Combined with the anisotropic nature of acoustic reflectance by a swimbladder this means the relationship between fish length and target strength is considerably more complex than that used for echo-integration and species discrimination in typical echosounder surveys [12,13]. Therefore alternative methods of discriminating between species and estimating abundance are being investigated [10].

This study acquired backscatter from 6 different schools of fish (5 different species) in waters off Western Australia to look at the acoustic packing density detected by Reson 8125 and 7125 multi-beam sonar systems. The species ensonified in this study were as follows:

1. Samsonfish (*Seriola hippos*) - a pelagic member of the Carangidae family endemic to Australia, Norfolk Island and New Zealand [14]. The species is distributed around the temperate waters of Australia in depths up to 100 m [15]. As a strong, pelagic fish the species has become renowned as a catch and release sports fish and length distributions from a recent study revealed a range of 55 to 160 cm fork length with a median of 107 cm during 2004/5 and 2005/6 summer seasons, off the Perth coast [16].

2. Skipjack trevally (*Pseudocaranx dentex*) - The skipjack trevally are widely distributed around warm temperate waters. It is a streamlined, fast-swimming, schooling Carangid species that grows to a maximum length of 94 cm. Adults tend to occur in large schools near the sea floor in coastal waters in depths of up to 120 m with pelagic schools formed by batch spawners which aggregate in summer [15, 17].

3. Bight redfish (*Centroberyx Gerrardi*) - This species mainly inhabit deep waters along the edge of the continental shelf and can live to at least 64 years and 66 cm [9]. Inshore migration has been reported in *C. gerrardi* around the Cape Naturaliste region to form spawning aggregations numbering in the thousands between February and April [9].

4. West Australian dhufish (*Glaucosoma hebraicum*) - Endemic to coastal waters of western and south western Australia *G. hebraicum* is a slow growing, sedentary, demersal species inhabiting reefs and caves to depths of 200 m, with the maximum reported *G. hebraicum* being 1.22 m long (total length) and weighing approximately 26 kg [9, 18-20]. Although 100 by 10 m deep "ghost patches" of thousands of *G. hebraicum* have been historically reported in the Capes region of Western Australia, the species is now typically found in groups of three and, to a lesser extent, up to ten [9]. Occasionally groups numbering in the tens of G. hebraicum have been observed along the West Coast Bio-region.

5. Unidentified baitfish - While video evidence could not identify the species of the fish these fish were estimated to be approximately 10 cm in length.

METHODS

Multi-beam sonar surveys of numerous schools of fish were conducted aboard *RV Naturaliste*, a 21.6 m Fisheries vessel, in October 2005 and February 2007. The 2005 survey employed a RESON Seabat 8125 (operating at 455 kHz) and the 2007 survey a RESON Seabat 7125 (400 kHz). Each system was mounted on the port side of the vessel, 2.77 m below the water surface and 3.95 m from the vessel centreline. During surveys the vessel speed was kept to between 4 and 5 knots. The maximum operating rates were approximately 4.5 s between pings for the

2005 survey and 1.2 s for the 2007 survey, translating to horizontal inter-ping distances of 5.4 to 7.2 m and 2.3 to 2.9 m in 2005 and 2007, respectively. Accounting for the fore-aft beam angles, but excluding the effects of pitch and yaw, at 80 m depth the distances between the edges of the acoustic swaths of two consecutive pings was 4.1 to 5.9 m in the 2005 survey and 0.8 to 1.3 m for the 2007 survey. Individual acoustic samples represented an along-beam sample depth of 10 cm and a width that varied with range, e.g. ~60cm at 70 m range. Comparison of acoustic packing densities of fish targets required standardising the number of pings in a given along-track distance. This is particularly important if the distance between pings is such that the likelihood of missing targets between pings is high. The number of detected targets in the 8125 study was therefore artificially increased by the ratio in inter-ping distance between the two surveys (2.53 times) to be comparable with the number of targets detected in the 7125 survey.

Ships positions were recorded using a Furuno Differential GPS system. Octopus F180 and Applanix POSMV motion sensors supplied pitch, roll and yaw data, which were logged in PDS2000 software together with sound velocity profile (SVP) data (Seabird). Towed underwater video transects were conducted before and after acoustic surveys to verify site species presence and confirm school structure. Settings of each system can be found in [10].

Noise was evident in each survey and was removed as per Parsons et al. [21], using Echoview v4.1. In each survey acoustic targets were detected using the "multi-beam target detection", using height, width and length dimensions of more than 0.02 m (i.e. the size of an individual sample). After school detection algorithms had been applied each ping was visually scrutinised to identify any remaining noise samples which were manually identified. In many cases individual fish reflected backscatter in a number of acoustic samples [21], which made up an acoustic target. The locations of these targets within the swath were exported from Echoview and into Matlab, along with the GPS and motion sensor data. Here roll and heading adjustments were made to each swath and the target positions

geo-referenced in Cartesian coordinates accordingly. Each acoustic target was linked to its three nearest neighbours to form a tetrahedron. These tetrahedrons were linked together to form an object which reflected the overall volume of the aggregation of fish. To standardise the method of determining which targets were considered part of the school and maximum linking distance was applied to exclude fish not considered part of the aggregation, based on how far they were from their nearest neighbours. Various threshold distances were applied (1 m intervals) until 85% of all detected targets were included in the object. The volume of the object was then calculated in Matlab to represent the volume of the aggregation.

RESULTS

During the February 2007 surveys, numerous small schools of fish were observed, however, only one aggregation of *G. hebraicum* and one of *C. gerrardi* were encountered where video tows could ground truth species composition. At a suspected *G. hebraicum* spawning site in Geographe Bay a school numbering in the tens of *G. hebraicum* was observed on towed video. The video GPS stamp confirmed the location of the tight *G. hebraicum* school in an area of high coverage of seagrass and small limestone lumps, with five larger *G. hebraicum* separated to the north and a school of baitfish to its southwest (Figure 3). A MBS acoustic transect was conducted five minutes after the video tow and acoustic backscatter suggested two schools of fish, one at each of the locations identified by the video tow. Data from the two acoustically derived groups revealed differences in aggregation features that suggested *G. hebraicum*, sparsely populating an area to the north west of a seabed lump, and a school of baitfish hovering above the seabed lump. Target counting and aggregation volume calculation of the *G. hebraicum* revealed 129 acoustic targets encompassed by a volume of 2,381 m³ based on a threshold 9 m nearest neighbour linking distance. This produced an estimate of 18.5 m³ per acoustic target
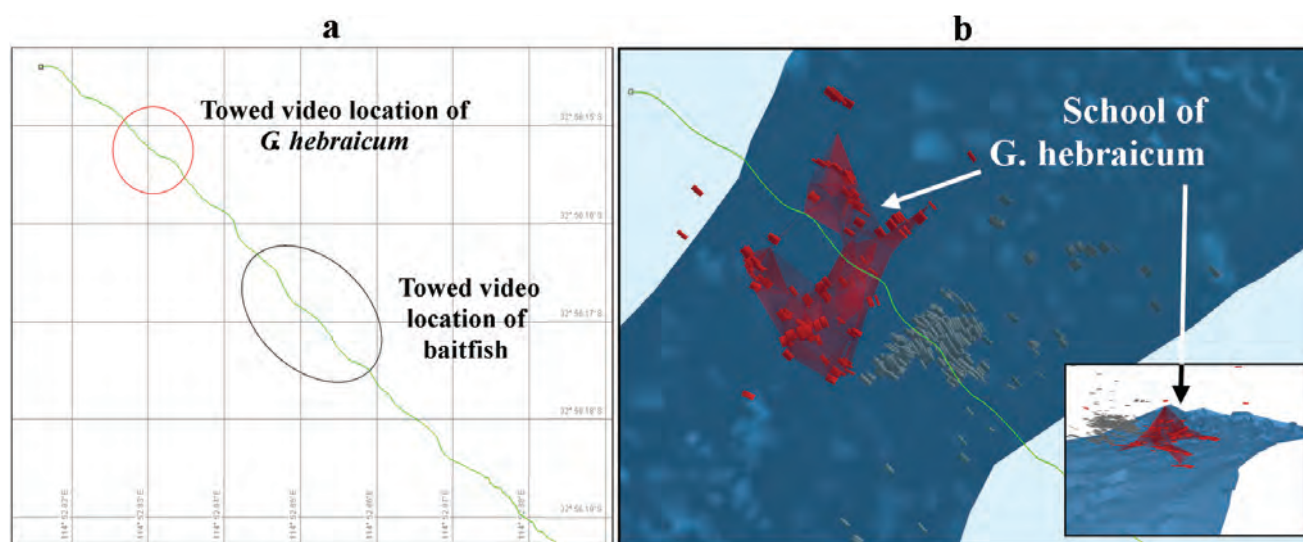

Figure 3. Map outlining locations of *G. hebraicum* and baitfish confirmed by towed video (a). Plan and aerial view (inset) of 3-D visualisation of targets in the areas where *G. hebraicum* (red) and baitfish (grey) were detected on camera (b)
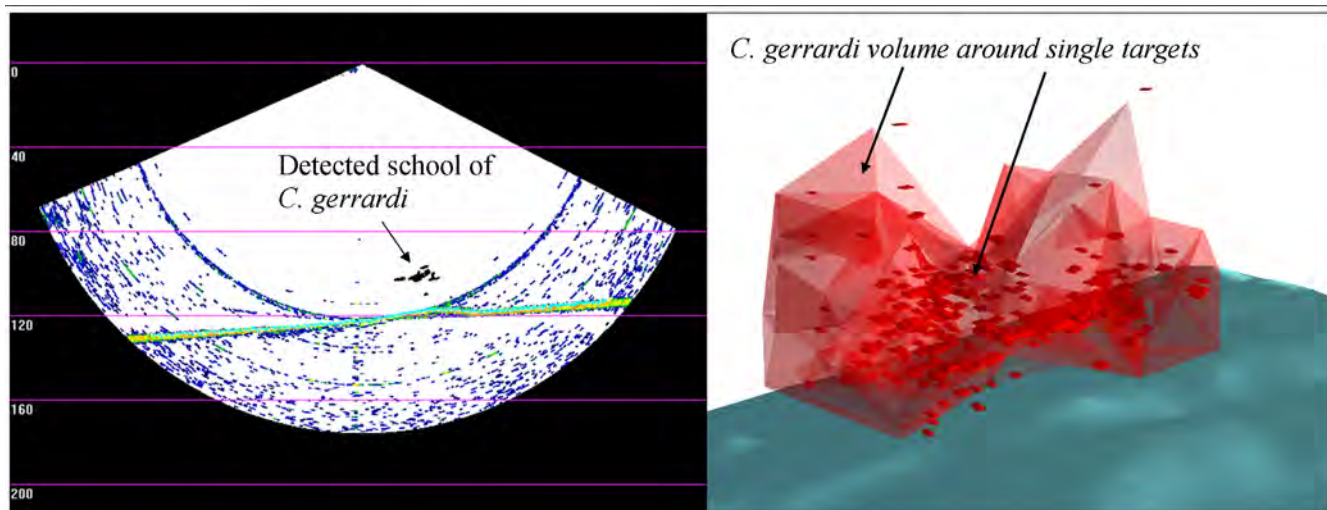
Figure 4. Acoustic multi-beam swath of a predominantly *C. gerrardi* school (left) and 3-D visualisation (right)

(mean nearest neighbour distance based on body length was not calculated due to lack of biological sampling and therefore no accurate known mean length). Video data displayed tens of *G. hebraicum* (a minimum of 18), and while it was certain that not all fish were observed by the towed video, this was far less than the number of acoustic targets detected. The school of small fish numbered 237 acoustic targets in 1,529 m³ (9 m nearest neighbour linking distance) at 6.5 m³ per target (body lengths unknown).

The surveys of *C. gerrardi* at sites close to Cape Naturaliste recommended by local fishermen revealed several small multi-species aggregations which included *C. gerrardi*. This survey highlighted the need to ground truth using video data, since the aggregations were initially thought to predominantly comprise *C. gerrardi* based on line fished biological sampling. By contrast, video evidence displayed not only *C. gerrardi*, but individuals from at least two other, similar sized species. An example of a RESON 7125 acoustic swath over a speculated *C. gerrardi* aggregation acquired in February, 2007 and the subsequent 3-D visualisation are shown in Figure 4. The detected targets displayed visible school structure and backscatter differences from aggregations of *S. hippos* surveyed with the same system and settings. Target counting and aggregation volume revealed 262 individual acoustic targets in a volume of 10,739 m³ based on a threshold 9 m nearest neighbour linking distance (41 m³ per target). At the centre of the aggregation *C. gerrardi* acoustic targets were more closely linked than those of *S. hippos* and comprised fewer individual samples with each target.

Adjusted acoustic target density for dense areas of *P. dentex* from the 8125 survey produced an acoustic packing density of 1.3 ±0.4m³ per target with least squares regression correlation of $R^2 = 0.87$ (Figure 5). By comparison the sparse area of *S. hippos* produced 23.8 ±5.1 m³ ($R^2 = 0.91$) and 13.9 ±4.1 m³ ($R^2 = 0.97$) for the October Reson 8125 and February Reson 7125 surveys respectively. These acoustic target densities equated to approximately 3 (*P. dentex*), 2 (*S. hippos*, 8125 survey) and 1.6 (*S. hippos*, 7125 survey) body lengths as nearest neighbour distances.
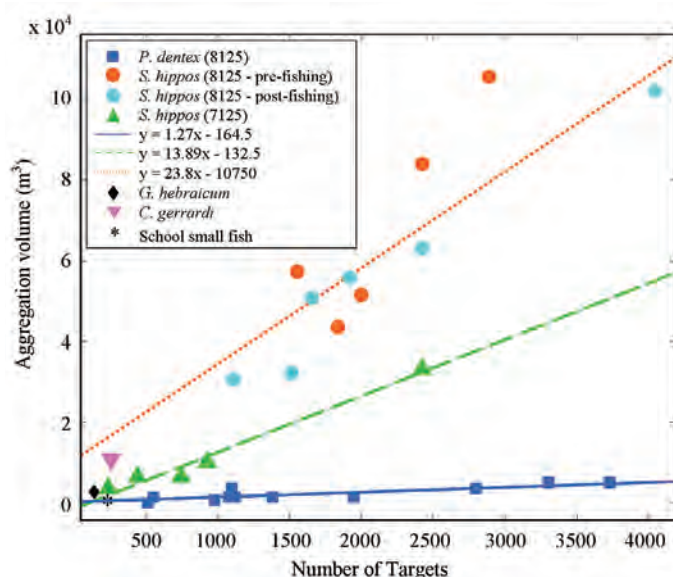
Figure 5. Detected acoustic target to aggregation volume relationships for a dense volume of *P. dentex* (■), *S. hippos* (● pre-fishing, ● post-fishing) (as detected by the RESON 8125 – not all points are shown) and *S. hippos* (▲) as detected by the RESON 7125). Calculated single transect values for *G. hebraicum* (♦), *C. gerrardi* (▼) and small fish school (*) are also shown

DISCUSSION

Though based on a small sample this study has illustrated several considerations associated with abundance estimates and discrimination of fish species via multi-beam sonar. All nearest neighbour distances of acoustic targets observed in this survey were of a similar order to nearest neighbour distances of fish in previous reports [22, 23]. Packing density is reportedly related primarily to body length and behaviour [23, 24], and to a smaller extent species [22]. Parsons [10] illustrated that it is possible to discriminate between two schools comprising fish of significantly different body lengths, surveyed at the same

time, by the packing density of acoustic targets. However, comparison of packing density of schools of the same species in different stages of their life cycle also showed significant differences (compare the 8125 and 7125 survey packing densities). This highlights the need for ground truth data in MBS surveys before species composition can be confidently determined.

Despite the difference in body size between fish such as *G. hebraicum* and *C. gerrardi*, the acoustic packing densities of small schools were similar. This suggests that there is a minimum number of fish and school size required before differences in packing density can be observed and that species discrimination via acoustic packing density will increase with school size. In the schools reported here, visual ground truthing of species was a necessity.

The discrepancy between the number of *G. hebraicum* discerned on the towed video was notable. Part of this disparity could be explained by fish hiding in habitat as the towed video passed, the narrow field of vision on a towed camera not detecting some of the school, or the difficulty in counting mobile fish using video techniques. There is also the possibility of multiple acoustic detections of the same fish, similar to that observed in *S. hippos* surveys [21] and the *P. dentex* and baitfish schools shown here. However, the fact remains that around five times as many acoustic targets were detected than fish observed on the video. These points reiterate the need for multiple transects of a school to minimise bias and the necessity to understand avoidance behaviour of each species. The need to accurately normalise for sampling effort in acoustic and video techniques is as important as it is in traditional methods, such as catch per unit effort. It also suggests that target counting is currently most useful for large fish with large nearest neighbour distances.

The shortening and elongation of an aggregation's volume in successive transects, combined with decrease and increase of acoustic targets (i.e. a change in volume and targets numbers, but a constant packing density) may be indicative of avoidance behaviour and that the larger volumes and target numbers are due to fish swimming along with the direction of the survey vessel [21]. The towed video data on *G. hebraicum*, compared with the number of acoustic targets detected in that school adds credence to the argument. This suggests that when estimating abundance via multi-beam sonar detected target counting and/or school volumes multiple transects are required and the lower target numbers and/or smaller volumes are more representative of the number of fish that are present. The comparison of acoustic packing densities between the original Reson 8125 survey [25] and that described here, highlights the need to ensure that the number of targets missed between acoustic pings is minimised.

It is the authors' opinion that while acoustic packing density, as detected by MBS, may identify two different schools of different sized fish, the smaller the number of fish, the less chance of correctly discriminating species. The maximum available ping rate must be sufficient to limit the number of missed targets and the effects of avoidance behaviour must be accounted for. In multiple transects of the same school, where across track avoidance is not observed, it is the transect which detects the least number of targets that is most likely to be an accurate representation of the number of fish present.

REFERENCES

[1] P. Freon, F. Gerlotto and M.O. Misund, "Consequences of fish behaviour for stock assessment", *ICES Journal of Marine Science* **196**, 181-191 (1993)

[2] M.V. Trevorrow, "Volumetric multi-beam sonar measurements of fish, zooplankton and turbulence", *Proceedings of the 1st International Conference on Underwater Acoustic Technologies: Measurements and Results*, Heraklion, Crete, 28 June–1 July 2005

[3] M. Wilson, I.R. Higginbottom and B. Buelens, "Four-dimensional visualisation and analysis of water column data from multi-beam echosounders and scanning sonars using Sonardata Echoview for fisheries applications", *Proceedings of the 1st International Conference on Underwater Acoustic Measurements: Technologies and Results*, Heraklion, Crete, 28 June–1 July 2005

[4] L. Nøttestad, M. Aksland, A. Beltestad, A. Fernö, A. Johannessen and O.A. Misund, "Schooling dynamics of norwegian spring spawning herring (Clupea harengus L.) in a coastal spawning area", *Sarsia* **80**(4) 277-284 (1996)

[5] L. Mayer, Y. Lic and G. Melvin, "3D visualization for pelagic fisheries research and assessment", *ICES Journal of Marine Science* **59**(1), 216-225 (2002)

[6] F. Gerlotto, J. Castillo, A. Saaverdra, M.A. Barbieri, M. Espejo and P. Cotel, "Three dimensional structure and avoidance behaviour of anchovy and common sardine schools in central southern Chile", *ICES Journal of Marine Science* **61**(7), 1120-1126 (2004)

[7] B. Buelens, M. Wilson and J.K. Horne, "Multi-beam water column data analysis for fisheries research: a worked example in Echoview", *Proceedings of the 2nd International Conference on Underwater Acoustic Measurements: Results and Technologies*, Heraklion, Crete, pp. 669-677, June 2007

[8] M. Soria, P. Freon and F. Gerlotto, "Analysis of vessel influence on spatial behaviour of fish schools using a multi-beam sonar and consequences for biomass estimates by echo-sounder", *ICES Journal of Marine Science* **53**(2), 453-458 (1996)

[9] M.C. Mackie, R. McCauley, H. Gill, H. and D. Gaughan, *Management and monitoring of fish spawning aggregations within the west coast bio-region of Western Australia*, Final report to Fisheries Research and Development Corporation on Project No. 2004/051. Fisheries Research Report No. 187 Department of Fisheries, Western Australia, 2009

[10] M.J.G. Parsons, "Active acoustic techniques for monitoring fish aggregations", In *An investigation into active and passive acoustic techniques to study aggregating fish species*, PhD Thesis, Curtin University, Australia, 2010, pp. 44-131

[11] C. Malzone, D. Lockhart, T. Meurling and M. Baldwin, "The progression and impact of the latest generation of multi-beam acoustics upon multidisciplinary hydrographic-based applications", *International Journal of the Society of Underwater Technology* **27**(4), 151-60 (2008)

[12] J.E. Simmonds and D.M. MacLennan, *Fisheries Acoustics, Theory and Practice*, 2nd edition, Blackwell Science, Oxford, 2005, pp. 437

[13] D.L. Burwen, P.A. Nealson, S.J. Fleischman, T.J. Mulligan and J.K. Horne, "The complexity of narrowband echo envelopes as a function of fish side-aspect angle", *ICES Journal of Marine Science* **64**, 1066–1074 (2007)

[14] J.R. Paxton, "Fish otoliths: do sizes correlate with taxonomic group, habitat and/or luminescence?", *Philosophical Transactions of the Royal Society of London* **355**, 1299-1303 (2000)

[15] B. Hutchins, *Sea fishes of southern Australia*, 2nd edition, Swainston Publishing and Gary Allen Pty Ltd, 1999

[16] A. Rowland, *The biology and ecology of Samson fish (Seriola hippos), with emphasis on the sport fishery targeting deep water spawning aggregations west of Rottnest Island*, PhD Thesis, Murdoch University, Australia, 2010

[17] R.H. Kuiter, *Guide to sea fishes of Australia*, New Holland Publishers, Australia, 1996

[18] P.J. Kailola, M.J. Williams, R.C. Stewart, R.E. Reichelt, A. McNee and C. Grieve, *Australian Fisheries Resources*, Department of Primary Industries and Energy, Bureau of Resource Sciences, Fisheries Research and Development Corporation, Australia, 1993

[19] R.J. McKay, *Pearl perches of the world (Family Glaucosomatidae)*, FAO species catalogue **17**, Rome, 1997

[20] J. St John and C.J. Syers, "Mortality of the demersal West Australian dhufish, Glaucosoma hebraicum (Richardson 1845) following catch and release: The influence of capture depth, venting and hook type", *Fisheries Research* **76**, 106-116 (2005)

[21] M.J.G. Parsons, I.M. Parnum and R.D. McCauley, "Visualising Samsonfish (Seriola hippos) with a Reson 7125 Seabat multi-beam sonar", *ICES Journal of Marine Science* (2013)

[22] A. Mogilner, L. Edelstein-Keshet, L, Bent and A. Spiros, "Mutual interactions, potentials, and individual distance in a social aggregation", *Mathematical Biology* **47**, 353-389 (2003)

[23] O.A. Misund, "Dynamics of moving masses: variability in packing density, shape, and size among herring, sprat, and saithe schools", *ICES Journal of Marine Science* **50**, 145-160 (1993)

[24] N. Niwa, "Power-law scaling in dimension-to-biomass relationship of fish schools", *Journal of Theoretical Biology* **235**, 419-430 (2005)

[25] M.J.G. Parsons, R.D. McCauley and M.C. Mackie, "Evaluation of acoustic backscatter data collected from Samson Fish (Seriola hippos) spawning aggregations in Western Australia", *Proceedings of the Eighth European Conference on Underwater Acoustics*, Caroeiro, Portugal, 2006, pp. 347-352

Inter-Noise 2014

MELBOURNE AUSTRALIA 16-19 NOVEMBER 2014

The Australian Acoustical Society will be hosting Inter-Noise 2014 in Melbourne, from 16-19 November 2014. The congress venue is the Melbourne Convention and Exhibition Centre which is superbly located on the banks of the Yarra River, just a short stroll from the central business district. Papers will cover all aspects of noise control, with additional workshops and an extensive equipment exhibition to support the technical program. The congress theme is *Improving the world through noise control*.

Key Dates
The dates for Inter-Noise 2014 are:
Abstract submission deadline: 10 May 2014
Paper submission deadline: 25 July 2014
Early Bird Registration by: 25 July 2014

Registration Fees
The registration fees have been set as:

Delegate	$840	$720 (early bird)
Student	$320	$255 (early bird)
Accompanying person	$140	

The registration fee will cover entrance to the opening and closing ceremonies, distinguished lectures, all technical sessions and the exhibition, as well as a book of abstracts and a CD containing the full papers.

The Congress organisers have included a light lunch as well as morning and afternoon tea or coffee as part of the registration fee. These refreshments will be provided in the vicinity of the technical exhibition which will be held in the Main Foyer.

The Congress Banquet is not included in the registration fee.

Technical Program
After the welcome and opening ceremony on Sunday 16 November, the following three days will involve up to 12 parallel sessions covering all fields of noise control. Major areas will include Community and Environmental Noise, Building Acoustics, Transport Noise and Vibration, Human Response to Noise, Effects of Low Frequencies and Underwater Noise.

A series of distinguished lectures will cover topics such as:
- Acoustic virtual sources
- Wind turbine noise
- Active noise control
- Aircraft noise
- Soundscapes

Organising and Technical Committee
- Congress President: Dr Norm Broner
- Technical Program Chair: Adjunct Professor Charles Don
- Technical Program Co-Chair: Adjunct Professor John Davy
- Technical Program Advisor: Mrs Marion Burgess
- Proceedings Editor: Mr Terry McMinn
- Sponsorship and Exhibition Manager: Dr Norm Broner
- Congress Treasurer: Ms Dianne Williams
- Social Program Chair: Mr Geoff Barnes
- Congress Secretariat: Ms Liz Dowsett

Further details are available on the congress website
www.internoise2014.org

UNDERWATER PASSIVE ACOUSTIC MONITORING & NOISE IMPACTS ON MARINE FAUNA—A WORKSHOP REPORT

Christine Erbe

Centre for Marine Science and Technology, Curtin University, GPO Box U1987, Perth 6845, Western Australia
Christine.erbe@curtin.edu.au

The marine ecosystem is being increasingly subjected to underwater noise from industrial operations. Our ability to monitor the marine soundscape using passive acoustic technology is important to determine the potential impacts of anthropogenic sound. The objectives of this workshop were to define our current capabilities with regard to passive acoustic monitoring (PAM); to define our current state of knowledge of the marine soundscape, and of underwater noise in particular, and of noise impacts; to identify the needs and concerns of the various stakeholders; and to determine future research and development needs. The workshop was held in Fremantle, Western Australia, on 21 November 2012, the day before the Australian Acoustical Society's annual conference. Three tutorial sessions were presented by leading researchers in the field on underwater acoustic terminology, metrics, the basics of sound propagation, noise modelling and prediction, the marine soundscape (physical ambient, anthropogenic and biological sources), sound recording technology and methods, noise impacts on marine fauna, mitigation and environmental management. Tutorials were followed by rapid-fire presentations of current research associated with the themes of passive acoustic monitoring and noise impact. Discussions pursued on the presented topics, with emphasis on stakeholder needs, prevailing problems, knowledge gaps, potential solutions and future initiatives. The workshop was attended by over 70 participants from within Australia and abroad, hosting a diverse range of expertise and representing the various stakeholders in the marine environment: the offshore oil and gas industry, consulting industry, fishing industry, defence, government (environmental officers, regulators, fisheries officers), environmental groups and academia. The outcomes of the workshop were:
- An appreciation of PAM for monitoring of marine fauna, for ecological studies, for measurements of anthropogenic noise, for studying noise impacts and for mitigation monitoring;
- A demonstration of the effectiveness of PAM for presence and abundance monitoring (with more acoustic detections than visual in certain circumstances);
- An understanding of the limitations of PAM (to vocalising animals) and the potential of combining PAM with visual observations and possibly active acoustic imaging to increase detection probability;
- An appreciation of the differences between regulatory approaches in different jurisdictions;
- The identification of the need to monitor (and address noise impacts on) entire ecosystems including less iconic (=non-mammalian) species;
- The identification of knowledge gaps with regards to unidentified sounds in marine soundscapes, natural variability in soundscapes with space and time necessitating long-term baseline recording, noise impacts on the vast majority of marine species, anthropogenic source signatures and sound transmission.

INTRODUCTION

The potential impacts of anthropogenic underwater noise (e.g. from seismic surveys, pile driving, dredging and defence operations) on marine fauna have grown in concern over the past few decades. An understanding of underwater sound emissions, sound propagation and bioacoustic impacts is necessary for sustainable development of marine resources. Passive acoustic monitoring of the marine soundscape, of anthropogenic operations and of—vocal—marine fauna is a non-invasive tool of rapidly growing application in bioacoustic

environmental impact assessments (EIA). There are no standards, however, neither domestically within Australia, nor internationally, relating to the measurement, data analysis, and data reporting for such EIAs. As a result, the quality of many environmental impact assessments is poor, the results are not reliable, data are not comparable, errors (which are hardly ever assessed or reported) are huge, outcomes (e.g. impact zones, imposed mitigation requirements) are arbitrary and costs are as random as the lottery. The problem is particularly topical in Western Australia due to the amount of offshore development.

The annual conferences of the Australian Acoustical Society

always attract a large number of underwater acousticians from within Australia and abroad. When Perth was announced as the site of the 2012 conference, the Centre for Marine Science and Technology (CMST) at Curtin University seized the opportunity to organise an underwater noise workshop in conjunction with the conference, as many experts would already be coming to Perth.

In addition to underwater acoustic researchers, various stakeholders in the marine environment were invited. Expecting differing backgrounds in acoustics, the workshop commenced with tutorial sessions on underwater acoustics, marine soundscapes and noise impacts. These were followed by contributed rapid-fire presentations and whole-audience discussions. It was hoped that by establishing an understanding of the fundamentals of underwater acoustics, participants could gain more insight from current research presented in the rapid-fire sessions. The aim was to create a more equal platform for all stakeholders to discuss outcomes, research needs and recommendations. Marine bioacoustics is a multi-disciplinary field in terms of both research and application, and the strength of this workshop came from the participation of a diverse group of stakeholders, including researchers, industry representatives, defence representatives, environmental officers, consultants and regulators. The workshop was organised into two themes: passive acoustic monitoring and underwater noise impacts on marine fauna.

UNDERWATER PASSIVE ACOUSTIC MONITORING

The morning session began with two tutorials: 1) an introduction to underwater acoustics presented by Alec Duncan of Curtin University, and 2) an overview of the marine soundscape presented by Rob McCauley of Curtin University.

Tutorials

Sound is a small periodic (in time) perturbation of density and pressure from their hydrostatic means. Water particles move back and forth; the perturbation travels, but the water particles don't (instead they oscillate). Water is 1000 times as dense as air; the speed of sound in water is three times that in air; sound travels much better (over longer ranges) under water than in air. Sound levels are given in decibel (dB), which is a ratio, not a unit. The reference pressure (or intensity) must be listed, which is 1 µPa in air and 20 µPa underwater. Continuous sound is best described in terms of root-mean-squared pressure *SPLrms*. Impulsive sound is best described in terms of sound exposure level *SEL* and/or peak pressure level *SPLpk*.

Transmission loss is the ratio of received pressure (or intensity) to source pressure (or intensity), and is usually given in dB as well. It's largely due to the spreading of sound over a larger and larger area as the sound propagates away from its source, and due to absorption (conversion of acoustic energy to heat due to vibration of water molecules). Geometrical formulae accounting for spherical and cylindrical spreading are commonly used to estimate transmission loss, but are hardly ever applicable. Sound can be ducted into a surface channel

when the speed of sound increases with depth. Sound can be ducted into the deep-ocean sound channel and traverse entire ocean basins. More sophisticated and environment-specific sound propagation models are available[1] and should be used, yet require significant expertise for correct implementation and application. Specifically, Australia's limestone seabeds are a challenge for sound propagation modelling [1].

Humans' air-filled ears hear poorly underwater, creating the misconception of a "quiet ocean". The ocean is indeed naturally noisy with contributions from wind, rain, ice, and—of course—animals (both vocalisations and activities such as breaching). The marine soundscape is very site-specific, not just because of different sources, but also because of different sound transmission regimes. Sites along the edge of the continental shelf usually have significant contributions (at frequencies < 100 Hz) from the deep ocean (e.g. wind and distant shipping). These sounds do not travel into shallow water and are not picked up on the continental shelf.

Biological and physical sea noise is believed to play a critical role in the life functions of marine animals. The ocean is naturally noisy and provides acoustic environmental cues to marine fauna. Fish choruses vary with season and moon phase [2]. Whale calls and song change over the years. The number of calling animals can sometimes be determined by counting overlapping calls. Migration routes of great whales can be pieced together from CMST noise logger data spanning 20 years and > 80 locations along the southern and western Australian coasts.

Ship noise is a continuous and chronic source, with a small number of very noisy ships contributing the majority of noise energy. Seismic surveying contributes significantly in certain areas and sound transmission environments. Airgun sound travels poorly in shallow water over limestone seafloors; yet surveys along the continental slope off southern WA were recorded at 2000 km range across the entire Great Australian Bight on noise loggers on the opposite continental slope. The same noise loggers also recorded colliding and calving icebergs in Antarctica 3000 km away.

Noise artefacts are often seen in EIA reports yet were not identified as such. Sources for artefacts are: hydrophone movement through the water, turbulent flow, cable strum, electronic noise, mooring noise, waves splashing against the deployment boat etc. Also, underwater moorings attract animals, and the sound recorded is no longer typical of the location in the absence of the mooring, e.g. crustaceans settle, fish move in, animals scratch and chew on the hydrophone and cables. Removing artefacts is particularly important when computing source levels of anthropogenic operations from levels received at some range; a common mistake is the inclusion and hence amplification of ambient noise, which should have been removed from the recording.

Rapid-fire presentations

Following the tutorials were rapid-fire presentations by participants, covering PAM applications from both research and industry. A common commendation of PAM from

---

[1] see e.g. http://cmst.curtin.edu.au/products/actoolbox.cfm

ecologists was its ability to open up monitoring regions that are otherwise remote and difficult or expensive to survey. Tracey Rogers of the University of New South Wales presented results from visual surveys and PAM of leopard seals (*Hydrurga leptonyx*) in Antarctica. Visual surveys were biased towards females mostly occupying the sea ice and missed males mostly occupying the water, where they could only be detected by PAM. Furthermore, as PAM allowed differentiating juveniles from adults by their differing vocalisations, it was discovered that sparsely distributed adults occupied prime habitat, forcing juveniles into densely-populated areas [3]. Contrary to common belief, high-quality habitat is not necessarily heavily occupied, hence density is not always a predictor for prime habitat, and the importance of protecting sparsely-populated habitat is likely underestimated in EIAs.

The use of PAM as a viable tool for long-term monitoring in remote locations was further stressed by Craig McPherson of JASCO Applied Sciences, who presented a multi-year acoustic monitoring program in the Arctic. Baseline ambient conditions, industrial sounds and the spatio-temporal distribution of marine mammals were monitored in open-water summers as well as under-ice in winters.

Given the vast amount of PAM data collected these days, automatic tools are needed for efficiency, reliability, comparability and objectivity. While a plethora of tools from pattern recognition or voice recognition research is available, these have mostly been applied to specific cases, e.g. the detection of a limited number of calls of one or more species in a specific type of noise [4]. A higher-level characterisation into all sounds biological versus anthropogenic versus physical ambient is quite a challenge, and is currently being tackled by Shyam Madhusudhana of Curtin University. Such a characterisation would allow the computation of noise budgets, i.e. the contribution of underwater acoustic energy by source type, without having to identify the specific sources of sound. It could be used on large spatio-temporal scales to aid in quantifying the contribution of sound from marine industrial operators to the underwater soundscape, in determining trends over time and in characterising geographical variability.

Andrew Parker of SLR Consulting presented a case study of PAM in conjunction with visual surveying for mitigation monitoring during port construction. PAM proved to be a useful tool for the environmental assessment process. A good correlation was seen between PAM and visual data for great whales.

In conclusion, the PAM rapid-fire presentations applauded PAM as a highly useful tool to add to the suite of ecological research methods. Its applicability to short-term, real-time mitigation monitoring as well as long-term, large-scale monitoring was demonstrated.

Discussion

An open-audience discussion followed the rapid-fire presentations. In this discussion, the importance of sound to marine organisms, the usefulness of bioacoustics as an ecological research tool, and the diverse applicability of PAM as a research and monitoring tool were repeated. Additional case studies were mentioned, e.g. the passive acoustic detection of false killer whales (*Pseudorca crassidens*) predating on fish caught in fishing gear.

Monitoring the presence of marine animals with visual observers alone is limited to good light and weather conditions and to animals that spend a significant amount of time near the surface. Binoculars only offer a limited field of view (of a few degrees), and many observers are needed for full-circle monitoring. Passive acoustics works in poor visibility (at night time, high sea state or fog), can detect vocalising animals from all directions over much longer ranges and often in higher numbers than visual observation alone [6].

It is comparatively easy to determine relative abundance of cetaceans from PAM data, yet much more difficult to derive absolute abundance or triangulate the location and distance of specific cetaceans. Along migration routes, animals can potentially be counted quite successfully as any one animal only passes by once. In areas where animals mill, abundance estimation is much more difficult.

PAM, however, is not the golden bullet. PAM is often used as a complementary tool alongside other methods. It has more value in some circumstances (environments, species) than in others. Not all species vocalise, and only a subset of a population vocalises. Calling behaviour depends on age, gender, health and context (e.g. other non-acoustic behaviour). Small cetaceans often travel in large groups, and the chances of at least some of them vocalising at any one time and hence the group being detected are high. Large whales often travel in smaller groups and the chances of PAM detection are much lower. Finally, calls change over time, and tools developed based on specific calls may not work in future.

Alternative methods, such as active acoustic (sonar) detection were discussed and can be useful for non-vocal species or in noisy environments where animal calls might be masked.

PAM is not only a tool for monitoring marine fauna, but also for monitoring anthropogenic development and marine soundscapes in general. A common step in the EIA process is the modelling and prediction of noise footprints of specific anthropogenic operations. At a later stage, model results can be validated in the field using passive acoustic techniques, in order to verify predictions of the EIA and in order to improve models.

Australia's neighbouring countries (Indonesia, Papua New Guinea and Singapore) are archipelagic nations. Indonesia is the largest archipelago on Earth with over 17,000 islands. These marine labyrinths are often characterised by the lack of a continental shelf (e.g., East Indonesia, PNG, SI), yet they are not open ocean either. These "deep-sea yet near-shore" habitats are often highly bio-diverse. The corresponding soundscapes are expected to be complex yet have hardly been studied at all. Both sound shielding and noise ducting likely play a significant role. These specific marine soundscape characteristics may have ramifications for effective management of anthropogenic underwater noise. One workshop participant voiced concern about sounds from seismic surveys in deep inter-island passages "driving" or "acoustically flushing out" marine life as the intense sound reverberates through such passages. This question is especially relevant for Indo-Pacific migration

corridors and other critical habitats for oceanic cetaceans and other marine life.

The value of long-term data sets on marine soundscapes was stressed several times. This data is useful to biologists and ecologists studying marine fauna. It is useful to oceanographers for the study of ambient noise, geographic variability and trends in time. It is useful to environmental scientists for studying human impacts. This data provides a record of the marine soundscape with future uses potentially not yet identified. For example, as the sources of currently unidentified sounds become known (e.g. if whale calls are identified through combined visual and acoustic surveys), we can go back in time picking these calls in old recordings in order to determine this species' whereabouts, migration and abundance.

The Australian Integrated Marine Observation System (IMOS) includes autonomous underwater acoustic recorders deployed and maintained by CMST, Curtin University, in four locations: off Sydney (New South Wales), off Portland (Victoria), off Perth (Western Australia) and off Scott Reef (Western Australia). Data from as early as 2008 is available online for free at http://www.imos.org.au/. A graphical user interface allows the display of sound spectrograms and the listening to sounds online. Sections can be selected for immediate download. Alternatively, entire recordings can be requested through the University of Tasmania. The more people use this free data set and tool, the more funding will likely be made available for the continuation of the IMOS program.

The benefits of data sharing were highlighted. CMST has collected soundscape data around Australia for over 20 years, on behalf of the offshore oil and gas industry, defence and government. The respective clients own individual data sets. Data sharing would allow a synthesis of soundscape data to determine geographical commonalities, trends over time, noise budgets, migration routes of great whales, habitat usage patterns etc. Under the oil and gas industry's Collaborative Environmental Research Initiative (CERI) some of this data is being shared for very specific syntheses such as migration patterns.

Future needs

During the presentations and discussion, a number of points were raised that should be addressed in the near future.

- The deployment of more PAM buoys was urged; ideally through public initiatives such as IMOS.
- The deployment of localisation arrays or time-synchronised autonomous recorders that can be used for localisation and tracking was encouraged—again ideally through programs like IMOS.
- The sharing of the data between stakeholders (academia, industry, government and public) was encouraged.
- The publication of raw data was desired.
- The timely publication of results was urged.
- Standards or guidelines for noise measurement, analysis and reporting are needed.
- Standards or guidelines for the usage of PAM in mitigation monitoring would be helpful (e.g. what a priori info on species present, calling behaviour and context is needed and where to find it; equipment and deployment guidelines; operational protocols).

IMPACTS OF UNDERWATER NOISE

The afternoon session began with a tutorial on bioacoustic impacts by Christine Erbe.

Tutorial

Similar types of impact have been described for marine mammals and fish. At long ranges, a sound source might merely be audible. With decreasing range, noise can cause a behavioural response, masking of communication or environmental cues, temporary hearing loss and potentially injury.

Behavioural and auditory evoked potential (AEP) audiograms have only been measured for few individuals of about 20 marine mammal species. There are no audiograms for polar bears under water, sea otters, sperm whales or baleen whales. In the absence of direct measurements, anatomical evidence for hearing sensitivity can be derived from structural properties of the ear [7,8].

Behavioural responses can sometimes be seen at very long ranges approaching the limit of audibility. Measurement indicators include changes in swim speed and direction, dive and surfacing duration and interval, respiration rate, and changes in contextual and acoustic behaviour. Behavioural responses can depend on prior exposure (habituation versus sensitisation), age, gender, health and current behavioural state. Case studies of behavioural responses were presented, including controlled exposure experiments of humpback whales (*Megaptera novaeangliae*) to a 2700 cui seismic array, undertaken by the Centre for Whale Research and Rob McCauley in 1996. Localised avoidance at 3 km range, without large-scale migratory changes were seen; cow-calf pairs were more responsive (at received levels of 129 dB re 1 μPa^{2}s) than males, who approached the air gun in 9 out of 16 trials [9]. The multi-year Behavioural Response of Australian Humpback whales to Seismic Surveys (BRAHSS) experiment exposed humpbacks to a single airgun and ramped-up signals in 2010 and 2011; data analysis is ongoing; the experiment will continue in 2013 and 2014 leading up to a full commercial array [10].

Noise can mask communication, echolocation and the sounds of predators, prey and the environment. Masking depends on the spectral and temporal characteristics of signal and noise. Masking is more complex than a mere energy comparison within frequency bands. Directional hearing, frequency and time discrimination capabilities, co-modulation masking release, and anti-masking strategies (increasing call level, frequency shifting, building in redundancy) help reduce the masking effect [11,12].

Noise exposure can cause hearing loss [13]. Klaus Lucke measured the onset of a Temporary Threshold Shift (TTS) in harbour porpoises (*Phocoena phocoena*) at a SEL of 164 dB re 1 μPa^{2}s and at a peak-to-peak sound pressure level (*SPLpkpk*) of 200 dB re 1 μPa [14]. Behavioural responses were documented at *SEL* = 145 dB re 1 μPa^{2}s and *SPLpkpk* = 174 dB re 1 μPa. This data (plus a "buffer" of a few dB) became Germany's official regulation thresholds for porpoises: *SEL* < 160 dB re 1 μPa^{2}s, *SPLpkpk* < 190 dB re 1 μPa. Mitigation methods (e.g. bubble curtains) have to be used around pile driving to keep levels low and animals out of this risk zone.

Jane Fewtrell and Rob McCauley exposed caged fish, turtles and squid to a 20 cui airgun in 1996. Fish swam faster, in tighter circles and deeper as the airgun approached. Hair cells in the inner ear were damaged at a cumulative *SEL* of 187 dB re 1 μPa^2s, and recovered over the duration of > 1 month [15]. In 2007, caged tropical fish exposed to a 2055 cui array at 45 m range showed no pathological damage, and only mild and insignificant TTS. Free fish dropped to the seafloor, and more fish were seen on echosounders > 500 m from the seismic transect. Zooplankton also showed signs of dispersing near the transect.

Noise—in certain circumstances—can also affect the vestibular system, reproductive system, nervous system and other tissues and organs. Stress is a physiological response to a stressor aimed at surviving the immediate threat, yet can cause health problems if it becomes chronic.

The biological significance of acoustic impacts is still poorly understood. What levels and impacts can threaten the survival of a population? Stressors can be additive and cumulative, with noise impacts "adding" to other impacts (chemical pollution, food depletion etc.).

Rapid-fire presentations

Bethan Parnum of Environmental Resources Management began the session with an overview of the environmental impact assessment process, which involves the following steps: baseline monitoring of the marine soundscape (PAM) and animal surveys, literature and database searches for anthropogenic source signatures, sound propagation modelling, literature searches for noise impacts on species present, comparison of modelled received levels to known impact (threshold) levels, and finally the design of situation-specific mitigation and management measures.

Roberto Racca of JASCO Applied Sciences presented a multi-year monitoring and mitigation project to protect grey whales (*Eschrichtius robustus*) from impacts of seismic surveys off Sakhalin Island. Individual whales were tracked visually; received levels were estimated via pre-season modelling and *in-situ* real-time measurements; shut-downs were imposed if whales within the near-shore feeding zone received *SEL* > 156 dB re 1 μPa^2s per pulse. Whale behaviour was variable. One animal travelling somewhat parallel to the seismic transect received increasing *SEL*/pulse and deflected as the received *SEL*/pulse reached 150 dB re 1 μPa^2s. Another whale paralleled the seismic transect further offshore outside of the feeding zone at received levels of up to 163 dB re 1 μPa^2s without deflecting. Received level alone is not a successful indicator for behaviour; rather, multiple variables such as behavioural state, environmental conditions, prey availability and demographic parameters must be included [16].

Chandra Salgado-Kent of Curtin University presented results of the BRAHSS experiment based on visual observations from the source vessel during control, ramp-up and active airgun trials. She showed that different groups of animals responded differently, with mother-calf pairs keeping a distance from the source, yet males occasionally approaching. Whether this puts them at higher risk for bioacoustic impact needs to be investigated. She highlighted the need for solid

statistical and spatial models to support data analysis.

Klaus Lucke of IMARES presented data from visual and acoustic observations of harbour porpoises around pile driving showing avoidance within 20 km range and increased detections at 25 – 50 km range. The effect was the stronger, the longer the pile driving duration.

Justin McDonald of Western Australian Fisheries and Marine Research Laboratories showed the "opposite" response: crustaceans, molluscs and ascidians were attracted to low-frequency noise and settled on ship hulls (biofouling). In a controlled experiment, *Ciona intestinalis* had a greater survival rate, faster settlement rate, and a faster rate of metamorphosis when exposed to vessel noise. As raised during the discussion, apart from noise, hydrodynamic flow might also affect settlement, as some whales have barnacles at different locations on their heads and bodies.

In contrast, Geoff McPherson of James Cook University showed how sound could intentionally be used to modify the behaviour of marine mammals around fishing gear. A specific case of mammal depredation around oceanic longline gear was presented. Passive acoustic sonar reflectors and active acoustic depredation mitigation pingers were shown to significantly mitigate depredation in Indo-Pacific longline fisheries by acoustically interfering with the terminal stages of depredation behaviour. Long-range acoustic detection of depredation behaviour is an option to modify fishing behaviour to minimise the need to expose mammals to behaviour modification techniques. Geoff argued that it was worth making short-range modifications to toothed whale behaviour to prevent mortality associated with fishing gear.

In conclusion, there was a great diversity in results presented, such as the ability of underwater sound to affect animal behaviour both negatively (source avoidance) and positively (biofouling settlement), both unintentionally (byproduct of acoustic surveying) and intentionally (active deterrence). Sound clearly has the potential to influence the ecology of marine organisms to various degrees.

Discussion

There was some discussion of metrics for impact assessment. We use decibels instead of linear units in order to handle the large dynamic range of sound levels underwater. Different types of impact relate to different quantities. For impulsive sound, the duration of the sound or the duty cycle seem to matter, which is why quantities such as *SEL* and cumulative *SEL* are useful. Also, peak pressure, pressure change and rise time have been related to impacts of impulsive sound, specifically effects other than auditory. Mammalian ears respond to intensity; other species' ears respond to pressure. Vibration of the seafloor is potentially critical for benthic organisms; CMST in collaboration with the University of Tasmania is currently investigating the impacts of seismics on benthic scallops and lobsters.

As sound propagates away from its source, the quantities that "matter" change. Close to an airgun, peak pressure might be critical, however, at longer ranges, pulses spread out, peak pressure drops and intensity and *SEL* become more critical. In addition, it is difficult to assign acoustic source signatures even

within one source type. For example, in the case of blasting, and specifically home-made bombs used by fishermen in Asia, the source signatures vary from case to case.

Dynamite fishing also happens in Australia with blast sounds recorded by CMST off Scott Reef and with two arrests of Indonesian fishing vessels illegally carrying dynamite in 2012. Blast effects in marine animals seem to correlate inversely with body mass; while sea turtles seem somewhat resistant to blast trauma. Multiple blasts in tight succession are worse than single blasts, with impact inversely correlated to the interblast interval.

This brought up a discussion of whether "one number" for a specific source and a specific species is "good enough" as a do-not-exceed threshold to adequately protect this species. Considering an airgun, the acoustic characteristics vastly differ close to the source compared to far from the source. Different quantities matter at different ranges. Also, would x dB from a single airgun have the same impact as x dB from an airgun array? What other factors and contexts need to be examined? This moved the discussion towards regulation.

Germany has regulations only for impulsive noise from pile driving. At 750 m from the source, SEL must be < 160 dB re 1 $\mu Pa^2 s$ and $SPLpkpk$ must be < 190 dB re 1 μPa. Mitigation methods such as bubble curtains must be employed to keep below these levels. In the Netherlands, pile driving is prohibited during the first six months of the year to protect fish larvae, and permitted without mitigation during the second six months of the year. Across the EU, impulsive noise and continuous noise are being monitored throughout the year to determine baselines and achievable thresholds [17], which will be set in the near future—likely individually by country.

In Australia, NOPSEMA came into existence on 1.1.2012 as the federal regulator for the offshore oil and gas industry operating in Commonwealth waters, handling all approvals for petroleum activities. NOPSEMA want to avoid having "one number" for all circumstances, and want to avoid that developers simply work towards "one number". Rather, developers are encouraged to engage with the research community to determine the best approach for local protection of the specific marine environment—under the ALARP (as low as reasonably practicable) principle. Proponents have to determine reasonable thresholds for the various operations and animal populations and demonstrate how they are going to meet these goals. The success of this process hinges on scientists publishing their results, and greatly benefits from the sharing of data and research outcomes.

Greater availability and accessibility of information on noise and impacts was repeatedly requested during the presentations and discussions. Workshops, such as this, were commended as they brought together multi-disciplinary scientists and stakeholders, and communicated results as well as knowledge gaps to a broad audience of people with different application requirements.

Future needs
- Science transfer: Results of research studies must be published and presented in order to guarantee uptake by industry and regulators and in order to guarantee best possible management of the marine environment.

- Environmental management would greatly benefit from the sharing of data.
- Underwater noise is an integral part of the soundscape and should be considered in fishery and environmental management plans as a factor (and potential pollutant) of water quality.
- Most of our knowledge relates to iconic (mammalian) species. With indications of anthropogenic impact on coral, crustacean and fish larvae and adults, it is clear that we must investigate impacts on all animals within an ecosystem, of which the better-studied, charismatic megafauna are only a small part.
- We know very little to nothing about noise impacts on most species and need to expand the database on basic hearing and hearing impacts, and non-auditory impacts.
- There is a place for experiments with captive animals and these should be supported; however, the translation of results from captive animals to wild animals has to be done with care, specifically if the experiments relate to behaviour.
- There should potentially be more 'real world' studies carried out in which the behaviour of animals and potential impacts on animals are studied in conjunction with a real activity such as a seismic survey. This would remove the significant issues of translating the results of 'artificial' studies using caged animals or an unrepresentative source into the 'real world'.
- We need to test a large number of individuals of a population in order to get statistically significant results and in order to assess variability within a population. E.g., young animals are often more susceptible than older animals, yet male adult humpback whales potentially expose themselves to higher sound levels.
- Individual impacts are likely not biologically significant; population effects are what we need to understand.

ACKNOWLEDGEMENTS

REFERENCES

[1] A.J. Duncan and A. Gavrilov, "Low-frequency acoustic propagation over calcarenite seabeds with thin, hard caps", *Proceedings of Acoustics 2012 Fremantle*, Western Australia, 21-23 November 2012

[2] R.D. McCauley, "Fish choruses from the Kimberley, seasonal and lunar links as determined by long term sea noise monitoring", *Proceedings of Acoustics 2012 Fremantle, Western Australia*, 21-23 November 2012

[3] T. Rogers, M. Ciaglia, H. Klinck and C. Southwell, "Can singing be used to predict critical habitats? ", *Proceedings of Acoustics 2012 Fremantle*, Western Australia, 21-23 November 2012

[4] C. Erbe and A.R. King, "Automatic detection of marine mammals using information entropy", *Journal of the Acoustical Society of America* **124**(5), 2833-2840 (2008)

[5] J. Barlow and B.L. Taylor, "Estimates of sperm whale abundance in the northeastern temperate Pacific from a combined acoustic and visual survey", *Marine Mammal Science* **21**(3), 429-445 (2005)

[6] S. Rankin, T.F. Norris, M.A. Smultea, C. Oedekoven, A.M. Zoidis, E. Silva and J. Rivers, "A visual sighting and acoustic detections of Minke whales, Balaenoptera acutoroshata (Cetacea: Balaenopteridae), in nearshore Hawaiian waters", *Pacific Science* **61**(3), 395-398 (2007)

[7] A. Tubelli, A.L. Zosuls, D. Ketten, M. Yamato and D. Mountain, "A prediction of the minke whale (Balaenoptera acutorostrata) middle-ear transfer function", *Journal of the Acoustic Society of America* **132**(5), 3263-3272 (2012)

[8] D.R. Ketten, "Cetacean Ears", in: W.L. Au, R.R. Fay, A.N. Popper (Eds.), *Hearing by whales and dolphins (SHAR Series for Auditory Research)*, Springer-Verlag, New York, 2000, pp. 43-108

[9] R.D. McCauley, J. Fewtrell, A.J. Duncan, C. Jenner, M.-N. Jenner, J.D. Penrose, R.I. T. Prince, A. Adhitya, J. Murdoch and K. McCabe, "Marine seismic surveys: a study of environmental implications", *Australian Petroleum Production Exploration Association (APPEA) Journal* **40**, 692-708 (2000)

[10] D.H. Cato, M.J. Noad, R.A. Dunlop, R.D. McCauley, N.J. Gales, C.P. Salgado-Kent, H. Kniest, D. Paton, C. Jenner, J. Noad, A.L. Maggi, I.M. Parnum and A.J. Duncan, "Project BRAHSS: Behavioural response of Australian humpback whales to seismic surveys", *Proceedings of Acoustics 2012 Fremantle*, Western Australia, 21-23 November 2012

[11] C. Erbe, "Critical ratios of beluga whales (Delphinapterus leucas) and masked signal duration", *Journal of the Acoustical Society of America* **124**(4), 2216-2223 (2008)

[12] C. Erbe and D.M. Farmer, "Masked hearing thresholds of a beluga whale (*Delphinapterus leucas*) in icebreaker noise", *Deep-Sea Research Part II* **45**(7), 1373-1388 (1998)

[13] D. Ketten, Marine mammal auditory system noise impacts: Evidence and incidence," in: A.N. Popper, A.D. Hawkins (Eds.), *The Effects of Noise on Aquatic Life. Advances in Experimental Medicine and Biology 730*, Springer Verlag, New York, 2012, pp. 207-212

[14] K. Lucke, U. Siebert, P.A. Lepper and M.-A. Blanchet, "Temporary shift in masked hearing thresholds in a harbor porpoise (*Phocoena phocoena*) after exposure to seismic airgun stimuli", *Journal of the Acoustical Society of America* **125**(6), 4060-4070 (2009)

[15] R.D. McCauley, J. Fewtrell and A.N. Popper, "High intensity anthropogenic sound damages fish ears", *Journal of the Acoustical Society of America* **113**, 638-642 (2003)

[16] R. Racca, A. Rutenko, K. Broker and G. Gailey, "Model based sound level estimation and in-field adjustment for real-time mitigation of behavioural impacts from a seismic survey and post-event evaluation of sound exposure for individual whales", *Proceedings of Acoustics 2012 Fremantle*, Western Australia, 21-23 November 2012

[17] M.L. Tasker, M. Amundin, M. Andre, A.D. Hawkins, W. Lang, T. Merck, A. Scholik-Schlomer, J. Teilman, F. Thomsen, S. Werner and M. Zakharia, *Marine Strategy Framework Directive: Task Group 11 Report: Underwater noise and other forms of energy*, JRC Scientific and Technical Report No. EUR 24341 EN - 2010, European Commission and International Council for the Exploration of the Sea, Luxembourg, 2010

Why You Hear What You Hear

An Experiential Approach to Sound, Music, and Psychoacoustics

Eric J. Heller

Eric Heller titled his book *Why You Hear What You Hear: An Experiential Approach to Sound, Music, and Psychoacoustics* because he hopes the reader will learn from doing. Much of these three areas of acoustics can be experienced via the ears or can be shown in animations, and these can often make topics accessible to students without much maths or physics background. Consequently, the book frequently directs readers to its extensive supporting website, http://www.whyyouhearwhatyouhear.com. That site contains suggestions on using a variety of readily available software for sound analysis and synthesis and for creating wave-behaviour animations. It also links to many other animations and sound media on the Web. For several decades now, books on acoustics have been supplemented with sound recordings and the use of the Web is an important next step.

Heller's topic order is somewhat unusual and, for that reason, *Why You Hear What You Hear* tells you "how to use this book": Because of the extensive cross-referencing, readers are encouraged to abandon the traditional linear approach and to navigate to chapters—and also the website—according to interest and need.

The book grew from a course called The Physics of Music and Sound that Heller taught at Harvard, first as a core curriculum course in physics, and later as a general education course. For non-physics majors taking music or any of the many other courses that involve sound, this book is a fresh alternative to some other possible texts. It's also deeper than most. However, for that audience, depth might not always be an advantage.

The first 15 of the book's 28 chapters develop the science of acoustics in logical but often novel ways. They're followed by five chapters on musical instruments and the voice; six on psychoacoustics, with an emphasis on pitch perception and consonance; one on room acoustics; and another on outdoor sound. For some humanities students, the book's equations and some serious physics discussion may trigger an allergic reaction. However, derivations for equations relating to topics such as the exponential horn or Sabine's reverberation are often sequestered in coloured boxes, an organisation that indicates to readers with a distaste for this side of physics that they can get by without those sections.

Why You Hear What You Hear also has much to interest physicists and physics students. As with many other excellent acousticians, Heller's primary specialty is not acoustics—his other research areas include chemical physics, surface waves, and quantum scattering. In general, a good physicist can bring novel insights to a new field as well as understanding of the standard approach. This book contains a lot of physical insight, and I think it will be the rare acoustician who does not enjoy reading it. I particularly liked the use of colour coding to introduce (with a minimum of maths) a graphical algorithm to represent autocorrelation. Also interesting are the author's diversions into history, including a story in which John William Strutt and William Henry Bragg seem to have been mistaken about an echo transposed in pitch.

I enjoy and applaud the book's experiential approach, although the experimentalist in me would like to have seen more suggestions for experiments that go beyond the computer keyboard. Also, I should declare a bias. Instead of writing a book, I publish educational acoustics material extensively on the Web, precisely because it's so easy to include sound files and other resources.

The successful integration of the book and its associated website invites the question: Why not an entirely electronic or web-based package? One answer is that some discussions are long and have beautiful, still graphics; those work well in a book chapter. Another reason may be the business model: A pay wall would be unpopular on the Web, but in this case the hard copy book could possibly subsidise an extensive website. Heller's experiment deserves to work.

The author specifically addresses musicians in the introduction. Many will read the book: Musicians are often passionate enough to undertake deep study of things related to their art and have usually accepted that excellence requires a significant investment of effort. I think, though, that quite a few sales will also be to people from the other end of the music-physics spectrum: Acousticians will enjoy its interesting perspectives, and physicists and engineers outside of acoustics will find it an attractive introduction to some important parts of the discipline.

Joe Wolfe
The University of New South Wales

Joe Wolfe does research on the voice and musical instruments. He has won awards for research and education. He is the author of the Web-based acoustics resources, Physclips (http://www.animations.physics.unsw.edu.au) and Music Acoustics (http://www.phys.unsw.edu.au/music). This review first appeared in *Physics Today*.

NEWS

Standards Australia

There are some actions within Standards Australia relating to acoustics standards. One project in process is an update to a part of AS/NZS 1269.4 which relates to audiometric testing facilities. Another, for which the project was submitted by the Australian Acoustical Society, is for the direct text adoption of the ISO standard which deals with measurement and assessment of hand arm vibration in the workplace plus the adoption, in accordance with the ISO amendment, of an amendment to the AS for whole body vibration.

A number of acousticians participated in a seminar held at Standards Australia on 25 February 2013 to discuss the proposal put forward by the Federal Department of Infrastructure and Transport for a revision of the AS 2021 on aircraft noise. The Department is seeking that a revision of the standard be undertaken to update some of the technical information in the tables and also to include means for describing aircraft noise other than only the ANEF. There was some heated discussion in this forum especially from the representatives of the organisations involved with planning and development. The next step would be for the Department to apply again to Standards Australia in the next round of submissions for projects to undertaken.

At the AAS conference in Perth in November 2012, the workshop on Standards identified some standards which desperately needed to be revised/updated. One of these was the AS/NZS 2107 which lists the design sound levels for areas of occupancy in buildings. It is intended that a submission for a project to revise AS/NZS 2107 will be prepared in time for consideration in the next round at Standards Australia. If any members can summarise key changes that they consider need to be made in AS/NZS 2107, can they please send these to Norbert Gabriels [norbert@gabriels.net.au] who is the chair of the relevant committee and Marion Burgess [m.burgess@adfa.edu.au] by 25 May 2013. These comments would be used to define the scope of the revision of the standard.

Noise – A human history

BBC Radio 4 has launched a 30-part series entitled *Noise – A human history* which explores how our interactions with sound have shaped us over 100,000 years. Recorded on location around the world and featuring treasures from the British Library's Sound Archive, it takes us from prehistory to the present, encompassing the shamanistic music of our cave-dwelling ancestors, the babel of ancient Rome, the massacre of noisy cats in pre-revolutionary Paris, the nerve-destroying din of trench warfare, right through to the cacophony of the modern metropolis. All episodes are available for listening at http://www.bbc.co.uk/programmes/b01rglcy/episodes/guide

GRANTS & AWARDS

AAS Research Grants

A special committee of the AAS Federal Council was formed at the last AAS Conference in Fremantle to look at research grants. The committee members are Matthew Stead (Chair, SA), Luke Zoontjens (WA), Matt Terlich (QLD), Neil Gross (NSW), Geoff Barnes (VIC), Norm Broner (President), Peter Heinze (Past President) and Tracy Gowen (AA and NSW). One outcome from the committee is a survey to seek YOUR input on the proposal for research grants and to identify priority areas for research that the AAS may partly fund.

The survey can be accessed at: http://www.surveymonkey.com/s/9DNB6M6 and will be open to the end of April. It is proposed that funding would need to be at least equally matched from other sources as identified in any application. Additional information and selection criteria for applications will be released after the survey results are analysed. For additional questions please email the AAS General Secretary Richard Booker or contact Matthew Stead at matthew.stead@resonateacoustics.com

NSW Division Travel Award

The New South Wales Division of the Australian Acoustical Society is offering up to three (3) awards to research students and one (1) award to an early career researcher (ECR) in acoustics, to attend the Acoustics 2013 conference at Victor Harbor, South Australia, 17-20 November 2013. The amount of each award is $1000 and is to be spent towards the conference registration fee, travel to and from the conference venue, and accommodation.

The award is open to all research students who are AAS student members of NSW Division as well as research students endorsed by AAS members of the NSW Division. The award is open to all ECRs in acoustics who are AAS members of the NSW Division. If not already a member, the ECR applicant must apply to become a member of the Australian Acoustical Society before submitting his/her application. The closing date for the applications is Thursday 9th May 2013. For more information and the application form go to http://www.acoustics.asn.au/joomla/notices.html

NEW PRODUCTS

GPS Synchronisation for the SoundBook

Want to know where you are? SAVTek offers a specially modified Garmin GPS unit to connect into the SoundBook. The GPS device records your longitude and latitude in SAMURAI during measurements in the field. When data is exported to Excel, the time synced GPS data includes longitude, latitude, angle of travel, ground speed, height above sea level and geoid separation. When using two or more SoundBook MK2s, the GPS devices can be used to synchronise the time clocks to within 200ns of each other. For further information contact Darryl Watkins, SAVTek, tel: (07) 3300 0363, dwatkins@savtek.com.au or visit www.savtek.com.au

DIVISIONAL NEWS

NSW Division

On 7th March, Matthew Stead, the director of Resonate Acoustics, gave a technical talk titled *Is infrasound from wind turbines significant?*. His talk outlined the findings of a recent report commissioned by the SA Environment Protection Authority (EPA) and jointly authored by Resonate Acoustics, titled *Infrasound levels near windfarms and in other environments*. The report found that the level of infrasound from wind turbines is insignificant and no different to any other source of noise. It also found that the worst contributors to household infrasound are air-conditioners, traffic and noise generated by people.

WA Division

The Western Australian Division held a technical meeting on the 21st of February to allow members to table ideas for Research Grants funded by the AAS. The meeting began with a presentation by division president Luke Zoontjens, who discussed funding models that could be considered by the AAS, and the purpose of the grants. Around twenty ideas for research grants were tabled by the WA members, covering many aspects of acoustics. Discussion was kept to the premise of the following statement, "*The Australian Acoustical Society aims to promote and advance the science and practice of acoustics in all its branches to the wider community and provide support to acousticians*". The WA division will shortly formalise the ideas discussed at the meeting for consideration by the Federal Council.

SA Division

The South Australian division has kicked-off 2013 with two technical talks, both followed by informal dinners at local hotels. On 26 February, Tom Evans of Resonate Acoustics presented a topical talk entitled *Infrasound Levels near Wind Farms and in Other Environments*, outlining the findings of a recent study undertaken by the South Australian Environment Protection Authority (EPA) in conjunction with Resonate Acoustics.

Tom, who has seven years of experience in the assessment of noise and vibration on a wide range of projects, was one of the study authors.

On 26 March, Darren Jurevicius, Director at AECOM, discussed the new Minister's Specification SA 78B: *Construction requirements for the control of external sound*. Specification SA 78B is a government initiative to provide an improved health standard for those living adjacent major transport corridors or within new mixed use zones. Darren, who has over 17 years of diverse experience on government and private sector projects across Australia, gave an overview of the specification and also provided valuable insight in to how it will work in practice. The presentation generated numerous in-depth questions regarding bedroom noise criteria, noise source spectra, entertainment premises and the minimisation of the size of sterile zones, rail noise sources/criteria and existing SA draft criteria. For example, there were some interesting discussions around the acceptability of an LAeq 9 hour average limit of 35 dB in people's bedrooms; such a metric may not adequately account for single or multiple sleep disturbing loud events such as train pass-bys.

The South Australian division is also being kept busy with preparations for Acoustics 2013 Victor Harbor *Science, Technology and Amenity*. We look forward to hosting this event in November against the backdrop of the beautiful Fleurieu Peninsula region.

QLD Division

The QLD Division has had a great start to 2013. Technical talks and a council policy workshop have provided an excellent platform for acoustic professionals to mix with policy makers. All attendees were able to share ideas and learn from each other regarding acoustic matters. It was exciting to hear debate between our senior members over Australian Standard 2021: *Acoustics-Aircraft Noise Intrusion – Building Siting and Construction* with regards to potential aircraft noise issues from an expanding Brisbane Airport. We look forward to working closely with policy makers on many more acoustic matters and we encourage all acoustic professionals to have your say in many more acoustic matters.

The first technical meeting of 2013 was held on Wednesday 27th February. A good turnout was experienced with 27 members present. The technical meeting consisted of presentations by Laurence Nicol (the 2012 recipient of the RJ Hooker Bursary) and Nick Tang (the 2012 recipient of the Acoustics Bursary). Laurence presented the results of his research into the prediction of patron noise in restaurants and dining areas, which included a novel way of modelling noise building-up in enclosed spaces. Nick outlined the acoustical defects and potential treatments associated with a large open plan office used by research personnel at the University of Queensland. Both presentations were of a high quality and provided insights

that will be beneficial to people faced with similar problems in the future.

On Tuesday 20th March the Queensland Division hosted a workshop on the proposed changes contained within the Brisbane City Council's Draft City Plan 2012. Frank Henry (Program Delivery Manager, Pollution Control, Brisbane City Council) and Alex Marchuk (Senior Program Office, Noise Policy, Brisbane City Council) presented to an interested audience of 56 people. The presentations outlined how transport, entertainment, commercial and industrial noise associated with new development will be managed in the future. The new noise criteria were explained along with how a noise impact assessment will need to be prepared in the future. A discussion forum at the conclusion of Council's presentations was convened by Russell Brown, James Heddle and Gillian Adams and enabled the attendees to ask questions and provide feedback on the proposed changes to City Plan.

FUTURE CONFERENCES

International Congress on Acoustics (ICA 2013)

The 21st International Congress on Acoustics will be held from 2-7 June 2013 at the Palais des congrès in downtown Montréal. This is a joint meeting with the American Acoustical Society and the Canadian Acoustical Society. The high standard technical program will include plenary, distinguished, invited, contributed, and poster papers covering all aspects of acoustics. There will be an extensive technical exposition highlighting the latest advances in acoustical products. The information about registration and details of the conference are available from the website. For more information visit www.ica2013montreal.org/index.html

International Symposium on Room Acoustics

The International Symposium on Room Acoustics, ISRA 2013, will be held in Toronto, Canada, from 9-11 June 2013, immediately following the ICA congress in Montreal. ISRA 2013 will be a single stream conference on acoustical issues related to performance spaces. ISRA 2013 will include presentations by 4 internationally acclaimed keynote speakers and a number of special sessions. Sessions will include both invited and contributed papers presented in either lecture or poster format. There will also be technical tours of performance spaces and an extended tutorial session. For more information visit www.ISRA2013.com

Inter-Noise 2013

Inter-Noise 2013 is the 42nd International Congress and Exposition on Noise Control

Engineering, and will be held in Innsbruck, Austria, from 15-18 September 2013. Inter-Noise 2013 will be held at the Congress Center Innsbruck. The Congress is sponsored by the International Institute of Noise Control Engineering (I-INCE), and is being organized by the Austrian Noise Abatement Association. The theme of the congress is Noise Control for Quality of Life. The early bird registration fee deadline is 15 May 2013. For more information visit www.internoise13.org

Inter-Noise 2014

With about eighteen months to go, the organisation of Inter-Noise 2014 in Melbourne is well on track. The venue will be the Melbourne Convention Centre on the banks of the Yarra River, with 12 rooms on the second floor available for the parallel technical sessions on Monday to Wednesday, while an expanded exhibition space will be located in the foyer. Morning and afternoon refreshments and a light lunch will be available in the middle of the exhibition area, permitting good interaction of delegates and exhibitors. Intending exhibitors should contact Norm Broner [NBroner@globalskm.com] about securing one of the prime display locations.

The Congress will commence on the afternoon of Sunday 16 November with a welcoming ceremony, followed by the first plenary lecture and light refreshments. We anticipate there will be four keynote lectures and two plenary talks during the Congress. Details of the speakers and their subject will be posted on our web-site, www.internoise2014.org once they are finalised. Already, over 80 people from many parts of Europe, UK, USA and Asia have agreed to chair or co-chair sessions during the Congress with, we are delighted to note, many Australian based researchers and consultants agreeing to assist. Topics include transport noise and vibration, low frequency effects on people and buildings, soundscapes in parks, wind turbine and gas-turbine noise, jet-noise and computational aero-acoustics, signal processing for active noise control, education and policy, light-weight building acoustics, low-noise tyres, virtual sources and underwater noise as well as psychoacoustics in noise evaluation and noise effects on humans, to name but a few. While this may seem comprehensive, there are many more topics still to be covered if anyone wishes to help organise a session.

We also have a banquet planned which will begin a little differently to the standard sit down banquet. We will be making various Australian animals available in the foyer of the banquet venue in the Convention Centre. Delegates will be able to pet these animals and take their own photos.

In September this year, Charles Don and John Davy will be attending Inter-Noise 2013 in Innsbruck with the purpose of explaining to the I-INCE board how the Melbourne plans are unfolding and to obtain further assistance with technical session planning and chairs. However, probably the main purpose is the opportunity to talk to delegates and exhibitors about attending

Michael John Smith

26/03/1947 – 11/01/2013

Managing Director and CEO of Vipac Engineers & Scientists Ltd

Michael J. Smith, Managing Director and CEO of Vipac Engineers & Scientists, passed away in January.

Michael graduated with a BEng(Mech) from Monash University in 1971, and was one of four young engineers who established Vipac Engineers and Scientists in Sydney in 1973. Over the next 40 years he steered it to become an engineering powerhouse, employing 280 staff in offices located throughout all Australian capital cities and in South East Asia.

Michael, a true innovator led the company, incorporating advanced technologies with sound engineering principles, and employing those in a wide range of applications; from wind, acoustics and vibration, to fluid mechanics and thermodynamics, across many industries including building and construction, defence, mining, transport and consumer appliances.

Under Michael's leadership, Vipac provided consultancy services on some of the most recognised landmark buildings around the world including the MCG, Melbourne Convert Hall, Etihad Stadium, the Academy of Performing Arts in Hong Kong, the Kuala Lumpur Convention Centre, Scotts Tower in Singapore, and the Burj Khalifa in the UAE - the world's tallest building.

When called upon to provide consultancy services in the areas of acoustics and air conditioning for Changi Airport's Terminal 2 in 1988, Michael moved his family to Singapore and set up Vipac's first office in Asia. While there Michael's family immersed themselves in local culture and his children attended local school.

Michael was presented with two EA Engineering Excellence Awards in 1999, the national engineering excellence award for research and development, and the award for innovation. Michael accepted these awards for Vipac's work on the BAMbino, a portable bearing monitor for conveyors

Michael is survived by his wife, four children and two grandchildren. Michael will be remembered by his colleagues as a caring and considerate leader, innovator, mentor, colleague, and friend, and an irrepressible force of nature.

Rob Connolly, MAAS MIOA, Vipac Engineers & Scientists, WA 6104

Inter-Noise 2014. As well as satchel inclusions, we plan to have a booth and there will be a presentation about Melbourne as part of the closing ceremony. Marion Burgess will be there to give moral support, however, we would like to know about any other AAS members intending to go to Innsbruck who are willing to "fly the flag", with perhaps an hour at the booth and especially helping at the closing activities. Please let Charles know [charlesdon@bigpond.com] and become part of the Inter-Noise 2014 team.

ICSV20, Bangkok

The 20th International Congress on Sound and Vibration (ICSV20) will be held from 7 to 11 July 2013 at Imperial Queen`s Park Hotel, Bangkok, Thailand. Theoretical and experimental research papers in the fields of acoustics, noise, sound, and vibration are invited for presentation. The ICSV20 Scientific Programme includes invited and contributed papers as well as technical exhibitions and a social program. For more information see http://www.icsv20.org

International Congress on Ultrasonics

The International Congress of Ultrasonics will be held at the Novotel Singapore Clark Quay, Singapore from 2-5 May 2013. This is the 4th in the series of International Congresses on Ultrasonics which started in 2007 in Vienna, Austria. It will be the first ICU to be held in Asia. The technical program includes both oral and poster presentations. Participation by students is encouraged. For more information see www.icu2013.com.sg

PRUAC 2013, Hangzhou

The Hangzhou Applied Acoustics Institute Research Institute (HAARI) and Zhejiang University are organising the 4th Pacific Rim Underwater Acoustics Conference in Hangzhou, China from 9-11 October 2013. PRUAC 2013 has the conference theme of "Underwater Acoustics and Ocean Dynamics". Every conference attendee will have the opportunity to participate in productive discussions on this specific theme. For more information see http://pruac.zju.edu.cn/index.htm

ISMA 2014, Leuven, Belgium

The 26th International Noise and Vibration Engineering Conference, ISMA2014, will be held in Leuven (Belgium) from 15 to 17 September 2014. It will be organised in conjunction with the 5th edition of the International Conference on Uncertainty in Structural Dynamics - USD2014. Both conferences are organised by the division PMA of the KU Leuven. ISMA2014 follows the biennial international conferences on noise and vibration engineering, structural dynamics and modal testing. A single registration will grant access to both the ISMA and the USD conference. Information on the conference topics, as well as on the procedure for submitting abstracts are available from http://www.isma-isaac.be. The first important dates are 1st October 2013 for the start of online abstract submission and 15th January 2014 as deadline for submission of abstracts.

DIARY

2013

2 - 5 May, Singapore
International Congress on Ultrasonics
(ICU 2013)
http://www.icu2013.com.sg/

26 – 31 May, Vancouver, Canada
IEEE International Conference on Acoustics,
Speech, and Signal Processing (ICASSP)
http://www.icassp2013.com

2 – 7 June, Montréal, Canada
21st International Congress on Acoustics
(ICA 2013)
http://www.ica2013montreal.org

9 - 11 June, Toronto, Canada
International Symposium on Room
Acoustics (ISRA 2013)
http://www.isra2013.com

7 –11 July, Bangkok, Thailand
20th International Congress on Sound
and Vibration (ICSV20)
http://www.icsv20.org

23 – 26 July, Glasgow, UK
Invertebrate Sound and Vibration (ISV
2013)
http://www.isv2013.org

26 – 28 August, Denver, USA
Noise-Con 2013
http://www.inceusa.org/nc13

27 – 30 August, Denver, USA
Wind Turbine Noise 2013
http://www.windturbinenoise2013.org

15 – 18 September, Innsbruck, Austria
Inter-Noise 2013
http://www.internoise2013.com

9 – 11 October, Hangzhou, China
4th Pacific Rim Underwater Acoustics
Conference
http://pruac.zju.edu.cn/index.htm

2014

6 –10 July, Beijing, China
21st International Congress on Sound and
Vibration (ICSV21)
http://www.iiav.org/index.
php?va=congresses

7 -12 September, Krakow, Poland
Forum Acusticum 2014
http://www.fa2014.pl/

17 – 19 November, Melbourne, Australia
Inter-Noise 2014
http://www.internoise2014.org/

2015

10 – 15 May, Metz, France
International Congress on Ultrasonics
(2015 ICU)
http://www.me.gatech.edu/2015-ICU-Metz/

2016

**5-9 September, Buenos Aires,
Argentina**
22nd International Congress on Acoustics
(ICA 2016)
http://www.ica2016.org.ar/

*Meeting dates can change so please
ensure you check the conference
website: http://www.icacommission.
org/calendar.html*

beware of imitations

SOUNDLAG
has been embossed as a
quality signature

Pyrotek Noise Control is introducing embossing to its Soundlag range. Embossing is more than clever marketing – it delivers tangible benefits to our customers:

- Embossing gives confidence that a genuine Pyrotek Noise Control product has been installed.
- During building audits, inspectors can see at a glance the specified product has been installed
- Project managers can also see instantly that the correct lagging has been installed

Embossing is a simple way to identify and distinguish Pyrotek products, giving customers confidence that their noise issues are being controlled with the actual specified product, with all the performance that was expected, from acoustic to environmental concerns.

www.pyroteknc.com

Pyrotek
noise control

SUSTAINING MEMBERS

The following are Sustaining Members of the Australian Acoustical Society.
Full contact details are available from http://www.acoustics.asn.au/sql/sustaining.php

3M AUSTRALIA

www.3m.com

ACOUSTIC RESEARCH LABORATORIES

www.acousticresearch.com.au

ACRAN

www.acran.com.au

ACU-VIB ELECTRONICS

www.acu-vib.com.au

ADAMSSON ENGINEERING

www.adamsson.com.au

AERISON PTY LTD

www.aerison.com

**ASSOCIATION OF AUSTRALIAN
ACOUSTICAL CONSULTANTS**

www.aaac.org.au

BARRISOL AUSTRALIA

www.barrisol.com.au

BORAL PLASTERBOARD

www.boral.com.au/plasterboard

BRUEL & KJAER AUSTRALIA

www.bksv.com.au

CSR BRADFORD INSULATION

www.bradfordinsulation.com.au
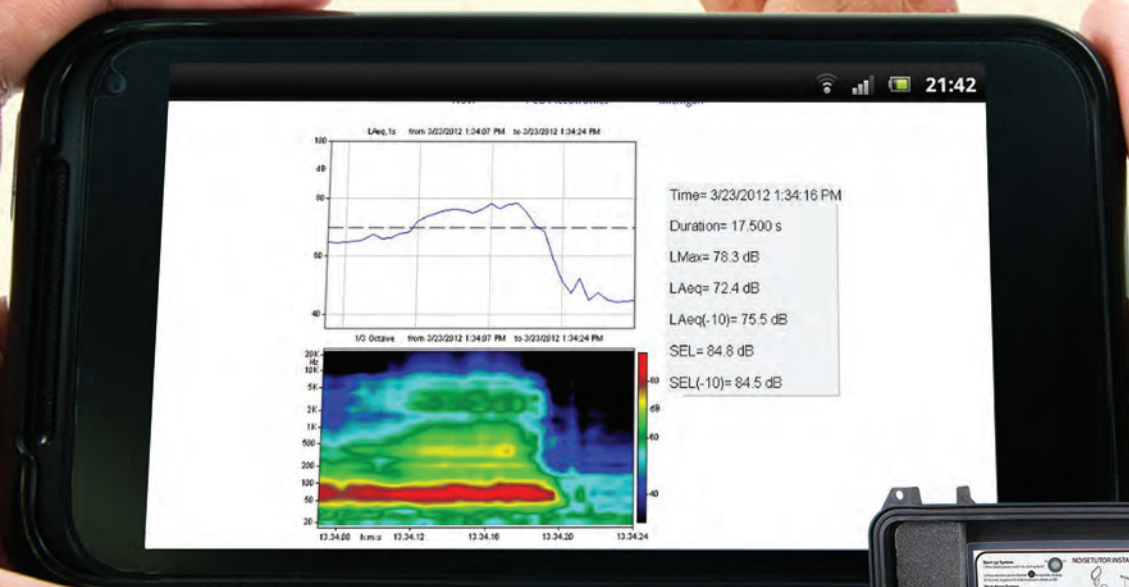
EMBELTON

www.vibrationisolation.com.au

HOWDEN AUSTRALIA

www.howden.com.au

IAC COLPRO

industrialacoustics.com/australia

**NSW DEPT OF ENVIRONMENT &
CLIMATE CHANGE**

www.environment.nsw.gov.au

PEACE ENGINEERING

www.peaceengineering.com

PYROTEK NOISE CONTROL

www.pyroteknc.com

SINCLAIR KNIGHT MERZ

www.globalskm.com

SOUND CONTROL

www.soundcontrol.com.au

SOUNDSCIENCE

www.soundscience.com.au

VIPAC ENGINEERS AND SCIENTISTS

www.vipac.com.au

AUSTRALIAN ACOUSTICAL SOCIETY ENQUIRIES

NATIONAL MATTERS

* Notification of change of address
* Payment of annual subscription
* Proceedings of annual conferences

Richard Booker - General Secretary
Australian Acoustical Society
PO Box 1843 Toowong DC QLD 4066
Tel: (07) 3122 2605
email: GeneralSecretary@acoustics.asn.au
www.acoustics.asn.au

SOCIETY SUBSCRIPTION RATES
For 2012/13 Financial Year:

Fellow and Member $130.00
Graduate, Associate and Subscriber . . $100.00
Retired $40.00
Student $30.00
Including GST

DIVISIONAL MATTERS

Enquiries regarding membership and sustaining membership should be directed to the appropriate State Division Secretary

AAS - NSW Division
Laura Allison
c/- AECOM
Level 21, 420 George Street
Sydney, NSW 2000
Tel: (02) 8934 0035
Fax: (02) 8934 0001
Laura.Allison@aecom.com

AAS - Queensland Division
PO Box 760
Spring Hill Qld 4004
Sec: Richard Devereux
Tel: (07) 3217 0055
Fax: (07) 3217 0066
rdevereux@acran.com.au

AAS - SA Division
AECOM,
Level 28, 91 King William St
ADELAIDE S.A. 5005
Sec: Darren Jurevicius
Tel: (08) 7100 6400
Fax: (08) 7100 6499
darren.jurevicius@aecom.com

AAS - Victoria Division
c/- Simon de Lisle
Arup Acoustics
Level 17, 1 Nicholson Street
Melbourne VIC 3000
Tel: (03) 9668 5580
Fax: (03) 9663 1546
simon.delisle@arup.com.au

AAS–WA Division
Unit 3
2 Hardy Street,
SOUTH PERTH 6151
Sec: Norbert Gabriels
Tel (08) 9474 5966
Fax (08) 9474 5977
gabriels@iinet.net.au

ACOUSTICS AUSTRALIA INFORMATION

GENERAL BUSINESS
Advertising Subscriptions

Mrs Leigh Wallbank
PO Box 70, OYSTER BAY 2225
Tel (02) 9528 4362
Fax (02) 9589 0547
wallbank@zipworld.com.au

ARTICLES & REPORTS NEWS, BOOK REVIEWS NEW PRODUCTS

The Editor, Acoustics Australia
c/o Nicole Kessissoglou
School of Mechanical & Manufacturing Engineering
University of New South Wales
NSW 2052 Australia
Mobile: +61 401 070 843
acousticsaustralia@acoustics.asn.au

PRINTING, ARTWORK
Cliff Lewis Printing
91-93 Parraweena Road
CARINGBAH NSW 222
Tel (02) 9525 6588   Fax (02) 9524 8712
email: matthew@clp.com.au

SUBSCRIPTION RATES

	Aust	Overseas
1 year	A$77.20	A$88.33
2 year	A$133.10	A$157.30
3 year	A$189.00	A$227.27

Australian rates include GST.
Overseas subscriptions go by airmail
Discounted for new subscriptions
20% Discount for extra copies
Agents rates are discounted.

ADVERTISING RATES

B&W	Non-members	Sus Mem
1/1 Page	$784.00	$699.15
1/2 Page	$509.40	$457.40
1/3 Page	$392.00	$352.90
1/4 Page	$326.70	$294.00

Spot colour: available
Prepared insert: $424.70 Conditions apply
Column rate: $26.40 per cm (1/3 p 5.5cm width)
All rates include GST

Discounted rates for 3 consecutive ads in advance

Special rates available for 4-colour printing

All enquiries to: Mrs Leigh Wallbank
Tel (02) 9528 4362 Fax (02) 9589 0547
wallbank@zipworld.com.au

ACOUSTICS AUSTRALIA ADVERTISER INDEX - VOL 41 No 1

Locate, quantify and rank noise sources accurately and rapidly

90	
88,5	
87	
85,5	
84	
82,5	
81	
79,5	
78	
76,5	
75	
75	
76,5	
78	
79,5	
81	
82,5	
84	
85,5	
87	
88,5	
90	
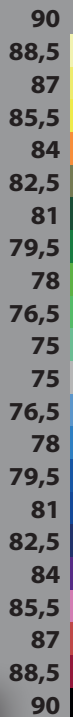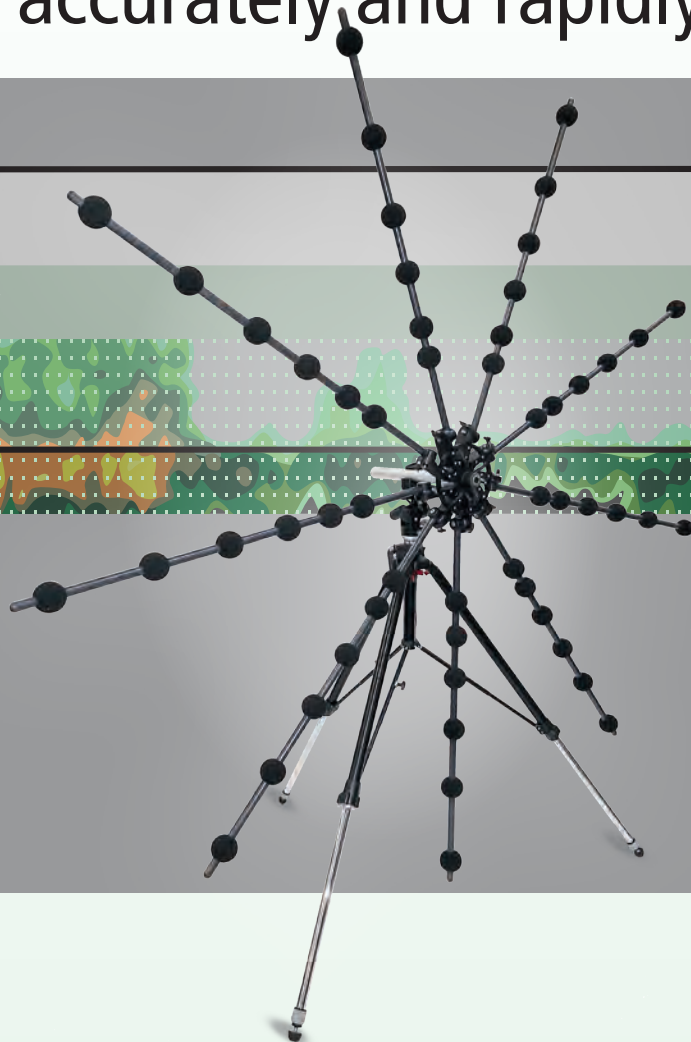
Noise source identification solutions for high-speed trains

Whether you deal with the aerodynamic noise generated by pantographs or rail/wheel interaction, Brüel & Kjær can provide you with the optimal acoustical array for your task, together with all the tools necessary for accurate, rapid and reliable noise source identification both outdoors and in wind tunnels.

Our array acoustics suite offers all the main noise source identification applications such as acoustical holography (STSF, SONAH*, ESM*), beamforming and spherical beamforming, together with a broad range of options (refined beamforming, transient, conformal and sound quality metrics calculations).

* patent pending

ALL FROM ONE PARTNER

Brüel & Kjær has the world's most comprehensive range of sound and vibration test and measurement systems

Brüel & Kjær

creating sustainable value

BN 1286–11